Analysis of Systems Described by Partial Differential Equations Using Convex Optimization

Mohamadreza Ahmadi

Keble College

University of Oxford

A thesis submitted for the degree of

Doctor of Philosophy

Trinity 2016

Acknowledgements

Oxford is an enchanting place! In addition to its beautiful colleges and stimulating atmosphere to do a DPhil, Oxford has taught me about different cultures from all over the world. It has also exposed me to other subjects, running the gamut of social sciences to plant sciences, that I had little knowledge of, before starting my DPhil course. This whole astounding experience was not possible without the financial support from the Clarendon Scholarship and the Sloane-Robinson Scholarship, for which I am deeply grateful.

Working with Prof. Antonis Papachristodoulou at Oxford was an amazing experience. Antonis is a caring and devoted supervisor. Throughout my DPhil studies, he provided me with invaluable advice and unwavering support both in life and in research. I should admit that Antonis is a model for me, and, if, at some point, I become a supervisor, I shall do my best to treat my students as he treated me. At the end of this DPhil, I can say that he made me a better person both in terms of attitude and in terms of research.

I am also grateful to Prof. Giorgio Valmorbida, who co-supervised my DPhil project. I am indebted to him for all the time he spent and all the discussions (though, on several occasions, a bit intense) we had on research. He has been very meticulous and passionate with respect to research, for which I am thankful.

At Oxford, I had the pleasure of making many marvelous friends. Specially, I am appreciative of the lovely couple, Dr. Matin Mavaddat and Mrs. Mahsa Aghdas Zadeh, for their priceless friendship and support from my very first days in the UK. I was also glad to have the companionship of Mr. Ali Pir Ataei, Dr. Cornelius Christian, Mr. Matthias Lalisse,

Mr. Stefan Saftescu, Mr. Charl Sevel, Mr. Sahba Shayani, Dr. Olumide Famuywa, Mr. Leo Davoudi, Miss Smaranda Ioana Maria, Dr. Hamed Nili, Mr. Chris Roth, Mr. Peter Bent, Prof. Dominic Brookshaw, Dr. Chinedu Ugwu, Dr. Victoria Truebody and Mr. Christopher Coghlan, who have been truly wonderful friends. Without your company, cozy Oxford wouldn't have been tolerable! Moreover, special thanks go to my colleagues and members of the Control Group at Oxford University, to name but a few, Mr. Mehdi Imani Masouleh, Mr. Dhruva Raman, Mr. Andreas Kisling Harris, Mr. Rainer Manuel Schaich, Mr. Ross Drummond, Dr. James Anderson, Dr. Xuan Zhang, Mr. Bartolomeo Stellato and Dr. Moritz Schulze Darup. I shall never forget those Age of Empires nights and our fantastic time in Japan! My appreciation should also go to my best friend in Iran, Dr. Kaveh Sadighi.

During my DPhil, I also had the honor to interact with several wonderful academics, among whom I should mention Prof. Sergei Chernyshenko, Prof. Dennice Gayme, Prof. Mihailo Jovanovic and Prof. Bassam Bamieh, who, in particular, further enriched my knowledge on problems in fluid mechanics.

Last but not least, I would like to express my greatest gratitude to my father Mr. Bahman Ahmadi, my mother Mrs. Masoumeh Yousef Zadeh, and my brother Dr. Milad Ahmadi for their unconditional love and support. You provided the best environment for me to grow and to be a better person. I dedicate this dissertation to you.

Abstract

In this dissertation, computational methods based on convex optimization, for the analysis of systems described by partial differential equations (PDEs), are proposed.

Firstly, motivated by the integral inequalities encountered in the Lyapunov stability analysis of PDEs, a method based on sum-of-squares (SOS) programming is proposed to verify integral inequalities with polynomial integrands. This method parallels the schemes based on linear matrix inequalities (LMIs) for the analysis of linear systems and approaches based on SOS programming for the analysis of polynomial nonlinear systems.

Secondly, dissipation inequalities for input-state/output analysis of PDE systems are formulated. Similar to the case of systems described by ordinary differential equations (ODEs), it is demonstrated that the dissipation inequalities can be used to check input-state/output properties, such as passivity, reachability, induced norms, and input-to-state stability (ISS). Furthermore, it is shown that the proposed input-state/output analysis method based on dissipation inequalities allows one to infer properties of interconnected PDE-PDE or PDE-ODE systems. In this regard, interconnections at the boundaries and interconnections over the domain are considered. It is also shown that an appropriate choice of the storage functional structure casts the dissipation inequalities into integral inequalities, which can be checked via convex optimization.

Thirdly, a method is proposed for safety verification of PDE systems. That is, the problem of checking whether all the solutions of a PDE, starting from a given set of initial conditions, do not enter some undesired or unsafe set. The method hinges on an extension

of barrier certificates to infinite-dimensional systems. To this end, a functional of the states of the PDE called the barrier functional is introduced. If this functional satisfies two inequalities along the solutions of the PDE, then the safety of the solutions is verified. If the barrier functional takes the form of an integral functional, the inequalities convert to integral inequalities that can be checked using convex optimization in the case of polynomial data. Furthermore, the proposed safety verification method is used for bounding output functionals of PDEs.

Finally, the tools developed in this dissertation are applied to study the stability and input-output analysis problems of fluid flows. In particular, incompressible viscous flows with constant perturbations in one of the coordinates are studied. The stability and input-output analysis is based on Lyapunov and dissipativity theories, respectively, and subsumes exponential stability, energy amplification, worst case input amplification and ISS. To the author's knowledge, this is the first time that ISS of flow models is being studied. It is shown that an appropriate choice of the Lyapunov/storage functional leads to integral inequalities with quadratic integrands. For polynomial base flows and polynomial data on flow geometry, the integral inequalities can be solved using convex optimization. This analysis includes both channel flows and pipe flows. For illustration, the proposed method is used for input-output analysis of several flows, including Taylor-Couette flow, plane Couette flow, plane Poiseuille flow and (pipe) Hagen-Poiseuille flow.

We conclude this dissertation with a summary and an account for future research directions.

Contents

List of Figures

Chapter 1

Introduction

The need for accurate models to study complex dynamical systems [20, 21, 130, 25] has driven research efforts towards PDE systems - equations involving derivatives with respect to more than one independent variable. Many, seemingly distinct, physical phenomena running the gamut of electrostatics to quantum mechanics can be mathematically formalized by PDEs. The PDEs involve rates of change of (spatially) *continuous* variables; whereas, the ODEs involve (spatially) *discrete* variables[1]. For instance, the configuration of a fluid is given by a continuous distribution of several variables, while the position of a rigid body is described by six numbers. Alternatively, we can say that the dynamics of the fluid take place in an infinite-dimensional space; whereas, the dynamics of a rigid body occur in a finite-dimensional space.

One example of a system that is best described by a PDE is the Tokamak plasma (see Figure 1.1). In [137], control-oriented PDE models for the physical variables in the Tokamak plasma were proposed. One such variable is the poloidal flux $\psi(R, Z)$ of the magnetic field $B(R, Z)$. The flux passes through a disc centered on the toroidal axis at height Z and with a surface $S = \pi R^2$, where R is the large plasma radius as depicted in Figure 1.2. The

[1]We call a variable *continuous* in an interval, if it can accept two particular real values such that it can also accept all real values between them (even values that are arbitrarily close together). On the other hand, if the variable can take on a value such that there is a non-infinitesimal gap on each side of it containing no values that the variable can take on, then it is *discrete* around that value.

Figure 1.1: Installation work inside the plasma vessel of the Tokamak reactor at IPP Max-Planck Institut för Plasmaphysik. The transformer coil is situated behind the column. The plasma vessel is surrounded by the main and the vertical-field coils (`http://www.ipp.mpg.de/16208/einfuehrung`).

flux per radians is defined as

$$\psi(R,Z) := \frac{1}{2\pi}\int_S \boldsymbol{B}(R,Z)\cdot d\boldsymbol{S}.$$

Let $\rho = (2\phi/B_{\phi_0})^{1/2}$ be the toroidal flux coefficient indexing the magnetic surfaces, where $\phi(t,\rho)$ is the toroidal flux per radians and $B_{\phi_0}(t)$ is the central magnetic field. The dynamics of the poloidal flux are described by the linear parabolic PDE

$$\frac{\partial\psi(t,\rho)}{\partial t} = D(t,\rho)\frac{\partial^2\psi(t,\rho)}{\partial\rho^2} + G(t,\rho)\frac{\partial\psi(t,\rho)}{\partial\rho} + S(t,\rho),$$

where $D(t,\rho)$ and $G(t,\rho)$ are transport coefficients, and $S(t,\rho)$ is the source term.

Another interesting PDE pertains to the turbulence phenomena in chemistry and combustion [119, Chapter III, Section 4.1]. The Kuramoto-Sivashinsky equation is a nonlinear PDE that models reaction-diffusion systems and can be used to describe pattern formation

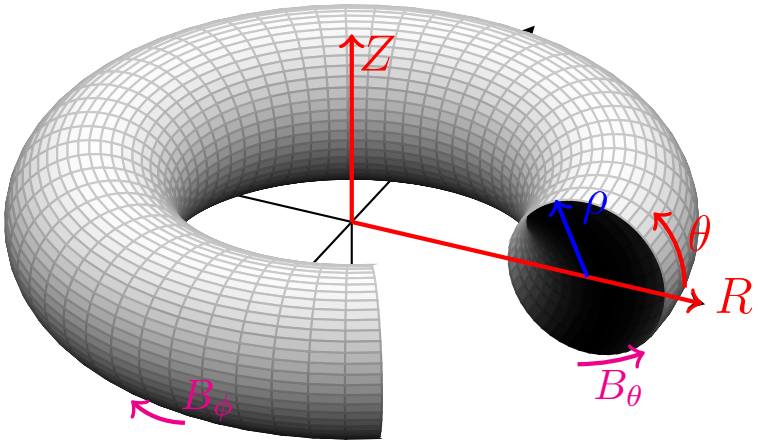

Figure 1.2: Diagram of the Tokamak system.

phenomena in the presence of turbulence and chaos. For an experimental setup, consider a combustor consisting of two concentric cylinders with a narrow gap filled with combustible gas as illustrated in Figure 1.3. The flame front develops wrinkles that are described by the Kuramoto-Sivashinsky equation

$$\frac{\partial u(t,x)}{\partial t} = -\frac{\partial^4 u(t,x)}{\partial x^4} - \mu\frac{\partial^2 u(t,x)}{\partial x^2} - u(t,x)\frac{\partial u(t,x)}{\partial x}, \qquad t > 0,\ x \in (0,1),$$

where $\mu > 0$ is called the anti-diffusion parameter.

The infinite dimensional nature of PDE models, such as the two examples above, make them challenging to study both analytically and numerically. Conventional numerical approaches to study PDEs rely on spectral or spatial discretization and use tools developed for ODEs [42, 32]. Computational methods which do not require finite-dimensional approximations are needed to mitigate the conservatism in the system analysis using numerical approaches.

In the forthcoming sections, we outline some of the interesting analysis problems for PDEs and review the literature on each of them. We also explain briefly how the latter analysis problems are addressed in this dissertation.

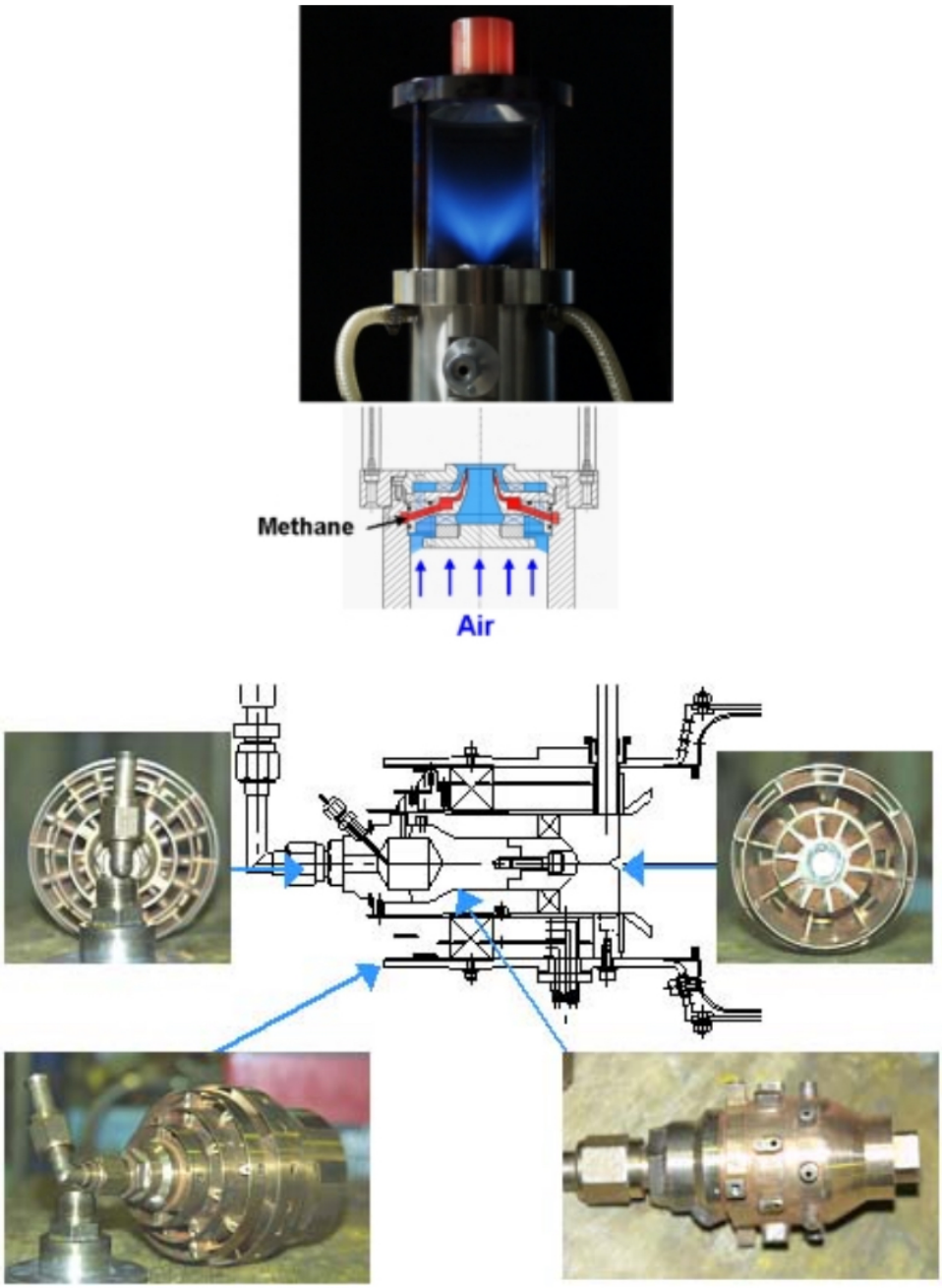

Figure 1.3: Experimental setup for the Kuramoto-Sivashinsky equation. (top) Gas turbine model combustor for swirled methane flames (`http://www.dlr.de/vt/en/desktopdefault.aspx/tabid-3080/4657_read-15212`) (bottom) A prototype of the combustor (`http://www.osakagas.co.jp/rd/sheet/126e.html`).

1.1 Stability Analysis of PDEs

The study of properties of solutions to PDEs, such as stability, parallels the study of ODEs in several aspects. As for ODEs, conditions for stability of the zero solution can be specified via spectral analysis when the PDE system is defined by a linear operator. Moreover, it is possible to infer stability from the semi-group generated by the linear or nonlinear operators which is analogous to the ODE approach of computing solutions to establish stability [26].

Similar to ODEs, another approach to stability analysis is through Lyapunov's second method. Early results on the extension of Lyapunov's second method to PDEs included the stability problem of elastic systems [75]. Although [75] studied the stability of an elastic beam, the formulation provided was general. Also, in [83], a construction method for Lyapunov functionals applied to linear PDE systems was proposed. Lyapunov theorems for PDE systems were obtained in [131] and [49], as well. For linear PDE systems, following in the footsteps of [28] associated with strongly continuous semi-groups, in [26, Theorem 5.1.3, p. 217], a Lyapunov equation is formulated which, if solved, ensures the exponential stability of the semi-group (see Theorem A.1.4 and the subsequent discussions). This Lyapunov equation is in terms of operators, and is a reminiscent of the one for linear ODE systems. To illustrate, consider the abstract Cauchy problem

$$\dot{\zeta}(t) = \mathscr{A}\zeta(t),\ \zeta(0) = \zeta_0 \in \mathscr{Z}. \tag{1.1}$$

Let $\mathscr{A}$ be the infinitestimal generator[2] of the C^0-semigroup $T(t)$ on a Hilbert space $\mathscr{Z}$, e.g. a linear differential operator. Then, $T(t)$ is exponentially stable if and only if there exists a bounded positive linear operator $\mathscr{P} : \mathscr{Z} \to \mathscr{Z}$ such that the following Lyapunov equation

[2]The infinitesimal generator $\mathscr{A}$ of a strongly continuous semigroup T is defined by

$$\mathscr{A}\zeta = \lim_{t \to 0^+} \frac{T(t)\zeta - \zeta}{t},$$

whenever the limit exists. The domain of $\mathscr{A}$, $Dom(\mathscr{A})$, is the set of $\zeta \in \mathscr{Z}$ for which this limit exists; $Dom(\mathscr{A})$ is a linear subspace and $\mathscr{A}$ is linear on this domain.

is satisfied

$$\langle \mathscr{A}\zeta, \mathscr{P}\zeta \rangle_{\mathcal{Z}} + \langle \mathscr{P}\zeta, \mathscr{A}\zeta \rangle_{\mathcal{Z}} = -\langle \zeta, \zeta \rangle_{\mathcal{Z}} \tag{1.2}$$

for all $\zeta \in Dom(\mathscr{A})$, which is a linear operator equation. Indeed, the left-hand side of (1.2) can be derived by calculating the time derivative of the following Lyapunov functional

$$V(\zeta) = \langle \mathscr{P}T(t)\zeta, T(t)\zeta \rangle_{\mathcal{Z}}\,. \tag{1.3}$$

Solving (1.2) can be cumbersome in the infinite-dimensional linear PDE case. In order to tackle this drawback, in [26], the authors use a high-dimensional ODE approximation instead of the (infinite-dimensional) linear PDE. Then, (1.2) reduces to a linear matrix equation in high dimensions. Despite attempts to overcome the difficulty in solving the resultant high dimensional matrix equations [76], solving these matrix equations remains burdensome.

In the case of nonlinear PDEs, however, *a priori* choices for Lyapunov functionals for a particular PDE system are difficult to find and are often too conservative. For example, the energy of the state (which is a norm defined on a function space in the case of PDEs) is a frequent choice, since it simplifies the analysis of a large set of nonlinear PDE systems, especially, when the nonlinearities are energy-preserving, e.g. convection [116]. Let us illustrate the steps followed for the stability analysis of a nonlinear PDE through an example.

Example 1.1.1 *Let $u = u(t,x)$ where $t > 0$ and $x \in (0,1)$. Consider Burgers' equation*

$$\frac{\partial u}{\partial t} = \frac{\partial^2 u}{\partial x^2} - u\frac{\partial u}{\partial x}, \qquad u(t,0) = u(t,1) = 0, \tag{1.4}$$

and the energy as a candidate Lyapunov functional:

$$E(u) = \frac{1}{2}\int_0^1 u^2 \;\; dx. \tag{1.5}$$

The time derivative of $E(u)$ *along the trajectories of* (1.4) *is*

$$\frac{dE(u)}{dt} = \int_0^1 u\frac{\partial u}{\partial t}\ dx = \int_0^1 u\left(\frac{\partial^2 u}{\partial x^2} - u\frac{\partial u}{\partial x}\right)\ dx. \tag{1.6}$$

Applying integration by parts, we obtain

$$\frac{dE(u)}{dt} = -\int_0^1 \left(\frac{\partial u}{\partial x}\right)^2\ dx + \left(u\frac{\partial u}{\partial x}\right)|_{x=0}^1 - \frac{1}{3}u^3|_{x=0}^1 \tag{1.7}$$

and since $u(t,0) = u(t,1) = 0$*, this results in*

$$\frac{dE(u)}{dt} = -\int_0^1 \left(\frac{\partial u}{\partial x}\right)^2\ dx. \tag{1.8}$$

Notice that the convection term uu_x *(energy preserving nonlinearity) in* (1.4) *was integrated to zero thanks to the boundary conditions. In order to demonstrate exponential stability of* (1.4)*, one needs to relate* $\int_0^1 \left(\frac{\partial u}{\partial x}\right)^2\ dx$ *to* $\int_0^1 u^2\ dx$*, so as to relate* $\frac{dE(u)}{dt}$ *to* $E(u)$*. This is done by employing the following inequality (known as the Poincaré inequality) on* $\Omega = (0,1)$ *with Dirichlet boundary conditions* $u(t,0) = u(t,1) = 0$

$$\int_0^1 u^2\ dx \leq \frac{1}{\pi^2}\int_0^1 \left(\frac{\partial u}{\partial x}\right)^2\ dx. \tag{1.9}$$

Combining (1.8) *and* (1.9)*, we get*

$$\frac{dE(u)}{dt} \leq -\pi^2\int_0^1 u^2\ \ dx = -2\pi^2 E(u) \tag{1.10}$$

which proves the exponential decay for $E(u(t,x))$*, since* $E(u(t,x)) \leq E(u(0,x))e^{-2\pi^2 t}$*.*

Note that the key tool in the above calculations was integration-by-parts. Use (or knowledge) of inequalities relating variables and their spatial derivatives in the domain such as Wirtinger [108], Poincaré and the Sobolev Embedding Theorem [33, Sec 5.6] was also required.

Analytical Lyapunov stability analysis of PDE systems becomes more involved for systems of several dependent variables, different nonlinearities (e.g., cubic terms) and for systems with spatially varying properties (inhomogeneous PDEs). For such systems, the energy functional may lead to poor stability bounds.

One alternative class of Lyapunov functional candidates for PDE systems is the weighted $\mathcal{H}^q$-norms (Sobolev norms). These functionals yield Lyapunov conditions requiring the verification of integral inequalities. In this context, computing the Lyapunov functionals requires the solution of integral inequalities [116].

1.1.1 Contribution

In Chapter 3, we present a method to verify integral inequalities with integrands that are polynomials in the dependent variables. The polynomial structure allows for a quadratic-like representation of the integrand and we formulate conditions for the positivity of integral expressions in terms of differential matrix inequalities. For the case of integrands that are polynomial in the *independent* variables as well, the differential matrix inequality formulated by the proposed method becomes a polynomial matrix inequality. We then exploit the SDP formulation [84] of optimization problems with linear objective functions and polynomial constraints [24] to obtain a numerical solution to the integral inequalities. Several analysis and feedback design problems have been studied using polynomial optimization, to name but a few, the stability of time-delay systems [86], synthesis of control laws [129, 94], applied to optimal controller design [66] and system analysis [48]. In the context of PDEs, [80] laid the first bricks, where the stability analysis of linear parabolic PDEs was formulated as an SOS program.

The proposed method to solve integral inequalities is then applied to study the stability of PDE systems using the weighted Sobolev norms as the Lyapunov functional candidate. A preliminary version of the contributions described in Chapter 3 was presented in the 2014 53rd IEEE Conference on Decision and Control [126]. The extended version of the results

was published in [128].

1.2 Dissipation Inequalities for Input-Output Analysis of PDEs

1.2.1 Literature Review

A powerful tool in the study of robustness and input-state/output properties of dynamical systems is dissipation inequalities [135, 51]. A dissipation inequality relates a storage function/functional, which characterizes the internal energy in the system, and a supply rate, which represents a generalized power supply function. Given a supply rate, the solution to the dissipation inequality is a storage function/functional, which, according to the supply rate, can certify different system properties such as passivity, induced $\mathcal{L}^2$-norm boundedness, reachability, and ISS. One major advantage of dissipation inequalities is that, in the case of systems consisting of an interconnection of subsystems, once some property of the subsystems is known in terms of dissipation inequalities, we can infer properties of the overall system [102].

For linear systems described by ODEs, quadratic storage functions of states are known to be both necessary and sufficient solutions to dissipation inequalities with quadratic supply rates [124]. For example, the Kalman-Yakubovic-Popov lemma [60] presents necessary and sufficient conditions to construct quadratic storage functions certifying the dissipation inequality for passivity of linear ODE systems. These conditions are given in terms of quadratic expressions, which can be checked computationally via LMIs [18, Chapter 2]. For ODEs with polynomial vector fields, [31] proposes an approach for constructing polynomial storage functions based on SOS programming. For general nonlinear ODEs, however, the solution to dissipation inequalities may require *ad hoc* techniques.

With respect to PDEs, the solution (state) is a function of both space and time. Moreover, the solution belongs to an infinite-dimensional (function) space, as opposed to a Euclidean space in the case of ODEs. Unlike Euclidean spaces, for function spaces, say

Sobolev spaces, different norms are not equivalent [33]. Therefore, input-state/output properties differ from one norm to another.

In the context of PDEs, solutions to dissipation inequalities have been recently proposed. For linear time-varying hyperbolic PDEs, the weighted $\mathcal{L}^2$-norm functional was considered as a certificate for ISS in [97]. ISS storage functionals were suggested in [71], for semi-linear parabolic PDEs. In [20], ISS of a semi-linear diffusion equation was analyzed using the weighted $\mathcal{L}^2$-norm as the storage functional and a control approach was formulated for a model of magnetic flux profile in Tokamak plasma. In this particular case, the calculation of the storage functional was formulated as the solution of a differential inequality, which was solved using a numerical method. More general ISS definitions were presented in [27], and a small gain theorem for the interconnection of PDEs was formulated.

However, once a dissipation inequality is formulated for an input-state/output property characterized by a supply rate, solving the dissipation inequality is difficult in general, especially in the case of nonlinear PDEs.

1.2.2 Contribution

In Chapter 4, we present a framework for input-state/output analysis of a class of nonlinear PDEs based on dissipation inequalities. Each input-state/output property, namely passivity, reachability, induced input-output norms and ISS, is defined in the appropriate Sobolev norm. For each property, the relevant dissipation inequality is formulated. We consider PDEs with inputs and outputs defined over the domain, and PDEs with inputs and outputs defined at the boundaries of the domain. Equipped with these dissipation inequalities, we study interconnections of PDE-PDEs and PDE-ODEs with the interconnection either at the boundary and/or over the domain. In this case, we formulate small-gain type theorems. Additionally, we use convex optimization to systematically solve the dissipation inequalities for PDEs described by polynomials on the independent and the dependent variables.

Preliminary results on the material presented in Chapter 4 were presented in the 2014 53rd IEEE Conference on Decision and Control [2]. The journal version of the results was also published in [6].

1.3 Barrier Functionals for the Analysis of PDEs

1.3.1 Safety Verification

One interesting problem in the analysis of PDEs is safety verification. That is, given the set of initial conditions, check whether the solutions of a PDE satisfy a set of constraints, or, in other words, whether they avoid an unsafe set. Reliable safety verification methods are fundamental to the design of safety critical systems such as life support systems (to ensure that the carbon dioxide and oxygen concentrations in a Variable Configuration CO2 Removal subsystem never reach unacceptable values) [41], and wind turbines (to guarantee safe emergency shutdown in the case of a fault or a large wind gust) [136].

The safety verification problem is well-studied for ODE systems (see the survey paper [44]). Methods based on the approximation of the reachable sets are considered in [63] for linear systems and in [121] for nonlinear systems. Another method for safety verification, which does not require the approximation of reachable sets, uses barrier certificates. Barrier certificates [91] were introduced for model invalidation of ODEs with polynomial vector fields and have been used to address safety verification of nonlinear and hybrid systems [93] and safety analysis of time-delay systems [92]. In [7], model validation and invalidation of biological models using exponential barrier certificates was considered. Exponential barrier functions were proposed in [115] for finite-time regional verification of stochastic nonlinear systems, as well. Moreover, compositional barrier certificates and converse results were studied in [110] and [95], respectively.

The application of barrier certificates goes beyond just the analysis. In [134], inspired by the notion of control Lyapunov functions (CLFs) [8] and Sontag's formula [111], Wei-

land and Allgöwer introduced control barrier functions (CBFs) and formulated a controller synthesis method that ensures safety with respect to an unsafe set.

1.3.2 Bounding Output Functionals of PDEs

In many engineering design problems, one may merely be interested in computing a functional of the solution to the underlying PDE rather than the solution itself (see the review article [10] for a number of applications in structural mechanics). For instance, the far-field pattern in electromagnetics and acoustics [73] and energy release rate in elasticity theory [139] are both functionals of the solutions to the governing PDEs.

The ubiquity of applications has motivated the development of computational algorithms for output functional approximation. In [88], an augmented Lagrangian-based approach was proposed for the calculation of upper and lower bounds to linear output functionals of coercive PDEs. In [73], adjoint and defect methods for obtaining estimates of linear output functionals for a class of stationary (time-independent) PDEs were suggested. In [138], the authors formulated an *a posteriori* bound methodology for linear output functionals of finite element solutions to linear coercive PDEs. Adjoint and defect methods for computing estimates of the error in integral functionals of solutions to stationary linear PDEs were discussed in [89]. In [14], an SDP-based bound estimation scheme for linear output functionals of linear elliptic PDEs, based on the moments problem, was formulated.

However, most of the methods proposed to date require finite element approximations of the solution, which is susceptible to inherent discretization errors. Furthermore, it may not be clear whether an attained bound from finite element approximations on the output functionals is an upper or lower bound estimate. Consequently, we need certificates to verify an obtained bound (see [139, 82] for finite element based methods with certificates for linear/quadratic output functionals of stationary linear elliptic PDEs).

1.3.3 Contribution

In Chapter 5, Section 5.1, we present a method for safety verification of systems described by PDEs. In this case, the considered sets that are subsets of Hilbert spaces rather than only subsets of Euclidean spaces as in the case of systems described by ODEs. The proposed method relies on barrier functionals, which are functionals of the dependent and independent variables. We show that if there exists a barrier functional that satisfies two inequalities along the solutions of the PDE, then we can conclude that the solutions avoid an unsafe set for all time or at some specific time instant. If the barrier certificate is defined as an integral functional, the latter inequalities become integral inequalities. In the case of polynomial data, we solve these integral inequalities by convex optimization.

In Chapter 5, Section 5.2, we apply the safety verification framework to compute bounds on output functionals of a class of time-dependent PDEs, without the need to approximate the solutions. The method is based on reformulating the output functional estimation method into a safety verification scenario using an appropriate definition of the unsafe set in terms of the output functional of interest. For each upper bound, the proposed method provides a barrier functional as a certificate. For the case of polynomial PDEs and polynomial output functionals (in both dependent and independent variables), SOS programming can be used to construct the barrier functionals and therefore to compute upper bounds. This reduces the problem to solving SDPs.

The results pertaining to bounding output functionals of PDEs, were presented in the 2015 American Control Conference [3]. A journal version which contains the safety verification method and more discussions is currently under preparation [5].

1.4 Input-Output Analysis of Fluid Flows

1.4.1 Literature Review

The dynamics of incompressible fluid flows is described by a set of nonlinear PDEs known as the Navier-Stokes equations. The properties of such flows are then characerized in terms of a dimensionless parameter Re called the Reynolds number. Experiments show that many flows have a critical Reynolds number Re_C below which the flow is stable with respect to disturbances of any amplitude. However, spectrum analysis of the linearized Navier-Stokes equations, considering only infinitesimal perturbations, predicts a linear stability limit Re_L which upper-bounds Re_C [30]. On the other hand, the bounds using energy methods Re_E, the limiting value for which the energy of arbitrary large perturbations decreases monotonically, are much below Re_C [55]. For Couette flow, for instance, $Re_E = 32.6$ computed by [106] using energy functional, $Re_L = \infty$ using spectrum analysis [101] and $Re_C \approx 350$ estimated empirically by [120].

The discrepancy between Re_L and Re_C have long been attributed to the eigenvalues analysis approach [123], citing a phenomenon called *transient growth* as the culprit; *i.e.*, although the perturbations to the linearized Navier-Stokes equation are stable (and the eigenvalues have negative real parts), they undergo high amplitude transient amplifications that steer the trajectories out of the region of linearization. This has led to studying the resolvent operator or ε-pseudospectra based on the general solution to the linearized Navier-Stokes equations [103].

Another method for studying stability is based on spectral truncation of the Navier-Stokes equations into an ODE system. This method is fettered by truncation errors and by the mismatch between the dynamics of the truncated model and the Navier-Stokes PDE. To alleviate this drawback, recently in [42, 22], a method was proposed based on keeping a number of modes from Galerkin expansion and bounding the energy of the remaining

modes. It was shown in [52] that, in the case of rotating Couette flow, this method can find a global stability limit which is better than the energy method. The method was also extended in [22] to address the problem of finding bounds for time-averaged flow parameters with applications to flow control for drag reduction.

Since the seminal paper by [99], it was observed that external excitations and body forces play an important role in flow instabilities. Mechanisms such as energy amplification of external excitations have shown to be crucial in understanding transition to turbulence as highlighted by [55]. Energy amplification of stochastic forcings to the linearized Navier-Stokes equations in unbounded shear and deformation flows was studied in [37]. In a similar vein, in [13], using the linearized Navier-Stokes equation, it was shown analytically, through the calculation of traces of operator Lyapunov equations, that the $\mathcal{H}^2$-norm from streamwise constant excitations to perturbation velocities in channel flows is proportional to Re^3. The amplification mechanism of the linearized Navier-Stokes equation was verified in [59] and [58], where the influence of each component of the body forces was calculated in terms of $\mathcal{H}^2$ and $\mathcal{H}^\infty$-norms based on finding analytical solutions to the Lyapunov equations. Input-output analysis of a model of plane Couette flow was carried out in [40] to study the nonlinear mechanisms associated with turbulence. In another vein, an input-state analysis method for the linearized Navier-Stokes equation by calculating the spatio-temporal impulse responses was given in [57]. Linear energy amplification of turbulent channel flows, by considering the turbulent mean velocity profiles and turbulent eddy viscosities, was studied in [29] with the corresponding transient growth analysis given in [98]. Linear non-normal energy amplification for harmonic and stochastic excitations to small coherent perturbations in turbulent channel flows was considered in [53]. The literature on input-output analysis methods is vast, but a review of input-output analysis methods was presented in [12], where the authors apply linear robust control theory techniques to the discretized version of the linearized complex Ginzburg-Landau equation. Linear robust control theory methods were also used in [11] for input-output analysis and control of

two-dimensional perturbations to a spatially evolving boundary layer on a flat plate.

1.4.2 Contribution

In Chapter 6, we consider the stability and input-output properties of incompressible, viscous fluid flows. We study input-output properties such as maximum energy growth, worst-case input amplification (induced $\mathcal{L}^2$-norms from body forces to perturbation velocities) and ISS. In particular, we consider flow perturbations constant in one of the three spatial coordinates. This is motivated by the transient growth analyses of the linearized Navier-Stokes equations for channel flows [77, 45, 37] suggesting that the streamwise constant modes receive largest energy growth and pseudo-spectral analysis of the linearized Navier-Stokes [123] implying that streamwise constant perturbations have the maximum energy growth. Our main tools for the input-output analysis are the dissipation inequalities developed in Chapter 4. For flows with streamwise constant perturbations, we find a suitable structure as a Lyapunov/storage functional that converts the dissipation inequalities into integral inequalities with quadratic integrands in dependent variables. Then, using these functionals, we propose conditions based on matrix inequalities. In the case of polynomial base velocity profiles, e.g. Couette and Poiseuille flows, these inequalities can be checked via convex optimization using available computational tools.

The preliminary version of the formulation described in Chapter 6 was presented at the 2015 54th IEEE Conference on Decision and Control [4]. A journal article including the discussions on pipe flows and more examples is currently under preparation.

1.5 List of Publications from The Dissertation

1. M. Ahmadi, G. Valmorbida and A. Papachristodoulou, Safety Verification for Distributed Parameter Systems Using Barrier Functionals, *Systems & Control Letters*, Under Review.

2. M. Ahmadi, A. W. K. Harris, and A. Papachristodoulou, An Optimization-based Method for Bounding State Functionals of Nonlinear Stochastic Systems, *in The 55th IEEE Conference on Decision and Control*, Las Vegas, USA, 2016.

3. M. Ahmadi, G. Valmorbida and A. Papachristodoulou, Dissipation Inequalities for the Analysis of a Class of PDEs, *Automatica*, vol. 66, pp. 163-171, 2016.

4. G. Valmorbida, M. Ahmadi and A. Papachristodoulou, Stability Analysis for a Class of Partial Differential Equations via Semi-Definite Programming, *IEEE Transactions on Automatic Control*, vol. 61, no. 6, pp. 1649-1654, 2016.

5. M. Ahmadi, G. Valmorbida, and A. Papachristodoulou, A Convex Approach to Hydrodynamic Analysis, *in The 54rd IEEE Conference on Decision and Control*, Osaka, Japan, pp. 7262-7267, 2015.

6. G. Valmorbida, M. Ahmadi, and A. Papachristodoulou, Convex Solutions to Integral Inequalities in Two Dimensions, *in The 54rd IEEE Conference on Decision and Control*, Osaka, Japan, pp. 7268-7273, 2015.

7. M. Ahmadi, G. Valmorbida, and A. Papachristodoulou, Barrier Functionals for Output Functional Estimation of PDEs, *in The 2015 American Control Conference*, July 1?3, Chicago, IL, pp. 2594-2599, 2015.

8. M. Ahmadi, G. Valmorbida, and A. Papachristodoulou, Input-Output Analysis of Distributed Parameter Systems Using Convex Optimization, *in The 53rd IEEE Conference on Decision and Control*, Los Angeles, California, USA, pp. 4310-4315, 2014.

9. G. Valmorbida, M. Ahmadi, and A. Papachristodoulou, Semi-definite Programming and Functional Inequalities for Distributed Parameter Systems, *in 53rd IEEE Conference on Decision and Control*, Los Angeles, California, USA, pp. 4304-4309, 2014.

1.6 Notation

The notation throughout this thesis is as follows.

Let $\mathbb{R}, \mathbb{R}_{\geq 0}, \mathbb{R}_{>0}$ and $\mathbb{R}^n$ denote the field of reals, the set of non-negative reals, the set of positive reals and the n-dimensional Euclidean space, respectively. The sets of natural numbers and non-negative natural numbers are denoted $\mathbb{N}$ and $\mathbb{N}_{\geq 0}$, respectively.

We use M' to denote the transpose of matrix M. The set of real symmetric matrices is denoted $\mathbb{S}^n = \{A \in \mathbb{R}^{n\times n} | A = A'\}$. For $A \in \mathbb{S}^n$, denote $A \geq 0$ ($A > 0$) if A is positive semidefinite (definite), the linear operator $He(\cdot)$ satisfies $He(A) := A + A'$. $diag(A, B)$ denotes the block-diagonal matrix formed by matrices A and B. We denote by $\mathrm{I}_{n\times n}$ the unit matrix of size $n \times n$.

The closure of set Ω is denoted $\overline{\Omega}$. The boundary $\partial\Omega$ of set Ω is defined as $\overline{\Omega} \setminus \Omega$ with $\setminus$ denoting set subtraction. The ring of polynomials, the ring of positive polynomials, and the ring of sum-of-squares polynomials on a real variable x are denoted $\mathcal{R}[x]$, $\mathcal{P}[x]$ and $\Sigma[x]$ respectively. The ring of SOS square matrices of dimension n, *i.e.,* matrices $M(x) \in \mathcal{R}^{n\times n}[x]$ satisfying $M(x) = \sum_{i=1}^{n_M} N_i'(x)N_i(x)$ with $N_i(x) \in \mathbb{R}^{d_i\times n}$, is denoted $\Sigma^{n\times n}[x]$. For $n, k \in \mathbb{N}_{\geq 0}$, define the matrix $K \in \mathbb{N}^{n\times\sigma(n,k)}$, $\sigma(n,k) := \binom{n+k-1}{n-1} = \frac{(n+k-1)!}{(n-1)!k!}$, of which the columns satisfy $\sum_{i=1}^{n} K_{ij} = k$, $\forall j$, without repetition. The multi-index notation is used to define the vector of all monomials of degree $k \in \mathbb{N}$ on vector $w = (w_1, w_2, \ldots, w_n) \in \mathbb{R}^n$, as $w^{\{k\}} := \begin{bmatrix} (w^{K_{(\cdot 1)}})' & \ldots & (w^{K_{(\cdot\sigma(n,k))}})' \end{bmatrix}$ where $w^{K_{(\cdot j)}} := \prod_{i=1}^{n} w_i^{K_{ij}}$. The number of terms in $w^{\{k\}}$ is hence given by $\sigma(n,d)$. For instance, with $n = 2$ and $k = 2$, we have $K = \left[\begin{smallmatrix} 2 & 1 & 0 \\ 0 & 1 & 2 \end{smallmatrix}\right]$, and $w^{\{2\}} = (w_1^2, w_1w_2, w_2^2)$. Define the vector containing all monomials in w up to degree k as $\eta^k(w) := \begin{bmatrix} 1 & (w^{\{1\}})' & \ldots & (w^{\{k\}})' \end{bmatrix}'$.

The set $\mathcal{T}$ of (vector) functions, mapping Ω into $\mathcal{A}$, is denoted $\mathcal{T}(\Omega; \mathcal{A})$ and we use the notation $\mathcal{T}(\Omega)$ or $\mathcal{T}_\Omega$ whenever the range can be understood from the context. In particular, we denote $\mathcal{T} = \mathcal{C}^k$ for the set of continuous vector functions, which are k-times differentiable and have continuous derivatives. Alternatively, $p \in \mathcal{C}^k[x]$ implies p is k-times continuous differentiable with respect to variable x. If $p \in \mathcal{C}^1(\Omega)$, then $\partial_x p$ is used to

denote the derivative of p with respect to variable x, i.e. $\partial_x := \frac{\partial}{\partial x}$. In addition, we adopt Schwartz's multi-index notation. For $u \in \mathcal{C}^k(\Omega; \mathbb{R}^n)$, $\alpha \in \mathbb{N}_0^n$, define

$$D^\alpha u := (u_1, \partial_x u_1, \ldots, \partial_x^{\alpha_1} u_1, \ldots, u_n, \partial_x u_n, \ldots, \partial_x^{\alpha_n} u_n)\,.$$

We use $\mathcal{T} = \mathcal{W}^{q,p}$ to represent the *Sobolev space* of p-th power, up to q-th derivative integrable functions u endowed with the norm

$$\|u\|_{\mathcal{W}_\Omega^{q,p}} = \left(\int_\Omega \sum_{i=0}^{q} \left| \partial_x^i u \right|^p \, \mathrm{d}x \right)^{\frac{1}{p}},$$

for $1 \leq p < \infty$ and $q \in \mathbb{N}_{\geq 0}$, and

$$\|u\|_{\mathcal{W}_\Omega^{q,\infty}} = \max_{i=0,\ldots,q} \left(\sup_{x \in \Omega} \left| \partial_x^i u \right| \right),$$

for $p = \infty$, where $|\cdot|$ signifies the absolute value. We denote the case $p = 2$ simply as the Hilbert space $\mathcal{H}_\Omega^q$. For $q = 0$, we use the notation $\mathcal{L}_\Omega^p$ for the Lebesgue space. Also, we use the following notation

$$\|u\|_{\mathcal{H}_{[0,T),\Omega}^q} = \left(\int_0^T \langle u, u \rangle_{\mathcal{H}_\Omega^q} \, \mathrm{d}t \right)^{\frac{1}{2}},$$

where $\langle u, u \rangle_{\mathcal{H}_\Omega^q}$ is the inner product in $\mathcal{H}_\Omega^q$. We remove the subscript of $\mathcal{H}_{[0,T),\Omega}^q$, *i.e.,* $\mathcal{H}^q$, when $T = \infty$.

For a function $f \in \mathcal{C}^1(\Omega)$ and $g \in \mathcal{C}^2(\Omega)$, ∇f denotes the gradient vector, $\nabla^2 g$ denotes the Hessian matrix and Δg is the Laplacian operator. The ceiling function is denoted $\lceil \cdot \rceil$.

A continuous, strictly increasing, function $k : [0, a) \to \mathbb{R}_{\geq 0}$, satisfying $k(0) = 0$, belongs to class $\mathcal{K}$. If $a = \infty$ and $\lim_{x \to \infty} k(x) = \infty$, k belongs to class $\mathcal{K}_\infty$. We recall that for any class $\mathcal{K}$ function, the inverse exists and belongs to class $\mathcal{K}$. Furthermore, for any positive $a, b > 0$ and $k \in \mathcal{K}$, we have [112, Inequality (12)]

$$k(a + b) \leq k(2a) + k(2b). \tag{1.11}$$

For a symmetric matrix function $S(x) : \Omega \to \mathbb{R}^{n \times n}$, we define $\lambda_m(S) = \inf_{x \in \Omega} |\lambda_{min}(S(x))|$, where $\lambda_{min} : \mathbb{S}^n \to \mathbb{R}$ is the minimum eigenvalue function. Similarly, $\lambda_M(S) = \sup_{x \in \Omega} |\lambda_{max}(S(x))|$, where $\lambda_{max} : \mathbb{S}^n \to \mathbb{R}$ is the maximum eigenvalue function.

Finally, $Dom(\mathscr{A})$ and $Ran(\mathscr{A})$ denote the domain and range of the operator $\mathscr{A}$, respectively.

Chapter 2

Preliminaries

In this chapter, we present some mathematical definitions and preliminary results that will be used in the sequel. We begin this chapter by presenting some results on stability of PDE solutions. Then, we touch upon a number of inequalities that are used in this dissertation. Finally, we provide a brief review of SOS programming.

2.1 Partial Differential Equations

We succinctly describe the stability notions pertained to PDEs. For the sake of self-containment, Appendix A reviews some results and definitions regarding semi-group theory and well-posedness of linear and nonlinear PDEs. While these results are important from a mathematical perspective, they are not central to our discussions in this dissertation. Throughout the dissertation, we assume that the PDEs under study satisfy the well-posedness conditions as outlined in Appendix A.

2.1.1 Stability of PDEs

Fundamental to our results is the notion of stability or convergence for the solutions of a PDE. Unlike the finite-dimensional systems, stability or convergence for solutions to a PDE

system should be understood in the sense of the norm one considers. In this dissertation, we study the stability and input-state/output properties in the sense of Sobolev norms.

In this section, we detail the formulation presented in [49] for stability of PDEs. Similar formulations are found in [75], [83] and [131], as well.

We begin by defining an equilibrium and afterwards stability.

Definition 2.1.1 (Definition 4.1.2 in [49]) *Let* $\{T(t),\ t \geq t_0\}$ *be a nonlinear semi-group (dynamical system) on a complete metric space* $\mathcal{U}$ *and for any* $u \in \mathcal{U}$*, let* $Y(u) = \{T(t)u,\ t \geq t_0\}$ *be the* orbit *through* u*. We say* u *is an equilibrium point if* $Y(u) = \{u\}$.

An orbit $Y(u)$ is *stable* if for any $\epsilon > 0$, there exists $\delta(\epsilon) > 0$ such that for all $t \geq t_0$, $\|T(t)u - T(t)v\|_{\mathcal{U}} < \epsilon$ whenever $\|u - v\|_{\mathcal{U}} < \delta(\epsilon)$, $v \in \mathcal{U}$, where $\|\cdot\|_{\mathcal{U}}$ is a norm defined on $\mathcal{U}$. An orbit is *uniformly asymptotically stable* if it is stable and also there is a neighbourhood $\mathcal{V} = \{v \in \mathcal{U} \mid \|u - v\|_{\mathcal{U}} < r\}$ such that $\|T(t)u - T(t)v\|_{\mathcal{U}} \to 0$ as $t \to \infty$, uniformly for $v \in \mathcal{V}$ [1]. Similarly, it is *exponentially stable* if there exist $\sigma, \gamma > 0$ such that

$$\|T(t)u - T(t)v\|_{\mathcal{U}} \leq \gamma \|u - v\|_{\mathcal{U}} e^{-\sigma(t-t_0)},$$

for all $t \geq t_0$ and all $u, v \in \mathcal{U}$.

We are interested in studying the stability of PDEs based on Lyapunov's second method. We need the definition of a Lyapunov function first.

Definition 2.1.2 (Definition 4.1.3 in [49]) *Let* $\{T(t),\ t \geq t_0\}$ *be a nonlinear semi-group on* $\mathcal{U}$*. A Lyapunov function is a continuous real-valued function* V *on* $\mathcal{U}$ *such that*

$$\partial_t V(u) = \lim_{t \to 0^+} \frac{V(T(t)u) - V(u)}{t} \leq 0, \tag{2.1}$$

for all $u \in \mathcal{U}$.

[1] i.e. $\forall \varepsilon > 0, \exists t_0 > 0 :\ t > t_0$ such that $\|T(t)u - T(t)v\|_{\mathcal{U}} < \varepsilon,\ \forall v \in \mathcal{U}$.

Theorem 2.1.3 (Lyapunov Theorem for Nonlinear Semi-groups, [49, Theorem 4.1.4]), *Let* $\{T(t),\ t \geq t_0\}$ *be a nonlinear semi-group, and let* ψ *be an equilibrium point in* $\mathcal{U}$*. Suppose* V *is a Lyapunov function on* $\mathcal{U}$ *which satisfies* $V(\psi) = 0$*, and* $V(u) \geq \alpha_1 \|u - \psi\|_{\mathcal{U}}$ *for* $\alpha_1 > 0$ *and* $u \in \mathcal{U}$*. Then,* $\psi(x)$ *is stable. In addition, if* $\partial_t V(u) \leq -\alpha_2 \|u - \psi\|_{\mathcal{U}}$ *for* $\alpha_2 > 0$*, then* ψ *is uniformly asymptotically stable.*

For the proof of the above theorem, refer to [49, p. 84]. The exponential stability of linear semi-groups can also be certified by the solution to the Lyapunov equation presented in [26, Theorem 5.1.3].

In particular, in this dissertation, we consider stability in Sobolev spaces $\mathcal{H}^q_\Omega$.

Definition 2.1.4 (Stability in $\mathcal{H}^q_\Omega$) *Consider the PDE*

$$\partial_t u = F(x, D^\alpha u), \quad x \in \Omega,\ t > 0. \tag{2.2}$$

Let ψ *be an equilibrium of* (2.2)*, satisfying* $F(x, D^\alpha \psi) = 0$*,* $x \in \Omega$*, and* $u(0, x) = u_0(x)$*. Then,* ψ *is*

- *stable in* $\mathcal{H}^q_\Omega$*, if for any* $\varepsilon > 0$*,* $\exists \delta = \delta(\varepsilon) > 0$ *such that*

$$\|u_0 - \psi\|_{\mathcal{H}^q_\Omega} < \delta \Rightarrow \|u(t, \cdot) - \psi\|_{\mathcal{H}^q_\Omega} < \varepsilon,\ t \geq 0,$$

- *asymptotically stable in* $\mathcal{H}^q_\Omega$*, if it is stable and* $\exists \delta > 0$ *such that*

$$\|u_0 - \psi\|_{\mathcal{H}^q_\Omega} < \delta \Rightarrow \lim_{t \to \infty} \|u(t, \cdot) - \psi\|_{\mathcal{H}^q_\Omega} = 0,$$

- *exponentially stable in* $\mathcal{H}^q_\Omega$*, if there exists scalars* $\lambda > 0$ *and* $M > 0$*,*

$$\|u(t, \cdot) - \psi\|^2_{\mathcal{H}^q_\Omega} \leq M \|u_0 - \psi\|^2_{\mathcal{H}^q_\Omega} e^{-\lambda t},\ t \geq 0.$$

In this dissertation, we consider stability to the null solution, *i.e.,* $\psi(x) = 0,\ \forall x \in \Omega$ in Definition 2.1.4.

2.2 Some Useful Inequalities

In the sequel, we use a number of inequalities that are listed below for the reader's convenience.

Lemma 2.2.1 (Hölder's Inequality [47]) *Let $p, q \in [1, \infty]$ satisfying $\frac{1}{p} + \frac{1}{q} = 1$. Then, for all measurable functions f and g, it holds that*

$$\|fg\|_{\mathcal{L}^1} \leq \|f\|_{\mathcal{L}^p} \|g\|_{\mathcal{L}^q}.$$

Lemma 2.2.2 (Young's Inequality [47]) *For any $a, b \in \mathbb{R}_{\geq 0}$ and $p, q > 0$ satisfying $\frac{1}{p} + \frac{1}{q} = 1$, then*

$$ab \leq \frac{a^p}{p} + \frac{b^q}{q}.$$

Lemma 2.2.3 (Poincaré Inequality [85]) *Assume Ω is a bounded, convex, Lipschitz domain with diameter D, and $u \in \mathcal{C}^1(\Omega)$ with Dirichlet $u|_{\partial\Omega} = 0$ or periodic $\int_\Omega u \, d\Omega = 0$ boundary conditions. Then, the following inequality holds*

$$\frac{\pi}{D} \|u\|_{\mathcal{L}^2_\Omega} \leq \|\nabla u\|_{\mathcal{L}^2_\Omega}.$$

2.3 Sum-of-Squares Programming

We employ SOS programming in our computational formulations. That is, we convert different analysis problems into a sum-of-squares program (SOSP), *i.e.,* an optimization problem involving a linear objective function subject to a set of polynomial constraints as

given below

$$\begin{aligned}
&\underset{c\in\mathbb{R}^N}{\text{minimize}} \quad w'c \\
&\text{subject to} \\
&a_{0,j}(x) + \sum_{i=1}^{N} p_i(x)a_{i,j}(x) = 0, \;\; j = 1, 2, \ldots, \bar{J}, \\
&a_{0,j}(x) + \sum_{i=1}^{N} p_i(x)a_{i,j}(x) \in \Sigma[x], \;\; j = \bar{J}+1, \bar{J}+2, \ldots, J,
\end{aligned} \tag{2.3}$$

where $w \in \mathbb{R}^N$ is a vector of weighting coefficients, $c \in \mathbb{R}^N$ is a vector formed of the (unknown) coefficients of $\{p_i\}_{i=1}^{\bar{N}} \in \mathcal{R}[x]$ and $\{p_i\}_{i=\bar{N}+1}^{N} \in \Sigma[x]$, $a_{i,j}(x) \in \mathcal{R}[x]$ are given scalar constant coefficient polynomials, $p_i(x) \in \Sigma[x]$ are SOSP variables.

The gist of the idea behind SOS programming is that if there exists an SOS decomposition for $p(x) \in \mathcal{R}[x]$, *i.e.*, if there exist polynomials $f_1(s), \ldots, f_m(x) \in \mathcal{R}[x]$ such that

$$p(x) = \sum_{i=1}^{m} f_i^2(x),$$

then it follows that $p(x)$ is non-negative. Unfortunately, the converse does not hold in general[2] ; that is, there exist non-negative polynomials which do not have an SOS decomposition. An example of this class of non-negative polynomials is the Motzkin's polynomial [74] given by

$$p(x) = 1 - 3x_1^2x_2^2 + x_1^2x_2^4 + x_1^4x_2^2, \tag{2.4}$$

which is non-negative for all $x \in \mathbb{R}^2$ but is not a SOS. This imposes some degree of conservatism when utilizing SOS based methods. Generally, determining whether a given

[2]Exceptions [100]:

- Univariate polynomials of any even degree,
- Quadratic polynomials in any number of variables,
- Quartic polynomials in two variables.

polynomial is positive is an NP-hard problem [16] (except for degrees less than 4); but, SOS decompositions provide a conservative, yet computationally feasible method for checking non-negativity. The next lemma gives an intriguing formulation to the SOS decomposition problem.

Lemma 2.3.1 ([24]) *A polynomial $p(x)$ of degree $2d$ belongs to $\Sigma[x]$ if and only if there exist a positive semi-definite matrix Q (known as the Gram matrix) and a vector of monomials $Z(x)$ which contains all monomial of x of degree $\leq d$ such that $p(x) = Z^T(x)QZ(x)$.*

In [23] and [84], it was demonstrated that the answer to the query that whether a given polynomial $p(x)$ is SOS or not can be investigated via semi-definite programming methodologies.

Lemma 2.3.2 ([84]) *Given a finite set $\{p_i\}_{i=0}^m \in \mathcal{R}[x]$, the existence of a set of scalars $\{a_i\}_{i=1}^m \in \mathbb{R}$ such that*

$$p_0 + \sum_{i=1}^{m} a_i p_i \in \Sigma[x] \tag{2.5}$$

is a linear matrix inequality (LMI)[3] feasibility problem.

In the sequel, we need to verify whether a matrix with polynomial entries is positive (semi)definite. To this end, we use the next lemma from [96].

Lemma 2.3.3 ([96]) *Denote by $\otimes$ the Kronecker product. Suppose $F(x) \in \mathcal{R}^{n\times n}[x]$ is symmetric and of degree $2d$ for all $x \in \mathbb{R}^n$. In addition, let $Z(x) \in \mathcal{R}^{n\times 1}[x]$ be a column vector of monomials of degree no greater than d and consider the following conditions*

(A) $F(x) \geq 0$ *for all* $x \in \mathbb{R}^n$

(B) $v^T F(x) v \in \Sigma[x, v]$, *for any* $v \in \mathbb{R}^n$.

[3] An LMI is an expression of the form

$$A_0 + x_1 A_1 + x_2 A_2 + \cdots + x_m A_m \geq 0,$$

where $x \in \mathbb{R}^m$ and $A_i \in \mathbb{S}^n,\ i = 1, 2, \ldots, m$. The above LMI specifies a convex constraint on x.

(C) There exists a positive semi-definite matrix Q such that

$$v^T F(x) v = (v \otimes Z(x))^T Q (v \otimes Z(x)),$$

for any $v \in \mathbb{R}^n$.

Then $(A) \Leftarrow (B)$ and $(B) \Leftrightarrow (C)$.

Furthermore, we are often interested in checking positivity of a matrix with polynomial entries $F(x) \in \mathcal{R}^{n \times n}[x]$ inside a set $\Omega \subset \mathbb{R}^n$. It turns out that if the set is semi-algebraic[4], Putinar's Positivstellensatz [65, Theorem 2.14] can be used.

Corollary 2.3.4 *For $F(x) \in \mathcal{R}^{n \times n}[x]$, $\omega \in \mathcal{R}[x]$ and $\Omega = \{x \in \mathbb{R}^n \mid \omega(x) \geq 0\}$, if there exists $N(x) \in \Sigma^{n \times n}[x]$ such that*

$$F(x) - N(x)\omega(x) \in \Sigma^{n \times n}[x], \tag{2.6}$$

then $F(x) \geq 0,\ \forall x \in \Omega$.

If the coefficients of $F(x)$ depend affinely in unknown parameters and the degree of $N(x)$ is fixed, checking whether (2.6) holds can be cast as a feasibility test of a convex set of constraints, an SDP, whose dimension depends on the degree of the polynomial entries of $F(x)$ and $N(x)$.

Algorithms for solving SOS programs are automated in MATLAB toolboxes such as SOSTOOLS [79] and YALMIP [68], in which the SOS problem is parsed into an SDP formulation and the SDPs are solved by LMI solvers such as SeDuMi [117]. In this dissertation, we use the SOSTOOLS toolbox for the numerical experiments.

[4] A semi-algebraic set $\mathcal{S} \subset \mathbb{R}^n$ for some closed field, say $\mathbb{R}$, is defined by a set of polynomial equalities and inequalities as follows

$$\mathcal{S} = \{x \in \mathbb{R}^n \mid p_i(x) \geq 0,\ i = 1, 2, \ldots, n_p,\ q_i(x) = 0,\ i = 1, 2, \ldots, n_q\},$$

where $\{p_i\}_{i=1}^{n_p}, \{q_i\}_{i=1}^{n_q} \in \mathcal{R}[x]$.

Chapter 3

Stability Analysis of PDEs: A Convex Method to Solve Integral Inequalities

We begin our research in the analysis of PDEs with studying stability. In particular, we are interested in studying stability using Lyapunov methods for PDEs [75, 28].

As highlighted in the Introduction and Example 1.1.1, Lyapunov analysis of PDEs leads to a set of integral inequalities. This chapter is concerned with formulating a method to verify the non-negativity of integral inequalities using convex optimization. We begin this chapter by discussing integral inequalities that are defined over the 1-dimensional domain. We study integral inequalities with integrands that are polynomial in the dependent variables. This allows for a quadratic representation of the integrands. The integral inequalities are subject to constraints on the dependent variables over the boundary of the domain of integration. Based on these boundary constraints, we show how the Fundamental Theorem of Calculus can be used to introduce terms that characterize the non-uniqueness of the integral kernels. This reformulates the problem of checking the positivity of the integral into checking the positivity of a matrix inequality over some domain. In the case of polynomial dependence in the independent variables, checking the matrix inequalities becomes an SOS program.

The proposed method for solving integral inequalities is then applied to the Lyapunov stability analysis problem of PDEs. We choose a Lyapunov functional structure in the form of weighted Sobolev norms. We show that if the Lyapunov functional satisfies two integral inequalities for a given PDE system, we can conclude the exponential stability of the solutions.

Finally, the proposed results are illustrated through several examples.

A preliminary version of the contributions described in this chapter was presented in the 2014 53rd IEEE Conference on Decision and Control [126]. The extended version of the results was published in [128].

3.1 Integral Inequalities with Polynomial Integrands in 1D

In this section, we study inequalities given by polynomials on the dependent variables evaluated at the boundaries of the domain of integration and integral terms with polynomial integrands on the dependent variables.

Consider the integral inequality

$$f_b\left(D^{\alpha-1}u(t,1),D^{\alpha-1}u(t,0)\right)+\int_0^1 f_i\left(x,D^{\alpha}u\right)\,dx\geq 0,\qquad \forall t\geq 0,$$

with $[0,1]=(0,1)$ (note that any bounded domain on $\mathbb{R}$ can be mapped into $[0,1]=(0,1)$ with an appropriate change of variables), $u:\mathbb{R}_{\geq 0}\times[0,1]\to\mathbb{R}^n$, $f_b\in\mathcal{R}[D^{\alpha-1}u(t,1),D^{\alpha-1}u(t,0)]$, $f_i(\cdot,D^{\alpha}u)\in\mathcal{R}[D^{\alpha}u]$ (f_i is a polynomial on its second argument). In order to simplify the exposition, let us define

$$D_b^{\alpha-1}u:=\left[\begin{array}{cc}\left(D^{\alpha-1}u(t,1)\right)' & \left(D^{\alpha-1}u(t,0)\right)'\end{array}\right]'.$$

For $\max(deg(f_b),deg(f_i))=k$, we can express the polynomials f_b and f_i in the quadratic-

like forms

$$f_b(D_b^{\alpha-1}u) = \left(\eta^{\lceil \frac{k}{2} \rceil}(D_b^{\alpha-1}u)\right)' F_b\, \eta^{\lceil \frac{k}{2} \rceil}(D_b^{\alpha-1}u) \tag{3.1}$$

$$f_i(x, D^{\alpha}u) = \left(\eta^{\lceil \frac{k}{2} \rceil}(D^{\alpha}u)\right)' F_i(x)\, \eta^{\lceil \frac{k}{2} \rceil}(D^{\alpha}u) \tag{3.2}$$

where the symmetric matrix $F_b \in \mathbb{S}^{\sigma(2n\alpha, \lceil \frac{k}{2} \rceil)}$ and the symmetric matrix function $F_i : [0,1] \to \mathbb{S}^{\sigma(n\alpha, \lceil \frac{k}{2} \rceil)}$. The dependent variable u is assumed to belong to sets of the form

$$\mathcal{U}_b := \left\{ u \in \mathcal{C}^{\alpha}([0,1]) \mid BD_b^{\alpha-1}u = 0 \right\}, \tag{3.3}$$

with $B \in \mathbb{R}^{n_b \times 2n\alpha}$, where n_b is the number of constraints on the boundary.

We study the following problem:

Problem 3.1.1 *Check whether the following integral inequality holds*

$$f_b(D_b^{\alpha-1}u) + \int_0^1 f_i(x, D^{\alpha}u)\, dx \geq 0, \quad \forall t \geq 0,\ \forall u \in \mathcal{U}_b. \tag{3.4}$$

For a given polynomial f_b, F_b in the representation (3.1) may be non-unique and is taken as an element of the set

$$\begin{aligned} \mathcal{F}_b(k,\alpha) = \Big\{ & F_b + G_b \in \mathbb{S}^{\sigma(n\alpha, \lceil \frac{k}{2} \rceil)} \\ & \mid f_i = (\eta^{\lceil \frac{k}{2} \rceil}(D_b^{\alpha-1}u))' F_b \eta^{\lceil \frac{k}{2} \rceil}(D_b^{\alpha-1}u),\ 0 = (\eta^{\lceil \frac{k}{2} \rceil}(D_b^{\alpha-1}u))' G_b \eta^{\lceil \frac{k}{2} \rceil}(D_b^{\alpha-1}u) \Big\}. \end{aligned} \tag{3.5}$$

Similarly, for a given function f_i, the set of quadratic-like representation (3.2) is taken as an element of the set

$$\begin{aligned} \mathcal{F}_i(k,\alpha) = \Big\{ & F_i + G_i : [0,1] \to \mathbb{S}^{\sigma(n\alpha, \lceil \frac{k}{2} \rceil)} \\ & \mid f_i = (\eta^{\lceil \frac{k}{2} \rceil}(D^{\alpha}u))' F_i(x) \eta^{\lceil \frac{k}{2} \rceil}(D^{\alpha}u),\ 0 = (\eta^{\lceil \frac{k}{2} \rceil}(D^{\alpha}u)' G_i(x) \eta^{\lceil \frac{k}{2} \rceil}(D^{\alpha}u) \Big\}. \end{aligned} \tag{3.6}$$

Example 3.1.2 *Consider* $f_i(x,(u,\partial_x u)) = x^2\partial_x u + 2u(\partial_x u)^2$, $u \in \{u \mid u(t,0) = u(t,1)\}$, *yielding* $k = 3$, $\alpha = 1$, *and* $D^1u = (u, \partial_x u)$, $\eta^{\lceil \frac{3}{2} \rceil}(D^1u) = (1, u, \partial_x u, u^2, u\partial_x u, (\partial_x u)^2)$. *The quadratic representation* (3.2) *and the set* (3.3) *are obtained with* $D_b^0 u = \left[\begin{smallmatrix} u(t,1) & u(t,0) \end{smallmatrix}\right]'$,

$$F_i(x) = \begin{bmatrix} 0 & 0 & \frac{x^2}{2} & 0 & 0 & 0 \\ 0 & 0 & 0 & 0 & 0 & 1 \\ \frac{x^2}{2} & 0 & 0 & 0 & 0 & 0 \\ 0 & 0 & 0 & 0 & 0 & 0 \\ 0 & 0 & 0 & 0 & 0 & 0 \\ 0 & 1 & 0 & 0 & 0 & 0 \end{bmatrix}, B = \begin{bmatrix} 1 & -1 \end{bmatrix}.$$

The set $\mathcal{F}_i(3,1)$ *is defined by matrices* $G_i(x)$ *as*

$$G_i(x) = \begin{bmatrix} 0 & 0 & 0 & g_1(x) & g_2(x) & g_3(x) \\ 0 & -2g_1(x) & -g_2(x) & 0 & 0 & 0 \\ 0 & -g_2(x) & -2g_3(x) & 0 & 0 & 0 \\ g_1(x) & 0 & 0 & 0 & 0 & g_4(x) \\ g_2(x) & 0 & 0 & 0 & -2g_4(x) & 0 \\ g_3(x) & 0 & 0 & g_4(x) & 0 & 0 \end{bmatrix}.$$

A complete quadratic representation of the integral expression (3.4), must also account for the differential relation among the entries of $D^{\alpha}u$. To this end, we define matrix $H_i(x) \in \mathcal{C}^1\left([0,1]; \mathbb{S}^{\sigma(2n\alpha, \lceil \frac{k}{2} \rceil)}\right)$ and the matrix of its boundary values $H_b \in \mathbb{S}^{\sigma(2n\alpha, \lceil \frac{k}{2} \rceil)}$, which contains the terms induced by integration-by-parts. That is, $H_i(x)$ and H_b satisfy

$$\begin{aligned}\int_0^1 \left(\frac{d}{dx} \left((\eta^{\lceil \frac{k}{2} \rceil}(D^{\alpha-1}u)))' H_i(x) \eta^{\lceil \frac{k}{2} \rceil}(D^{\alpha-1}u) \right) \right) \, dx \\ = \left[\left(\eta^{\lceil \frac{k}{2} \rceil}(D^{\alpha-1}u) \right)' (H_i(x)) \eta^{\lceil \frac{k}{2} \rceil}(D^{\alpha-1}u) \right]_{x=0}^{1} \\ = (\eta^{\lceil \frac{k}{2} \rceil}(D_b^{\alpha-1}u))' H_b \eta^{\lceil \frac{k}{2} \rceil}(D_b^{\alpha-1}u) \quad (3.7)\end{aligned}$$

The complete quadratic representation is then characterized by the set $\mathcal{I}$ as follows

$$\begin{aligned}\mathcal{I} := \Bigg\{ F_b \in \mathcal{F}_b(k,\alpha), F_i \in \mathcal{F}_i(k,\alpha) \mid (\eta^{\lceil \frac{k}{2} \rceil}(D_b^{\alpha-1}u))'(F_b + H_b)\eta^{\lceil \frac{k}{2} \rceil}(D_b^{\alpha-1}u) \\ + \int_0^1 \left[(\eta^{\lceil \frac{k}{2} \rceil}(D^{\alpha}u)' F_i(x) \eta^{\lceil \frac{k}{2} \rceil}(D^{\alpha}u) + \frac{d}{dx} \left((\eta^{\lceil \frac{k}{2} \rceil}(D^{\alpha-1}u)))' H_i(x) \eta^{\lceil \frac{k}{2} \rceil}(D^{\alpha-1}u) \right) \right] \, dx \Bigg\} \quad (3.8)\end{aligned}$$

The example below illustrates matrices H_b and $H_i(x)$ for an element of set (3.8).

Example 3.1.3 *Consider* (3.4) *with* $f_b = 2u(t,1)\partial_x u(t,0)$, $f_i(x,(u,\partial_x u)) = \sin^2(x)u\partial_x u + 2u\partial_x^2 u$, *yielding* $k = 2$, $\alpha = 2$, *and* $D^2 u = (u, \partial_x u, \partial_x^2 u)$. *Since the expression is homogeneous of degree* $k = 2$, *we replace the inhomogeneous vector* $\eta^{\lceil \frac{2}{2} \rceil}(D^2 u)$ *by a homogeneous vector* $(D^2 u)^{\{\frac{2}{2}\}}$ *to obtain the quadratic expressions with* $(D_b^1 u)^{\{1\}} = (u(t,1), \partial_x u(t,1), u(t,0), \partial_x u(t,0))$, $(D^2 u)^{\{1\}} = (u, \partial_x u, \partial_x^2 u)$. *The representation* (3.2) *is defined by*

$$F_b = \begin{bmatrix} 0 & 0 & 0 & 1 \\ 0 & 0 & 0 & 0 \\ 0 & 0 & 0 & 0 \\ 1 & 0 & 0 & 0 \end{bmatrix}, \; F_i(x) = \begin{bmatrix} 0 & -\frac{\sin^2(x)}{2} & 1 \\ -\frac{\sin^2(x)}{2} & 0 & 0 \\ 1 & 0 & 0 \end{bmatrix},$$

and the terms characterizing the multiplicity of the integral as described by

$$\frac{d}{dx}\left((D^{\alpha-1}u)'H_i(x)(D^{\alpha-1}u)\right)$$
$$= (D^{\alpha}u)'\begin{bmatrix} \frac{d}{dx}h_{11}(x) & \frac{d}{dx}h_{12}(x)+h_{11}(x) & \frac{1}{2}h_{12}(x) \\ \frac{d}{dx}h_{12}(x)+h_{11}(x) & \frac{d}{dx}h_{22}(x)+h_{12}(x) & h_{22}(x) \\ \frac{1}{2}h_{12}(x) & h_{22}(x) & 0 \end{bmatrix}(D^{\alpha}u) \quad (3.9)$$

and (3.8) *as given by*

$$(D_b^1u)'H_b(D_b^1u) = (D_b^1u)'\begin{bmatrix} -H_i(1) & 0 \\ 0 & H_i(0) \end{bmatrix}(D_b^1u).$$

Note that the non-uniqueness associated with the algebraic relations in the vector describing the quadratic representation is characterized by the sets $\mathcal{F}_b$ and $\mathcal{F}_i$. The Fundamental Theorem of Calculus shows the non-uniqueness of the integral expression associated with the differential relations of the elements in $D^{\alpha}u$, characterizing the set (3.8).

In order to simplify the presentation of the next result, let us introduce the function $\bar{H}_i(x)$, which satisfies

$$\frac{d}{dx}\left((\eta^{\lceil\frac{k}{2}\rceil}(D^{\alpha-1}u))'H_i(x)\eta^{\lceil\frac{k}{2}\rceil}(D^{\alpha-1}u)\right) = (\eta^{\lceil\frac{k}{2}\rceil}(D^{\alpha}u))'\bar{H}_i(x)\eta^{\lceil\frac{k}{2}\rceil}(D^{\alpha}u) \quad (3.10)$$

and allows us to denote the quadratic form in the integrand of (3.8) in terms of matrix $F_i(x)+\bar{H}_i(x)$. The quadratic-like characterization of the integrand in terms of the algebraic and the differential relations leads to conditions for integral inequalities in terms of matrix inequalities as follows:

Theorem 3.1.4 *If there exist $F_b \in \mathcal{F}_b$, $F_i(x) \in \mathcal{F}_i$, satisfying* (3.1)-(3.2)*, and $H_i(x) \in \mathcal{C}^1([0,1])$, yielding H_b as in* (3.8) *and $\bar{H}_i(x)$ as in* (3.10) *such that*

$$(\eta^{\bar{k}}(D_b^{\alpha-1}u))'\,(F_b+H_b)\,\eta^{\bar{k}}(D_b^{\alpha-1}u) \geq 0 \quad \forall u \in \mathcal{U}_b, \quad (3.11)$$

$$F_i(x) + \bar{H}_i(x) \geq 0 \quad \forall x \in [0,1], \tag{3.12}$$

where $\bar{k} = \lceil \frac{k}{2} \rceil$*, then inequality* (3.4) *holds in the subspace defined by* $\mathcal{U}_b$*.*

Proof: For given polynomials f_b and f_i satisfying $k = \max(deg(f_b), deg(f_i))$ we can express an integral expression as in (3.4). Let

$$\phi(u) = f_b(D_b^{\alpha-1}u) + \int_0^1 f_i(x, D^\alpha u)\, dx.$$

Using the quadratic forms as defined in (3.1)–(3.2) with $F_b \in \mathcal{F}_b(k,\alpha)$, $F_i(x) \in \mathcal{F}_i(k,\alpha)$, we have

$$\begin{aligned} \phi(u) &= f_b(D_b^{\alpha-1}u) + \int_0^1 f_i(x, D^\alpha u)\, dx \\ &= (\eta^{\bar{k}}(D_b^{\alpha-1}u))' F_b \eta^{\bar{k}}(D_b^{\alpha-1}u) + \int_0^1 (\eta^{\bar{k}}(D^\alpha u))' F_i(x) \eta^{\bar{k}}(D^\alpha u)\, dx. \end{aligned}$$

Following the definition of set $\mathcal{I}$ in (3.8) and the definition of $\bar{H}_i$ in (3.10), we obtain

$$\begin{aligned} \phi(u) = (\eta^{\bar{k}}(D_b^{\alpha-1}u))'(F_b + H_b)\eta^{\bar{k}}(D_b^{\alpha-1}u) \\ + \int_0^1 (\eta^{\bar{k}}(D^\alpha u))' \left(F_i(x) + \bar{H}_i(x)\right) \eta^{\bar{k}}(D^\alpha u)\, dx. \end{aligned} \tag{3.13}$$

Hence, if the boundary term satisfies (3.11), and the integral term satisfies (3.12) then $\phi(u) \geq 0,\ \forall u \in \mathcal{U}_b$. □

Note that inequality (3.12) is a differential matrix inequality since the elements $\bar{H}_i(x)$ involve continuously differentiable functions and their derivatives.

3.2 Verifying Integral Inequalities with Integral Constraints

In some PDE analysis applications (an example is the computational formulation in Chapter 5), we require verifying an integral inequality subject to a number of integral constraints. That is, the following class of problems

$$\int_0^1 f_i(\theta, D^\alpha u)\, d\theta \geq 0,$$

subject to

$$\int_0^1 s_i(\theta, D^\alpha u)\, d\theta \geq 0,\ i = 1, 2, \ldots, r. \tag{3.14}$$

where f_i is described as (3.2) and

$$s_i(x, D^\alpha u) = \left(\eta^{\lceil \frac{k}{2} \rceil}(D^\alpha u)\right)' S_i(x)\, \eta^{\lceil \frac{k}{2} \rceil}(D^\alpha u)$$

with $S_i : [0, 1] \to \mathbb{S}^{\sigma(n\alpha, \lceil \frac{k}{2} \rceil)}$.

The approach we develop here is reminiscent of the S-procedure [90] for LMIs. The S-procedure provides conditions under which a particular quadratic inequality holds subject to some other quadratic inequalities (for example, within the intersection of several ellipsoids). Similar conditions for checking polynomial inequalities within a semi-algebraic set were developed in [81, 84] thanks to Putinar's Positivstellensatz [65, Theorem 2.14]. However, current machinery for including integral constraints includes multiplying the integral constraint and subtracting it from the inequality (see Proposition 9 in [81]). In the following, we propose an alternative to the latter method that can be used to verify the feasibility problem (3.14).

Consider the following set of integral constraints

$$\mathcal{S} = \left\{ u \in \mathcal{C}^\alpha_{[0,1]} \mid \int_0^1 s_i(\theta, D^\alpha u)\, d\theta \geq 0,\ i = 1, 2, \ldots, r \right\}. \tag{3.15}$$

Note that in this setting, we can also represent sets as $\left\{u \mid \int_0^1 g(\theta, D^\alpha u)\, d\theta = 0\right\}$ by selecting $s_1 = g$ and $s_2 = -g$.

Define

$$v_i(t,x) := \int_0^x s_i(\theta, D^\alpha u)\, d\theta, \tag{3.16}$$

which satisfies

$$\begin{cases} v_i(t,0) = 0, \\ \partial_x v_i(t,x) - s_i(x, D^\alpha u(t,x)) = 0, \end{cases} \tag{3.17}$$

for $i = 1, 2, \ldots, r$. Using (3.16), we can represent $\mathcal{S}$ as

$$\mathcal{S} = \left\{u \in \mathcal{C}^\alpha_{[0,1]} \mid v_i(t,1) \geq 0,\ i = 1, 2, \ldots, r\right\}.$$

Lemma 3.2.1 *Consider problem* (3.14) *and let* $t \in \mathcal{T} \subseteq \mathbb{R}_{\geq 0}$. *Let* $v(t,x) = \left[\begin{smallmatrix} v_1(t,x) & \cdots & v_r(t,x) \end{smallmatrix}\right]'$ *and* $s(x, D^\alpha u) = \left[\begin{smallmatrix} s_1(x,D^\alpha u) & \cdots & s_r(x,D^\alpha u) \end{smallmatrix}\right]'$. *If there exists a function* $m : \mathcal{T} \times [0,1] \to \mathbb{R}^r$ *and a vector* $n \in \mathbb{R}^r_{\geq 0}$ *such that*

$$\int_0^1 f_i(x, D^\alpha u)\, dx - n' v(t,1) + \int_0^1 m'(t,x)\Big(\partial_x v(t,x) - s\left(x, D^\alpha u(t,x)\right)\Big)\, dx > 0, \tag{3.18}$$

for all $u \in \mathcal{U}$ *and all* $t \in \mathcal{T}$, *then* (3.14) *is satisfied.*

Proof: From (3.17), we have that for any $m : \mathbb{R}_{\geq 0} \times [0,1] \to \mathbb{R}^r$

$$m'(t,x)\left(\partial_x v(t,x) - s(x, D^\alpha u(t,x))\right) = 0, \quad \forall x \in [0,1].$$

Hence, since v and u are related according to (3.17), we obtain

$$\int_0^1 m'(t,x)\left(\partial_x v(t,x) - s(x, D^\alpha u(t,x))\right)\, dx = 0.$$

Consequently, if inequality (3.18) is satisfied, we infer

$$\int_0^1 f_i(x, D^\alpha u)\, dx > n'v(t,1), \quad \forall t \in \mathcal{T}.$$

Finally, since $n'v(t,1) \geq 0$, for all $u \in \mathcal{S}$, we conclude that problem (3.14) is verified. $\square$

Note that inequality (3.18) is a particular case of (3.4). In order to incorporate the integral constraints, we introduced the (dummy) dependent variables $v_i(t,x)$, satisfying (3.17), and their partial derivative with respect to x.

3.2.1 Semidefinite Programming Formulation

Whenever a matrix $F_i(x)$ is a polynomial of the variable x and we impose polynomial dependence of $\bar{H}_i(x)$ on the variable x, inequality (3.12) can be addressed by a straightforward application of Putinar's Positivstellensatz [65, Theorem 2.14] or Corollary 2.3.4. Note that the set $[0,1] = [0,1]$, can be described as the semi-algebraic set $\{x|[0,1](x) := x(1-x) \geq 0\}$.

Corollary 3.2.2 *For $F_i(x) + \bar{H}_i(x) \in \mathcal{R}^{n_M \times n_M}[x]$, if there exists $N(x) \in \Sigma^{n_M \times n_M}[x]$ such that*

$$F_i(x) + \bar{H}_i(x) - N(x)[0,1](x) \in \Sigma^{n_M \times n_M}[x] \tag{3.19}$$

then (3.12) *holds.*

If the coefficients of $F_i(x)$ and $\bar{H}_i(x)$ depend affinely in unknown parameters and the degree of $N(x)$ is fixed, checking whether (3.19) holds can be cast as a feasibility test of a convex set of constraints, an SDP, whose dimension depends on the degree of $F_i(x) + \bar{H}_i(x)$ and $N(x)$ and on the dimension of matrix $F_i(x) + \bar{H}_i(x)$ which depends on the degree k and the order α as in (3.1)-(3.2).

Remark 3.2.3 *Although Positivstellensatz gives necessary and sufficient conditions for checking inequality* (3.12)*, in order to make these conditions computationally tractable the de-*

gree of the sum-of-squares polynomial $N(x)$ *in* (3.19) *must be fixed, hence yielding only sufficient conditions for a given value of* $deg(N(x))$. □

The formulation of inequalities (3.11) and (3.12) is possible thanks to the application of the Fundamental Theorem of Calculus to characterize the set of quadratic-like representations of an integral inequality, as described by the set (3.8). The terms introduced in the integrand by matrix H_i do not affect the value of the integral and allow for a test for positivity based on the positivity of the matrices in the quadratic-like representation. This is similar to the quadratic representation that is used in sum-of-squares when checking positivity of a polynomial. Also, for polynomial expressions, the algebraic relations in the quadratic representation of integrand polynomials are here defined in terms of functions, (see (3.6)) instead of scalars. With the solution to (3.11), we can verify inequalities in subspaces as in (3.3), incorporating boundary values of the dependent variables.

3.3 Integral Inequalities for Stability Analysis of PDEs

In what follows, we present the class of PDE systems and Lyapunov functionals studied in this chapter. Consider the following PDE system

$$\partial_t u(t,x) = F\left(x, D^\alpha u(t,x)\right), \quad t > t_0,\ x \in [0,1], \tag{3.20}$$

$u(t_0,x) = u_0(x) \in \mathcal{M} \subset \mathcal{H}^q([0,1];\mathbb{R}^n)$, where $q \in \mathbb{N}_{\geq 0}$. Let $F(x, D^\alpha u) = \mathscr{A}u$, where $\mathscr{A}$ is an operator defined on $\mathcal{M}$, a closed subset of $\mathcal{H}^q_{[0,1]}$.

Theorem 3.3.1 *Consider system* (3.20). *Suppose there exist a function* $V \in \mathcal{C}^1[t]$ *, with* $V(0) = 0$*, and scalars* c_1*,* c_2*,* $c_3 \in \mathbb{R}_{>0}$ *such that*

$$c_1\|u\|^2_{\mathcal{H}^q_{[0,1]}} \leq V(u) \leq c_2\|u\|^2_{\mathcal{H}^q_{[0,1]}}, \tag{3.21}$$

and

$$\partial_t V(u) \leq -c_3 \|u\|^2_{\mathcal{H}^q_{[0,1]}}, \tag{3.22}$$

along the solutions of (3.20)*, then the* $\mathcal{H}^q_{[0,1]}$*-norm of the trajectories of* (3.20) *satisfy*

$$\|u(t,x)\|^2_{\mathcal{H}^q_{[0,1]}} \leq \frac{c_2}{c_1} \|u_0(x)\|^2_{\mathcal{H}^q_{[0,1]}} e^{-\frac{c_3}{c_2}(t-t_0)}, \quad t > t_0 \tag{3.23}$$

where $u_0 = u(t_0, x)$.

Proof: From (3.21)-(3.22), one has $\frac{\frac{dV(u)}{dt}}{V(u)} \leq -\frac{c_3}{c_2}$. Since $\frac{\frac{dV(u)}{dt}}{V(u)} = \frac{d(\ln(V(u)))}{dt}$, the integral in time of the above expression over $[t_0, t]$ yields

$$\begin{aligned}
\int_{[t_0,t]} \frac{d\left(\ln(V(u(\tau,x)))\right)}{d\tau}\, d\tau &\leq -\frac{c_3}{c_2}(t-t_0) \\
\ln(V(u(t,x))) - \ln(V(u(t_0,x))) &\leq -\frac{c_3}{c_2}(t-t_0) \\
\frac{V(u(t,x))}{V(u(t_0,x))} &\leq e^{-\frac{c_3}{c_2}(t-t_0)} \\
V(u(t,x)) &\leq V(u(t_0,x)) e^{-\frac{c_3}{c_2}(t-t_0)}.
\end{aligned}$$

Finally (3.23) is obtained by applying the bounds of (3.21) on the above inequality. □

Remark 3.3.2 *The above stability result is analogous to the stability theorems for nonlinear ODEs [61]. However, in the context of PDEs, one has to consider the norm in which the stability properties are defined. Next, we describe a class of Lyapunov functionals that one has to consider to prove stability in some* $\mathcal{H}^q_{[0,1]}$*-norm.*

We consider candidate Lyapunov functionals of the form

$$V(u) = \frac{1}{2} \int_0^1 (D^q u)' P(x) (D^q u)\ dx, \tag{3.24}$$

with $P(x) > 0,\ \forall x \in [0,1]$ to study stability in $\mathcal{H}^q_{[0,1]}$. That is, $V(u)$ is the squared $P(x)$-

weighted $\mathcal{H}^q_{[0,1]}$-norm. Since

$$\lambda_m(P)\|u\|^2_{\mathcal{H}^q_{[0,1]}} \leq V(u) \leq \lambda_M(P)\|u\|^2_{\mathcal{H}^q_{[0,1]}},$$

$V(u)$ is equivalent to the $\mathcal{H}^q_{[0,1]}$-norm.

Remark 3.3.3 *For $q_1 < q_2$, the space $\mathcal{H}^{q_1}_{[0,1]}$ is embedded in $\mathcal{H}^{q_2}_{[0,1]}$ [33, Sec 5.6]. Therefore, stability in $\mathcal{H}^{q_2}_{[0,1]}$-norm implies stability in $\mathcal{H}^{q_1}_{[0,1]}$-norm, but the converse does not hold.*

It turns out that, if we choose Lyapunov functional (3.24), the conditions of Theorem 3.3.1 become integral inequalities.

Proposition 3.3.4 *If there exists a function $P(x)$ and positive scalars ϵ_1, ϵ_2 such that*

$$\int_0^1 \left[(D^q u)' P(x)(D^q u) - \epsilon_1 (D^q u)'(D^q u)\right]\, dx \geq 0 \tag{3.25a}$$

$$-\int_0^1 \left[2(D^q u)' P(x) F(x, D^\alpha u) + \epsilon_2 (D^q u)'(D^q u)\right]\, dx \geq 0 \tag{3.25b}$$

then the $\mathcal{H}^q_{[0,1]}$-norm of solutions to (3.20) *satisfy* (3.23) *with $c_1 = \lambda_m(P(x))$, $c_2 = \lambda_M(P(x))$, and $c_3 = \epsilon_2$, i.e., the solutions to* (3.20) *converge to the null solution in the $\mathcal{H}^q_{[0,1]}$-norm exponentially.*

Inequalities (3.25a)-(3.25b) are integral inequalities such as the ones studied in Section 3.1. The sets $\mathcal{U}_b$ as in (3.3) associated to the inequalities are defined by the domain of the PDE operators. The results of Sections 3.1 can therefore be applied to (3.25a)-(3.25b) whenever the integrand is a polynomial on the dependent variables.

3.4 Examples

In this section, we illustrate the results of this chapter with three examples. We begin with the problem of minimizing the constant in the Poincaré inequality. We then apply

the tools developed to solve the Lyapunov inequalities (3.25a) and (3.25b) for two PDE systems, namely, the transport equation and a system of coupled nonlinear PDEs with spatially varying coefficients.

3.4.1 Poincaré inequality

Consider

$$\int_0^1 \left(C(\partial_x u)^2 - u^2\right) \ dx \geq 0, \tag{3.26}$$

with $u(t,0) = u(t,1) = 0$, which is an integral inequality of the form (3.4). Notice that the integrand is affine on C. Such an inequality holds for all $u \in \mathcal{H}^1_{[0,1]}$ and establishes bounds for $\|u\|^2_{\mathcal{L}^2_{[0,1]}}$ in terms of $\|(\partial_x u)\|^2_{\mathcal{L}^2_{[0,1]}}$. Let $\mathcal{U} = \left\{u \in \mathcal{H}^1_{[0,1]} \mid u(t,0) = u(t,1) = 0\right\}$. We are interested in obtaining a tight bound for (3.26), *i.e.,* to solve

$$\begin{gathered}\text{minimize } C \\ \text{subject to} \\ \textstyle\int_0^1 \left(C(\partial_x u)^2 - u^2\right) \ dx \geq 0, \quad \forall u \in \mathcal{U},\end{gathered} \tag{3.27}$$

with $[0,1] = [0,1]$ and $u(t,0) = u(t,1) = 0$. The results of Section 3.1 can now be applied since the integrand involves only u and its spatial derivative $\partial_x u$. Following Proposition 3.1.4, problem (3.27) can be relaxed (upper-bounded) as

$$\begin{gathered}\underset{h}{\text{minimize}}\ C \\ \text{subject to} \\ \begin{bmatrix} -1 + \partial_x h(x) & h(x) \\ h(x) & C \end{bmatrix} \geq 0, \quad \forall x \in [0,1].\end{gathered} \tag{3.28}$$

By imposing a polynomial structure to $h(x)$ and applying the Positivstellensatz as described in Section 3.2.1, (3.28) holds if the following SOSP is satisfied

$$\begin{aligned} &\underset{h,N}{\text{minimize}} \;\; C \\ &\text{subject to} \\ &\begin{bmatrix} -1+\partial_x h(x) & h(x) \\ h(x) & C \end{bmatrix} + N(x)x(x-1) \in \Sigma^{2\times 2}[x], \\ &N(x) \in \Sigma^{2\times 2}[x]. \end{aligned} \tag{3.29}$$

We solve Problem (3.29) by fixing different degrees of polynomial $h(x)$ (with $deg(N(x)) = deg(h(x))+2$). Figure 3.1 depicts the optimal value C^* as a function of the degree of $h(x)$. The figure also presents the optimal bound π^{-2} for the problem [85].

As it can be observed by increasing the degree of the polynomials up to 35, there is still a gap between the bound obtained from the proposed method and the optimal constant in the Poincaré inequality. This discrepancy results from the fact that, by Weierstrass' theorem, only *continuous* functions defined on a closed interval $[a, b] \subset \mathbb{R}$ can be uniformly

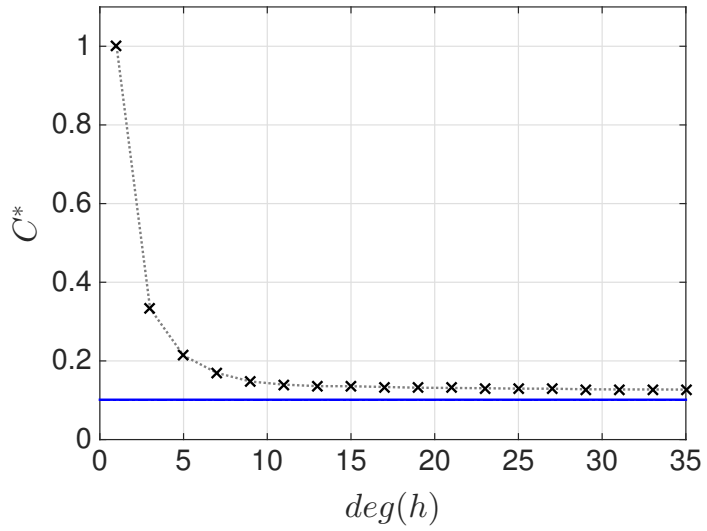

Figure 3.1: Optimal values for Problem (3.29) as a function of the degree of $h(x)$.

approximated as closely as desired by *polynomial* functions.

To illustrate, in the following, we derive the function $h(x)$ that corresponds to the optimal value $C^* = \frac{1}{\pi^2}$ and show that this is not a continuous function on $[0, 1]$. If we set $C = \frac{1}{\pi^2}$ in (3.28), we have

$$M(x) = \begin{bmatrix} -1 + \partial_x h(x) & h(x) \\ h(x) & \frac{1}{\pi^2} \end{bmatrix} \geq 0, \ x \in [0, 1]. \tag{3.30}$$

For the optimal C^*, the function $h(x)$ should be such that the rank of $M(x)$ in (3.30) drop by one and the inequality lose strictness. That is, $M(x)$ can be represented as

$$M(x) = \begin{bmatrix} M_1(x) \\ M_2(x) \end{bmatrix} \begin{bmatrix} M_1(x) & M_2(x) \end{bmatrix} = \begin{bmatrix} M_1^2(x) & M_1(x)M_2(x) \\ M_1(x)M_2(x) & M_2^2(x) \end{bmatrix}.$$

Then, $M_2 = \frac{1}{\pi}$, $M_1 = \pi h(x)$, and $M_1^2 = -1 + \partial_x h(x)$. Solving the nonlinear differential equation $\partial_x h(x) - \pi^2 h^2(x) - 1 = 0$ gives $h(x) = \frac{1}{\pi} \tan(\pi x + c)$, where c is an integration constant. Since $h(x)$ is not a continuous function over the $[0, 1]$ domain, a polynomial approximation of $h(x) = \frac{1}{\pi} \tan(\pi x + c)$ may not have satisfactory convergence properties. This justifies the gap in Figure 3.1. However, using polynomial bases in $h(x)$ provides a means based on SDPs to upper bound the optimal value C^*. □

3.4.2 Transport Equation

Consider the equation

$$\partial_t u = -\partial_x u \quad x \in [0, 1], \ t > 0 \quad u(t, 0) = 0, \tag{3.31}$$

which gives $\mathcal{U}_b = \left\{ u \in \mathcal{C}^2([0,1]) \mid \left[\begin{smallmatrix} 0 & 1 \end{smallmatrix}\right] \left[\begin{smallmatrix} u(t,1) \\ u(t,0) \end{smallmatrix}\right] = 0 \right\}$. Given $\lambda > 0$, let

$$V(u) = \frac{1}{2} \int_0^1 p(x) u^2(x) \ \ dx,$$

be the candidate function to certify

$$-\lambda V(u) - \dot{V}(u) = \int_0^1 \left(-\frac{1}{2} \lambda p(x) u^2(x) + p(x) u \partial_x u(x) \right) \ \ dx \geq 0$$

(proving the exponential stability with convergence rate λ). We apply Theorem 3.1.4 to the Lyapunov inequalities in Proposition 3.3.4 to obtain

$$p(x) > 0, \quad \forall x \in [0,1], \tag{3.32a}$$

$$\begin{bmatrix} u(t,1) \\ u(t,0) \end{bmatrix}' \begin{bmatrix} -h(1) & 0 \\ 0 & h(0) \end{bmatrix} \begin{bmatrix} u(t,1) \\ u(t,0) \end{bmatrix} > 0, \quad \forall \begin{bmatrix} u(t,1) \\ u(t,0) \end{bmatrix} \in \mathcal{U}_b, \tag{3.32b}$$

$$M(x) = \frac{1}{2} \begin{bmatrix} -\lambda p(x) - \partial_x h(x) & h(x) + p(x) \\ h(x) + p(x) & 0 \end{bmatrix} \geq 0, \quad \forall x \in [0,1]. \tag{3.32c}$$

We solve (3.32c) by imposing $h(x) = -p(x)$ and the differential equation $\partial_x h(x) + \lambda h(x) = 0$, to obtain $h(x) = -e^{-\lambda x}$, which satisfies (3.32a) (*i.e.,* $-h(x) = p(x) > 0$). Notice that with $p(x) = -h(x) = e^{-\lambda x}$ the inequality of (3.32c) holds for all $x \in \mathbb{R}$. Inequality (3.32b) is expressed as $-h(1)u^2(1) > 0$, which clearly holds since $-h(1) = e^{-\lambda} > 0$. The inequalities then hold for any $\lambda > 0$ which proves the exponential stability of the $\mathcal{L}^2_{[0,1]}$-norm of the solution for *any* convergence rate. This is expected as, for bounded domains, the transport equation presents *finite-time* stability.

The inequalities in (3.25a)-(3.25b) were also formulated with polynomial weighting function $p(x)$, with $q = 0$ (giving $D^q u = u$) and $\epsilon_2 = \lambda$. Theorem 3.1.4 is applied to the resulting inequalities and we use the Positivstellensatz to formulate the SOSP as

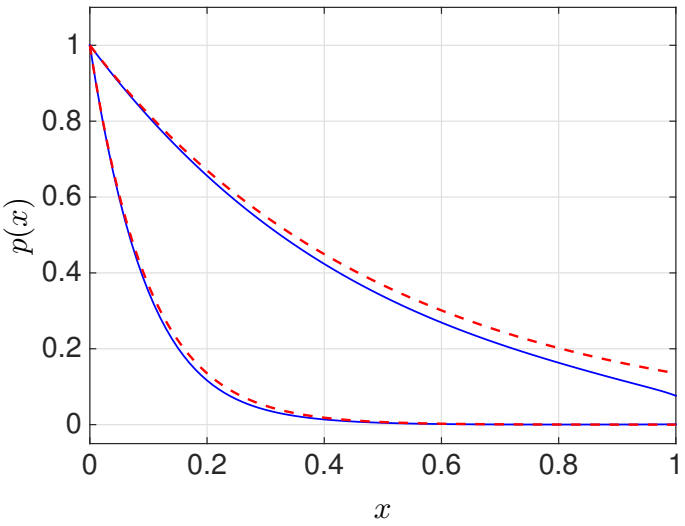

Figure 3.2: Weighting functions proving exponential stability for convergence rates $\lambda \in \{2, 10\}$. The red dotted curves depict the solution $p(x) = e^{-\lambda x}$. The solid blue lines correspond to the polynomials obtained by solving (3.33).

in Corollary 2.3.4

$$\text{Find } p, h, N$$

$$\text{subject to}$$

$$M(x) + N(x)x(x-1) \in \Sigma^{2\times 2}[x],$$

$$N(x) \in \Sigma^{2\times 2}[x]. \tag{3.33}$$

Solutions to the above inequalities were obtained for $\lambda \in (0, 10]$ (the value $\lambda^* = 10$ was solved with $deg(p(x)) = deg(h(x)) = 30$). The numerical results provide polynomial Lyapunov certificates for the $\mathcal{L}^2_{[0,1]}$ stability of the solutions of (3.31). A comparison of the solution $p(x) = e^{-\lambda x}$ and the numerical solutions are depicted in Figure 3.2. □

In the next example we study the stability of a nonlinear, inhomogeneous PDE.

3.4.3 System of Nonlinear Inhomogeneous PDEs

Let $R > 0$. Consider the following PDE

$$\begin{cases} \partial_t u = \frac{1}{R}\partial_x^2 u - (x-0.5)v\partial_x w \\ \partial_t v = \frac{1}{R}\partial_x^2 v + xu + (x-0.5)u\partial_x w \\ \partial_t w = \frac{1}{R}\partial_x^2 w + xu - x^2 v, \end{cases} \tag{3.34}$$

subject to the boundary conditions $u(t,0) = u(t,1) = v(t,0) = v(t,1) = w(t,0) = w(t,1) = 0$. In order to obtain the asymptotic stability bound in terms of the parameter R a straightforward approach is to take the energy as the Lyapunov functional. In this case, the nonlinear terms, given by $\left(-\frac{1}{2}+x\right)\left[\, u_2\partial_x u_3 \;\; -u_1\partial_x u_3 \;\; 0 \,\right]'$, are removed from the expression of the time-derivative of the energy and the remaining expression is influenced only by the linear terms. This choice results in conservatism since the stability may not be certified by the energy of the state taken as the Lyapunov functional. Instead consider the weighted $\mathcal{L}^2_{[0,1]}$-norm as a Lyapunov functional candidate and solve (3.25a) and (3.25b) to obtain $P(x)$, the weighting function. In order to illustrate this solution, we compute the largest value of parameter R for which stability could be certified both with energy and the weighted $\mathcal{L}^2_{[0,1]}$-norm.

The results are depicted in Table 3.1.

Table 3.1: Stability intervals for parameter $R \in (0, R^*]$ for different degrees of $P(x)$.

$deg(P(x))$	0, $P(x) = I$	1	2	3
R^*	6.3	10.5	17.5	21

3.5 Further Discussions: PDEs with Non-Polynomial Nonlinearity

The proposed computational method in this chapter applies to PDEs with polynomial dependence in the dependent and independent variables. In this section, we present hints on the case where PDEs involve non-polynomial nonlinearity.

Let us first clarify the two different cases of non-polynomial data in the dependent variable $D^\alpha u$ and non-polynomial data in the independent variable θ in the quadratic-like integral expression as

$$\int_0^1 \eta'(D^\alpha u)\, M(\theta)\, \eta(D^\alpha u)\ \ d\theta.$$

For nonlinear $\eta(D^\alpha u)$, the non-uniqueness of the quadratic forms is related to the algebraic and differential relations of the entries of vector $\eta(D^\alpha u)$. For instance, for polynomial $\eta(u)$, consider $D^0 u = \begin{bmatrix} u_1 \\ u_2 \end{bmatrix}$ and

$$\eta(u) = \begin{bmatrix} u_1^2 \\ u_1 u_2 \\ u_2^2 \end{bmatrix}.$$

We have

$$\eta'(u)M(\theta)\eta(u) = \begin{bmatrix} u_1^2 \\ u_1 u_2 \\ u_2^2 \end{bmatrix}' \left(M(\theta) + \begin{bmatrix} 0 & 0 & \alpha(\theta) \\ 0 & -2\alpha(\theta) & 0 \\ \alpha(\theta) & 0 & 0 \end{bmatrix} \right) \begin{bmatrix} u_1^2 \\ u_1 u_2 \\ u_2^2 \end{bmatrix}.$$

For a different nonlinear dependence on u, say trigonometric with

$$\eta(u) = \begin{bmatrix} 1 \\ \sin(u) \\ \cos(u) \end{bmatrix}.$$

Since $\int_{[0,1]} \alpha(\theta) \left(\sin^2(u) + \cos^2(u) - 1\right) \ d\theta = 0$, we obtain

$$\eta'(u)M(\theta)\eta(u) = \begin{bmatrix} 1 \\ \sin(u) \\ \cos(u) \end{bmatrix}' \left(M(\theta) + \begin{bmatrix} -\alpha(\theta) & 0 & 0 \\ 0 & \alpha(\theta) & 0 \\ 0 & 0 & \alpha(\theta) \end{bmatrix} \right) \begin{bmatrix} 1 \\ \sin(u) \\ \cos(u) \end{bmatrix}.$$

With the above example, we illustrate that a quadratic-like form can also account for non-polynomial dependence in the dependent variables. However, existing optimization software packages easily handle polynomial vectors, whereas other non-polynomial dependence requires *ad-hoc* construction methods.

The approach presented in this chapter leads to an infinite-dimensional semidefinite constraint in terms of the independent variables. This is illustrated using a simple example below. Consider

$$\partial_t u = \partial_x^2 u + \lambda(x)u, \ u(t,0) = u(t,1) = 0.$$

and the Lyapunov functional $V(u) = \int_0^1 p(x)u^2 \ dx$. Following the steps in Section 3.3 for stability analysis, $p(x) > 0$ and in addition $\partial_t V(u) < 0$. After introducing the differential relation among the dependent variables and accounting for the boundary conditions, we

obtain the differential matrix inequality

$$\left[\begin{array}{c:ccc} 0_{2\times 2} & \multicolumn{3}{c}{0} \\ \hdashline & 2p(x)\lambda(x) & 0 & p(x) \\ 0 & 0 & 0 & 0 \\ & p(x) & 0 & 0 \end{array}\right]$$
$$+\left[\begin{array}{cc:ccc} h_3(1) & 0 & \multicolumn{3}{c}{0} \\ 0 & -h_3(0) & & & \\ \hdashline & & \partial_x h_1(x) & h_1(x)+\partial_x h_2(x) & h_2(x) \\ \multicolumn{2}{c:}{0} & h_1(x) & 2h_2(x)+\partial_x h_3(x) & h_3(x) \\ & & h_2(x) & h_3(x) & 0 \end{array}\right] \geq 0,\ \forall x \in [0,1]. \quad (3.35)$$

Notice that the above differential matrix inequality may be difficult to solve in the general case (nonlinear problem data). For constant λ, the solution to matrix inequality (3.35) can be found analytically as

$$p(x) = \epsilon \sin\left(\sqrt{\frac{\lambda}{2}}x\right),\ h_2(x) = -p(x),\ h_3(x) = 0,\ h_1(x) = -2\frac{d}{dx}h_2(x),$$

where $\epsilon > 0$.

However, in order to obtain a finite-dimensional SDP for inequality (3.35), we have to select a set of basis functions to parametrize the decision variables. In other words, using the basis set $F = \{f_1(x), \ldots, f_n(x)\}$, we can write $p(x) = \sum_{i=1}^{n} c_i f_i(x)$ in terms of a finite number of c_i's. The choice adopted in the chapter is the set of monomials $\{1, x, x^2, \ldots\}$. The reason for such choice is that the associated differential matrix inequalities like (3.35) become polynomial matrix inequalities. For this class of matrix inequalities, there exists efficient numerical optimization softwares such as SOSTOOLS [79]. The numerical examples in the chapter take advantage of these software tools.

The proposed formulation in terms of matrix inequalities does not impose polynomial dependence. However, in order to obtain solutions that take advantage of convex optimization tools, we require the problem data to be polynomial.

3.6 Conclusions

This chapter proposed tests for positivity of integral expressions with integrands that are polynomial on the dependent variables. This was motivated by inequalities encountered in Lyapunov analysis of PDEs. A set of quadratic-like representations for the polynomial integrand is obtained thanks to the Fundamental Theorem of Calculus, which embeds the boundary values of the dependent variables. The positivity of the integral is then studied by analyzing the matrices associated with the quadratic-like representation. Under the assumption that the integrand is also polynomial in the independent variable, matrix positivity tests are cast as SDPs. We then studied integral inequalities from Lyapunov stability conditions for PDEs. The proposed Lyapunov functionals were given by the weighted $\mathcal{H}^q_{[0,1]}$-norms.

In the subsequent chapter, we formulate dissipation inequalities for input-output analysis of PDEs. We show that a suitable choice of storage functional structure converts the input-output analysis problem into checking a set of integral inequalities. We solve these inequalities based on the methodology developed here.

Chapter 4

Dissipation Inequalities for Input-State/Output Analysis of PDEs

In the previous chapter, we developed tools for verifying integral inequalities and applied these tools to the Lyapunov stability analysis problem of PDEs.

Probably more important than stability analysis is the input-state or input-output analysis problem of PDEs. To this end, we use dissipation inequalities, which are widely employed in the context of ODEs [118]. In particular, we are interested in input-state/output properties, such as, passivity, reachability, induced input-output norms and ISS. For each of these properties, we formulate the corresponding dissipation inequality.

We consider PDEs with inputs and outputs that are defined over the domain and PDEs with inputs and outputs at the boundaries. For these systems, the formulation based on dissipation inequalities allows us to characterize input-state/output properties in the context of appropriate Sobolev norms. Furthermore, it enables us to study the interconnections of PDE systems, in which we propose small gain conditions. Also, we demonstrate that the interconnection results can be extended to ODE-PDE interconnections.

In the case of polynomial data, we show that the choice of the weighted Sobolev norms as the storage functionals converts the dissipation inequalities into integral inequalities that

can be solved by SOS programming based on the method introduced in Chapter 3.

We illustrate these discussions by several examples.

Preliminary results on the material presented in this chapter were presented in the 2014 53rd IEEE Conference on Decision and Control [2]. The journal version of the results, which included the small gain results, was also disseminated in [6].

4.1 PDEs with In-Domain Inputs and In-Domain Outputs

In this section, we consider the class of PDE systems described by

$$\begin{cases} \partial_t u(t,x) = F\left(x, D^{\alpha_u} u(t,x), D^{\alpha_d} d(t,x)\right), \\ y(t,x) = H(x, D^{\delta} u), \qquad (t,x) \in \mathbb{R}_{\geq 0} \times \Omega, \\ B \begin{bmatrix} D^{\alpha_u - 1} u(t,1) \\ D^{\alpha_u - 1} u(t,0) \end{bmatrix} = 0, \; B \begin{bmatrix} D^{\alpha_d - 1} d(t,1) \\ D^{\alpha_d - 1} d(t,0) \end{bmatrix} = 0, \end{cases} \tag{4.1}$$

and initial conditions $u(0,x) = u_0(x)$, where $0 \leq \delta \leq \alpha_u$. The dependent variables $u : \mathbb{R}_{\geq 0} \times \Omega \to \mathbb{R}^{n_u}$, $d : \mathbb{R}_{\geq 0} \times \Omega \to \mathbb{R}^{n_d}$, and $y : \mathbb{R}_{\geq 0} \times \Omega \to \mathbb{R}^{n_y}$ represent states, inputs, and outputs, respectively, and B is a matrix of appropriate dimension defining the boundary conditions. We assume throughout the section that the solutions to (4.1) possess sufficient regularity for all required derivatives to exist.

In order to study input-state/output properties of system (4.1), we define each property as follows.

Definition 4.1.1

A. *Passivity: System* (4.1) *is* passive*, if it satisfies the following inequality*

$$\langle d, y \rangle_{\mathcal{L}^2_{[0,\infty),\Omega}} \geq 0, \tag{4.2}$$

whenever $u_0(x) \equiv 0, \; \forall x \in \Omega$.

B. $\mathcal{H}^p$-to-$\mathcal{H}^q_\Omega$ Reachability: System (4.1) *is* $\mathcal{H}^p$*-to-*$\mathcal{H}^q_\Omega$ reachable*, if for* $d \in \mathcal{H}^p(\mathbb{R}_{\geq 0} \times \Omega; \mathbb{R}^{n_d})$ *with* $\alpha_d \geq p$*, the solutions of* (4.1) *satisfy*

$$\|u(T,\cdot)\|_{\mathcal{H}^q_\Omega} \leq \beta\left(\|d\|_{\mathcal{H}^p_{[0,T),\Omega}}\right), \quad \forall T > 0 \tag{4.3}$$

with $\beta \in \mathcal{K}_\infty$ *and* $u_0(x) \equiv 0,\ \forall x \in \Omega$*.*

C. Induced $\mathcal{H}^p$-to-$\mathcal{H}^q$-norm Boundedness: System (4.1) *has a* bounded induced $\mathcal{H}^p$-to-$\mathcal{H}^q$-norm*, if for* $d \in \mathcal{H}^p(\mathbb{R}_{\geq 0} \times \Omega; \mathbb{R}^{n_d})$ *with* $\alpha_d \geq p$ *and some* $\gamma > 0$*,*

$$\|y\|_{\mathcal{H}^q_{[0,\infty),\Omega}} \leq \gamma \|d\|_{\mathcal{H}^p_{[0,\infty),\Omega}} \tag{4.4}$$

subject to zero initial conditions $u_0(x) \equiv 0,\ \forall x \in \Omega$*.*

D. D^p-Input-to-State Stability in $\mathcal{H}^q_\Omega$: System (4.1) *is* D^p-Input-to-State Stable in the $\mathcal{H}^q_\Omega$-norm*, if for* $d \in \mathcal{W}^{p,\infty}(\Omega; \mathbb{R}^{n_d})$ *with* $\alpha_d \geq p$*, some scalar* $\psi > 0$*, functions* $\beta, \tilde{\beta}, \chi \in \mathcal{K}_\infty$*, and* $\sigma \in \mathcal{K}$*, it holds that*

$$\begin{aligned}\|u(t,\cdot)\|_{\mathcal{H}^q_\Omega} \leq\ & \beta\Big(e^{-\psi t}\chi\left(\|u_0\|_{\mathcal{H}^q_\Omega}\right)\Big) \\ & + \tilde{\beta}\Big(\sup_{\tau\in[0,t)}\big(\int_\Omega \sigma\big(\,|D^p d(\tau,x)|\,\big)\,dx\big)\Big),\ \forall t > 0,\ \forall u_0 \in \mathcal{H}^q_\Omega,\end{aligned} \tag{4.5}$$

where $|\cdot|$ *is the Euclidean norm.*

Remark 4.1.2 *The above definition of passivity was used in [109], where a passivity-based design strategy for flow control is presented.*

Given $T > 0$ and the information on the $\mathcal{H}^p_{[0,T),\Omega}$-norm of the input, inequality (4.3) shows how the $\mathcal{H}^q_\Omega$-norm evolves at $t = T$. In fact, a minimization over $\beta \in \mathcal{K}_\infty$ results in an upper bound on the reachable set at time $t = T$ in the $\mathcal{H}^q_\Omega$-norm.

In item C in Definition 4.1.1, for the PDE system (4.1), we are interested in estimating upper bounds on $\gamma^* > 0$ defined as

$$\gamma^* = \sup_{0<\|d\|_{\mathcal{H}^q}<\infty} \frac{\|y\|_{\mathcal{H}^q}}{\|d\|_{\mathcal{H}^p}}, \tag{4.6}$$

i.e., the induced $\mathcal{H}^p$-to-$\mathcal{H}^q$-norm.

Note that the D^p-ISS property (4.5) assures asymptotic convergence to the null solution in $\mathcal{H}^q_\Omega$ when $d \equiv 0$. Moreover, when $d \neq 0$, as $t \to \infty$, the first term on the right-hand side of (4.5) vanishes, yielding

$$\lim_{t\to\infty} \|u(t,\cdot)\|_{\mathcal{H}^q_\Omega} \leq \tilde{\beta}\left(\int_\Omega \|\sigma(|D^p d(\cdot,x)|)\|_{\mathcal{L}^\infty_{[0,\infty)}}\, dx\right) \leq \tilde{\beta}\left(\int_\Omega \sigma(\|d(t,x)\|_{\mathcal{W}^{p,\infty}_{[0,\infty)}})\, dx\right), \tag{4.7}$$

wherein, the fact that $\sigma, \beta \in \mathcal{K}_\infty \subset \mathcal{K}$ is used. Hence, when all the spatial derivatives of the input up to order p are bounded in $\mathcal{L}^\infty_{[0,\infty)}$, the *state* u is bounded in the $\mathcal{H}^q_\Omega$-norm. This is analogous to the ISS property for ODEs [113].

Remark 4.1.3 *The reachability property is often referred to as controllability [64, Section 9.6.7] and the induced norm boundedness property is often studied in the context of trace regularity (e.g. see the trace regularity results for hyperbolic PDEs [64, Section 8A] and the Schrödinger equation [64, Section 10.9.3]).*

In the sequel, we use the concept of *zero-state detectability* for PDEs, which is defined next (for the case of ODEs refer to [46, p. 362]).

Definition 4.1.4 *A system is zero-state detectable (ZSD) in $\mathcal{H}^q_\Omega$, if $\|y\|_{\mathcal{H}^q_\Omega} = 0$ implies $\|u\|_{\mathcal{H}^q_\Omega} = 0$.*

Zero-state detectability imposes constraints on H in (4.1) ($\|H(x, D^\delta u)\|_{\mathcal{H}^q_\Omega} = 0 \Rightarrow \|u\|_{\mathcal{H}^q_\Omega} = 0$). In the special case of $H(x, D^\delta u) = h(x)u$ and $q = 0$, this is equivalent to $\nexists x \in \Omega$ such that $h(x) = 0$, thereby $y = 0$ implies $u = 0$.

A powerful tool in the study of robustness and input-state/output properties of systems is dissipation inequalities [135, 51]. For linear ODEs, quadratic storage functions of states are both necessary and sufficient solutions to dissipation inequalities with quadratic supply rates [124]. For polynomial ODEs, [31] proposes an approach for constructing polynomial storage functions based on SOSPs.

For PDEs, dissipation inequalities were proposed for particular systems. For linear time-varying hyperbolic PDEs, the weighted $\mathcal{L}^2$-norm functional was considered as a certificate for ISS in [97]. In [20], ISS of a semi-linear diffusion equation was analyzed using the weighted $\mathcal{L}^2$-norm as the storage functional. However, the formulation of dissipation inequalities for PDEs and the construction of storage functionals in the latter contributions is based on *ad hoc* methods.

In the next theorem, we formulate the dissipation inequalities associated with properties A-D in Definition 4.1.1, which can be applied to a larger class of PDEs, including nonlinear PDEs.

Theorem 4.1.5 *Consider the PDE system described by* (4.1). *If there exist a positive semidefinite storage functional*[1] $S(u) \in \mathcal{C}^1[t]$, *scalars* $\gamma, \psi > 0$, *and functions* $\beta_1, \beta_2 \in \mathcal{K}_\infty$, $\alpha, \sigma \in \mathcal{K}$ *satisfying* $\psi|U| \leq \alpha(|U|)$, *such that*

A)
$$\partial_t S(u) \leq \langle d, y \rangle_{\mathcal{L}^2_\Omega}, \ \forall t \geq 0, \tag{4.8}$$

then, system (4.1) *is passive as in* (4.2).

B)
$$\beta_1(\|u\|_{\mathcal{H}^q_\Omega}) \leq S(u), \tag{4.9}$$

$$\partial_t S(u) \leq \gamma^2 \langle d, d \rangle_{\mathcal{H}^p_\Omega}, \ \forall t \geq 0, \tag{4.10}$$

[1] We refer to a functional $J(u)$ as positive semidefinite, if it satisfies $J(0) = 0$ and $J(u) \geq 0, \ \forall u \neq 0$.

then, system (4.1) *is* $\mathcal{H}^p$*-to-*$\mathcal{H}^q_\Omega$ *reachable as in* (4.3) *with* $\beta(\cdot) = \beta_1^{-1}(\gamma(\cdot))$.

C) $$\|y\|_{\mathcal{H}^q_\Omega} = 0 \Rightarrow \|u\|_{\mathcal{H}^q_\Omega} = 0, \tag{4.11}$$

$$\partial_t S(u) \leq -\langle y, y\rangle_{\mathcal{H}^q_\Omega} + \gamma^2 \langle d, d\rangle_{\mathcal{H}^p_\Omega}, \ \forall t \geq 0 \tag{4.12}$$

then, system (4.1) *is asymptotically stable and its induced* $\mathcal{H}^p$*-to-*$\mathcal{H}^q$*-norm is bounded by* γ *as in* (4.4).

D) $$\beta_1(\|u\|_{\mathcal{H}^q_\Omega}) \leq S(u) \leq \beta_2(\|u\|_{\mathcal{H}^q_\Omega}), \tag{4.13}$$

$$\partial_t S(u) \leq -\alpha(S(u)) + \int_\Omega \sigma(|D^p d|)\, dx, \ \forall t \geq 0, \tag{4.14}$$

then system (4.1) *is* D^p*-ISS in* $\mathcal{H}^q_\Omega$ *and satisfies* (4.5) *with* $\chi = \beta_2$, $\beta = \beta_1^{-1} \circ 2$ *and* $\tilde{\beta} = \beta_1^{-1} \circ \frac{2}{\psi}$.

Proof: Each item is proven in turn:

A) Integrating both sides of (4.8) over time from 0 to ∞ yields

$$\int_0^\infty \partial_t S(u) \ \ dt \leq \int_0^\infty \int_\Omega d'y \ dx \ dt.$$

That is,

$$\lim_{t\to\infty} S\left(u(t,x)\right) - S\left(u_0\right) \leq \int_0^\infty \int_\Omega d'y \ dx \ dt.$$

By hypothesis, $S(u)$ is positive semidefinite. Hence, for $u(0,x) = 0$, we have $S(u(0,x)) = 0$. Moreover, $\lim_{t\to\infty} S\left(u(t,x)\right)) \geq 0$. Therefore, we obtain the passivity estimate (4.2).

B) Integrating both sides of (4.10) over time from 0 to T yields

$$\int_0^T \partial_t S(u) \ \ dt \leq \gamma \int_0^T \|d\|^2_{\mathcal{H}^q_\Omega} \ \ dt.$$

That is,

$$S(u(T,x)) - S(u(0,x)) \leq \gamma \|d\|_{\mathcal{H}^p_{[0,T),\Omega}}.$$

Noting that, with $u(0,x) \equiv 0$, from (4.9), we have

$$\beta_1(\|u(T,\cdot)\|_{\mathcal{H}^q_\Omega}) \leq S(u(T,x)) \leq \gamma \|d\|_{\mathcal{H}^p_{[0,T),\Omega}}.$$

Since $\beta_1 \in \mathcal{K}_\infty$, its inverse exists and belongs to $\mathcal{K}_\infty$. Thus,

$$\|u(T,\cdot)\|_{\mathcal{H}^q_\Omega} \leq \beta_1^{-1}\left(\gamma \|d\|_{\mathcal{H}^p_{[0,T),\Omega}}\right).$$

Therefore, an estimate of the reachable set at $t = T$ in terms of $\|d\|_{\mathcal{H}^p_{[0,T),\Omega}}$ is attained.

C) Subject to zero inputs $d \equiv 0$, (4.12) becomes

$$\partial_t S(u) \leq -\|y\|^2_{\mathcal{H}^q_\Omega}. \tag{4.15}$$

Inequality (4.15) implies that the time derivative of the storage functional $S(u)$ is negative semidefinite. Moreover, from Definition 3, condition (4.11) is equivalent to system (4.1) being ZSD in $\mathcal{H}^q_\Omega$. Thus, $\partial_t S(u) = 0$ only if $\|u\|_{\mathcal{H}^q_\Omega} = 0$. Hence, from LaSalle's invariance principle [70, Theorem 3.64, p. 161], it follows that u converges to the null solution $u = 0$ in $\mathcal{H}^q_\Omega$-norm asymptotically.

Furthermore, by integrating both sides of (4.12) from 0 to ∞, we obtain

$$\int_0^\infty \partial_t S(u)\ \ dt \leq -\int_0^\infty \|y\|^2_{\mathcal{H}^q_\Omega}\ \ dt + \gamma^2 \int_0^\infty \|d\|^2_{\mathcal{H}^p_\Omega}\ \ dt.$$

That is,

$$\lim_{t\to\infty} S(u(t,x)) - S(u_0) \leq -\int_0^\infty \|y\|^2_{\mathcal{H}^q_\Omega}\ \ dt + \gamma^2 \int_0^\infty \|d\|^2_{\mathcal{H}^p_\Omega}\ \ dt.$$

Since $u_0(x) \equiv 0,\ x \in \Omega$, we have

$$\lim_{t\to\infty} S(u(t,x)) \leq -\int_0^\infty \|y\|^2_{\mathcal{H}^q_\Omega}\ dt + \gamma^2 \int_0^\infty \|d\|^2_{\mathcal{H}^p_\Omega}\, dt,$$

and because $S(\cdot)$ is positive semidefinite, we obtain

$$\int_0^\infty \|y\|^2_{\mathcal{H}^q_\Omega}\ dt \leq \gamma^2 \int_0^\infty \|d\|^2_{\mathcal{H}^p_\Omega}\ dt.$$

D) By rearranging the terms in (4.14) and noting that $\psi|U| \leq \alpha(|U|)$, we have $\partial_t S(u) + \psi S(u) \leq \int_\Omega \sigma(|D^p d|)\ dx$. Multiplying both sides of the above inequality by the strictly increasing, positive function $e^{\psi t}$, we have $e^{\psi t}\left(\partial_t S(u) + \psi S(u)\right) \leq e^{\psi t}\int_\Omega \sigma(|D^p d|)\ dx$. Then, it follows that

$$\frac{d}{dt}\left(e^{\psi t} S\right) \leq e^{\psi t}\int_\Omega \sigma(|D^p d|)\ dx. \tag{4.16}$$

Integrating both sides of inequality (4.16) from 0 to t gives

$$\begin{aligned} e^{\psi t}S(u(t,x)) - S(u(0,x)) &\leq \int_0^t e^{\psi\tau}\left(\int_\Omega \sigma(|D^p d(\tau,x)|)\ dx\right)\ d\tau \\ &\leq \left(\int_0^t e^{\psi\tau}\ d\tau\right)\sup_{\tau\in[0,t)}\left(\int_\Omega \sigma(|D^p d(\tau,x)|)\ dx\right) \\ &\leq \frac{1}{\psi}(e^{\psi t}-1)\sup_{\tau\in[0,t)}\left(\int_\Omega \sigma(|D^p d(\tau,x)|)\ dx\right) \\ &\leq \frac{e^{\psi t}}{\psi}\sup_{\tau\in[0,t)}\left(\int_\Omega \sigma(|D^p d(\tau,x)|)\ dx\right), \end{aligned} \tag{4.17}$$

where Hölder's inequality is used in the second inequality above. Dividing both sides of the last inequality above by the positive term $e^{\psi t}$ gives

$$S(u) \leq e^{-\psi t}S(u_0) + \frac{1}{\psi}\sup_{\tau\in[0,t)}\left(\int_\Omega \sigma(|D^p d(\tau,x)|)\ dx\right).$$

Using (4.13), we infer that

$$\beta_1(\|u\|_{\mathcal{H}^q_\Omega}) \leq e^{-\psi t}\beta_2(\|u_0\|_{\mathcal{H}^q_\Omega}) + \frac{1}{\psi}\sup_{\tau\in[0,t)}\left(\int_\Omega \sigma(|D^p d(\tau,x)|)\,dx\right). \tag{4.18}$$

Since $\beta_1 \in \mathcal{K}_\infty$, its inverse exists and belongs to $\mathcal{K}_\infty$. Hence, taking the inverse of β_1 from both sides of (4.18) yields

$$\|u\|_{\mathcal{H}^q_\Omega} \leq \beta_1^{-1}\big(e^{-\psi t}\beta_2(\|u_0\|_{\mathcal{H}^q_\Omega}) + \frac{1}{\psi}\sup_{\tau\in[0,t)}\big(\int_\Omega \sigma(|D^p d(\tau,x)|)\,dx\big)\big),$$

and, applying inequality (1.11), it follows that

$$\|u\|_{\mathcal{H}^q_\Omega} \leq \beta_1^{-1}\left(2e^{-\psi t}\beta_2(\|u_0\|_{\mathcal{H}^q_\Omega})\right) + \beta_1^{-1}\left(\frac{2}{\psi}\sup_{\tau\in[0,t)}\big(\int_\Omega \sigma(|D^p d(\tau,x)|)\,dx\big)\right),$$

and (4.5) is obtained with $\chi = \beta_2$, $\beta = \beta_1^{-1}\circ 2$ and $\tilde{\beta} = \beta_1^{-1}\circ\frac{2}{\psi}$. □

Remark 4.1.6 *An important property of PDE systems, in particular in the study of hyperbolic systems, is conservativeness [133, 132], i.e., the system satisfies the relation*

$$\|u(T,\cdot)\|^2_{\mathcal{L}^2_\Omega} - \|u_0\|^2_{\mathcal{L}^2_\Omega} = \int_0^T \|d\|^2_{\mathcal{L}^2_\Omega}\ dt - \int_0^T \|y\|^2_{\mathcal{L}^2_\Omega}\ dt. \tag{4.19}$$

For $p = q = 0$, if we consider the squared $\mathcal{L}^2_\Omega$-norm as the storage functional, i.e., $S(u) = \|u\|^2_{\mathcal{L}^2_\Omega} = \int_\Omega u^2\,dx$, inequality (4.12) *in Theorem 4.1.5 can be re-written as*

$$\partial_t\left(\|u\|^2_{\mathcal{L}^2_\Omega}\right) \leq \gamma^2\|d\|^2_{\mathcal{L}^2_\Omega} - \|y\|^2_{\mathcal{L}^2_\Omega}.$$

Integrating both sides of the above inequality over time from 0 to $T > 0$ yields

$$\|u(T,\cdot)\|^2_{\mathcal{L}^2_\Omega} - \|u_0\|^2_{\mathcal{L}^2_\Omega} \leq \gamma^2\int_0^T \|d\|^2_{\mathcal{L}^2_\Omega}\ dt - \int_0^T \|y\|^2_{\mathcal{L}^2_\Omega}\ dt.$$

Then, in the special case when $\gamma = 1$ and equality holds, we obtain (4.19)*. Thus, conserva-*

tive PDEs are special cases of PDEs with bounded induced $\mathcal{L}^2$-to-$\mathcal{L}^2$-norm. That is, since $T > 0$ is arbitrary, the induced $\mathcal{L}^2$-to-$\mathcal{L}^2$-norm of the system is 1.

We illustrate Theorem 4.1.5 using an example.

Example 4.1.7 (ISS Analysis of Burgers' Equation) *Consider the following PDE system*

$$\begin{aligned} \partial_t u(t,x) &= \partial_x^2 u(t,x) - u(t,x)\partial_x u(t,x) + d(t,x), \\ y(t,x) &= u(t,x), \qquad\qquad x \in [0,1],\ t > 0 \end{aligned} \tag{4.20}$$

subject to $u(0,t) = u(1,t) = 0$. In the following, we show that for the above system the following storage functional

$$S(u) = \frac{1}{2}\int_0^1 u^2(t,x)\, dx. \tag{4.21}$$

satisfies inequalities (4.13)*, and* (4.14)*. In other words, using storage functional* (4.21)*, we demonstrate that the system is D^0-ISS in $\mathcal{L}^2_\Omega$. Note that the storage functional* (4.21) *satisfies $\frac{c}{2}\int_0^1 u^2\, dx \leq \frac{1}{2}\int_0^1 u^2\, dx \leq \frac{C}{2}\int_0^1 u^2\, dx$ for some $0 < c < 1$ and $C > 1$. Thus, inequality* (4.13) *is satisfied. Substituting* (4.21) *in* (4.14) *and noting that $\psi|U| \leq \alpha(|U|)$, we have*

$$-\frac{\psi}{2}\int_0^1 u^2\, dx + \int_0^1 \sigma(|d|)\, dx \geq \int_0^1 u \overbrace{\left(\partial_x^2 u - u\partial_x u + d\right)}^{\partial_t u}\, dx. \tag{4.22}$$

By integration by parts and using the boundary conditions, we have $\int_0^1 u\partial_x^2 u\, dx = -\int_0^1 (\partial_x u)^2\, dx$, and $\int_0^1 u^2\partial_x u\, dx = 0$. Then, inequality (4.22) *gives*

$$-\frac{\psi}{2}\int_0^1 u^2\, dx + \int_0^1 \sigma(|d|)\, dx \geq -\int_0^1 (\partial_x u)^2\, dx + \int_0^1 ud\, dx. \tag{4.23}$$

In addition, using Hölder and Young inequalities for $p = q = 2$, we have

$$\int_0^1 ud\, dx \leq \left(\int_0^1 u^2\, dx\right)^{\frac{1}{2}}\left(\int_0^1 d^2\, dx\right)^{\frac{1}{2}} \leq \frac{1}{2}\int_0^1 u^2\, dx + \frac{1}{2}\int_0^1 d^2\, dx. \tag{4.24}$$

Next, we show that the left hand side of (4.23) *is greater than a quantity which is greater than the right hand side of* (4.23)*. Thus, inequality* (4.23) *also holds. Applying inequality* (4.24)*, we check*

$$-\frac{\psi}{2}\int_0^1 u^2\,dx+\int_0^1 \sigma(|d|)\,dx\geq-\int_0^1 (\partial_x u)^2\,dx+\frac{1}{2}\int_0^1 u^2\,dx+\frac{1}{2}\int_0^1 d^2\,dx.$$

Moving the terms involving d *and* u *to the left and the right hand side of the above inequality, respectively, gives*

$$-\frac{\psi}{2}\int_0^1 u^2\,dx+\int_0^1 (\partial_x u)^2\,dx-\frac{1}{2}\int_0^1 u^2\,dx\geq-\int_0^1 \sigma(|d|)\,dx+\frac{1}{2}\int_0^1 d^2\,dx.$$

By choosing $\sigma(|d|)=\frac{d^2}{2}$*, we obtain* $-\left(\frac{\psi+1}{2}\right)\int_0^1 u^2\,dx+\int_0^1 (\partial_x u)^2\,dx\geq 0$*. From the Poincaré inequality, we infer that if we choose* ψ *and correspondingly* α *such that* $\frac{\psi+1}{2}\leq\pi^2$*, then the above inequality holds. Consequently, we demonstrated using storage functional* (4.21) *that system* (4.20) *is* D^0*-ISS in* $\mathcal{L}^2_\Omega$*.*

In Section 4.4, we shall demonstrate that for PDEs with polynomial data the dissipation inequalities can be solved by convex optimization. To this end, we employ the results for solving integral inequalities provided in Chapter 3.

4.2 PDEs with Boundary Inputs and Boundary Outputs

In this section, we formulate conditions to study the input-output properties of PDEs with boundary inputs and outputs. Consider the following PDE system

$$\begin{cases}\partial_t u(t,x)=F\left(x,D^\alpha u(t,x)\right),\\ y(t)=h\left(D^\beta u(t,0)\right),\ (t,x)\in\mathbb{R}_{\geq 0}\times\Omega\\ BD^{\alpha-1}u(t,0)=0,\ BD^{\alpha-1}u(t,1)=w(t),\end{cases}\tag{4.25}$$

and initial conditions $u(0,x) = u_0(x)$, where B is a matrix of appropriate dimension, $y : \mathbb{R}_{\geq 0} \to \mathbb{R}^{n_y}$, and $w : \mathbb{R}_{\geq 0} \to \mathbb{R}^{n_w}$. Next, we define input-state/output properties for PDE (4.25). We assume throughout the section that the solutions to (4.25) have sufficient regularity for all required derivatives to exist.

Definition 4.2.1

A. *Passivity [102]: System* (4.25) *is* passive*, if it satisfies the following inequality*

$$\langle w, y \rangle_{\mathcal{L}^2_{[0,\infty)}} \geq 0, \tag{4.26}$$

with $u_0(x) \equiv 0,\ \forall x \in \Omega$.

B. $\mathcal{L}^2_{[0,\infty)}$*-to-*$\mathcal{H}^q_\Omega$ *Reachability [102]: System* (4.25) *is* $\mathcal{L}^2_{[0,\infty)}$-to-$\mathcal{H}^q_\Omega$ reachable*, if for* $\forall w \in \mathcal{L}^2(\mathbb{R}_{\geq 0}; \mathbb{R}^{n_w})$*, the solutions of* (4.25) *satisfy*

$$\|u(T,\cdot)\|_{\mathcal{H}^q_\Omega} \leq \beta\left(\|w\|_{\mathcal{L}^2_{[0,T)}}\right), \quad \forall T > 0, \tag{4.27}$$

with $\beta \in \mathcal{K}_\infty$ *and with* $u_0(x) \equiv 0,\ \forall x \in \Omega$.

C. *Induced* $\mathcal{L}^2_{[0,\infty)}$*-norm Boundedness [102]: System* (4.25) *has* bounded induced $\mathcal{L}^2_{[0,\infty)}$-norm*, if for* $\forall w \in \mathcal{L}^2(\mathbb{R}_{\geq 0}; \mathbb{R}^{n_w})$*, there exits a* $\gamma > 0$ *such that*

$$\|y\|_{\mathcal{L}^2_{[0,\infty)}} \leq \gamma \|w\|_{\mathcal{L}^2_{[0,\infty)}} \tag{4.28}$$

with zero initial conditions $u_0(x) \equiv 0,\ \forall x \in \Omega$.

D. *Input-to-State Stability in* $\mathcal{H}^q_\Omega$*: System* (4.25) *is* input-to-state stable in $\mathcal{H}^q_\Omega$*, if for* $\forall w \in \mathcal{L}^\infty(\mathbb{R}_{\geq 0}; \mathbb{R}^{n_w})$*, there exists a scalar* $\psi > 0$*, functions* $\beta, \tilde{\beta}, \chi \in \mathcal{K}_\infty$*, and*

$\sigma \in \mathcal{K}$ *such that*

$$\|u(t,\cdot)\|_{\mathcal{H}^q_\Omega} \leq \beta\Big(e^{-\psi t}\chi\left(\|u_0\|_{\mathcal{H}^q_\Omega}\right)\Big) + \tilde{\beta}\Big(\sup_{\tau\in[0,t)} \sigma\left(|w(\tau)|\right)\Big),\ \forall t>0,\ \forall u_0 \in \mathcal{H}^q_\Omega, \quad (4.29)$$

Remark 4.2.2 *The Input-to-State Stability in $\mathcal{H}^q_\Omega$ property defined above parallels the ISS property for ODE systems as given in [112]. However, ISS in $\mathcal{H}^q_\Omega$ property for PDEs includes bounds on states u defined in the Sobolev norm of interest $\mathcal{H}^q_\Omega$, since the state u belongs to an infinite-dimensional space.*

The next result follows from Theorem 4.1.5.

Corollary 4.2.3 *Consider the PDE system described by* (4.25)*. If there exist a positive semidefinite storage functional $S(u) \in \mathcal{C}^1[t]$, scalars $\gamma, \psi > 0$, and functions $\beta_1, \beta_2 \in \mathcal{K}_\infty$, $\alpha, \sigma \in \mathcal{K}$ satisfying $\psi|U| \leq \alpha(|U|)$, such that*

A) $$\partial_t S(u) \leq w'(t)y(t),\ \forall t \geq 0, \quad (4.30)$$

then, system (4.25) *satisfies the passivity property* (4.26)*.*

B) $$\beta_1(\|u\|_{\mathcal{H}^q_\Omega}) \leq S(u), \quad (4.31)$$

$$\partial_t S(u) \leq \gamma^2 w'(t)w(t),\ \forall t \geq 0, \quad (4.32)$$

then, system (4.25) *satisfies the $\mathcal{L}^2_{[0,\infty)}$-to-$\mathcal{H}^q_\Omega$ reachability property* (4.27) *with $\beta(\cdot) = \beta_1^{-1}(\gamma^2(\cdot)^2)$.*

C) $$\partial_t S(u) \leq -y'(t)y(t) + \gamma^2 w'(t)w(t),\ \forall t \geq 0, \quad (4.33)$$

then system (4.25) *is stable and has its induced $\mathcal{L}^2_{[0,\infty)}$-norm bounded by γ as in* (4.28)*.*

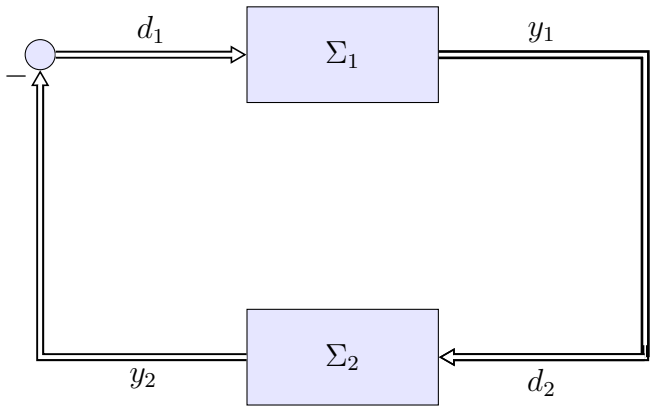

Figure 4.1: The interconnection of two PDE systems.

D) $$\beta_1(\|u\|_{\mathcal{H}^q_\Omega}) \leq S(u) \leq \beta_2(\|u\|_{\mathcal{H}^q_\Omega}), \tag{4.34}$$

$$\partial_t S(u) \leq -\alpha(S(u)) + \sigma(|w(t)|),\ \forall t \geq 0, \tag{4.35}$$

then system (4.25) *is ISS and satisfies* (4.29) *with* $\chi = \beta_2$, $\beta = \beta_1^{-1} \circ 2$ *and* $\tilde{\beta} = \beta_1^{-1} \circ \frac{2}{\psi}$.

Proof: The proof of Items *A*, *B*, and *D* follows the same lines as the proof of Theorem 4.1.5. For Item *C*, LaSalle's invariance principle cannot be used to conclude asymptotic stability as was the case in Theorem 4.1.5, since with $w \equiv 0$ inequality (4.33) is converted to $\partial_t S(u) \leq -y'(t)y(t)$ which implies that the solutions to (4.25) are stable. However, $y(t) = 0$ only contains information about the values at the boundaries; *i.e.,* $h\left(D^\beta u(t,0)\right) = 0$, which does not imply $u(t,x) = 0$ for all $(t,x) \in \mathbb{R}_{\geq 0} \times \Omega$. □

4.3 Interconnections

In this section, we consider several interconnection topologies for PDE-PDE or PDE-ODE systems. We show that, analogous to the ODE-ODE interconnections, once some properties of the subsystems in an interconnection hold in terms of dissipation inequalities, we can infer properties of the interconnection.

Remark that, if a system property holds, it is not necessarily equivalent to the existence of a storage functional satisfying some dissipation inequality. Though the converse holds for linear ODEs with quadratic storage functions and supply rates [124], even for nonlinear ODEs, this is still an open problem [102]. In this section, however, when we refer to a property of subsystems, we imply that the subsystem satisfies the associated dissipation inequality. In other words, we are interested in making conclusions about an overall system, once some property of subsystems is known in terms of dissipation inequalities.

4.3.1 PDE-PDE Interconnections

The next result is a small-gain theorem, which ensures stability or asymptotic stability of interconnected PDE systems under some assumptions. This demonstrates the applicability of dissipation inequalities for studying the stability of coupled or large-scale PDE systems.

Theorem 4.3.1 *Let*

$$\Sigma_i : \begin{cases} \partial_t u_i = F_i(x, D^{\alpha_u^i} u_i, D^{\alpha_d^i} d), \\ y_i = H_i(x, D^{\delta^i} u_i),\ (t,x) \in \mathbb{R}_{\geq 0} \times \Omega \\ B_i \begin{bmatrix} D^{\alpha_u^i - 1} u_i(t,1) \\ D^{\alpha_u^i - 1} u_i(t,0) \end{bmatrix} = 0,\ B_i \begin{bmatrix} D^{\alpha_d^i - 1} d_i(t,1) \\ D^{\alpha_d^i - 1} d_i(t,0) \end{bmatrix} = 0, \end{cases} \tag{4.36}$$

for $i = 1, 2$. Consider the interconnected PDE systems Σ_1 and Σ_2 as depicted in Figure 4.1. If Σ_1 and Σ_2 have induced $\mathcal{H}^q$-to-$\mathcal{H}^q$-norms γ_1 and γ_2, respectively, in the sense of (4.4) *and certified by dissipation inequality* (4.12)*, then, the interconnected system is stable in $\mathcal{H}^q_\Omega$, provided that*

$$\gamma_1 \gamma_2 < 1. \tag{4.37}$$

Furthermore, if each of subsystems Σ_1 and Σ_2 are ZSD in $\mathcal{H}^q_\Omega$, then asymptotic stability in $\mathcal{H}^q_\Omega$ holds for the interconnected system.

Proof: Let S_1 and S_2 be two storage functionals for Σ_1 and Σ_2. By hypothesis, it holds that

$$\partial_t S_i \leq -\langle y_i, y_i \rangle_{\mathcal{H}^q_\Omega} + \gamma_i^2 \langle d_i, d_i \rangle_{\mathcal{H}^q_\Omega}, \ i = 1, 2. \tag{4.38}$$

Let μ be a scalar satisfying $\gamma_1 < \mu < \frac{1}{\gamma_2}$. Therefore, $\gamma_1\gamma_2 < \mu\gamma_2 < 1$. Let $S = S_1 + \mu^2 S_2$. Then, from (4.38), it follows that

$$\partial_t S \leq -\langle y_1, y_1 \rangle_{\mathcal{H}^q_\Omega} + \gamma_1^2 \langle d_1, d_1 \rangle_{\mathcal{H}^q_\Omega} - \mu^2 \langle y_2, y_2 \rangle_{\mathcal{H}^q_\Omega} + \mu^2\gamma_2^2 \langle d_2, d_2 \rangle_{\mathcal{H}^q_\Omega}.$$

With the interconnection $y_1 = d_2$ and $y_2 = -d_1$, we have

$$\partial_t S \leq -(1 - \mu^2\gamma_2^2)\langle y_1, y_1 \rangle_{\mathcal{H}^q_\Omega} - (\mu^2 - \gamma_1^2)\langle y_2, y_2 \rangle_{\mathcal{H}^q_\Omega}.$$

Thus, from (4.37) and the definition of μ, it follows that the time derivative of the storage functional S is non-positive, which, in turn, implies that the interconnected PDE system is stable in $\mathcal{H}^q_\Omega$. Moreover, from ZSD property of Σ_1 and Σ_2, one can infer that $\|y_i\|_{\mathcal{H}^q_\Omega} = 0 \Rightarrow \|u_i\|_{\mathcal{H}^q_\Omega} = 0, i = 1, 2$. Hence, $\partial_t S(u) = 0$ only if $\|u_i\|_{\mathcal{H}^q_\Omega} = 0, i = 1, 2$. Consequently, from LaSalle's invariance principle [70, Theorem 3.64, p. 161], it follows that $(u_1, u_2) \to 0$ as $t \to \infty$ in $\mathcal{H}^q_\Omega$. This completes the proof. □

The next corollary asserts that stability in $\mathcal{H}^q_\Omega$ holds, if both subsystems of interconnection in Figure 4.1 with boundary inputs and boundary outputs have bounded $\mathcal{L}^2_{[0,\infty)}$-norms and satisfy a small gain criterion.

Corollary 4.3.2 *Let*

$$\Sigma_1 : \begin{cases} \partial_t u_1 = F_1(x, D^{\alpha_u^1} u_1) \\ y_1 = h_1(D^{\beta^1} u_1(t, 1)), \\ B_1 D^{\alpha_u^1 - 1} u_1(t, 0) = w_1(t), \ B_1 D^{\alpha_u^1 - 1} u_1(t, 1) = 0, \end{cases}$$

and

$$\Sigma_2 : \begin{cases} \partial_t u_2 = F_2(x, D^{\alpha_u^2} u_2) \\ y_2 = h_2(D^{\beta^2} u_2(t,0)), \\ B_2 D^{\alpha_u^2 - 1} u_2(t,0) = 0,\ B_2 D^{\alpha_u^2 - 1} u_2(t,1) = w_2(t), \end{cases}$$

with interconnection $w_1 = -y_2$ *and* $w_2 = y_1$. *If* Σ_1 *and* Σ_2 *have induced* $\mathcal{L}^2_{[0,\infty)}$*-norms* γ_1 *and* γ_2*, respectively, in the sense of* (4.28) *and certified by dissipation inequality* (4.33)*, then, the interconnected system is stable in* $\mathcal{H}^q_\Omega$*, provided that* $\gamma_1\gamma_2 < 1$.

Proof: Let S_1 and S_2 be two storage functionals for Σ_1 and Σ_2. By hypothesis, it holds that

$$\partial_t S_i \leq -y_i' y_i + \gamma_i^2 w_i' w_i,\ i = 1, 2. \tag{4.39}$$

Define μ such that $\gamma_1 < \mu < \frac{1}{\gamma_2}$. Therefore, $\gamma_1\gamma_2 < \mu\gamma_2 < 1$. Let $S = S_1 + \mu^2 S_2$. Then, from (4.39), it follows that

$$\partial_t S \leq -|y_1|^2 + \gamma_1^2|w_1|^2 - \mu^2|y_2|^2 + \mu^2\gamma_2^2|w_2|^2.$$

With the interconnection $y_1 = w_2$ and $y_2 = -w_1$, we have

$$\partial_t S \leq -(1 - \mu^2\gamma_2^2)|y_1|^2 - (\mu^2 - \gamma_1^2)|y_2|^2.$$

Thus, since $\gamma_1\gamma_2 < 1$, $(\mu\gamma_2)^2 < 1$ and $\mu^2 > \gamma_1^2$, it follows that the time derivative of the storage functional S is non-positive, which, in turn, implies that the interconnected PDE system is stable in $\mathcal{H}^q_\Omega$. □

4.3.2 PDE-ODE Interconnections

In the following, we consider interconnection of PDE systems and ODE systems, where the interconnection is assumed to be at the boundary of the domain. First, we show that if both the PDE subsystem and the ODE subsystem have bounded induced $\mathcal{L}^2$-norm then the interconnection has bounded induced $\mathcal{L}^2$-norm. Secondly, we demonstrate that PDE-ODE interconnections (cascades) preserve the ISS property, provided that each subsystem is ISS.

Theorem 4.3.3 *Consider the following PDE-ODE system subject to dynamic disturbance at the boundary*

$$\begin{cases} \partial_t u = F(x, D^\alpha u),\ x \in \Omega,\ t > 0, \\ y = H(x, D^\beta u), \\ D^{\alpha-1}u(t,0) = 0, \\ D^{\alpha-1}u(t,1) = z(t). \end{cases} \tag{4.40}$$

$$\begin{cases} \frac{dX(t)}{dt} = f\left(X(t), d(t)\right),\ d \in \mathcal{L}^2_{[0,\infty)}, \\ z(t) = X(t). \end{cases} \tag{4.41}$$

Let (4.40) *have bounded induced $\mathcal{L}^2_\Omega$-norm η and* (4.41) *have bounded induced $\mathcal{L}^2_{[0,\infty)}$-norm γ. Then, the overall interconnection has bounded induced $\mathcal{L}^2_{[0,\infty)}$-to-$\mathcal{L}^2_\Omega$-norm $\eta\gamma$.*

Proof: Since both systems (4.40) and (4.41) have bounded induced $\mathcal{L}^2$-norms with $\mathcal{L}^2$-gains $\eta > 0$ and $\gamma > 0$, respectively, they satisfy the following inequalities

$$\partial_t S(u) \leq -\int_\Omega y^2\, dx + \eta^2 z^2(t) \tag{4.42}$$

$$\partial_t s(X) \leq -z^2(t) + \gamma^2 d^2(t). \tag{4.43}$$

for storage functional $S(u)$ and storage function $s(X)$. Let us define the following storage functional for the interconnected system

$$\Sigma(u, X) = S(u) + \eta^2 s(X). \tag{4.44}$$

Then, the time derivative of the storage functional yields

$$\begin{aligned} \partial_t \Sigma(u, X) &= \partial_t S + \eta^2 \partial_t s(X) \\ &\leq -\int_\Omega y^2 \, dx + \eta^2 z^2(t) - \eta^2 z^2(t) + \eta^2 \gamma^2 d^2(t) \\ &= -\int_\Omega y^2 \, dx + \eta^2 \gamma^2 d^2(t). \end{aligned} \tag{4.45}$$

Therefore, the interconnected system has bounded induced $\mathcal{L}^2_{[0,\infty)}$-to-$\mathcal{L}^2_\Omega$-norm $\eta\gamma$. □

Theorem 4.3.4 *Consider the following ODE-PDE system in cascade interconnection*

$$\begin{cases} \partial_t u = F(x, D^\alpha u), \ x \in [0,1], \ t > 0, \\ D^{\alpha-1} u(t, 0) = 0, \\ D^{\alpha-1} u(t, 1) = z(t). \end{cases} \tag{4.46}$$

$$\begin{cases} \frac{dX(t)}{dt} = f\left(X(t), d(t)\right), \ d \in \mathcal{L}^\infty_{[0,\infty)} \\ z(t) = X(t). \end{cases} \tag{4.47}$$

If both systems (4.46) *and* (4.47) *satisfy the ISS property, then the interconnection is ISS, as well.*

Proof: If both systems (4.46) and (4.47) satisfy the ISS property, then there exist storage function/functionals S for the PDE system and storage function s for the ODE systems,

such that

$$\partial_t S(u) \leq -\alpha\left(S(u)\right) + \sigma\left(|X(t)|\right), \tag{4.48}$$

$$\partial_t s(X) \leq -2\sigma\left(|X(t)|\right) + \gamma(|d(t)|), \tag{4.49}$$

for some $\alpha, \sigma \in \mathcal{K}_\infty$ and $\gamma \in \mathcal{K}$. At this point, to show that the ISS-property of the cascade holds, we consider the following storage functional

$$\Sigma(u, X) = S(u) + s(X).$$

Then, functional Σ satisfies

$$\partial_t \Sigma(u, X) \leq -\alpha\left(S(u)\right) - \sigma\left(|X(t)|\right) + \gamma(|d(t)|). \tag{4.50}$$

□

4.4 Computation of Storage Functionals

For computational purposes, we assume that the studied PDEs are polynomial in the dependent and independent variables, *i.e.,* functions F and H in (4.1) and functions F and h in (4.25) are all polynomials. The following structure is also considered as a candidate storage functional to check the dissipation inequalities given in Theorem 4.1.5 and Corollary 4.2.3:

$$S(u) = \frac{1}{2}\langle u, P(x)u\rangle_{\mathcal{H}^q_\Omega} := \frac{1}{2}\int_0^1 (D^q u)' P(x)(D^q u)\, dx, \tag{4.51}$$

where, $P(x) : \Omega \to \mathbb{S}^{n(\alpha+1)}$ is a symmetric positive definite polynomial matrix function for all $x \in \Omega$. This storage functional candidate satisfies

$$\frac{1}{2}\lambda_m(P)\|u\|^2_{\mathcal{H}^q_\Omega} \leq S(u) \leq \frac{1}{2}\lambda_M(P)\|u\|^2_{\mathcal{H}^q_\Omega}. \tag{4.52}$$

Therefore, $(S(u))^{\frac{1}{2}}$ is equivalent to the $\mathcal{H}^q_\Omega$-norm.

4.4.1 PDEs with In-domain Inputs/Outputs

Next, we discuss how conditions of Theorem 4.1.5 can be checked via integral inequalities.

Remark 4.4.1 *From* (4.52)*, it follows that* (4.9) *and* (4.13) *are satisfied, respectively, with* $\beta_1(\cdot) = \frac{\lambda_m(P)}{2}(\cdot)^2$, $\beta_1^{-1}(\cdot) = \sqrt{\frac{2}{\lambda_m(P)}(\cdot)}$, *and* $\beta_2(\cdot) = \frac{\lambda_M(P)}{2}(\cdot)^2$. □

Let $\eta = \gamma^2$. For reachability analysis, we solve the following minimization problem:

Problem 1: (Reachability for system (4.1))

$$\begin{gathered}\underset{P(x)}{\text{minimize}}\ \eta \\ \text{subject to} \\ (4.10),\ \text{and}\ \nu^2 I < P(x),\end{gathered} \tag{4.53}$$

where, $\nu > 0$ is a constant.

In this case, the reachability estimate (4.3) transforms to

$$\|u(T,\cdot)\|_{\mathcal{H}^q_\Omega} \leq \frac{\gamma}{\nu}\|d\|_{\mathcal{H}^p_{[0,T),\Omega}}, \quad \forall T > 0. \tag{4.54}$$

Similarly, for induced $\mathcal{H}^p$-to-$\mathcal{H}^q$-norm, the following minimization problem is solved:

Problem 2: (Induced $\mathcal{H}^p$-to-$\mathcal{H}^q$ norm for system (4.1))

$$\begin{aligned} &\underset{P(x)}{\text{minimize}}\ \eta \\ &\text{subject to} \\ &(4.12). \end{aligned} \tag{4.55}$$

When adopting the storage functional structure (4.51) for D^p-ISS in $\mathcal{H}^q_\Omega$, it is possible to check the condition

$$\partial_t S(u) \leq -\int_\Omega (D^q u)' \alpha(x) (D^q u)\, dx + \int_\Omega \sigma(|D^p d(t,x)|)\, dx,$$

instead of (4.14), where $\alpha : \Omega \to \mathbb{S}^n$ is a symmetric positive definite polynomial function for all $x \in \Omega$ and σ is chosen as the sum of some even monomials of d. In this case, the D^p-ISS estimate translates to

$$\|u(t,\cdot)\|_{\mathcal{H}^q_\Omega} \leq \left(e^{-\frac{\lambda_m(\alpha)}{\lambda_m(P)}t}\left(\|u_0\|^2_{\mathcal{H}^q_\Omega}\right)\right)^{\frac{1}{2}} + \left(\frac{1}{\lambda_m(\alpha)} \sup_{\tau\in[0,t)} \left(\int_\Omega \sigma(|D^p d(\tau,x)|)\, dx\right)\right)^{\frac{1}{2}}. \tag{4.56}$$

4.4.2 PDEs with Boundary Inputs and Boundary Outputs

In this subsection, we discuss a computational formulation of Corollary 4.2.3. To formulate the problem in terms of integral inequalities with polynomial integrands, we assume that the function σ in inequality (4.35) is polynomial, while the storage functional is given by (4.51).

Substituting (4.25) in inequalities (4.30), (4.32), (4.33), and (4.35) respectively yields

$$\text{I)} \qquad \partial_t S(u) \leq \left(D^{\alpha-1}u(t,1)\right)' B' h \left(D^\beta u(t,0)\right), \tag{4.57}$$

$$\text{II)} \quad \partial_t S(u) \leq \gamma^2 \left(D^{\alpha-1}u(t,1)\right)' B'B \left(D^{\alpha-1}u(t,1)\right), \tag{4.58}$$

$$\begin{aligned} \text{III)} \qquad \partial_t S(u) \;&\leq\; -h'\left(D^{\beta}u(t,0)\right) h\big(D^{\beta}u(t,0)\big) \\ &\quad +\gamma^2\big(D^{\alpha-1}u(t,1)\big)'B'B\big(D^{\alpha-1}u(t,1)\big), \end{aligned} \tag{4.59}$$

$$\text{IV)} \quad \partial_t S(u) \leq -\int_{\Omega} (D^q u)'\alpha(x)(D^q u)\, dx + \sigma\left(\left|BD^{\alpha-1}u(t,1)\right|\right), \tag{4.60}$$

where $\alpha : \Omega \to \mathbb{S}^{n(\alpha+1)}$ is a symmetric positive definite polynomial matrix function for all $x \in \Omega$. Let $\eta = \gamma^2$. For reachability analysis, the following minimization problem is solved:

Problem 3: (Reachability for system (4.25))

$$\begin{gathered} \underset{P(x)}{\text{minimize}}\ \eta \\ \text{subject to} \\ \text{(4.58), and } \nu^2 I < P(x) \quad , \end{gathered} \tag{4.61}$$

where, $\nu > 0$ is a constant.

Then, the reachability estimate (4.27) transforms to

$$\|u(T,\cdot)\|_{\mathcal{H}^q_\Omega} \leq \frac{\gamma}{\nu}\|w\|_{\mathcal{L}^2_{[0,T)}}, \quad \forall T > 0. \tag{4.62}$$

Analogously, we solve the following minimization problem for $\mathcal{L}^2_{[0,\infty)}$-to-$\mathcal{H}^q$-norm:

Problem 4: (Induced $\mathcal{L}^2_{[0,\infty)}$-to-$\mathcal{H}^q$ norm for system (4.25))

$$\begin{gathered} \underset{P(x)}{\text{minimize}}\ \eta, \\ \text{subject to} \\ \text{(4.59).} \end{gathered} \tag{4.63}$$

Provided that the problem data are polynomial in the dependent variables, we can formulate SOS programs as discussed in Chapter 3 to solve the inequalities discussed in this section.

4.5 Numerical Examples

In this section, we illustrate the proposed results in this chapter using four numerical examples.

4.5.1 Heat Equation with Reaction Term

Consider the following PDE system

$$\begin{cases} \partial_t u = \partial_x^2 u + \lambda(x)u + \epsilon(x)d, \quad \forall x \in [0,1] \text{ and } \forall t \geq 0 \\ y = u, \\ u(0,t) = u(1,t) = 0, \ t \geq 0. \end{cases} \tag{4.64}$$

For $d = 0$, the system is exponentially stable for $\lambda(x) = \lambda_0 < \pi^2$ [116, p. 11]. For passivity analysis, let $\epsilon(x) = 1$ and $\lambda(x) = \lambda_0$. Applying condition (4.8) in Theorem 4.1.5, certificates could be found that passivity property holds for $\lambda_0 < 0.2\pi^2$.

With respect to reachability analysis, let $\epsilon(x) = 100x(1-x)$ and $\lambda = 0$. With this choice of the function $\epsilon(x)$, the in-domain input d has its maximum amplification at $x = 0.5$. The polynomial $P(x)$ is set to 1, so that the Lyapunov functional represents the $\mathcal{L}^2_\Omega$-norm of solutions. Table 4.1 provides the attained results. As expected, for larger values of parameter λ, as the system approaches the instability bound, the reachable set is enlarged.

In the case of induced $\mathcal{L}^2$-to-$\mathcal{L}^2$-norm, certificates were found for $\mathcal{L}^2$-to-$\mathcal{L}^2$-norm boundedness for $\lambda(x) = \lambda_0 \leq 0.4\pi^2$. Table 4.2 presents the results from the numerical experi-

Table 4.1: Reachability analysis results for Equation (4.64).

$\frac{\lambda}{\pi^2}$	0	0.2	0.4	0.6	0.8
γ	5.76	6.79	8.62	12.46	29.71

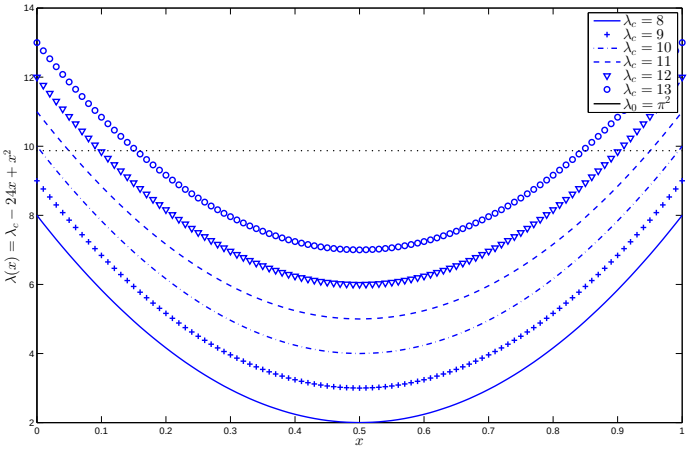

Figure 4.2: The spatially varying coefficients for Equation (4.69).

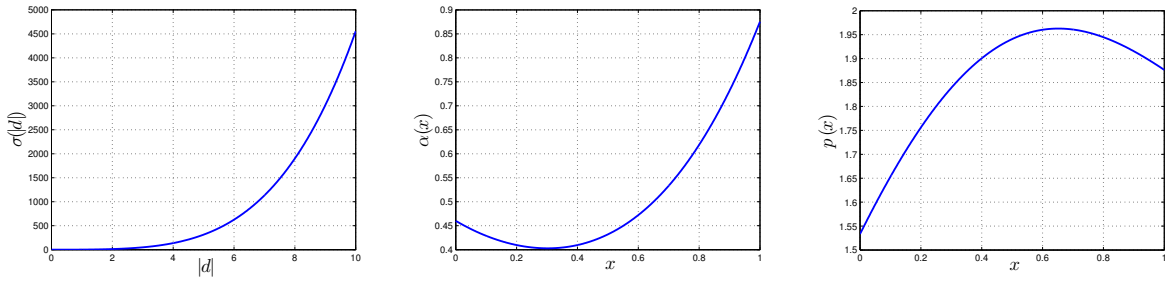

Figure 4.3: ISS certificates for Equation (4.69) (with $\lambda = 0.2\pi^2$).

ments. It can be deduced from the table that, from $\lambda_0 = 0.3\pi^2$ to $\lambda_0 = 0.4\pi^2$, the induced $\mathcal{L}^2$-gain increases.

Take $\lambda(x) = \lambda_c - 24x + 24x^2$ and $\epsilon(x) = 100x(1-x)$. Figure 4.2 depicts the spatially varying parameter $\lambda(x)$ with different values of λ_c. As it can be observed, for $\lambda_c \in \{10, 11, 12, 13\}$, the coefficients exceed the stability bound for constant λ; *i.e.,* $\lambda(x) = \lambda_0 = \pi^2$. Table 4.3 summarizes the obtained results.

Finally, certificates for ISS are studied. The experiments were performed with construction of polynomials $P(x)$, $\alpha(x)$, and $\sigma(u)$ to certify ISS property. Certificates for ISS

Table 4.2: Induced $\mathcal{L}^2$-norm results for Equation (4.64) subject to constant coefficients.

$\frac{\lambda}{\pi^2}$	0	0.2	0.3	0.35	0.39
γ^2	0.0560	0.1876	0.5465	1.296	6.158
Total Time (s)	16.87	18.09	18.35	16.89	18.23

Table 4.3: Induced $\mathcal{L}^2$-norm results for Equation (4.64) subject to spatially varying coefficients.

λ_c	8	9	10	11	12	13
γ^2	6.503	6.987	4.612	5.989	7.676	10.261
Total Time (s)	16.87	18.09	18.35	16.89	18.23	17.22

property were constructed for $\lambda(x) = \lambda_0 \leq 0.5\pi^2$. Fig. 4.3 presents the results obtained from numerical experiments for $\lambda_0 = 0.2\pi^2$.

4.5.2 Coupled Reaction-Diffusion PDEs

Consider the following system of coupled reaction-diffusion PDEs

$$\Sigma : \begin{cases} \partial_t u = \partial_x^2 u + \lambda u - v \\ \partial_t v = \partial_x^2 v + \lambda v + u \end{cases}, \; x \in [0,1], \; t > 0 \tag{4.65}$$

subject to $u(t,0) = u(t,1) = v(t,0) = v(t,1) = 0$, where $\lambda > 0$. In the following, we show that system (4.65) is exponentially stable in $\mathcal{L}^2_\Omega$ for $\lambda < \pi^2$. We consider the following energy functional in $\mathcal{L}^2_\Omega$

$$E(u,v) = \frac{1}{2}\|(u,v)\|^2_{\mathcal{L}^2_\Omega} = \frac{1}{2}\int_0^1 \left(u^2 + v^2\right) \, dx. \tag{4.66}$$

Table 4.4: Obtained bounds on induced $\mathcal{L}^2_\Omega$-norm for Equation (4.68).

$\frac{\lambda}{\pi^2}$	0	0.3	0.5	0.75	0.8
γ^2	0.014	0.033	0.079	0.712	1.318

The time derivative of the above energy functional along the solutions of (4.65) is given by

$$\begin{aligned}
\partial_t E(u,v) &= \int_0^1 \left(u\left(\partial_x^2 u + \lambda u - v\right) + v\left(\partial_x^2 v + \lambda v + u\right)\right)\, dx \\
&= \int_0^1 \left(u\partial_x^2 u + \lambda u^2 + v\partial_x^2 v + \lambda v^2\right)\, dx \\
&= \left(u\partial_x u\right)|_{x=0,1} + \left(v\partial_x v\right)|_{x=0,1} + \int_0^1 \left(-\left(\partial_x u\right)^2 + \lambda u^2 - \left(\partial_x v\right)^2 + \lambda v^2\right)\, dx \\
&= -\int_0^1 \left(\left(\partial_x u\right)^2 + \left(\partial_x v\right)^2\right)\, dx + \lambda \int_0^1 \left(u^2 + v^2\right)\, dx,
\end{aligned}$$

where in the last inequality the boundary conditions $u(t,0) = u(t,1) = v(t,0) = v(t,1) = 0$ is used. Applying the Poincaré inequality to the last equality above, we obtain

$$\begin{aligned}
\partial_t E(u,v) &\leq -\pi^2 \int_0^1 \left(u^2 + v^2\right)\, dx + \lambda \int_0^1 \left(u^2 + v^2\right)\, dx \\
&= -2\pi^2 \left(1 - \frac{\lambda}{\pi^2}\right) E(u,v). \qquad (4.67)
\end{aligned}$$

That is, $E(u,v) \leq E(u_0,v_0)e^{-2\pi^2\left(1-\frac{\lambda}{\pi^2}\right)t}$ for $\lambda < \pi^2$.

However, we can infer the stability properties of Σ by decomposing it into an interconnection of two PDEs, *i.e.,* Σ_1 and Σ_2 given by

$$\Sigma_i : \begin{cases} \partial_t u_i = \partial_x^2 u_i + \lambda u_i \\ y_i = u_i \end{cases}, \; i = 1,2. \qquad (4.68)$$

where $u_1 = u$ and $u_2 = v$ with the interconnection as in Figure 4.1. Remark that both Σ_1 and Σ_2 are ZSD in $\mathcal{L}^2_\Omega$, since $y_i = 0$ implies $u_i = 0$, for $i = 1,2$. From Table 4.4, it can be inferred that we could find certificates that equation (4.64) with $\epsilon(x) = 0$ has induced $\mathcal{L}^2_\Omega$-norm $\gamma < 1$ for $\lambda \leq 0.75\pi^2$. Since both Σ_1 and Σ_2 are in the form of (4.64) with

Table 4.5: Results pertained to induced $\mathcal{L}^2$-to-$\mathcal{L}^2$-norm for PDE (4.69).

$\frac{\sqrt{2}\beta}{\pi}$	0	0.1	0.12	0.15	0.18	0.2
γ^2	0.195	0.306	0.351	0.452	0.666	1.062

$\epsilon(x) = 0$, we infer that $\gamma_1 < 1$ and $\gamma_2 < 1$ for $\lambda \leq 0.75\pi^2$. Thus, $\gamma_1\gamma_2 < 0.507 < 1$ for $\lambda \leq 0.75\pi^2$. Therefore, conditions of Theorem 4.3.1 are satisfied. Thus, system Σ, which is the interconnection of Σ_1 and Σ_2 is asymptotically stable for $\lambda \leq 0.75\pi^2$. This is consistent with the results from energy stability analysis, *i.e.,* $\lambda < \pi^2$.

4.5.3 Burgers' Equation with Nonlinear Forcing [116, 62]

Consider the following PDE

$$\begin{cases} \partial_t u = \frac{1}{R}\partial_x^2 u - \delta u \partial_x u + \beta u^2 + d, \\ u(t,0) = 0,\ u(t,1) = w(t),\ \ (t,x) \in \mathbb{R}_{\geq 0} \times [0,1] \end{cases} \tag{4.69}$$

subject to $d(t,0) = d(t,1) = 0$ for all $t \geq 0$, where R, δ, β are constants.

4.5.3.1 In-domain Analysis ($w \equiv 0$, $R = 1$ and $\delta = 1$)

Let $y(t,x) = u(t,x),\ (t,x) \in \mathbb{R}_{\geq 0} \times [0,1]$. The system without inputs ($d \equiv 0,\ w \equiv 0$) is exponentially stable for $\beta < \frac{\pi}{\sqrt{2}}$ [116, p. 20]. Using condition (4.8) in Theorem 4.1.5, certificates were found for passivity just for $\beta = 0$. For the induced $\mathcal{L}^2$-to-$\mathcal{L}^2$-norm, Table 4.5 provides the numerical details of the numerical experiments. From numerical experiments, certificates were constructed for $\mathcal{L}^2$-to-$\mathcal{L}^2$-norm boundedness of system (4.69) for $\beta \leq 0.2\frac{\pi}{\sqrt{2}}$.

At this point, let $\beta = 0$. Similar to nonlinear ODEs, we expect the nonlinear PDE to have a nonlinear induced $\mathcal{L}^2$-to-$\mathcal{L}^2$ gain function [39]. Figure 4.4 illustrates the obtained (upper bound) gain functions from numerical experiments. There are three noteworthy regions in the gain curve. For small values of the input $\mathcal{L}^2$-norm, the nonlinear gain curve

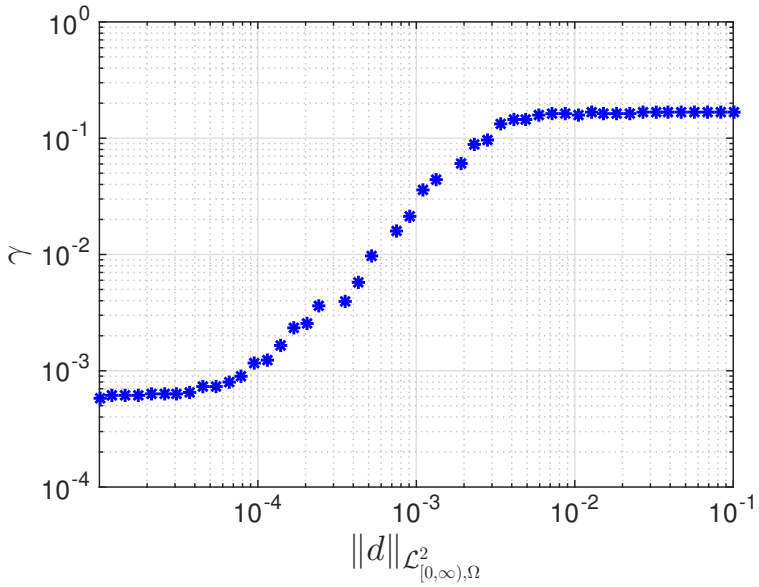

Figure 4.4: The $\mathcal{L}^2$-to-$\mathcal{L}^2$ gain curve.

is relatively constant until a threshold is reached. This section corresponds only to the linear part of the PDE. Then, the gain nonlinearly increases until it reaches an upper bound which is approximately the bound obtained using only energy as the storage functional.

In addition, for different values of the parameter R, we computed the induced $\mathcal{L}^2$-to-$\mathcal{L}^2$ norms using the energy functional $P(x) = I$ and using storage functional (4.51) of degree 8. The results are illustrated in Figure 4.5. As it can be observed, the bounds obtained using the energy method remain constant for all values of input norm for fixed R. Moreover, they upper-bound the induced norms computed by storage functional (4.51). This implies that the energy functional is not suitable for capturing the nonlinear dynamics of the PDE.

4.5.3.2 Boundary Analysis ($d \equiv 0$)

Assume $y(t) = \partial_x u(t, 0),\ t > 0$. Let $\delta = \beta = 0$. First, we study the upper bounds on γ as in (4.28). It is assumed $u_0(x) \equiv 0,\ \forall x \in [0, 1]$. Figure 4.6 illustrates the results obtained for $R \in [0.01, 10]$. For each R, Problem 4 is solved and the minimum γ is shown in the figure. As it can be inferred from the figure, as R increases and therefore the diffusion term

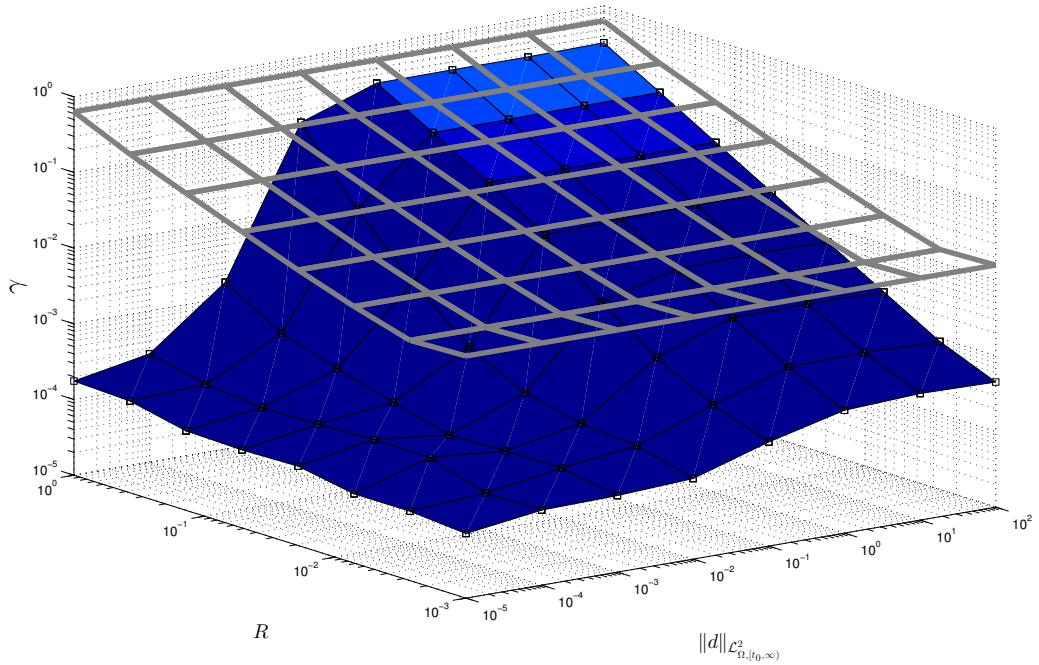

Figure 4.5: The $\mathcal{L}^2$-to-$\mathcal{L}^2$ gain curve in terms of R. The gray net illustrates the induced $\mathcal{L}^2$-to-$\mathcal{L}^2$ norms using the energy functional and the blue surface represents the induced $\mathcal{L}^2$-to-$\mathcal{L}^2$ norms obtained using storage functional (4.51).

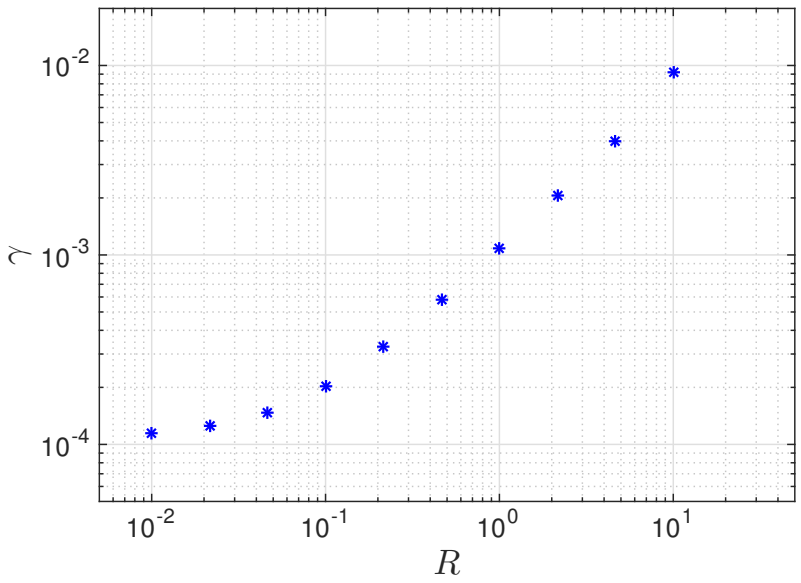

Figure 4.6: The obtained upper bounds on induced $\mathcal{L}^2_{[0,\infty)}$-to-$\mathcal{L}^2$-norm.

attenuates, the obtained bounds on γ increase.

At this point, we study the ISS property in $\mathcal{L}^2_\Omega$ of system (4.69) with $\delta = 1$ and $R = 1$. The ISS bound on β for which ISS certificates could be found was $\beta = (0.43)\frac{\pi}{\sqrt{2}}$. Figure 4.7 depicts the constructed certificates $P(x)$ and $\alpha(x)$ for $\beta = (0.43)\frac{\pi}{\sqrt{2}}$. Also, certificate $\sigma(w)$ is calculated as

$$\sigma(w) = 0.9506w^4 + 7.1271w^2.$$

4.5.4 Example IV: Kuramoto-Sivashinsky Equation [54, 34]

Consider the following PDE

$$\begin{cases} \partial_t u = -\partial_x^4 u - \lambda \partial_x^2 u - u\partial_x u + d, \\ y = u, \quad (t,x) \in \mathbb{R}_{\geq 0} \times [0,1], \\ u(t,0) = u(t,1) = \partial_x u(t,0) = \partial_x u(t,1) = 0. \end{cases} \tag{4.70}$$

It was demonstrated in [67] that for *constant* λ the system is exponentially stable in $\mathcal{H}^2_\Omega$-norm (thus, from Sobolev Embedings, stable in $\mathcal{H}^1_\Omega$-norm as well) for $\lambda \leq 4\pi^2$.

First, we consider computing upper bounds on the induced $\mathcal{L}^2$-to-$\mathcal{H}^1$-norm of the system. The results are presented in Table 4.6. Figure 4.8 shows the elements of the 2×2 matrix $P(x)$ in the storage functional and its eigenvalues for $\lambda = (0.9)4\pi^2$.

Finally, let $\lambda(x) = \lambda_0 - 16\pi^2 x(1-x)$. Then, in (4.70), the spatially varying coefficient $\lambda(x)$ crosses the stability bound $\lambda = 4\pi^2$ (at least) at subsets of the domain for $\lambda_0 \geq 4\pi^2$. We seek upper bounds on λ_0 such that certificates for D^1-ISS in $\mathcal{H}^1_\Omega$ can be found. For constant λ, certificates could only be found up to $\lambda = (0.62)4\pi^2$. However, for the spatially varying λ, we could construct certificates for D^1-ISS in $\mathcal{H}^1_\Omega$ for $\lambda_0 = (1.83)4\pi^2$. Figure 4.9

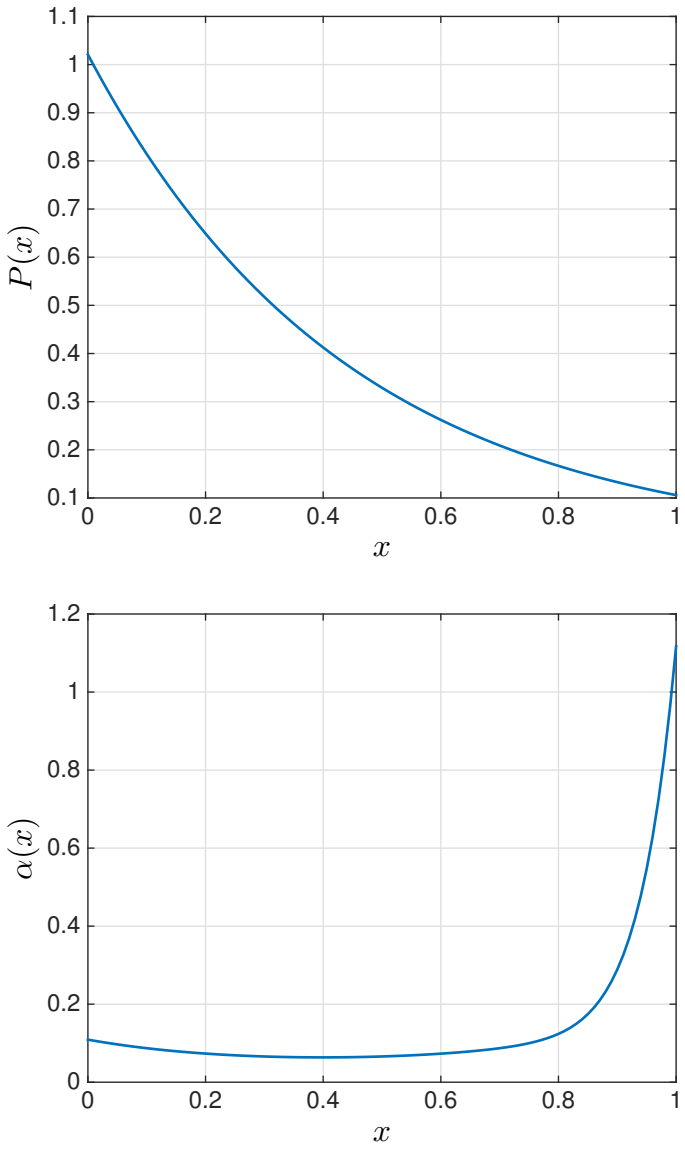

Figure 4.7: The ISS certificates $P(x)$ (top) and $\alpha(x)$ (bottom).

illustrates the eigenvalues of certificates $P(x)$ and $\alpha(x)$ for the case $\lambda_0 = (1.83)4\pi^2$ and $\sigma(d, \partial_x d)$ was calculated as

$$\sigma(d, \partial_x d) = 3.2314d^2 + 4.0093(\partial_x d)^2.$$

Table 4.6: Results pertained to induced $\mathcal{L}^2$-to-$\mathcal{H}^1$-norm for PDE (4.70).

$\frac{\lambda}{4\pi^2}$	0.3	0.5	0.55	0.6	0.7	0.9
γ^2	0.003	0.048	0.517	1.211	3.229	9.840

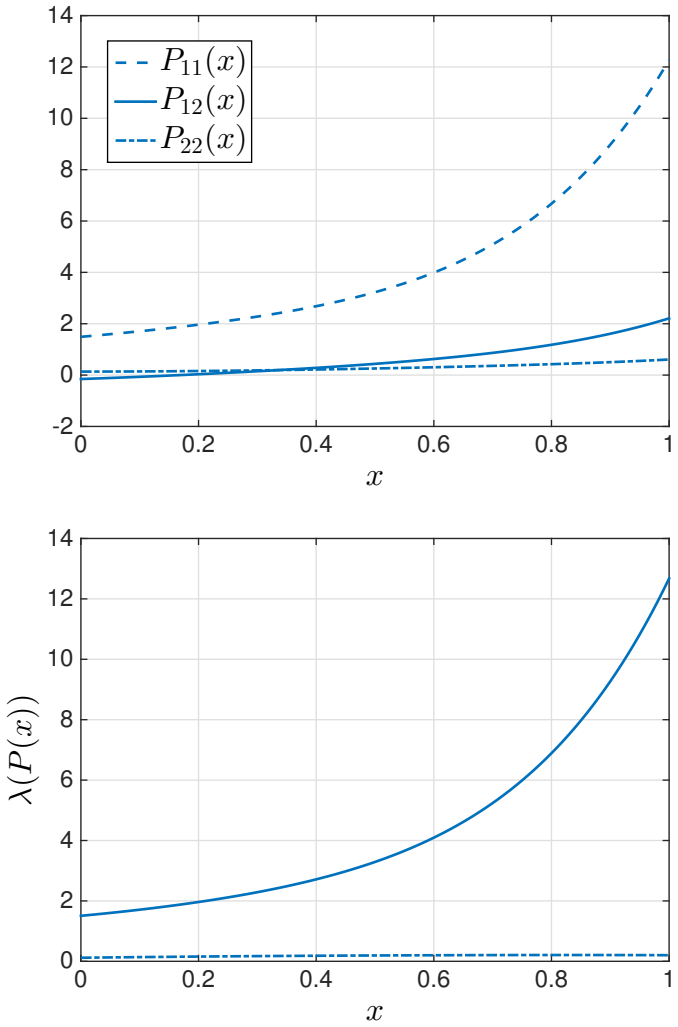

Figure 4.8: The entries of $P(x)$ (top) and the eigenvalues of $P(x)$ (bottom) for the case $\lambda = (0.9)4\pi^2$.

4.6 Further Discussions: Finite-Dimensional Inputs and Outputs

In this section, we elaborate on some further remarks. In particular, we delve further into the case when the PDE system is subject to finite-dimensional inputs and outputs.

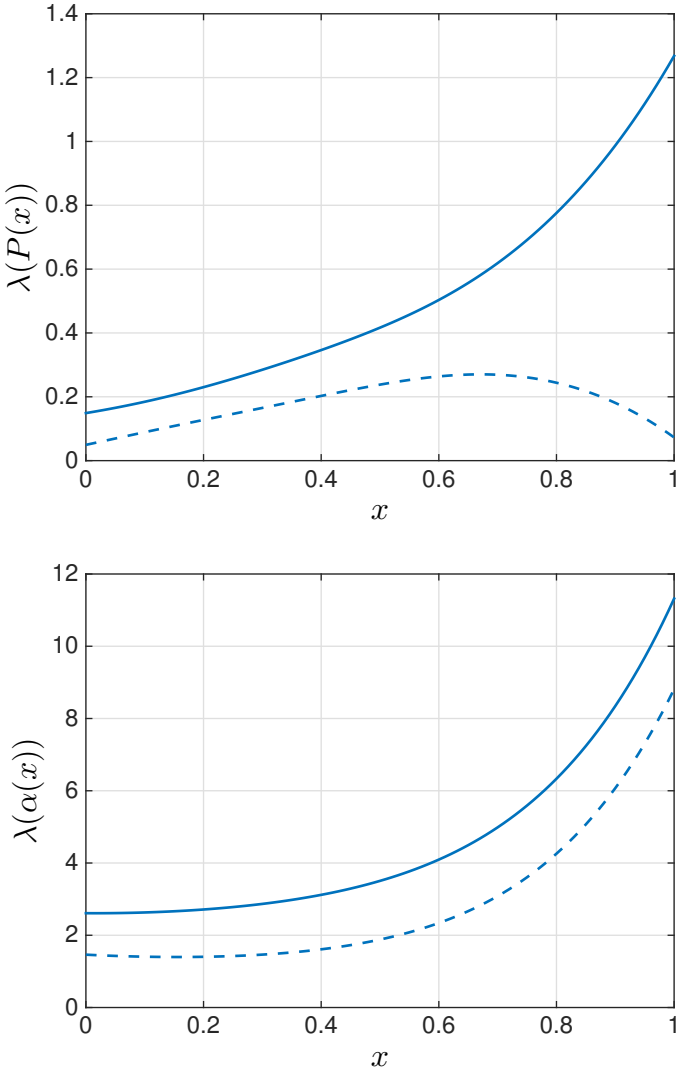

Figure 4.9: D^1-ISS in $\mathcal{H}^1_\Omega$ certificates for PDE (4.70) with $\lambda_0 = (1.8)4\pi^2$.

The case of finite dimensional inputs and outputs defined at the boundaries was discussed in Section 4.2. Regarding inputs and outputs of the form

$$\bar{d}(t,x) = b(x)d(t), \tag{4.71}$$

$$y(t) = \int_\Omega c(x)u(t,x)\,dx, \tag{4.72}$$

we describe how the proposed formulation in this chapter can address these types of inputs and outputs as follows.

With respect to $\bar{d}(t,x)$, note that

$$\|\bar{d}(t,x)\|_{\mathcal{H}^q_{[0,T),\Omega}} = \|b(x)d(t)\|_{\mathcal{H}^q_{[0,T),\Omega}} = \left(\int_0^T \langle b(x)d(t), b(x)d(t)\rangle_{\mathcal{H}^q_\Omega} \ dt\right)^{\frac{1}{2}}$$
$$= \left(\int_0^T d'(t)d(t)\|b(x)\|^2_{\mathcal{H}^q_\Omega} \ dt\right)^{\frac{1}{2}} = \|b(x)\|_{\mathcal{H}^q_\Omega}\|d(t)\|_{\mathcal{L}^2_{[0,T)}}. \quad (4.73)$$

Thus, for $\bar{d}(t,x)$, we can obtain bounds on its $\mathcal{H}^q$ norm as the ones presented in Section 4.1, as long as $b \in \mathcal{H}^q_\Omega$ and $d \in \mathcal{L}^2_{[0,T)}$.

Regarding $y(t)$, consider the class of PDE systems described by

$$\begin{cases} \partial_t u(t,x) = F\left(x, D^{\alpha_u}u(t,x)\right) + G(x)d(t), \\ y(t) = \int_0^1 h(x, D^\beta u(t,x))\, dx, \quad (t,x) \in \mathbb{R}_{\geq 0} \times \Omega, \\ B\begin{bmatrix} D^{\alpha_u - 1}u(t,1) \\ D^{\alpha_u - 1}u(t,0) \end{bmatrix} = 0, \end{cases} \quad (4.74)$$

and initial conditions $u(0,x) = u_0(x)$. The dependent variables $u : \mathbb{R}_{\geq 0} \times \Omega \to \mathbb{R}^{n_u}$, $d : \mathbb{R}_{\geq 0} \to \mathbb{R}^{n_d}$, and $y : \mathbb{R}_{\geq 0} \to \mathbb{R}^{n_y}$ represent states, inputs, and outputs, respectively, $G(x) = diag(g_1(x), g_2(x), \ldots, g_{n_d}(x))$, $\beta < \alpha_u$, B is a matrix of appropriate dimension defining the boundary conditions, and h is a nonlinear function. In order to apply the methods proposed in Chapter 3, let us define a new dependent variable $\bar{y}(t,x)$ as

$$\bar{y}(t,x) = \int_0^x h(\eta, D^\beta u(t,\eta)) \ d\eta,$$

with the boundary values

$$\bar{y}(t,0) = 0, \ \bar{y}(t,1) = y(t), \quad (4.75)$$

and the differential equation

$$\partial_x \bar{y}(t,x) - h(x, D^\beta u(t,x)) = 0. \quad (4.76)$$

We can then include the differential equation (4.76) in system (4.74) as an equality constraint relating u and $\bar{y}$. In order to illustrate how we incorporate equality constraints in the proposed formulation, *i.e.,* in the integral constraints, we provide the following steps. Let

$$\begin{aligned}\mathcal{M} = &\int_{\Omega} \left(D^{\alpha} v(t,x)\right)' M(x) D^{\alpha} v(t,x)\, dx \\ &- \left(\left(D^{\alpha-1} v(t,1)\right)' M_1 \left(D^{\alpha-1} v(t,1)\right) - \left(D^{\alpha-1} v(t,0)\right)' M_0 \left(D^{\alpha-1} v(t,0)\right) \right) \end{aligned} \tag{4.77}$$

and

$$\mathcal{V}_S(B) = \left\{ v \mid B \begin{bmatrix} D^{\alpha-1} v(t,1) \\ D^{\alpha-1} v(t,0) \end{bmatrix} = 0 \right\}. \tag{4.78}$$

We are interested in solving the following problem:

$$\begin{aligned} &\text{Verify} \quad \mathcal{M} \geq 0 \\ &v \in \mathcal{V}_S(B),\ p\left(x, D^{\beta} v(t,x)\right) = 0. \end{aligned} \tag{4.79}$$

Since $p\left(x, D^{\beta} v(t,x)\right) = 0$ holds for all $x \in \Omega$, we have $N(x) p\left(x, D^{\beta} v(t,x)\right) = 0,\ \forall x \in \Omega$ for any $N(x) : \Omega \to \mathbb{R}^{M_p}$. Hence,

$$\bar{\mathcal{M}} = \mathcal{M},\ \ \forall v \in \mathcal{V}_S(B) \text{ and } \forall v \in \left\{ v \mid p\big(x, D^{\beta} v(t,x)\big) = 0 \right\},$$

where

$$\begin{aligned}\bar{\mathcal{M}} = &\int_{\Omega} \left(\left(D^{\alpha} v(t,x)\right)' M(x) D^{\alpha} v(t,x) + N(x) p\left(x, D^{\beta} v(t,x)\right) \right) dx \\ &- \left(\left(D^{\alpha-1} v(t,1)\right)' M_1 \left(D^{\alpha-1} v(t,1)\right) - \left(D^{\alpha-1} v(t,0)\right)' M_0 \left(D^{\alpha-1} v(t,0)\right) \right). \end{aligned} \tag{4.80}$$

Thus, we can convert the constrained feasibility problem (4.79) into the following uncon-

strained feasibility problem

$$\begin{aligned} &\text{Verify} \quad \bar{\mathcal{M}} \geq 0 \\ &v \in \mathcal{V}_S(B), \end{aligned} \tag{4.81}$$

which fits the framework discussed in Chapter 3.

The input-output properties of interest are then studied by Corollary 4.2.3 for finite dimensional inputs and outputs defined at the boundary.

4.7 Conclusions

In this chapter, we proposed a methodology for input-state/output analysis of PDEs using dissipation inequalities and we provided a systematic computational method for solving the dissipation inequalities in the case of polynomial data. Based on these tools, we studied passivity, reachability, induced norms and ISS for PDEs with in-domain inputs and outputs and PDEs with boundary inputs and outputs. The dissipation inequalities allowed us to establish properties of the interconnected PDE-PDE and PDE-ODE systems. We illustrated the proposed method by several examples of linear and nonlinear PDE systems.

In the next chapter, we look into another analysis problem of PDEs, *i.e.,* safety verification of PDEs. We also demonstrate that the safety verification method can be used for bounding output functionals of PDEs.

Chapter 5

Barrier Functionals for Safety Verification of PDEs

In the previous chapter, we discussed methods for input-state/output analysis of PDEs. Apart from input-output analysis, in many safety-critical applications in engineering, we are concerned with the so called safety verification problem, *i.e.,* given a set of initial conditions, checking whether all of the solutions of a given PDE do not violate a set of constraints characterized by an unsafe set, especially in bounded time intervals. Moreover, in many cases, we are interested in determining bounds on an output functional of the solutions of the PDE, rather than the PDE solutions. In both of these problems, solving the PDE directly for all initial conditions in a given set of initial conditions is overly computationally costly. Also, numerical methods often do not provide certificates.

In this chapter, we propose a method for safety verification of PDEs based on the construction of a functional of the states of the PDE that we refer to as the Barrier Functional. The method does not require solving the PDEs and, parallels the storage functionals or Lyapunov functionals for, respectively, input-output analysis or stability analysis of PDEs. We demonstrate that if such barrier functional exists, satisfying a set of inequalities, then the PDE solutions are safe. When the barrier functional is an integral functional, these

inequalities become integral inequalities, which can be checked via convex optimization in the case of polynomial data.

Furthermore, we show how the output functional estimation problem can be reformulated as a safety verification problem. Then, we can find upper-bounds on the output functionals by solving a polynomial optimization problem.

Two examples illustrate the proposed method.

The results associated with bounding output functionals of PDEs, were presented in the 2015 American Control Conference [3]. A journal version including the discussions on safety verification is currently under preperation [5].

5.1 Safety Verification for PDE Systems

In the current section, we define the safety verification problem and present a method based on an extension of barrier certificates to PDEs. We then illustrate the proposed method by an analytical example.

5.1.1 Problem Formulation

We study a class of forward-in-time PDE systems. Let $\mathcal{U}$ be a Hilbert space. Consider the following differential equation

$$\begin{cases} \partial_t u(t,x) = \mathscr{F} u(t,x), \quad x \in \Omega \subset \mathbb{R}^n,\ t \in [0,T], \\ y(t) = \mathscr{H} u(t,x) \\ u(0,x) = u_0(x) \in \mathcal{U}_0 \subset Dom(\mathscr{F}) \\ u \in \mathcal{U}_b \end{cases} \tag{5.1}$$

where $\mathcal{U}_b$ is a subspace of $\mathcal{U}$, the state-space of system (5.1), defined by the boundary conditions, $\mathscr{H} : \mathcal{U} \to \mathbb{R}$ and $Dom(\mathscr{H}) \supseteq \mathcal{U}$, the state-space of system (5.1).

We call the set

$$\mathcal{Y}_u := \{u \in \mathcal{U} \mid \mathscr{H}u \leq 0\},$$

the *unsafe set*.

As an example of system (5.1), consider the following system, $x \in [0,1],\ t \in [0,T]$,

$$\begin{cases} \partial_t u(t,x) = \partial_x^2 u(t,x) - u(t,x)\partial_x u(t,x), \\ y(t) = 5 - \int_\Omega u^2(t,\theta)\, d\theta - \partial_x u(t,1) \\ \mathcal{U}_0 = \{u_0 \in \mathcal{L}_2 \mid \|u_0\|_{\mathcal{L}_2} \leq 1; \partial_x u_0 \leq 0\} \\ \mathcal{U}_b = \left\{ u \in \mathcal{H}^1_\Omega \mid \begin{bmatrix} 1 & 0 & 0 & 0 \\ 0 & 0 & 1 & 0 \end{bmatrix} \begin{bmatrix} u(t,0) \\ \partial_x u(t,0) \\ u(t,1) \\ \partial_x u(t,1) \end{bmatrix} = 0 \right\}. \end{cases}$$

Then, by definition, we have

$$\mathcal{Y}_u = \left\{ u \in \mathcal{U}_b \mid 5 \leq \int_\Omega u^2(t,\theta)\, d\theta + \partial_x u(t,1) \right\}.$$

In this section, we present conditions to obtain certificates that trajectories starting in the set $\mathcal{U}_0$ are *safe* with respect to the set $\mathcal{Y}_u$. In other words, we present a method for *safety verification* of a PDE system.

Consider the following properties of trajectories related to an initial set $\mathcal{U}_0$ and an unsafe set $\mathcal{Y}_u$.

Definition 5.1.1 (Safety Verification at Time T) *Let $u \in \mathcal{U}$. For a set $\mathcal{U}_0 \subseteq \mathcal{U}$, an unsafe set $\mathcal{Y}_u$, satisfying $\mathcal{U}_0 \cap \mathcal{Y}_u = \emptyset$, and a positive scalar T, system* (5.1) is safe with respect to $\mathcal{Y}_u$ at time T, *if, for all $u(0,x) \in \mathcal{U}_0$, the solutions $u(t,x)$ of system* (5.1) *satisfy $y(T) \notin \mathcal{Y}_u$.*

Definition 5.1.2 (Safety Verification) *System* (5.1) *is safe with respect to* $\mathcal{Y}_u$*, if it is safe with respect to* $\mathcal{Y}_u$ *in the sense of Definition 5.1.1 for all* $T > 0$*.*

We are interested in solving the following problem:

Problem 5.1.3 *Given sets* $\mathcal{Y}_u$*,* $\mathcal{U}_0$ *and* $T > 0$*, verify that system* (5.1) *is safe with respect to* $\mathcal{Y}_u$ *at time* T*.*

To this end, we define a functional of the states of the PDE and time

$$B(t, u) = \mathscr{B}(t)u, \tag{5.2}$$

where $\mathscr{B}(t) : Dom(\mathscr{B}) \to \mathbb{R}$. We refer to this functional as the barrier functional. Note that this extension of barrier certificates [91] enables us to address sets that are defined on infinite-dimensional spaces. In the subsequent section, we show that the barrier functional provides the means to characterize a barrier between the set of initial conditions and the unsafe set.

5.1.2 Safety Verification Using Barrier Functionals

In the next theorem, we provide a solution to Problem 5.1.3 for PDE systems based on the construction of barrier functionals satisfying a set of inequalities.

Theorem 5.1.4 (Safety Verification for Forward PDE Systems) *Consider the PDE system described by* (5.1)*. Let* $u \in \mathcal{U}$*. Given a set of initial conditions* $\mathcal{U}_0 \subseteq \mathcal{U}$*, an unsafe set* $\mathcal{Y}_u$*, such that* $\mathcal{U}_0 \cap \mathcal{Y}_u = \emptyset$*, and a constant* $T > 0$*, if there exists a barrier functional* $B(t, u(t, x)) \in \mathcal{C}^1[t]$ *as in* (5.2)*, such that the following inequalities hold*

$$B(T, u(T, x)) - B(0, u_0(x)) > 0, \quad \forall u(T, x) \in \mathcal{Y}_u,\ \forall u_0 \in \mathcal{U}_0, \tag{5.3a}$$

$$\frac{dB(t, u(t, x))}{dt} \leq 0, \quad \forall t \in [0, T],\ \forall u \in \mathcal{U}, \tag{5.3b}$$

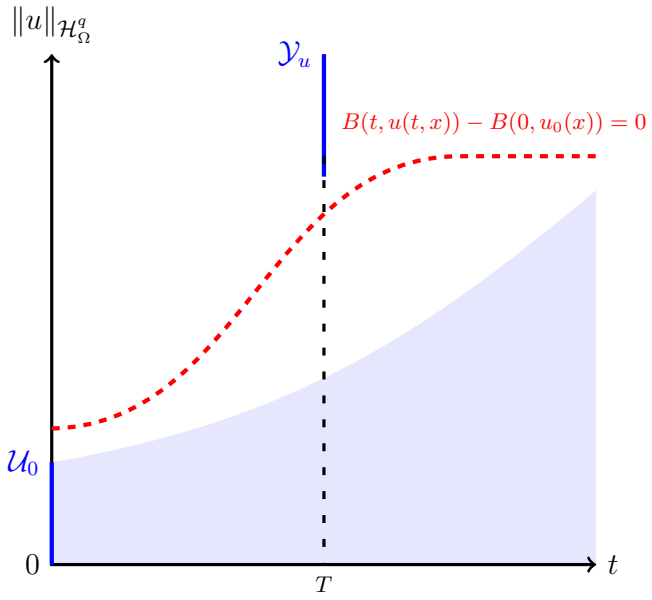

Figure 5.1: Illustration of a barrier functional for a PDE system: any solution $u(t,x)$ with $u(0,x) \in \mathcal{U}_0$ (depicted by the shaded area) satisfies $u(T,x) \notin \mathcal{Y}_u$. The system avoids $\mathcal{Y}_u$ at time $t = T$ but not for $\forall t > 0$.

along the solutions of (5.1)*, then the solutions of* (5.1) *are safe with respect to* $\mathcal{Y}_u$ *at time* T *(cf. Definition 5.1.1).*

Proof: The proof is by contradiction. Assume there exists a solution of (5.1) such that, at time T, $u(T,x) \in \mathcal{Y}_u$ and inequality (5.3a) holds. From (5.3b), it follows that

$$\frac{dB(t,u(t,x))}{dt} \leq 0, \tag{5.4}$$

for all $t \in [0,T]$, and $u \in \mathcal{U}$. Integrating both sides of (5.4) with respect to t from 0 to T yields

$$\int_0^T \frac{dB(t,u)}{dt}\, dt = B(T,u(T,x)) - B(0,u(0,x)) \leq 0.$$

for all $u \in \mathcal{U}$. This contradicts (5.3a). □

The level sets of $B(t,u(t,x)) - B(0,u_0(x))$ represent barrier surfaces in the $\mathcal{U}$ space separating $\mathcal{U}_0$ and $\mathcal{Y}_u$ such that no solution of (5.1) starting from $\mathcal{U}_0$ is in $\mathcal{Y}_u$ at time T (hence, the term "barrier functional"). This property is illustrated in Figure 5.1.

Theorem 5.1.4 is concerned with conditions for safety verification with respect to the unsafe set $\mathcal{Y}_u$ at a particular time $T > 0$. The next corollary follows from Theorem 5.1.4 and gives conditions for safety verification with respect to an unsafe set $\mathcal{Y}_u$ for all time $t > 0$. In this case, the barrier functional can be independent of t.

Corollary 5.1.5 *Consider the PDE system described by* (5.1)*. Assume* $u \in \mathcal{U}$*. Given an unsafe set* $\mathcal{Y}_u \subset \mathcal{U}$*, such that* $\mathcal{U}_0 \cap \mathcal{Y}_u = \emptyset$*, if there exists a barrier functional* $B(u(t,x))$ *as in* (5.2) *such that*

$$B(u(t,x)) - B(u_0(x)) > 0, \quad \forall u \in \mathcal{Y}_u,\ \forall u_0 \in \mathcal{U}_0, \tag{5.5a}$$

$$\frac{dB(u(t,x))}{dt} \leq 0, \quad \forall u \in \mathcal{U}, \tag{5.5b}$$

along the solutions of (5.1)*, then the solutions of PDE* (5.1) *are safe with respect to* $\mathcal{Y}_u$ *(cf. Definition 5.1.2).*

Proof: The proof follows the same lines as the proof of Theorem 5.1.4. Assume that there exists a solution $u(t,x)$ to (5.1) such that, for some $t > 0$, we have $u(t,x) \in \mathcal{Y}_u$. Then, from (5.5a), it follows that $B(u(t,x)) - B(u_0(x)) > 0$. On the other hand, integrating inequality (5.5b) from 0 to t implies that $B(u(t,x)) - B(u_0(x)) \leq 0$, which is a contradiction. Thus, since t is arbitrary, the solutions to (5.1) avoid $\mathcal{Y}_u$ for all time. □

We conclude this section by illustrating Corollary 5.1.5 with an analytical example that uses a barrier functional to bound a performance index.

Example 5.1.6 ***(Performance Bounds)*** *Consider the heat equation defined over a domain* $\Omega \subset \mathbb{R}^2$ *with smooth boundary*

$$\partial_t u = \Delta u, \quad x \in \Omega,\ t > 0, \tag{5.6}$$

subject to $u|_{\partial\Omega} = 0$. *Then,* $\mathcal{U} = \{u \in \mathcal{H}^2_\Omega \mid u|_{\partial\Omega} = 0\}$. *The set of initial conditions*

$$u(0,x) \in \mathcal{U}_0 = \left\{ u_0 \in \mathcal{U} \mid \int_\Omega |\nabla u_0|^2 \, d\Omega \leq 1 \right\}. \tag{5.7}$$

Consider the output

$$y(t) = \gamma^2 - \int_\Omega u^2 \, d\Omega,$$

where $\gamma \geq 0$. *Then, the unsafe set is described as* $\mathcal{Y}_u = \left\{ u \in \mathcal{U} \mid y(t) = \gamma^2 - \int_\Omega u^2 \, d\Omega < 0 \right\}$. *We are interested in finding the minimum* γ *such that no solution of* (5.6) *enters* $\mathcal{Y}_u$ *for all* $u(0,x) \in \mathcal{U}_0$.

We consider the barrier functional (5.2) *with*

$$\begin{aligned} \mathscr{B} : \qquad & \mathcal{H}^1_\Omega \to \mathbb{R}_{\geq 0} \\ & u \mapsto \textstyle\int_\Omega (\nabla u)' \nabla u \, d\Omega, \end{aligned}$$

that is, $B(u(t,x)) = \int_\Omega (\nabla u)' \nabla u \, d\Omega$. *We first check inequality* (5.5b) *along the solutions of* (5.6)*:*

$$\begin{aligned} \frac{dB(u(t,x))}{dt} &= \int_\Omega 2 \nabla u \partial_t \left(\nabla u \right) \, d\Omega = 2 \left(\nabla u \partial_t u \right) |_{\partial\Omega} - 2 \int_\Omega \Delta u \partial_t u \, d\Omega \\ &= -2 \int_\Omega \left(\Delta u \right)^2 \, d\Omega \leq 0, \end{aligned}$$

where, in the second equality above, integration by parts and, in the third equality, the boundary conditions are used. Thus, inequality (5.5b) *is satisfied. At this point, let us check inequality* (5.5a). *We have*

$$\begin{aligned} B(u(t,x)) - B(u_0) &= \int_\Omega |\nabla u|^2 \, d\Omega - \int_\Omega |\nabla u_0|^2 \, d\Omega \geq \int_\Omega |\nabla u|^2 \, d\Omega - 1 \\ &\geq C(\Omega) \int_\Omega u^2 \, d\Omega - 1, \end{aligned}$$

where $u_0 \in \mathcal{U}_0$ *as in* (5.7) *is applied to obtain the first inequality and the Poincaré inequal-*

ity is used in the second inequality. Then, it follows that whenever $\gamma^2 > \frac{1}{C(\Omega)}$*, we have* $B(u(t,x)) - B(u_0) > 0$*, and thus, from Theorem 5.1.4, system* (5.6) *avoids* $\mathcal{Y}_u$*. Therefore, it holds that* $y \notin \mathcal{Y}_u$*, which implies* $y(t) = \gamma^2_{min} - \int_\Omega u^2 \, d\Omega \geq 0$*, i.e.,* $\gamma^2_{min} \geq \int_\Omega u^2 \, d\Omega$*, where* $\gamma^2_{min} = \frac{1}{C(\Omega)}$*. For example, whenever* $\Omega = \{(x,y) \in \mathbb{R}^2 \mid |x+y| \leq 1\}$*, we obtain* $\gamma^2 = \frac{2}{\pi^2}$.

5.2 Bounding Output Functionals of PDEs

In this section, we discuss an important application of the safety verification method, *i.e.,* bounding functional outputs of PDEs. We present a motivating example that is referred to throughout this section.

5.2.1 Motivating Example

The heat distribution over a heated rod is described by

$$\partial_t u = k\partial_x^2 u + f(t,x,u), \quad x \in \Omega, \; t > 0 \tag{5.8}$$

where $k > 0$ is the thermal conductivity, and $f(t,x,u)$ is the forcing, representing either a heat sink or a heat source. The initial heat distribution is $u(0,x) = u_0(x)$. We are interested in estimating bounds on the heat flux emanating from the boundary $x = 0$

$$y(t) = k\partial_x u(t,0), \; t > 0. \tag{5.9}$$

The available approaches for finding bounds on (5.9) rely on methods for approximating the solution to (5.8) and then computing (5.9) [88, 73, 89]. In addition, some existing methods [14, 88, 138] require convexity of the output functional $y(t)$ in the dependent variables.

5.2.2 Problem Formulation

Consider the following particular case of PDE systems (5.1)

$$\begin{aligned} \partial_t u(t,x) &= F(t,x,D^{\alpha}u(t,x)), \quad x \in \Omega,\ t > 0 \qquad (5.10)\\ y(t) &= \tilde{\mathscr{H}}u,\ t \geq 0 \qquad (5.11) \end{aligned}$$

subject to $u(0,x) = u_0(x)$ and boundary conditions given by

$$Q \begin{bmatrix} D^{\alpha-1}u(t,1) \\ D^{\alpha-1}u(t,0) \end{bmatrix} = 0, \qquad (5.12)$$

with B being a matrix of appropriate dimension and F being a nonlinear function. Define the following set with the Sobolev norm as the restriction of Hilbert space to the space of functions u satisfying boundary conditions (5.12)

$$\mathcal{U}_b = \left\{ u \in \mathcal{H}^{\alpha}_{\Omega} \mid Q \begin{bmatrix} D^{\alpha-1}u(t,1) \\ D^{\alpha-1}u(t,0) \end{bmatrix} = 0 \right\}. \qquad (5.13)$$

We assume the output functional (5.11) is defined by the operator $\tilde{\mathscr{H}}$ which is of the form

$$\tilde{\mathscr{H}}u = H_1\left(t, D^{\beta}u(t,x)\right) + \int_0^t H_2\left(\tau, D^{\beta}u(\tau,x)\right)\, d\tau,\ x \in \Omega,\ t > 0, \qquad (5.14)$$

wherein, $0 \leq \beta \leq \alpha$. $\{H_i\}_{i=1,2}$ are given by

$$H_i(t, D^{\beta}u) = h_1(t,x,D^{\beta}u(t,x)) + \int_{\tilde{\Omega}} h_2(t,\theta,D^{\beta}u(t,\theta))\, d\theta,\ x \in \Omega,\ t > 0,\ i = 1,2 \qquad (5.15)$$

with $\tilde{\Omega} \subseteq \Omega$ and $h_i,\ i = 1,2$ being nonlinear functions that map into $\mathbb{R}$. In this study, we discuss the cases where either $H_1 = 0$ or $H_2 = 0$.

Remark 5.2.1 *The functional given by* (5.11)*,* (5.14)*, and* (5.15) *represents an output functional either evaluated*

A. at a single point inside the domain ($h_2 = 0$),

B. over a subset of the domain ($h_1 = 0$ and $\tilde{\Omega} \subset \Omega$)

C. over the whole domain ($h_1 = 0$ and $\tilde{\Omega} = \Omega$).

We transform output functionals A-B to the output functional structure C, which we refer as full integral form in the sequel. This structure is consistent with the method for solving integral inequalities outlined in Chapter 3. The transformation methods for converting structure A to C and structure B to C are discussed in Appendix B.

The problem we are interested in solving can be stated as follows.

Problem 5.2.2 *Given PDE* (5.10) *with initial condition $u_0 \in \mathcal{U}_0$ and boundary conditions* (5.12)*, and a scalar $T \geq 0$, compute $\gamma \in \mathbb{R}$ such that $y(T) \leq \gamma$, where y is given in* (5.11) *and* (5.14)*.*

We are interested in finding barrier certificates to check whether the output functional y as in (5.11) satisfies $y(T) \leq \gamma$ for some $\gamma > 0$ and $T > 0$, e.g., $y(T) = k\partial_x u(T, 0)$ in the motivating example of Section 5.2.1. Let $\mathcal{Y}_u = \left\{ u \in \mathcal{H}^{\alpha}_{\Omega} \mid y(T) = \tilde{\mathscr{H}} u(T) > \gamma \right\}$. Note that the set $\mathcal{Y}_u$ defines a subset of function spaces. At this point, we observe that checking whether $y(T) \leq \gamma$ can be performed via safety verification. In this respect, the key step is to find certificates that there is no solution $u(t, x)$ to (5.10) starting at $u_0(x) \in \mathcal{U}_0$ such that $u(T, x) \in \mathcal{Y}_u$. The next theorem asserts that barrier functionals can be used as certificates for upper-bounding output functionals.

Corollary 5.2.3 *Consider the PDE system described by* (5.10) *subject to boundary conditions* (5.12) *and initial condition $u_0(x) \in \mathcal{U}_0 \subset \mathcal{U}_b$, where $\mathcal{U}_b$ is defined in* (5.13)*. Assume*

$u \in \mathcal{U} \subseteq \mathcal{U}_b$. *Let*

$$\mathcal{Y}_u = \left\{ u \in \mathcal{U} \mid y(T) = \int_0^1 h(T, x, D^\beta u(T, x))\, dx > \gamma \right\}, \tag{5.16}$$

define the unsafe set. If there exists a barrier functional $B(t, u) \in \mathcal{C}^1[t]$*, such that* (5.3) *hold, then it follows that there is no solution* $u(t, x)$ *of* (5.10) *such that* $u(0, x) = u_0(x) \in \mathcal{U}_0$ *and* $u(T, x) \in \mathcal{Y}_u$ *for* $T > 0$*. In other words, it holds that* $y(T) \leq \gamma$*.*

From Corollary 5.2.3, we can compute upper bounds on $y(T)$ by solving the minimization problem below

$$\begin{gathered} \underset{B(t,u)}{\text{minimize}}\ \gamma \\ \text{subject to} \\ B(T, u(T, x)) - B(0, u_0) > 0, \quad \text{for } \textstyle\int_0^1 \left(h(T, x, D^\beta u(T, x)) - \gamma \right)\, dx > 0, \quad (5.17) \\ -\tfrac{dB}{dt} \geq 0, \quad \text{for } t(T - t) > 0. \quad (5.18) \end{gathered}$$

where $u(T, x), u(t, x) \in \mathcal{U}_b$.

Thus far, output functionals of type (5.14) with $H_2 = 0$ were considered. In some applications, one might be interested in output functionals of type (5.14) with $H_1 = 0$. For example, referring to the motivating example in Section 5.2.1, we might be interested in the following quantity which represents the average temperature of the heated rod for time $T > 0$

$$y(T) = \int_0^T \int_\Omega u(t, x)\, dx\, dt.$$

In other words, bounds on inequalities of the following type are sought

$$y(T) = \int_0^T \int_0^1 h(t, x, D^\beta u(t, x))\, dx\, dt \leq \gamma^*. \tag{5.19}$$

Obtaining bounds for this type of output functionals can also be addressed as delineated in

the next corollary.

Corollary 5.2.4 *Consider the PDE system described by* (5.10) *with boundary conditions* (5.12) *and initial condition* $u_0 \in \mathcal{U}_0 \subset \mathcal{U}_b$*, where* $\mathcal{U}_b$ *is defined in* (5.13)*. Assume* $u \in \mathcal{U} \subseteq \mathcal{U}_b$*. Let*

$$\tilde{\mathcal{Y}}_u = \left\{ u \in \mathcal{U} \mid \int_0^1 h(t, x, D^\beta u(t,x))\, dx > \partial_t \gamma(t) \right\}, \tag{5.20}$$

with $\gamma(t) : \mathbb{R}_{\geq 0} \to \mathbb{R}$*,* $0 \leq \beta \leq \alpha$ *as in* (5.10)*, define the unsafe set. If there exists a barrier functional* $B(t,u) \in \mathcal{C}^1[t]$*, such that*

$$B(t, D^\beta u(t,x)) - B(0, D^\beta u_0(x)) > 0, \quad \forall u \in \tilde{\mathcal{Y}}_u,\ \forall u_0 \in \mathcal{U}_0,\ \forall t \in (0,T), \tag{5.21}$$

and (5.3b) *are satisfied, then it holds that* $y(T) \leq \gamma^\star$ *with* $y(T)$ *given by* (5.19) *and* $\gamma^\star = \gamma(T) - \gamma(0)$.

Proof: This follows from Corollary 5.2.3. If there exists a function $B(t,u)$ satisfying (5.21) and (5.3b), then, from Corollary 5.2.3, we conclude that there is no solution $u(t,x)$ of (5.10) satisfying $u(t,x) \in \tilde{\mathcal{Y}}_u$ for $t \in (0,T)$. That is, it holds that

$$\int_0^1 h(t, x, D^\beta u(t,x))\, dx \leq \partial_t \gamma(t),\ \forall t \in (0,T). \tag{5.22}$$

Integrating both sides of (5.22) from 0 to T yields

$$y(T) = \int_0^T \int_0^1 h(t, x, D^\beta u(t,x))\, dx\, dt \leq \int_0^T \partial_t \gamma(t)\, dt = \gamma(T) - \gamma(0). \tag{5.23}$$

This completes the proof. □

We can compute bounds on $\gamma^* = \gamma(T) - \gamma(0)$ via an optimization problem as follows.

If there exists a solution $\gamma^* = \gamma(T) - \gamma(0)$ to the minimization problem

$$\begin{gathered}\underset{B(t,u)}{\text{minimize}} \ (\gamma(T) - \gamma(0)) \\ \text{subject to} \\ B(t,u) - B(0,u_0) > 0, \text{ for } \int_0^1 \left(h(t,x,D^\beta u(t,x)) - \partial_t \gamma(t)\right)\, dx > 0 \text{ and } t(T-t) > 0, \\ -\tfrac{dB}{dt} \geq 0, \quad \text{for} \quad t(T-t) > 0. \end{gathered} \tag{5.24}$$

with $u(t,x) \in \mathcal{U}_b$, then the following inequality holds

$$\int_0^T \int_0^1 h(t,x,D^\beta u(t,x))\, dx\, dt \leq \gamma^* = \gamma(T) - \gamma(0). \tag{5.25}$$

Remark 5.2.5 *Note that inequality* (5.21) *in Corollary 5.2.4 requires the system to be safe for all* $t \in (0,T)$. *In this sense, Corollary 5.2.4 is more conservative than Corollary 5.2.3. The resulting barrier functional* B *may not be a barrier for the set*

$$\tilde{\mathcal{Y}}_u = \left\{ u \in \mathcal{U}_b \mid \int_0^T \int_0^1 g(t,x,D^\beta u(t,x))\, dx\, dt \leq \gamma^* \right\}.$$

However, the set described in (5.20) *can be used to compute the bound as in* (5.19).

5.3 Construction of Barriers Functionals

In this section, we study a specific class of barrier functionals. For the studied class and for particular sets $\mathcal{U}_0$, and $\mathcal{Y}_u$, the inequalities (5.3) and (5.21) become integral inequalities. For the case of polynomial data, the verification of the inequalities can be cast as constraints of an SDP based on the method discussed in Chapter 3.

In the previous sections, the barrier functionals were only assumed to be continuously differentiable with respect to time. In this section, we impose the following structure for

the barrier functionals

$$B(t,u) = \int_{\Omega} \eta^d(D^\alpha u(t,\theta))' \, \bar{B}(t,\theta) \, \eta^d(D^\alpha u(t,\theta)) \, d\theta \tag{5.26}$$

where $\Omega = [0,1]$, $\bar{B} : \mathbb{R}_{\geq 0} \times \Omega \to \mathbb{R}^{\sigma(n,d)\times\sigma(n,d)}$, $\bar{B}(t,x) \in \mathcal{C}^1[t], \forall x \in \Omega$, and the following quadratic-like structures for the unsafe and the initial sets

$$\mathcal{Y}_u = \left\{ u \in \mathcal{U} \mid \int_{\Omega} \eta^d(D^\alpha u(t,\theta))' \, Y(\theta) \, \eta^d(D^\alpha u(t,\theta)) \, d\theta \geq 0 \right\}, \tag{5.27a}$$

and the set of initial conditions

$$\mathcal{U}_0 = \left\{ u_0 \in \mathcal{U} \mid \int_{\Omega} \eta^d(D^\alpha u(t,\theta))' \, U_0(\theta) \, \eta^d(D^\alpha u(t,\theta)) \, d\theta \geq 0 \right\}. \tag{5.27b}$$

where, $Y : \mathbb{R}_{\geq 0} \times \Omega \to \mathbb{R}^{\sigma(n,d)\times\sigma(n,d)}$ and $U_0 : \mathbb{R}_{\geq 0} \times \Omega \to \mathbb{R}^{\sigma(n,d)\times\sigma(n,d)}$.

The following proposition applies Lemma 3.2.1 to formulate integral inequalities to verify the conditions of Theorem 5.1.4 considering the barrier functional (5.26). In this case, the constraint set $\mathcal{S}$ as defined in (3.15) is given by $\mathcal{S} = \mathcal{Y}_u \cup \mathcal{U}_0$, with the sets defined in (5.27), that is

$$\begin{aligned} s_1(x, D^\alpha u) &= \eta^d(D^\alpha u)' Y(x) \eta^d(D^\alpha u), \\ s_2(x, D^\alpha u) &= \eta^d(D^\alpha u)' U_0(x) \eta^d(D^\alpha u). \end{aligned} \tag{5.28}$$

Proposition 5.3.1 *If there exist* $\bar{B} : [0,T] \times \Omega \to \mathbb{R}^{\sigma(n,d)\times\sigma(n,d)}$ *or* $B(t,u)$ *as in* (5.26)*,* $m : \mathcal{T} \times \Omega \to \mathbb{R}^2$ *and* $n \in \mathbb{R}^2_{\geq 0}$ *such that the inequalities*

$$B(T,u(T,x)) - B(0,u_0) - n'v(T,1) + \int_{\Omega} m'(T,\theta) \left(\partial_\theta v(T,\theta) - s(x, D^\alpha u(T,\theta))\right) \, d\theta > 0, \tag{5.29a}$$

with $s(x, D^\alpha u) = \left[\begin{smallmatrix} s_1(x,D^\alpha u) & s_2(x,D^\alpha u) \end{smallmatrix} \right]'$ *defined by* (5.28) *and* $v(t,x) = \left[\begin{smallmatrix} v_1(t,x) & v_2(t,x) \end{smallmatrix} \right]'$ *as*

defined by (3.16)*, and*

$$\int_{\Omega} \left(\eta^d(D^\alpha u)' \partial_t \bar{B}(t,\theta) \eta^d(D^\alpha u) + 2\eta^d(D^\alpha u)' \bar{B}(t,\theta) \nabla \eta^d(D^\alpha u)' \partial_t (D^\alpha u) \right) \, d\theta \leq 0, \tag{5.29b}$$

$\forall t \in [0,T]$, $\forall u \in \mathcal{U}$*, then* (5.3) *holds and the PDE is* $\mathcal{Y}_u$*-safe at time* T.

The numerical results presented in the next section consider the problem data to be polynomial, *i.e.,* the functions $\bar{B}$, m, Y, U_0 appearing in the inequalities of Proposition 5.3.1 are polynomials on variables t and x, and the operator $\mathscr{F}$ in (5.1) may be nonlinear and defined by a polynomial on u and its spatial derivatives with coefficients that are polynomials on the spatial variables.

5.4 Examples

We now illustrate the proposed results with two numerical examples. The first example is associated with tuning a parameter such that the solutions to a (nonlinear) diffusion-reaction-convection PDE are safe. The second example is concerned with bounding two output functionals of a diffusion-reaction PDE.

5.4.1 Safety Verification of the Burgers' Equation with Reaction

Consider

$$\partial_t u = \partial_x^2 u + \lambda u - 2u\partial_x u, \; u(t,0) = u(t,1) = 0, \tag{5.30}$$

where $\lambda > 0$, $x \in [0,1]$ and $t > 0$. Due to the presence of a nonlinear convection term, the solutions with $\lambda \geq \pi^2$ (otherwise unstable) may converge to a different stationary solution. This stems from the fact that the convection term transfers low wave number components of the solutions to the high wave number ones for which the diffusion term has a stabilizing effect in a similar fashion to the effects of diffusion and anti-diffusion terms in

the Kuramoto-Sivashinsky equation [78]. Figure 5.2 depicts a solution to PDE (5.30) with $\lambda > \pi^2$.

We are interested in computing the maximum value for parameter λ, such that the solutions starting in

$$\mathcal{U}_0 = \left\{ u_0 \mid \int_0^1 \left(u_0^2 + (\partial_\theta u_0)^2 \right) \, d\theta \leq 1 \right\}, \tag{5.31}$$

which implies $\|u_0\|_{\mathcal{H}^1_{[0,1]}} \leq 1$, do not enter the set $\mathcal{Y}_u = \left\{ u \mid \int_0^1 \left(u^2 + (\partial_\theta u)^2 \right) \, d\theta \geq (6)^2 \right\}$, *i.e.,* $\|u\|_{\mathcal{H}^1_{[0,1]}} \geq 6$ for all $t > 0$. To this end, we consider the following barrier functional structure

$$B(t, u(t,x)) = \int_0^1 \left[\begin{smallmatrix} u(t,\theta) \\ \partial_\theta u(t,\theta) \end{smallmatrix} \right]' M(\theta) \left[\begin{smallmatrix} u(t,\theta) \\ \partial_\theta u(t,\theta) \end{smallmatrix} \right] \, d\theta, \tag{5.32}$$

where $M(\theta) \in \mathbb{R}^{2\times 2}$. Applying Corollary 5.1.5 and performing a line search for λ, the maximum parameter λ, for which the solutions avoid $\mathcal{Y}_u$, is found to be $\lambda = 1.198\pi^2$, for which the barrier functional (5.32) was constructed with a degree-16 $M(\theta)$, in less than 16 seconds, as given below

$$M(\theta) = \begin{bmatrix} M_{11}(\theta) & M_{12}(x) \\ M_{12}(\theta) & M_{22}(\theta) \end{bmatrix},$$

$$\begin{aligned} 10^4 M_{11}(\theta) = &- 12.96\theta^{16} + 27.92\theta^{15} - 55.38\theta^{14} - 160.6\theta^{13} - 222.4\theta^{12} + 180.8\theta^{11} \\ &+ 199.1\theta^{10} + 332.9\theta^9 - 343.5\theta^8 - 454.9\theta^7 - 390.1\theta^6 + 329.9\theta^5 \\ &+ 666.7\theta^4 - 83.37\theta^3 - 663.4\theta^2 + 418.7\theta - 74.97, \end{aligned}$$

$$\begin{aligned} 10^4 M_{12}(\theta) = &1.39\theta^{16} - 26.03\theta^{15} + 10.76\theta^{14} + 22.53\theta^{13} - 14.63\theta^{12} - 22.81\theta^{11} \\ &+ 52.28\theta^{10} - 67.56\theta^9 - 69.45\theta^8 - 87.54\theta^7 + 79.37\theta^6 + 262.8\theta^5 \\ &- 32.63\theta^4 - 447.1\theta^3 + 417.7\theta^2 - 157.6\theta + 23.88, \end{aligned}$$

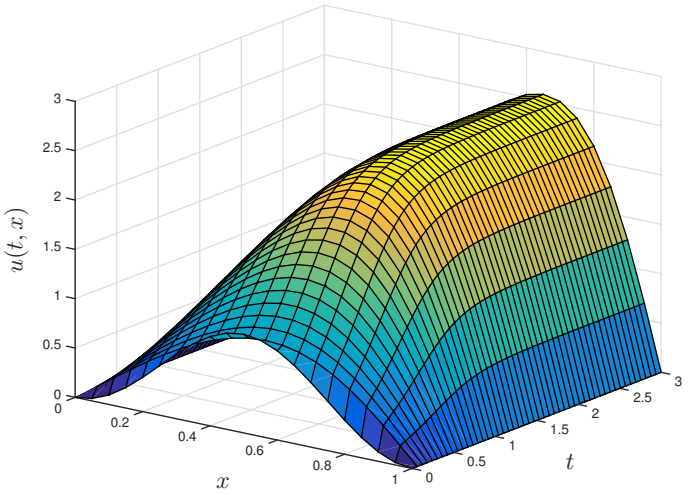

Figure 5.2: The solution to PDE (5.30) for $\lambda = 1.2\pi^2$.

$$\begin{aligned} 10^4 M_{22}(\theta) = &- 1.607\theta^{16} - 26.85\theta^{14} + 47.17\theta^{13} + 38.69\theta^{12} - 77.1\theta^{11} - 34.36\theta^{10} \\ &+ 66.47\theta^9 + 13.36\theta^8 - 34.57\theta^7 - 1.477\theta^6 + 17.13\theta^5 \\ &- 9.405\theta^4 + 2.768\theta^3. \end{aligned}$$

This is consistent with the numerical experiments shown in Figure 5.3, where the $\mathcal{H}^1_\Omega$-norm of the solution to PDE (5.30) with $\lambda = 1.2\pi^2$ was computed for four different initial conditions $u_0(x) \in \mathcal{U}_0$ as in (5.31).

5.4.2 Bounding the Heat Flux of a Heated Rod

In this example, we apply the safety verification method to find upper bounds on the heat equation. Consider

$$\partial_t u = \partial_x^2 u + \lambda u, \quad x \in [0,1],\ t > 0, \tag{5.33}$$

for all $u(t,0) = u(t,1) = 0$ and the initial condition $u_0(x) = \pi x(1-x)$. For comparison, the exact solution to PDE (5.33) can be found using the method of separation of variables

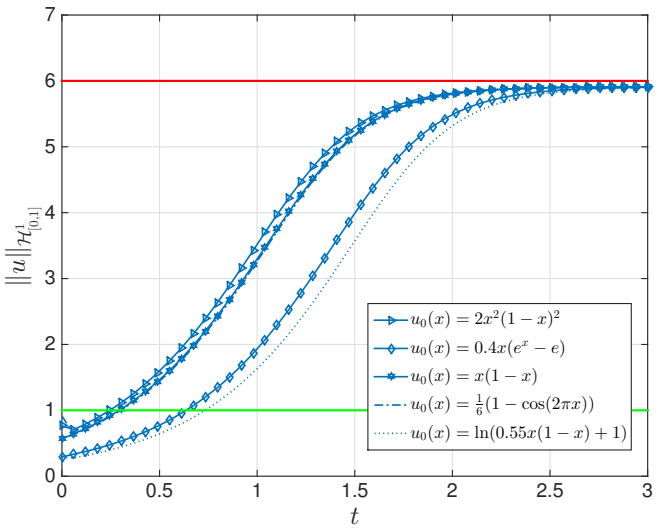

Figure 5.3: The evolution of $\mathcal{H}^1_{[0,1]}$-norm of solutions to (5.30) with $\lambda = 1.2\pi^2$ for different initial conditions. The red and green lines show the boundaries of $\mathcal{Y}_u$ and $\mathcal{U}_0$, respectively.

as

$$u(t,x) = \sum_{n=1}^{\infty} \frac{2\left(1-(-1)^n\right)}{\pi^2 n^3} e^{(\frac{\lambda}{\pi^2}-n^2)\pi^2 t} \sin(n\pi x). \tag{5.34}$$

The solutions to (5.33) are convergent to the null solution $u(t,x) = 0,\ x \in [0,1],\ t > 0$ in $\mathcal{L}^2_\Omega$ for $\lambda < \pi^2$ [116, p. 11]. In this example, we are interested in upper-bounding an output functional of the solutions when $\lambda = 10\pi^2$, *i.e.,* the unstable solutions. We consider the following barrier functional structure

$$B(t,u) = \int_0^1 b(t,x,D^1u)\, dx, \tag{5.35}$$

with $b \in \mathcal{R}[t,x,D^1u]$. We investigate the bounds on the heat flux emanating from the boundary $x = 0$ at time $T = 0.01$ given by

$$y(T) = \partial_x u(T,0). \tag{5.36}$$

The results are given in Table 5.1. It can be observed that the bounds approach the actual heat flux $y(0.01) \approx 3.2512$ as the degree of b increases. The constructed certificates of

Table 5.1: Obtained upper bounds of functional (5.36) of system (5.35).

$deg(b)$	1	2	3	4	5	6
$\gamma^\star$	8.0447	5.8035	3.9637	3.3418	3.2919	3.2555

degree 4 in b is given below

$$\begin{aligned}
b(t,x,D^1u) = &-7.1441t^2u^2 + 1.7154t^2u\partial_x u - 20.228t^2u - 7.5293t^2(\partial_x u)^2 - 3.0302t^2\partial_x u \\
&+ 84.477t^2 + 5.306txu^2 + 4.439tu^2 - 11.394txu\partial_x u + 4.0763tu\partial_x u \\
&+ 11.385tux + 9.753tu - 0.7447tx(\partial_x u)^2 + 0.55552t(\partial_x u)^2 - 4.2529tx\partial_x u \\
&+ 1.3549t\partial_x u - 42.631tx - 28.656t - 6.9887x^2u^2 + 5.7104xu^2 \\
&- 2.3317u^2 - 0.21259x^2u\partial_x u + 2.3274xu\partial_x u - 1.7012u\partial_x u + 5.7105x^2u \\
&- 6.7309xu - 0.23359u - 0.3866x^2(\partial_x u)^2 + 0.326x(\partial_x u)^2 - 0.04805(\partial_x u)^2 \\
&- 0.01152x^2\partial_x u + 0.062023x\partial_x u - 0.020951\partial_x u.
\end{aligned}$$

The second output functional of interest is given by

$$y(T) = \int_0^T \partial_x u(\tau, 0)\, d\tau. \tag{5.37}$$

with $T = 0.05$. We define the unsafe set as

$$\mathcal{Y}_u = \left\{ u \in \mathcal{U}_b \mid \int_0^1 \partial_x \left((x-1)\partial_x u(\tau, x)\right)\, dx d\tau \geq \partial_t \gamma \right\}.$$

With the above formulation, it is clear that the larger the set $\mathcal{Y}_u$ for which we can find a barrier functional, the tighter the upper bound of the output functional (5.37). Applying Corollary 5.2.4, the minimum $\gamma^\star$ such that certificates for safety verification at time $T = 0.05$ could be found are provided in Table 5.2. It can be inferred from the table that the results are converging to the exact solution of the functional which can be obtained from (5.34) as $y(0.05) \approx 1.2402$. In these numerical experiments, we set $deg(\gamma(t)) = deg(b) + 3$. The

Table 5.2: Obtained upper bounds of functional (5.37) of system (5.35).

$deg(b)$	1	2	3	4	5	6
$\gamma^\star$	6.7374	4.6736	2.2749	1.4175	1.2921	1.2524

obtained certificates for bounding the state functional with b of degree 4 were:

$$\gamma(t) = 964.11t^7 + 6.7729t^6 + 66.924t^5 + 32.375t^4 + 100.79t^3 - 4.5509t^2 + 5.7891t,$$

and (5.35) with

$$\begin{aligned} b(t,x,D^1u) = &- 1.6454t^2u^2 + 0.37053t^2u\partial_x u - 2.14t^2u - 1.2514t^2(\partial_x u)^2 \\ &+ 0.15851t^2\partial_x u + 3.8517t^2 + 2.6005txu^2 + 1.672tu^2 \\ &- 2.5321tu(\partial_x u)^2 + 0.69396tu\partial_x u + 3.6274txu + 1.3629tu \\ &- 0.13896tx(\partial_x u)^2 + 0.24091t(\partial_x u)^2 - 0.18622tx\partial_x u + 0.016255t\partial_x u \\ &- 7.0307tx - 2.1521t - 6.3404x^2u^2 + 4.1574xu^2 \\ &- 1.9985u^2 + 0.19901x^2u\partial_x u + 0.54298xu\partial_x u - 0.69336u\partial_x u \\ &+ 0.75643x^2u - 1.1887xu - 0.048215u - 0.20306x^2(\partial_x u)^2 \\ &+ 0.16273x(\partial_x u)^2 - 0.021415(\partial_x u)^2 - 0.0023234x^2\partial_x u + 0.014826x\partial_x u \\ &- 0.0032264\partial_x u. \end{aligned}$$

5.5 Conclusions

We considered the safety verification problem of PDEs, *i.e.,* given the set of initial conditions and the unsafe set, checking whether the solutions of the PDE avoid the unsafe set. The safety verification problem is reformulated as the existence of a barrier functional satisfying a set of integral inequalities. Furthermore, equipped with the safety verification method, we proposed a scheme to upper-bound output functionals of a class of PDEs by barrier functionals. In the case of polynomial dependence on both independent and depen-

dent variables, we used SOS programming to construct the barrier functionals by solving SDPs. The proposed method was illustrated using two examples.

In the following chapter, we apply the tools developed in Chapter 3 and Chapter 4 to fluid flow analysis.

Chapter 6

Input-Output Analysis of Fluid Flows

In Chapter 4, we discussed a method based on dissipation inequalities for the input-state/output analysis of PDEs. One important area in which PDE models are used is in describing the dynamics of incompressible fluid flows. For such flows, the dynamics is described by a set of nonlinear PDEs known as the Navier-Stokes equations. The input-output and stability properties of such flows are then characterized in terms of a dimensionless parameter Re called the Reynolds number.

In this chapter, we consider input-output and stability properties of a class of incompressible viscous fluid flows. To be precise, we study flows subject to perturbations that are constant in one of the three spatial coordinates. With this assumption, we obtain the perturbation dynamics-a nonlinear PDE with 3 vector fields in two spatial coordinates. Alternative forms of this model were used in [40] for modeling turbulence. In particular, we study streamwise constant perturbations. This is motivated by the transient growth analyses of the linearized Navier-Stokes equations for channel flows [77, 45, 37] suggesting that the streamwise constant modes receive largest energy growth, pseudo-spectral analysis of the linearized Navier-Stokes [123] implying that streamwise constant perturbations have the maximum energy growth, and the Squire's Theorem which states that the two-dimensional perturbations are the least stable among all perturbations [50].

The input-output analysis method proposed in this chapter entails both channel flows[1] and pipe flows.

Based on a set of dissipation inequalities, we study input-output properties such as maximum energy growth, induced $\mathcal{L}^2$-norms from body forces to perturbation velocities and ISS. We propose a class of Lyapunov and storage functionals that takes advantage of the flow structure and leads to a quadratic integrand in the resultant integral inequalities. For streamwise constant perturbations, we formulate conditions based on matrix inequalities. We show that in the case of polynomial base flow profiles, the matrix inequalities can be checked via convex optimization. We illustrate the proposed method by studying four flows, namely, the Taylor-Couette flow, the plane Couette flow, the plane Poiseuille flow and the Hagen-Poiseuille flow.

The preliminary version of the results discussed in this chapter was presented at the 2015 54th IEEE Conference on Decision and Control [4]. A journal article including the discussions on pipe flows and more examples is currently under preparation.

6.1 The Flow Perturbation Model

Let I be an index set corresponding to the spatial coordinates. The dynamics of incompressible viscous flows are described by the Navier-Stokes equations, given by

$$\begin{aligned} \partial_t \bar{\boldsymbol{u}} &= \frac{1}{Re}\nabla^2 \bar{\boldsymbol{u}} - \bar{\boldsymbol{u}} \cdot \nabla \bar{\boldsymbol{u}} - \nabla \bar{p} + F\bar{\boldsymbol{u}} + \boldsymbol{d}, \\ 0 &= \nabla \cdot \bar{\boldsymbol{u}}, \end{aligned} \tag{6.1}$$

where $t > 0$, $F \in \mathbb{R}^{3\times 3}$ represents terms coming from rotation, and $\mathrm{x} \in \Omega = \Omega_i \times \Omega_j \subset \mathbb{R} \times \mathbb{R}$ with $i \neq j$, $i, j \in I$ are the spatial coordinates. The dependent variable $\boldsymbol{d} : \mathbb{R}_{\geq 0} \times \Omega \to \mathbb{R}^3$ is the input vector representing exogenous excitations or body forces,

[1]The type of fluid flow within a conduit with a free surface, known as a channel. A channel flow has a free surface, whereas the pipe flow does not.

$\bar{\boldsymbol{u}} : \mathbb{R}_{\geq 0} \times \Omega \to \mathbb{R}^3$ is the velocity vector, and $\bar{p} : \mathbb{R}_{\geq 0} \times \Omega \to \mathbb{R}$ is the pressure.

We consider perturbations $(\boldsymbol{u}, p)$ to the steady solution $(\boldsymbol{U}, P)$, which are constant in one of the directions, say x_m, $m \in I$, *i.e.*, $\partial_{x_m} = 0$. Let $I_0 = I - \{m\}$. The perturbations are described as

$$\bar{\boldsymbol{u}} = \boldsymbol{u} + \boldsymbol{U},\ \bar{p} = p + P, \tag{6.2}$$

where $(\boldsymbol{U}, P)$ satisfy

$$\begin{aligned} 0 &= \frac{1}{Re}\nabla^2 \boldsymbol{U} - \boldsymbol{U} \cdot \nabla \boldsymbol{U} - \nabla P + F\boldsymbol{U}, \\ 0 &= \nabla \cdot \boldsymbol{U}. \end{aligned} \tag{6.3}$$

Substituting (6.2) in (6.1) and using (6.3), we obtain the perturbation dynamics

$$\begin{aligned} \partial_t \boldsymbol{u} &= \frac{1}{Re}\nabla^2 \boldsymbol{u} - \boldsymbol{u} \cdot \nabla \boldsymbol{u} - \boldsymbol{U} \cdot \nabla \boldsymbol{u} - \boldsymbol{u} \cdot \nabla \boldsymbol{U} - \nabla p + F\boldsymbol{u} + \boldsymbol{d}, \\ 0 &= \nabla \cdot \boldsymbol{u}. \end{aligned} \tag{6.4}$$

In the rest of the chapter, we study the properties of PDE (6.4). We concentrate on perturbations with no-slip boundary conditions $\boldsymbol{u}|_{\partial\Omega} \equiv 0$ (the fluid has zero velocity relative to the solid boundaries) and periodic boundary conditions (in the the direction with symmetry in the flow).

6.2 Flow Stability and Input-Output Analysis Using Dissipation Inequalities

Our analysis of the nonlinear flow model (6.4) is based on dissipativity theory for systems described by PDEs as outlined in Chapter 4. Next, we define the stability and input-output properties of interest. We use several terms from the hydrodynamics literature. Nonetheless, the connection to the input-output properties discussed in Chapter 4 will be clarified

whenever needed.

We study exponential stability of perturbation velocities.

Definition 6.2.1 (Exponential Stability) *Let* $p_0 \in \mathbb{R}^3$. *The stationary solution* $(0, p_0)$ *of* (6.4) *with* $\boldsymbol{d} \equiv 0$ *is exponentially stable in the* $\mathcal{L}^2_\Omega$*-norm, if there exist* $\lambda > 0$ *and* $c > 0$*, such that for all* $t \geq 0$

$$\|\boldsymbol{u}(t,\cdot)\|^2_{\mathcal{L}^2_\Omega} \leq c\|\boldsymbol{u}(0,\cdot)\|^2_{\mathcal{L}^2_\Omega} e^{-\lambda t}. \tag{6.5}$$

That is, system (6.1) *converges to the base flow* $(\boldsymbol{U}, P)$ *satisfying* (6.3).

If the perturbation velocities are exponentially stable, we can study bounds on the maximum energy growth from initial conditions. In the context of linear systems, this corresponds to maximum transient growth [123].

Definition 6.2.2 (Energy Growth Boundedness) *Let* $\boldsymbol{d} \equiv 0$ *in* (6.4). *There exists a constant* $\gamma > 0$ *such that*

$$\|\boldsymbol{u}\|^2_{\mathcal{L}^2_{[0,\infty),\Omega}} \leq \gamma^2 \|\boldsymbol{u}(0,\cdot)\|^2_{\mathcal{L}^2_\Omega}. \tag{6.6}$$

The energy growth bound inequality given in (6.6) determines how much the energy of initial perturbations is amplified. The minimum γ such that (6.6) holds provides an upper-bound to maximum energy growth for the flow. The next property of interest is related to amplifications from body forces or inputs rather than initial conditions.

Definition 6.2.3 (Worst-Case Input Amplification) *For some* $\eta_i > 0$*,* $i \in I$*,*

$$\|\boldsymbol{u}\|^2_{\mathcal{L}^2_{[0,\infty),\Omega}} \leq \sum_{i \in I} \eta_i^2 \|d_i\|^2_{\mathcal{L}^2_{[0,\infty),\Omega}}, \tag{6.7}$$

subject to zero initial conditions $\boldsymbol{u}(0, \mathrm{x}) \equiv 0,\ \forall \mathrm{x} \in \Omega$.

The above property is equivalent to the induced $\mathcal{L}^2$-norm. Due to nonlinear flow dynamics, the actual induced $\mathcal{L}^2$-norm of system (6.4) is a nonlinear function of $\|\boldsymbol{d}\|_{\mathcal{L}^2_{[0,\infty),\Omega}}$

(see Example 4.5.3). The quantities $\eta_i,\ i \in I$ provide upper-bounds on the actual induced $\mathcal{L}^2$-norms.

The definition of the worst-case input amplification requires the inputs (or forcings) to be square integrable. This automatically leads to the exclusion of persistent forcings, such as constant forcings and sinusoidal forcings that are defined for all time. To include these classes of forcings as well, we employ input-to-state stability. In this case, the only requirement on the forcings is that they should be upper-bounded.

Definition 6.2.4 (Input-to-State Stability) *For some scalar $\psi > 0$, functions $\beta, \tilde{\beta}, \chi \in \mathcal{K}_\infty$, and $\sigma \in \mathcal{K}$, it holds that*

$$\|\boldsymbol{u}(t,\cdot)\|_{\mathcal{L}^2_\Omega} \ \leq \ \beta\left(e^{-\psi t}\chi\left(\|\boldsymbol{u}(0,\cdot)\|_{\mathcal{L}^2_\Omega}\right)\right) + \tilde{\beta}\left(\sup_{\tau\in[0,t)}\left(\int_\Omega \sigma\big(|\boldsymbol{d}(\tau,\mathrm{x})|\big)\ d\Omega\right)\right), \quad (6.8)$$

for all $t > 0$.

The ISS property (6.8) implies the exponential convergence to the base flow $(\boldsymbol{U}, P)$ in $\mathcal{L}^2_\Omega$ when $\boldsymbol{d} \equiv 0$. Moreover, as $t \to \infty$, we obtain

$$\lim_{t\to\infty}\|\boldsymbol{u}(t,\cdot)\|_{\mathcal{L}^2_\Omega} \leq \tilde{\beta}\left(\int_\Omega \|\sigma(|\boldsymbol{d}(\cdot,\mathrm{x})|)\|_{\mathcal{L}^\infty_{[0,\infty)}}\ d\Omega\right) \leq \tilde{\beta}\left(\int_\Omega \sigma(\|\boldsymbol{d}(\cdot,\mathrm{x})\|_{\mathcal{L}^\infty_{[0,\infty)}})\ d\Omega\right), \quad (6.9)$$

wherein, the fact that $\sigma, \beta \in \mathcal{K}$ is used. Hence, as long as the external excitations or body forces $\boldsymbol{d}$ are bounded in the $\mathcal{L}^\infty_{[0,\infty)}$-norm, the perturbation velocities $\boldsymbol{u}$ are bounded in the $\mathcal{L}^2_\Omega$-norm.

The next result converts the tests for exponential stability, energy growth boundedness, worst-case input amplification (induced $\mathcal{L}^2$-norms), and ISS into verifying a set of dissipation inequalities, thanks to dissipativity theory, which allows for the analysis of the nonlinear flow model.

Theorem 6.2.5 *Consider the perturbation model* (6.4)*. If there exist a positive semidefinite storage functional* $V(\boldsymbol{u})$*, positive scalars* $\{\eta_i\}_{i\in I}$*,* $\{c_i\}_{i\in\{1,2,3\}}$*,* ψ*, and functions* $\beta_1, \beta_2 \in \mathcal{K}_\infty$*,* $\sigma \in \mathcal{K}$*, such that*

I) when $\boldsymbol{d} \equiv 0$*,*

$$c_1\|\boldsymbol{u}(t,\cdot)\|^2_{\mathcal{L}^2_\Omega} \leq V(\boldsymbol{u}) \leq c_2\|\boldsymbol{u}(t,\cdot)\|^2_{\mathcal{L}^2_\Omega}, \tag{6.10}$$

$$\frac{dV(\boldsymbol{u}(t,\mathrm{x}))}{dt} \leq -c_3\|\boldsymbol{u}(t,\cdot)\|^2_{\mathcal{L}^2_\Omega}, \tag{6.11}$$

then, system (6.4) *is exponentially stable.*

II) when $\boldsymbol{d} \equiv 0$*, the system is exponentially stable and*

$$V(\boldsymbol{u}) \leq \gamma^2\|\boldsymbol{u}(t,\cdot)\|^2_{\mathcal{L}^2_\Omega}, \tag{6.12}$$

$$\frac{dV(\boldsymbol{u}(t,\mathrm{x}))}{dt} \leq -\int_\Omega \boldsymbol{u}'(t,\mathrm{x})\boldsymbol{u}(t,\mathrm{x})\ d\Omega, \tag{6.13}$$

then, it has bounded energy growth as given by (6.6)*.*

III)

$$\frac{dV(\boldsymbol{u}(t,\mathrm{x}))}{dt} \leq -\int_\Omega \boldsymbol{u}'(t,\mathrm{x})\boldsymbol{u}(t,\mathrm{x})\ d\Omega + \int_\Omega \sum_{i\in I} \eta_i^2 d_i^2(t,\mathrm{x})\ d\Omega, \tag{6.14}$$

then system (6.4) *has induced* $\mathcal{L}^2$*-norm upper-bounds* η_i*,* $i \in I$ *as in* (6.7)*.*

IV)

$$\beta_1(\|\boldsymbol{u}(t,\cdot)\|_{\mathcal{L}^2_\Omega}) \leq V(\boldsymbol{u}) \leq \beta_2(\|\boldsymbol{u}(t,\cdot)\|_{\mathcal{L}^2_\Omega}), \tag{6.15}$$

$$\frac{dV(\boldsymbol{u}(t,\mathrm{x}))}{dt} \leq -\psi V(\boldsymbol{u}(t,\mathrm{x})) + \int_\Omega \sigma(|\boldsymbol{d}(t,\mathrm{x})|)\ d\Omega, \tag{6.16}$$

then system (6.4) *is ISS and satisfies* (6.8) *with* $\chi = \beta_2$*,* $\beta = \beta_1^{-1} \circ 2$ *and* $\tilde{\beta} = \beta_1^{-1} \circ \frac{2}{\psi}$*.*

Proof: Items I, III, and IV are direct applications of Theorem 3.3.1 in Chapter 3 and Theorem 4.1.5 in Chapter 4. For Item II, integrating both sides of (6.13) with respect to

time from 0 to ∞ yields

$$V(\boldsymbol{u}(\infty, \mathrm{x})) - V(\boldsymbol{u}(0, \mathrm{x})) \leq -\|\boldsymbol{u}\|^2_{\mathcal{L}^2_{[0,\infty),\Omega}}.$$

Since the system is exponentially stable, $\boldsymbol{u}(\infty, \mathrm{x}) = 0$ and therefore $V(\boldsymbol{u}(\infty, \mathrm{x})) = 0$. Thus, we obtain

$$-V(\boldsymbol{u}(0, \mathrm{x})) \leq -\|\boldsymbol{u}\|^2_{\mathcal{L}^2_{[0,\infty),\Omega}}.$$

Multiplying both sides of the above inequality by -1 yields

$$V(\boldsymbol{u}(0, \mathrm{x})) \geq \|\boldsymbol{u}\|^2_{\mathcal{L}^2_{[0,\infty),\Omega}}.$$

Applying (6.12), we get

$$\gamma^2 \|\boldsymbol{u}(0, \cdot)\|^2_{\mathcal{L}^2_\Omega} \geq V(\boldsymbol{u}(0, \mathrm{x})) \geq \|\boldsymbol{u}\|^2_{\mathcal{L}^2_{[0,\infty),\Omega}},$$

which is identical to (6.6). □

In this following, we derive classes of storage functionals $V(\boldsymbol{u})$ suitable for the analysis of perturbation dynamics (6.4) constant in one of the three spatial coordinates. We consider two classes of flows, namely, channel flows and pipe flows.

6.2.1 Channel Flows: Cartesian Coordinates

In Cartesian coordinates, for a scalar function v, $\nabla v = \sum_i \partial_{x_i} v \overrightarrow{e}_i$ and $\nabla^2 v = \sum_i \partial^2_{x_i} v$, where $\overrightarrow{e}_i$ is the unit vector in the direction x_i. For a vector valued function $\boldsymbol{w} = \sum_i w_i \overrightarrow{e}_i$, the divergence $\nabla \cdot \boldsymbol{w}$ is given by $\nabla \cdot \boldsymbol{w} = \sum_i \partial_{x_i} w_i$. In the following, $\{x_1, x_2, x_3\}$ corresponds to $\{x, y, z\}$ and $I = \{1, 2, 3\}$. Additionally, we adopt Einstein's multi-index notation over index j, that is the sum over repeated indices j, e.g., $v_j \partial_{x_j} u_i = \sum_j v_j \partial_{x_j} u_i$.

The perturbation model (6.4) can be re-written as

$$\begin{aligned} \partial_t u_i &= \frac{1}{Re}\nabla^2 u_i - u_j\partial_{x_j}u_i - U_j\partial_{x_j}u_i - u_j\partial_{x_j}U_i - \partial_{x_i}p + F_{ij}u_j + d_i, \\ 0 &= \partial_{x_j}u_j. \end{aligned} \tag{6.17}$$

where $i, j \in I$ and F_{ij} is the (i, j) entry of F. To simplify the exposition, without loss of generality, we assume that the perturbations are constant with respect to x_1. Since $x_i,\ i = 1, 2, 3$ are arbitrary, this does not affect the formulation. This assumption is used so that the presentation of the proof of Proposition 6.2.6 becomes more compact.

The next proposition states that, by choosing a suitable Lyapunov/storage functional structure, the time derivative of the Lyapunov/storage functional turns out to be a quadratic form in the dependent variables $\boldsymbol{u}$ and their spatial derivatives. This property paves the way for a convex optimization based method to check stability and input-output properties.

Proposition 6.2.6 *Consider the perturbation model* (6.17) *subject to periodic or no-slip boundary conditions* $\boldsymbol{u}|_{\partial\Omega} = 0$. *Assume the velocity perturbations in* (6.17) *are constant with respect to* x_1. *Let* $I_0 = \{2, 3\}$ *and*

$$V(\boldsymbol{u}) = \frac{1}{2}\int_\Omega \boldsymbol{u}' Q \boldsymbol{u}\ d\Omega, \tag{6.18}$$

where $Q = \begin{bmatrix} q_1 & 0 & 0 \\ 0 & q_i & 0 \\ 0 & 0 & q_j \end{bmatrix} > 0$, $q_i = q_j$ *for* $i \neq j$, $i, j \in I_0$, *be a candidate Lyapunov or storage functional. Then, the time derivative of* (6.18) *satisfies*

$$\partial_t V(\boldsymbol{u}) \leq -\sum_{i\in I} q_i \int_\Omega \left(\frac{C(\Omega)}{Re}u_i^2 + U_j u_i \partial_{x_j}u_i + u_j u_i \partial_{x_j}U_i - u_i F_{ij} u_j - u_i d_i \right) d\Omega, \tag{6.19}$$

where $C > 0$.

Proof: The time derivative of Lyapunov functional (6.18) along the solutions of (6.17) can be computed as

$$\partial_t V(\boldsymbol{u}) = \sum_{i\in I}\int_\Omega q_i\bigg(\frac{1}{Re}u_i\nabla^2 u_i - u_j u_i\partial_{x_j}u_i \\ - U_j u_i\partial_{x_j}u_i - u_j u_i\partial_{x_j}U_i - u_i\partial_{x_i}p + u_i F_{ij}u_j + u_i d_i\bigg)\, d\Omega. \quad (6.20)$$

Consider $\int_\Omega q_i u_j u_i \partial_{x_j} u_i \; d\Omega$. Using the boundary conditions, integration by parts and the incompressibility condition $\partial_{x_j} u_j = 0$, we obtain

$$\int_\Omega q_i u_j u_i \partial_{x_j} u_i \; d\Omega = \frac{1}{2}\int_{\Omega_i} q_i u_j u_i^2|_{\partial\Omega_j} \; dx_i - \frac{1}{2}\int_\Omega q_i u_i^2 \left(\partial_{x_j} u_j\right) \; d\Omega = 0.$$

Consider the pressure terms $\int_\Omega q_i u_i \partial_{x_i} p \; d\Omega$. Since the perturbations are assumed constant in x_1, we have

$$\int_\Omega \left(q_2 u_2 \partial_{x_2} p + q_3 u_3 \partial_{x_3} p\right) \; d\Omega \\ = \int_{\Omega_3} (q_2 u_2 p)|_{\partial\Omega_2} \; dx_3 + \int_{\Omega_2} (q_3 u_3 p)|_{\partial\Omega_3} \; dx_2 - \int_\Omega \left(q_2\partial_{x_2}u_2 p + q_3\partial_{x_3}u_3 p\right) \; d\Omega \\ = -\int_\Omega \left(q_2\partial_{x_2}u_2 + q_3\partial_{x_3}u_3\right) p \; d\Omega, \quad (6.21)$$

where, in the first equality above, we use integration by parts and, in the second inequality, we use the boundary conditions. Then, if $q_2 = q_3$, using the incompressibility condition $\partial_{x_2}u_2 + \partial_{x_3}u_3 = 0$, (6.21) equals zero. Therefore, the time derivative of the Lyapunov/storage functional (6.20) is modified to

$$\partial_t V(\boldsymbol{u}) \; = \; \sum_{i\in I}\int_\Omega q_i\bigg(\frac{1}{Re}u_i\nabla^2 u_i \; - \; U_j u_i\partial_{x_j}u_i \; - \; u_j u_i\partial_{x_j}U_i \; + \; u_i F_{ij}u_j \; + \; u_i d_i\bigg)\, d\Omega. \quad (6.22)$$

Integrating by parts the $u_i\nabla^2 u_i$ term and using the boundary conditions, we get

$$\partial_t V(\boldsymbol{u}) \;=\; \sum_{i\in I}\int_\Omega q_i\left(\frac{-1}{Re}(\partial_{x_i}u_i)^2 - U_j u_i\partial_{x_j}u_i - u_j u_i\partial_{x_j}U_i + u_i F_{ij}u_j + u_i d_i\right)\, d\Omega. \tag{6.23}$$

Applying the Poincaré inequality to (6.23), we obtain (6.19). □

Remark 6.2.7 *A special case of* (6.18) *was used in [56] to study the stability of viscous flows (subject to streamwise constant perturbations) in pipes and between rotating cylinders. The authors referred to this structure as* the two energy function*. In the formulation presented in this chapter, assuming constant perturbations in the x_1-direction, we can represent the two energy function as*

$$V(\boldsymbol{u}) = \frac{1}{2}\int_\Omega \boldsymbol{u}'\left[\begin{smallmatrix} q & 0 & 0\\ 0 & 1 & 0\\ 0 & 0 & 1\end{smallmatrix}\right]\boldsymbol{u}\; d\Omega,$$

where $q > 0$ is a constant. The "optimal" value for this constant was then calculated analytically for the pipe Poiseuille and the rotating Couette flow.

In the sequel, we use structure (6.18) as a Lyapunov functional when studying stability and as a storage functional when studying input-output properties.

The next corollary proposes integral inequalities under which properties such as stability, energy growth bounds, input-state induced $\mathcal{L}^2$ bounds and ISS can be inferred for the flow described by (6.17).

Corollary 6.2.8 *Consider the perturbation dynamics described by* (6.17) *subject to periodic or no-slip boundary conditions $\boldsymbol{u}|_{\partial\Omega} = 0$. Assume the velocity perturbations are constant with respect to x_1. Let $I_0 = \{2, 3\}$. If there exist positive constants q_i, $i \in I$, with $q_i = q_j$, $i, j \in I_0$, positive scalars $\{\psi_i\}_{i\in I}$, $\{\eta\}_{i\in I}$, and $\sigma \in \mathcal{K}$ such that*

I) when $\boldsymbol{d} \equiv 0$*,*

$$\sum_{i\in I} q_i \int_\Omega \left(\frac{C(\Omega)}{Re} u_i^2 + U_j u_i \partial_{x_j} u_i + u_j u_i \partial_{x_j} U_i - u_i F_{ij} u_j \right) d\Omega > 0, \tag{6.24}$$

II) when $\boldsymbol{d} \equiv 0$*,*

$$\sum_{i\in I} \int_\Omega \left(\left(\frac{q_i C(\Omega)}{Re} - 1 \right) u_i^2 + q_i U_j u_i \partial_{x_j} u_i + q_i u_j u_i \partial_{x_j} U_i - q_i u_i F_{ij} u_j \right) d\Omega \geq 0, \tag{6.25}$$

III)

$$\sum_{i\in I} \int_\Omega \left(\left(\frac{q_i C(\Omega)}{Re} - 1 \right) u_i^2 + q_i U_j u_i \partial_{x_j} u_i \right.$$
$$\left. + q_i u_j u_i \partial_{x_j} U_i - q_i u_i F_{ij} u_j - q_i u_i d_i + \eta_i^2 d_i^2 \right) d\Omega \geq 0 \tag{6.26}$$

IV)

$$\sum_{i\in I} \int_\Omega \left(\left(\frac{q_i C(\Omega)}{Re} - \psi_i q_i \right) u_i^2 + q_i U_j u_i \partial_{x_j} u_i + q_i u_j u_i \partial_{x_j} U_i - q_i u_i F_{ij} u_j \right.$$
$$\left. - q_i u_i d_i + \sigma(|\boldsymbol{d}|) \right) d\Omega \geq 0 \tag{6.27}$$

Then,

I) perturbation velocities given by (6.17) *are exponentially stable. Therefore, the flow converges to the base flow exponentially.*

II) system (6.17) *has bounded energy growth as described by* (6.6) *with* $\gamma^2 = \max_{i\in I} q_i$*.*

III) under zero perturbation initial conditions $\boldsymbol{u}(0, \mathrm{x}) \equiv 0$*, the induced* $\mathcal{L}^2$*-norm from inputs to perturbation velocities is bounded by* η_i*,* $i \in I$ *as in* (6.7)*.*

IV) the perturbation velocities described by (6.17) *are ISS in the sense of* (6.8)*.*

Proof: Each item is proven as follows.

I) Considering Lyapunov functional (6.18), inequality (6.10) is satisfied with $c_1 = \min_{i\in I} q_i$ and $c_2 = \max_{i\in I} q_i$. Re-arranging the terms in (6.24) gives

$$-\sum_{i\in I} q_i \int_\Omega \left(\frac{C(\Omega)}{Re} u_i^2 + U_j u_i \partial_{x_j} u_i + u_j u_i \partial_{x_j} U_i - u_i F_{ij} u_j - u_i d_i \right) d\Omega < 0. \quad (6.28)$$

Then, from Proposition 6.2.6, we infer that, for $d \equiv 0$, $\partial_t V(\boldsymbol{u}) < 0$. By continuity, we infer that there exists $c_3 > 0$ such that (6.11) holds. Then, form Item I in Theorem 6.2.5, we infer that the perturbation velocities are exponentially stable.

II) Given storage functional structure (6.18), we have

$$V(\boldsymbol{u}(t, \mathrm{x})) \leq \lambda_M(Q) \int_\Omega \boldsymbol{u}'\boldsymbol{u} \; d\Omega,$$

where $\lambda_M(Q)$ denotes the maximum eigenvalue of Q. Since Q is diagonal, we have $\lambda_M(Q) = \max_{i\in I} q_i$. Therefore, (6.12) is satisfied with $\gamma^2 = \max_{i\in I} q_i$. Re-arranging terms in (6.25) yields

$$-\sum_{i\in I} q_i \int_\Omega \left(\frac{C(\Omega)}{Re} u_i^2 + U_j u_i \partial_{x_j} u_i + u_j u_i \partial_{x_j} U_i - u_i F_{ij} u_j \right) d\Omega \leq \sum_{i\in I} \int_\Omega u_i^2 \; d\Omega.$$

Applying Proposition 6.2.6 with $d \equiv 0$, we obtain

$$\partial_t V(\boldsymbol{u}) \leq \sum_{i\in I} \int_\Omega u_i^2 \; d\Omega.$$

Thus, inequality (6.13) is also satisfied. Applying Item II from Theorem 6.2.5, we infer that the system has bounded energy growth.

III) Re-arranging terms in (6.26) yields

$$-\sum_{i\in I} q_i \int_\Omega \left(\frac{C(\Omega)}{Re} u_i^2 + U_j u_i \partial_{x_j} u_i + u_j u_i \partial_{x_j} U_i - u_i F_{ij} u_j - u_i d_i \right) d\Omega \\ \leq -\sum_{i\in I} \int_\Omega u_i^2 \; d\Omega + \sum_{i\in I} \int_\Omega \eta_i^2 d_i^2 \; d\Omega \quad (6.29)$$

Then, from (6.19) in Proposition 6.2.6, we deduce that

$$\partial_t V(\boldsymbol{u}) \leq -\sum_{i\in I} \int_\Omega u_i^2 \; d\Omega + \sum_{i\in I} \int_\Omega \eta_i^2 d_i^2 \; d\Omega.$$

From Item II in Theorem 6.2.5, we infer that, under zero initial conditions, the perturbation velocities satisfy (6.7).

IV) Adopting (6.18) as a storage functional, (6.15) is satisfied with $\beta_1(\cdot) = \min_{i\in I} q_i(\cdot)^2$ and $\beta_2(\cdot) = \max_{i\in I} q_i(\cdot)^2$. Re-arranging the terms in (6.27), we obtain

$$-\sum_{i\in I} \int_\Omega \left(\frac{q_i C(\Omega)}{Re} u_i^2 + q_i U_j u_i \partial_{x_j} u_i + q_i u_j u_i \partial_{x_j} U_i - q_i u_i F_{ij} u_j - q_i u_i d_i \right) d\Omega \\ \leq -\sum_{i\in I} \psi_i \int_\Omega q_i u_i^2 \; d\Omega + \int_\Omega \sigma(|\boldsymbol{d}|) \; d\Omega \quad (6.30)$$

From (6.19) in Proposition 6.2.6, it follows that

$$\partial_t V(\boldsymbol{u}) \leq -\psi V(\boldsymbol{u}) + \int_\Omega \sigma(|\boldsymbol{d}|) \; d\Omega, \quad (6.31)$$

with $\psi = \min_{i\in I} \psi_i$. Then, from Item III in Theorem 6.2.5, we infer that the perturbation velocities satisfy the ISS property (6.8). □

6.2.2 Pipe Flows: Cylindrical Coordinates

We now turn our attention to flows in cylindrical coordinates (r, θ, z). In cylindrical coordinates, the gradient and Laplacian operators are, respectively, defined as $\nabla_c(\cdot) = \partial_r(\cdot)\overrightarrow{e}_r +$

$\frac{1}{r}\partial_\theta(\cdot)\overrightarrow{e}_\theta + \partial_z(\cdot)\overrightarrow{e}_z$ and $\nabla_c^2(\cdot) = \frac{1}{r}\partial_r\left(r\partial_r(\cdot)\right) + \frac{1}{r^2}\partial_\theta^2(\cdot) + \partial_z^2(\cdot)$. The Navier-Stokes equations in cylindrical coordinates are then given by

$$\begin{aligned}
\partial_t \bar{u}_r &= \frac{1}{Re}\left(\nabla_c^2 \bar{u}_r - \frac{\bar{u}_r}{r^2} - \frac{2}{r^2}\partial_\theta \bar{u}_\theta\right) - \bar{\boldsymbol{u}}\cdot\nabla_c \bar{u}_r + \frac{\bar{u}_\theta^2}{r} - \partial_r \bar{p} + F_r'\bar{\boldsymbol{u}} + d_r \\
\partial_t \bar{u}_\theta &= \frac{1}{Re}\left(\nabla_c^2 \bar{u}_\theta - \frac{\bar{u}_\theta}{r^2} + \frac{2}{r^2}\partial_\theta \bar{u}_r\right) - \bar{\boldsymbol{u}}\cdot\nabla_c \bar{u}_\theta - \frac{\bar{u}_\theta \bar{u}_r}{r} - \frac{1}{r}\partial_\theta \bar{p} + F_\theta'\bar{\boldsymbol{u}} + d_\theta \\
\partial_t \bar{u}_z &= \frac{1}{Re}\nabla_c^2 \bar{u}_z - \bar{\boldsymbol{u}}\cdot\nabla_c \bar{u}_z - \partial_z \bar{p} + F_z'\bar{\boldsymbol{u}} + d_z \\
0 &= \frac{1}{r}\partial_r\left(r\bar{u}_r\right) + \frac{1}{r}\partial_\theta \bar{u}_\theta + \partial_z \bar{u}_z,
\end{aligned} \tag{6.32}$$

where $\bar{\boldsymbol{u}} = (\bar{u}_r, \bar{u}_\theta, \bar{u}_z)'$ and $\left[\begin{smallmatrix} F_r' & F_\theta' & F_z' \end{smallmatrix}\right]' = F \in \mathbb{R}^{3\times 3}$.

In this section, we consider the flow perturbations that are constant in z-direction. The base flow is given by $\boldsymbol{U} = U_m(r,\theta)\overrightarrow{e}_z$ and P. For such flows, substituting $\bar{\boldsymbol{u}} = \boldsymbol{u} + \boldsymbol{U}$ and $\bar{p} = P + p$ in (6.32), the perturbation dynamics is obtained as

$$\begin{aligned}
\partial_t u_r &= \frac{1}{Re}\nabla_c^2 u_r - u_r\partial_r u_r - \frac{u_\theta \partial_\theta u_r}{r} + \frac{u_\theta^2}{r} - \frac{u_r}{r^2 Re} - \frac{2\partial_\theta u_\theta}{r^2 Re} - \partial_r p + F_r'\boldsymbol{u} + d_r, \\
\partial_t u_\theta &= \frac{1}{Re}\nabla_c^2 u_\theta - u_r\partial_r u_\theta - \frac{u_\theta \partial_\theta u_\theta}{r} - \frac{u_r u_\theta}{r} - \frac{u_\theta}{r^2 Re} - \frac{2\partial_\theta u_\theta}{r^2 Re} - \frac{1}{r}\partial_\theta p + F_\theta'\boldsymbol{u} + d_\theta, \\
\partial_t u_z &= \frac{1}{Re}\nabla_c^2 u_z - u_r\partial_r u_z - u_r\partial_r U_m - \frac{u_\theta \partial_\theta U_m}{r} - \frac{u_\theta \partial_\theta u_z}{r} + F_z'\boldsymbol{u} + d_z, \\
0 &= \partial_r(r u_r) + \partial_\theta u_\theta,
\end{aligned} \tag{6.33}$$

wherein $\boldsymbol{u} = (u_r, u_\theta, u_z)'$.

Proposition 6.2.9 *Consider the perturbation dynamics in cylindrical coordinates* (6.33) *with periodic or no-slip boundary conditions* $u \mid_{\partial\Omega} = 0$. *The time derivative of Lyapunov/storage functional*

$$V(\boldsymbol{u}) = \frac{1}{2}\int_\Omega \begin{bmatrix} u_r \\ u_\theta \\ u_z \end{bmatrix}' \begin{bmatrix} q_r & 0 & 0 \\ 0 & q_\theta & 0 \\ 0 & 0 & q_z \end{bmatrix} \begin{bmatrix} u_r \\ u_\theta \\ u_z \end{bmatrix} \, r dr d\theta, \tag{6.34}$$

with $q_r = q_\theta$, satisfies

$$\partial_t V(\boldsymbol{u}) \leq -\int_\Omega \Big(\frac{q_r C}{Re} u_r^2 + q_z \partial_r U_m u_r u_z + \frac{q_z C}{Re} u_z^2 + \frac{q_z}{r} \partial_\theta U_m u_\theta u_z + \frac{q_\theta C}{Re} u_\theta^2 \\ - q_r u_r F_r' \boldsymbol{u} - q_\theta u_\theta F_\theta' \boldsymbol{u} - q_z u_z F_z' \boldsymbol{u} - q_r u_r d_r - q_\theta u_\theta d_\theta - q_z u_z d_z \Big)\, r dr d\theta, \quad (6.35)$$

where $C > 0$.

Proof: The time derivative of the Lyapunov/storage functional (6.34) is given by

$$\begin{aligned} \partial_t V(\boldsymbol{u}) = &\int_\Omega \Big(- r q_r u_r^2 \partial_r u_r - q_r u_r u_\theta \partial_\theta u_r + q_r u_r u_\theta^2 - r q_r \partial_r p u_r \\ &+ \frac{q_r}{Re} r u_r \nabla_c^2 u_r - \frac{q_r u_r^2}{Rer} - \frac{2 q_r u_r \partial_\theta u_\theta}{rRe} + q_r r u_r F_r' \boldsymbol{u} + q_r r u_r d_r \Big)\, d\theta dr \\ &+ \int_\Omega \Big(- r q_\theta u_r u_\theta \partial_r u_\theta - q_\theta u_r u_\theta \partial_\theta u_r - q_\theta u_r u_\theta^2 - q_\theta \partial_\theta p u_\theta \\ &+ \frac{q_\theta}{Re} r u_\theta \nabla_c^2 u_\theta - \frac{q_\theta u_\theta^2}{rRe} + \frac{2 q_\theta \partial_\theta u_r u_\theta}{rRe} + q_\theta r u_\theta F_\theta' \boldsymbol{u} + q_\theta r u_\theta d_\theta \Big)\, dr d\theta \\ &+ \int_\Omega \Big(- r q_z u_r u_z \partial_r u_z - r q_z u_r u_z \partial_r U_m - q_z \partial_\theta U_m u_\theta u_z - q_z u_\theta u_z \partial_r u_z \\ &+ \frac{q_z}{Re} r u_z \nabla_c^2 u_z + q_z r u_z F_z' \boldsymbol{u} + q_z r u_z d_z \Big)\, dr d\theta. \quad (6.36) \end{aligned}$$

From the incompressibility condition $\partial_r(r u_r) + \partial_\theta u_\theta = 0$ and the fact that $q_r = q_\theta$, we obtain

$$\begin{aligned} \int_\Omega (-r q_r \partial_r p u_r - q_\theta \partial_\theta p u_\theta)\; dr d\theta &= \int_\Omega (q_r \partial_r (r u_r) p + q_\theta \partial_\theta u p)\; dr d\theta \\ &= \int_\Omega q_r p\, (\partial_r (r u_r) + \partial_\theta u)\; dr d\theta = 0. \quad (6.37) \end{aligned}$$

where, in the first equality above, we used integration by parts and the boundary conditions. Furthermore, using integration by parts, boundary conditions and the incompressibility

condition it can be shown that

$$\int_\Omega \left(-rq_r u_r^2 \partial_r u_r - q_r u_r u_\theta \partial_\theta u_r\right)\ drd\theta = \int_\Omega \left(\frac{q_r u_r^2}{2}\partial_r(ru_r) + \frac{q_r u_r^2}{2}\partial_\theta u_\theta\right)\ drd\theta = 0,$$

$$\int_\Omega \left(-rq_\theta u_r u_\theta \partial_r u_\theta - q_\theta u_\theta^2 \partial_\theta u_\theta\right)\ drd\theta = \int_\Omega \left(\frac{q_\theta u_\theta^2}{2}\partial_r(ru_r) + \frac{q_\theta u_\theta^2}{2}\partial_\theta u_\theta\right)\ drd\theta = 0,$$

$$\int_\Omega (-rq_z u_r u_z \partial_r u_z - q_z u_\theta u_z \partial_\theta u_z)\ drd\theta = \int_\Omega \left(\frac{q_z u_z^2}{2}\partial_r(ru_r) + \frac{q_z u_z^2}{2}\partial_\theta u_\theta\right)\ drd\theta = 0,$$

and

$$\int_\Omega \left(-\frac{2q_r u_r \partial_\theta u_\theta}{rRe} - \frac{2q_\theta \partial_\theta u_r u_\theta}{rRe}\right)\ drd\theta = \int_\Omega \frac{2q_r}{rRe}\left(-u_r\partial_\theta u_\theta + u_r \partial_\theta u_\theta\right)\ drd\theta = 0.$$

Then, the time derivative expression (6.36) simplifies to

$$\begin{aligned}\partial_t V(\boldsymbol{u}) = &\int_\Omega \left(\frac{q_r}{Re} r u_r \nabla_c^2 u_r - \frac{q_r u_r^2}{Rer} + q_r r u_r F_r' \boldsymbol{u} + q_r r u_r d_r\right)\ d\theta dr \\ &+ \int_\Omega \left(\frac{q_\theta}{Re} r u_\theta \nabla_c^2 u_\theta - \frac{q_\theta u_\theta^2}{rRe} + q_\theta r u_\theta F_\theta' \boldsymbol{u} + q_\theta r u_\theta d_\theta\right)\ drd\theta \\ + \int_\Omega \Big(&- rq_z u_r u_z \partial_r U_m - q_z \partial_\theta U_m u_\theta u_z + \frac{q_z}{Re} r u_z \nabla_c^2 u_z + q_z r u_z F_z' \boldsymbol{u} + q_z r u_z d_z\Big)\ drd\theta.\end{aligned} \tag{6.38}$$

Factoring out r yields

$$\begin{aligned}\partial_t V(\boldsymbol{u}) = &\int_\Omega \left(\frac{q_r}{Re} u_r \nabla_c^2 u_r - \frac{q_r u_r^2}{r^2 Re} + q_r u_r F_r' \boldsymbol{u} + q_r u_r d_r\right)\ rd\theta dr \\ &+ \int_\Omega \left(\frac{q_\theta}{Re} u_\theta \nabla_c^2 u_\theta - \frac{q_\theta u_\theta^2}{r^2 Re} + q_\theta u_\theta F_\theta' \boldsymbol{u} + q_\theta u_\theta d_\theta\right)\ rdrd\theta \\ + \int_\Omega \Big(&- q_z u_r u_z \partial_r U_m - \frac{q_z}{r}\partial_\theta U_m u_\theta u_z + \frac{q_z}{Re} u_z \nabla_c^2 u_z + q_z u_z F_z' \boldsymbol{u} + q_z u_z d_z\Big)\ rdrd\theta.\end{aligned} \tag{6.39}$$

Since the terms $\frac{q_r u_r^2}{r^2 Re}$ and $\frac{q_\theta u_\theta^2}{r^2 Re}$ are non-negative, it follows that

$$\begin{aligned}\partial_t V(\boldsymbol{u}) \leq \int_\Omega \Bigg(& \frac{q_r}{Re} u_r \nabla_c^2 u_r + \frac{q_\theta}{Re} u_\theta \nabla_c^2 u_\theta + \frac{q_z}{Re} u_z \nabla_c^2 u_z - q_z u_r u_z \partial_r U_m - \frac{q_z}{r} \partial_\theta U_m u_\theta u_z \\ & - q_r u_r F_r' \boldsymbol{u} - q_\theta u_\theta F_\theta' \boldsymbol{u} - q_z u_z F_z' \boldsymbol{u} - q_r u_r d_r - q_\theta u_\theta d_\theta - q_z u_z d_z \Bigg) \, r dr d\theta \\ = - \int_\Omega \Bigg(& \frac{q_r}{Re} |\nabla_c u_r|^2 + \frac{q_\theta}{Re} |\nabla_c u_\theta|^2 + \frac{q_z}{Re} |\nabla_c u_z|^2 + q_z u_r u_z \partial_r U_m + \frac{q_z}{r} \partial_\theta U_m u_\theta u_z \\ & - q_r u_r F_r' \boldsymbol{u} - q_\theta u_\theta F_\theta' \boldsymbol{u} - q_z u_z F_z' \boldsymbol{u} - q_r u_r d_r - q_\theta u_\theta d_\theta - q_z u_z d_z \Bigg) \, r dr d\theta, \quad (6.40)\end{aligned}$$

where in the last equality above integration by parts and the boundary conditions were used. Applying the Poincaré inequality (Lemma 2.2.3), we obtain (6.35). □

6.3 Convex Formulation for Streamwise Constant Perturbations

In this section, we show that the input-output analysis problem for the class of streamwise constant perturbations can be converted into a set of matrix inequalities. These matrix inequalities can be solved by convex optimization, provided that the base flow is a polynomial in the spatial coordinates and the flow geometry is a semi-algebraic set.

6.3.1 Convex Formulation: Channel Flows

To present a convex method for checking the conditions in Corollary 6.2.8, we restrict our attention to streamwise constant perturbations in the x_1-direction with base flow $\boldsymbol{U} = U_m(\mathrm{x})\overrightarrow{e}_1$.

Corollary 6.3.1 *Consider the perturbation dynamics given by* (6.17)*, that are constant in the streamwise direction x_1 and with base flow $\boldsymbol{U} = U_m(\mathrm{x})\overrightarrow{e}_1$. Let $I_0 = \{2, 3\}$. If there exist positive constants $\{q_l\}_{l \in I}$ with $q_i = q_j$, $i, j \in I_0$, $\{\eta_l\}_{l \in I}$, $\{\psi_l\}_{l \in I}$, and functions*

$\{\sigma_l\}_{l\in I}$ *such that*

I)

$$M(\mathrm{x}) = \begin{bmatrix} \left(\frac{C}{Re} - F_{11}\right) q_1 & \frac{q_1(\partial_{x_j} U_m(\mathrm{x}) - F_{1j}) - q_j F j1}{2} & \frac{q_1(\partial_{x_i} U_m(\mathrm{x}) - F_{1i}) - q_i F i1}{2} \\ \frac{q_1(\partial_{x_j} U_m(\mathrm{x}) - F_{1j}) - q_j F j1}{2} & \left(\frac{C}{Re} - F_{jj}\right) q_j & -\frac{q_j F_{j1}}{2} \\ \frac{q_1(\partial_{x_i} U_m(\mathrm{x}) - F_{1i}) - q_i F i1}{2} & -\frac{q_j F_{j1}}{2} & \left(\frac{C}{Re} - F_{ii}\right) q_i \end{bmatrix} \geq 0,$$

$$i, j \in I_0, i \neq j, \ \mathrm{x} \in \Omega. \quad (6.41)$$

II) when $\boldsymbol{d} \equiv 0$*,*

$$M(\mathrm{x}) - \mathrm{I}_{3\times 3} \geq 0, \ \mathrm{x} \in \Omega, \quad (6.42)$$

III)

$$N(\mathrm{x}) = \left[\begin{array}{ccc:ccc} & M(\mathrm{x}) - \mathrm{I}_{3\times 3} & & -\frac{q_1}{2} & 0 & 0 \\ & & & 0 & -\frac{q_j}{2} & 0 \\ & & & 0 & 0 & -\frac{q_i}{2} \\ \hdashline -\frac{q_1}{2} & 0 & 0 & \eta_1^2 & 0 & 0 \\ 0 & -\frac{q_j}{2} & 0 & 0 & \eta_i^2 & 0 \\ 0 & 0 & -\frac{q_i}{2} & 0 & 0 & \eta_j^2 \end{array}\right] \geq 0, \quad (6.43)$$

for $i, j \in I_0, i \neq j$ *and* $\mathrm{x} \in \Omega$*,*

IV) $\sigma_l(\mathrm{x}) \geq 0, \ \mathrm{x} \in \Omega$*,* $l \in I$ *and*

$$Z(\mathrm{x}) = \left[\begin{array}{ccc:ccc} & M(\mathrm{x}) - W & & -\frac{q_1}{2} & 0 & 0 \\ & & & 0 & -\frac{q_j}{2} & 0 \\ & & & 0 & 0 & -\frac{q_i}{2} \\ \hdashline -\frac{q_1}{2} & 0 & 0 & \sigma_1(\mathrm{x}) & 0 & 0 \\ 0 & -\frac{q_j}{2} & 0 & 0 & \sigma_j(\mathrm{x}) & 0 \\ 0 & 0 & -\frac{q_i}{2} & 0 & 0 & \sigma_i(\mathrm{x}) \end{array}\right] \geq 0, \quad (6.44)$$

for $i, j \in I_0, i \neq j$ *and* $\mathrm{x} \in \Omega$*, where* $W = \begin{bmatrix} \psi_1 q_1 & 0 & 0 \\ 0 & \psi_j q_j & 0 \\ 0 & 0 & \psi_i q_i \end{bmatrix}$*. Then, it follows that*

I) the perturbation velocities are exponentially stable,

II) the system has energy growth bound $\gamma^2 = \max_{i\in I} q_i$ *as described by* (6.6)*,*

III) subject to zero initial conditions, the induced $\mathcal{L}^2$ *norm from inputs to perturbation velocities is bounded by* η_i*,* $i \in I$ *as in* (6.7)*,*

IV) the perturbation velocities are ISS in the sense of (6.8) *with* $\sigma(|\boldsymbol{d}|) = \sum_{i\in I} \sigma_i(\mathrm{x}) d_i^2$*.*

Proof: The proof is straightforward and follows from computing conditions (6.24)-(6.27) considering perturbations that are constant in x_1, the base flow $\boldsymbol{U} = U_m \overrightarrow{e}_1$, and $\sigma(|\boldsymbol{d}|) = \sum_{i\in I} \sigma_i(\mathrm{x}) d_i^2$. Since the flow perturbations are constant in x_1 and the base flow is given by $\boldsymbol{U} = U_m \overrightarrow{e}_1$, we have $U_j u_i \partial_{x_j} u_i = 0$, $i \in I$.

I) Inequality (6.24) is given by

$$\begin{aligned}\mathcal{A} = \int_\Omega \Bigg(& \left(\frac{C(\Omega)}{Re} - F_{ii}\right) q_i u_i^2 - u_i(q_i F_{ij}) u_j - u_i(q_i F_{i1}) u_1 \\ & + \left(\frac{C(\Omega)}{Re} - F_{jj}\right) q_j u_j^2 - u_j(q_j F_{ji}) u_i - u_j(q_j F_{j1}) u_1 \\ & \left(\frac{C(\Omega)}{Re} - F_{11}\right) q_1 u_1^2 + u_1(\partial_{x_i} U_m - F_{1i}) u_i + u_1(\partial_{x_j} U_m - F_{1j}) \Bigg)\, d\Omega \geq 0 \end{aligned} \quad (6.45)$$

for $i, j \in I_0$, $i \neq j$, which can be rewritten as

$$\int_\Omega \begin{bmatrix} u_1 \\ u_j \\ u_i \end{bmatrix}' M(\mathrm{x}) \begin{bmatrix} u_1 \\ u_j \\ u_i \end{bmatrix} \, d\Omega \geq 0. \quad (6.46)$$

with $M(\mathrm{x})$ given in (6.41). Therefore, if (6.41) is satisfied, (6.46) also holds and from Item I in Corollary 6.2.8 we infer that the perturbation velocities are exponentially stable.

II) The proof follows from the proof of Item I. Inequality (6.25) can be re-written as

$$\int_\Omega \begin{bmatrix} u_1 \\ u_j \\ u_i \end{bmatrix}' M(\mathrm{x}) \begin{bmatrix} u_1 \\ u_j \\ u_i \end{bmatrix} \, d\Omega - \int_\Omega \begin{bmatrix} u_1 \\ u_j \\ u_i \end{bmatrix}' \begin{bmatrix} u_1 \\ u_j \\ u_i \end{bmatrix}' \, d\Omega \geq 0. \quad (6.47)$$

Thus, if inequality (6.42) holds, inequality (6.47) is satisfied. Therefore, from Corollary 6.2.8, we infer that the energy growth is bounded.

III) Inequality (6.26) is changed to

$$\mathcal{A} + \int_{\Omega} (q_i u_i d_i + q_j u_j d_j + q_1 u_1 d_1)\ d\Omega - \int_{\Omega} (u_i^2 + u_j^2 + u_1^2)\ d\Omega \\ + \int_{\Omega} (\eta_i^2 d_i^2 + \eta_j^2 d_j^2 + \eta_1^2 d_1^2)\ d\Omega \geq 0, \quad (6.48)$$

for $i, j \in I_0$, $i \neq j$, which can be rewritten as

$$\int_{\Omega} \begin{bmatrix} u_1 \\ u_j \\ u_i \\ d_1 \\ d_j \\ d_i \end{bmatrix}' N(\mathrm{x}) \begin{bmatrix} u_1 \\ u_j \\ u_i \\ d_1 \\ d_j \\ d_i \end{bmatrix}\ d\Omega \geq 0, \quad (6.49)$$

where N is defined in (6.43). Consequently, if (6.43) is satisfied for all $\mathrm{x} \in \Omega$, (6.49) holds and from Item II in Corollary 6.2.8 we infer that, subject to zero initial conditions, the induced $\mathcal{L}^2$-norm from inputs to perturbation velocities is bounded by η_i, $i \in I$ as in (6.7).
IV) The proof follows the same lines as the proof of Item III above. □

When $U_m(\mathrm{x}) \in \mathcal{R}[\mathrm{x}]$, inequalities (6.41)-(6.44) are polynomial matrix inequalities that should be checked for all $\mathrm{x} \in \Omega$. If the set Ω is a semi-algebraic set, *i.e.,*

$$\Omega = \left\{ \mathrm{x} \in \mathbb{R}^2 \mid g_l(\mathrm{x}) = 0,\ f_k(\mathrm{x}) > 0,\ l = 1, 2, \ldots, L,\ k = 1, 2, \ldots, K \right\},$$

where $\{g_l\}_{l=1}^{L} \in \mathcal{R}[\mathrm{x}]$ and $\{f_k\}_{k=1}^{K} \in \mathcal{R}[\mathrm{x}]$, then these inequalities can be cast as a SOS program by applying Corollary 2.3.4.

We are interested in estimating bounds on the maximum energy growth of the flow

under study. To this end, we solve the following optimization problem

$$\min_{\{q_i\}_{i\in I}} \left(\max_{i\in I} q_i \right)$$
$$\text{subject to}$$
$$M(\mathrm{x}) - \mathrm{I}_{3\times 3} \geq 0,$$
$$q_i > 0,\ i \in I. \tag{6.50}$$

In order to find upper-bounds on the induced $\mathcal{L}^2$-norm from the body forces or disturbances $\boldsymbol{d}$ to the perturbation velocities $\boldsymbol{u}$, we solve the following optimization problem

$$\min_{\{q_i\}_{i\in I}} \sum_{i\in I} \eta_i^2$$
$$\text{subject to}$$
$$N(\mathrm{x}) \geq 0,$$
$$q_i > 0,\ i \in I. \tag{6.51}$$

6.3.2 Convex Formulation: Pipe Flows

Similar to the case of channel flows, in the following, we propose a convex formulation for pipe flows. The method relies on inequality (6.35). Note that for cylindrical coordinates $I = \{r, \theta, z\}$ and $I_0 = \{r, \theta\}$.

Corollary 6.3.2 *Consider the perturbation dynamics given by* (6.33)*, streamwise constant in the z-direction with base flow $\boldsymbol{U} = U_m(r,\theta)\overrightarrow{e}_z$. Suppose that there exist positive constants $\{q_l\}_{l\in I}$ with $q_r = q_\theta$, $\{\psi_l\}_{l\in I}$, and functions $\{\sigma_l\}_{l\in I}$ such that*

I)

$$M_c(r,\theta) = \begin{bmatrix} \left(\frac{C}{Re}-F_{z,3}\right)q_z & \frac{1}{2}(q_z\partial_r U_m - q_r F_{r,3} - q_z F_{z,1}) & \frac{q_z}{2}\left(\frac{\partial_\theta U_m}{r}-F_{z,2}\right)-q_\theta F_{\theta,3} \\ \frac{1}{2}(q_z\partial_r U_m - q_r F_{r,3} - q_z F_{z,1}) & \left(\frac{C}{Re}-F_{r,1}\right)q_r & -\frac{1}{2}\left(q_r F_{r,2}+q_\theta F_{\theta,2}\right) \\ \frac{q_z}{2}\left(\frac{\partial_\theta U_m}{r}-F_{z,2}\right)-q_\theta F_{\theta,3} & -\frac{1}{2}\left(q_r F_{r,2}+q_\theta F_{\theta,2}\right) & \left(\frac{C}{Re}-F_{\theta,2}\right)q_\theta \end{bmatrix} \geq 0,$$

$$(r,\theta) \in \Omega. \quad (6.52)$$

II) the system is exponentially stable when $\mathbf{d} \equiv 0$ *and*

$$M_c\left(r,\theta\right) - \mathrm{I}_{3\times 3} \geq 0, \quad (r,\theta) \in \Omega, \tag{6.53}$$

III)

$$N_c(r,\theta) = \left[\begin{array}{ccc:ccc} & & & -\frac{q_z}{2} & 0 & 0 \\ & M_c(r,\theta) - \mathrm{I}_{3\times 3} & & 0 & -\frac{q_r}{2} & 0 \\ & & & 0 & 0 & -\frac{q_\theta}{2} \\ \hdashline -\frac{q_z}{2} & 0 & 0 & \eta_z^2 & 0 & 0 \\ 0 & -\frac{q_r}{2} & 0 & 0 & \eta_r^2 & 0 \\ 0 & 0 & -\frac{q_\theta}{2} & 0 & 0 & \eta_\theta^2 \end{array}\right] \geq 0, \quad (r,\theta) \in \Omega, \tag{6.54}$$

IV) $\sigma_l(r,\theta) \geq 0,\ (r,\theta) \in \Omega$*,* $l \in I$ *and*

$$Z_c(r,\theta) = \left[\begin{array}{ccc:ccc} & & & -\frac{q_z}{2} & 0 & 0 \\ & M_c(r,\theta) - W_c & & 0 & -\frac{q_r}{2} & 0 \\ & & & 0 & 0 & -\frac{q_\theta}{2} \\ \hdashline -\frac{q_z}{2} & 0 & 0 & \sigma_z(r,\theta) & 0 & 0 \\ 0 & -\frac{q_r}{2} & 0 & 0 & \sigma_r(r,\theta) & 0 \\ 0 & 0 & -\frac{q_\theta}{2} & 0 & 0 & \sigma_\theta(r,\theta) \end{array}\right] \geq 0, \quad (r,\theta) \in \Omega, \tag{6.55}$$

where $W_c = \begin{bmatrix} \psi_z q_z & 0 & 0 \\ 0 & \psi_r q_r & 0 \\ 0 & 0 & \psi_\theta q_\theta \end{bmatrix}$*. Then, it follows that*

I) the perturbation velocities are exponentially stable,

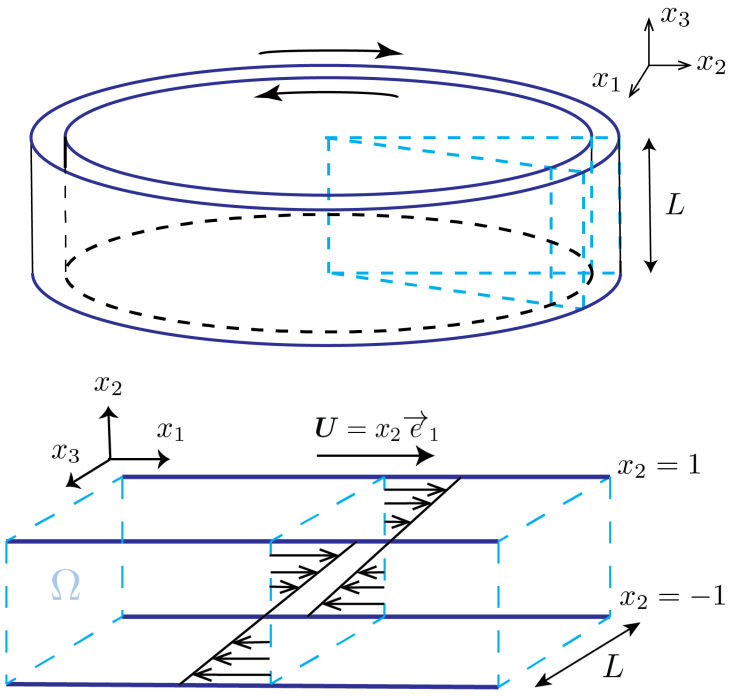

Figure 6.1: Schematic of the Taylor-Couette flow geometry.

II) the flow has bounded energy growth $\gamma^2 = \max(q_r, q_\theta, q_z)$ *as given by* (6.6)*,*

III) subject to zero initial conditions, the induced $\mathcal{L}^2$ *norm from inputs to perturbation velocities is bounded,*

IV) the perturbation velocities are ISS in the sense of (6.8) *with* $\sigma(|\boldsymbol{d}|) = \sum_{l\in I} \sigma_l(r,\theta) d_l^2$.

Note that, depending on $\partial_\theta U_m$, M_c and therefore N_c and Z_c can be functions of $\frac{1}{r}$. Then, inequalities (6.52)-(6.55) become intractable. To circumvent this problem, since r is positive, we can multiply (6.52)-(6.55) by positive powers of r making the resulting inequalities solvable by convex optimization methods.

6.4 Examples

In this section, we illustrate the proposed method by analyzing four benchmark flows, namely, Taylor-Couette flow, plane Couette flow, plane Poiseuille flow and Hagen-Poiseuille flow.

6.4.1 Taylor-Couette Flow

We consider the flow of viscous fluid between two co-axial cylinders, where the gap between the cylinders is much smaller than their radii. In this setting, the flow is schematically illustrated in Figure 6.1. The axis of rotation is parallel to the x_3-axis and the circumferential direction corresponds to x_1-axis. Then, the dynamics of the perturbation velocities is described by (6.4). The perturbations are assumed to be constant with respect to x_1 ($\partial_{x_1} = 0$) and periodic in x_3 with period L. The domain is, therefore, defined as

$$\Omega = \{(x_2, x_3) \mid (x_2, x_3) \in (-1, 1) \times (0, L)\}.$$

The base flow is given by $\boldsymbol{U} = (x_2, 0, 0)' = x_2 \overrightarrow{e}_1$ and $P = P_0$. In addition, $F = \begin{bmatrix} 0 & Ro & 0 \\ -Ro & 0 & 0 \\ 0 & 0 & 0 \end{bmatrix}$, where $Ro \in [0, 1]$ is a parameter representing the Coriolis force[2]. Notice that the cases $Ro = 0, 1$ correspond to the Couette flow. We consider no-slip boundary conditions $\boldsymbol{u}|^1_{x_2=-1} = 0$ and $\boldsymbol{u}(t, x_2, x_3) = \boldsymbol{u}(t, x_2, x_3 + L)$. The Poincaré constant is then given by $C = \frac{\pi^2}{L^2+2^2}$.

We are interested in finding estimates of the critical Reynolds number Re_C using the following Lyapunov functional

$$V(u) = \int_0^L \int_{-1}^1 \begin{bmatrix} u_1 \\ u_2 \\ u_3 \end{bmatrix}' \begin{bmatrix} q_1 & 0 & 0 \\ 0 & q_2 & 0 \\ 0 & 0 & q_2 \end{bmatrix} \begin{bmatrix} u_1 \\ u_2 \\ u_3 \end{bmatrix} \, dx_2 dx_3,$$

which is the same as Lyapunov functional (6.18) assuming invariance with respect to x_1.

For stability analysis, we need to check inequality (6.41) according to Item I in Corol-

[2] That is, $Ro = 0$ ($Ro = 1$) corresponds to the case where only the outer (inner) cylinder is rotating and $Ro = 0.5$ is the case where both cylinders are rotating with the same velocity but in opposite direction.

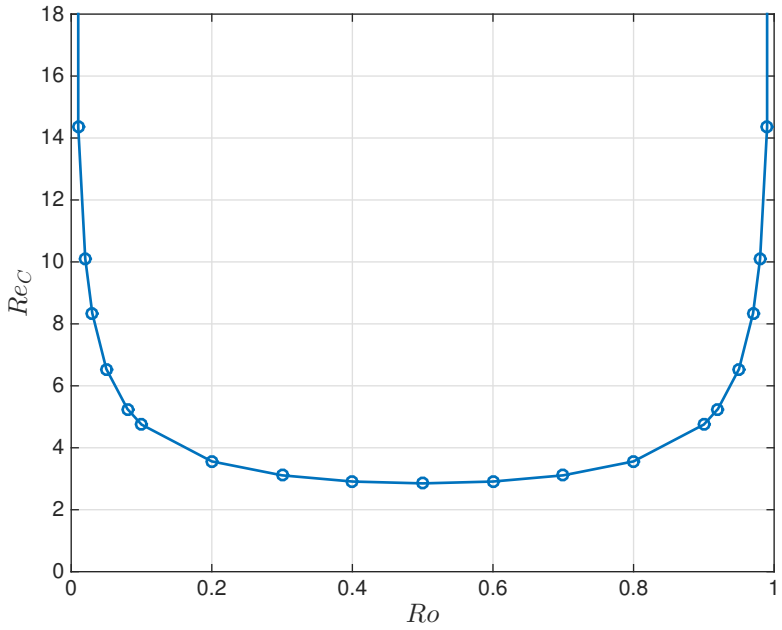

Figure 6.2: Estimated critical Reynolds numbers Re in terms of Ro for Taylor-Couette flow.

lary 6.3.1. For this flow ($m = 1, j = 2, i = 3$), we have

$$M = \begin{bmatrix} \frac{q_1 C}{Re} & \frac{q_2 Ro - q_1(Ro-1)}{2} & 0 \\ \frac{q_2 Ro - q_1(Ro-1)}{2} & \frac{q_2 C}{Re} & 0 \\ 0 & 0 & \frac{q_2 C}{Re} \end{bmatrix} \geq 0. \tag{6.56}$$

This is a LMI feasibility problem with decision variables $q_1, q_2 > 0$.

Let $L = \pi$. Figure 6.2 illustrates the estimated lower bounds on the critical Reynolds numbers Re_C as a function of Ro obtained from solving the LMI (6.56) and performing a line search over Re. These quantities are obtained by fixing Ro and increasing Re until LMI (6.56) becomes unfeasible. Notice that for the cases $Ro = 0, 1$ the flow is stable for all Reynolds numbers.

For induced $\mathcal{L}^2$-norm analysis, we apply inequality (6.43), which for this particular flow is given by the following LMI

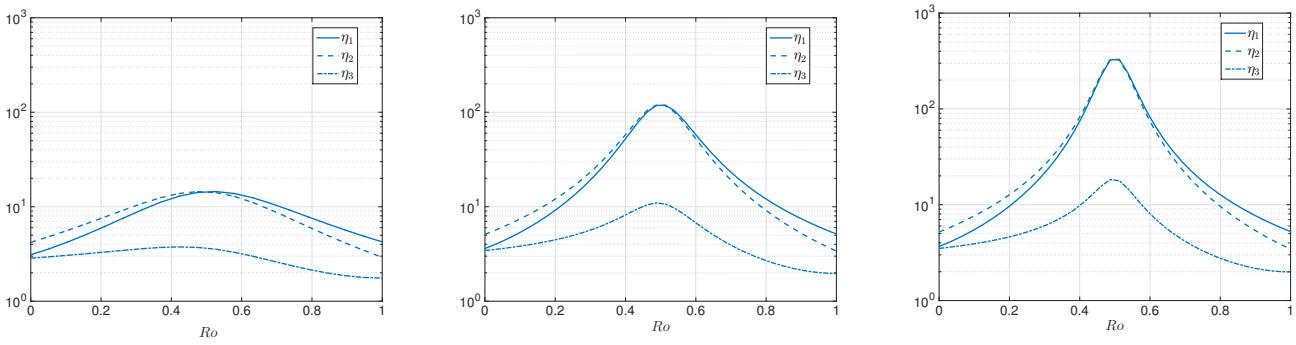

Figure 6.3: Upper bounds on induced $\mathcal{L}^2$-norms from $\boldsymbol{d}$ to perturbation velocities $\boldsymbol{u}$ of Taylor-Couette flow for different Reynolds numbers: $Re = 2$ (left), $Re = 2.8$ (middle), and $Re = 2.83$ (right).

$$N = \left[\begin{array}{ccc:ccc} & & & -\frac{q_1}{2} & 0 & 0 \\ & M - \mathrm{I}_{3\times 3} & & 0 & -\frac{q_2}{2} & 0 \\ & & & 0 & 0 & -\frac{q_2}{2} \\ \hdashline -\frac{q_1}{2} & 0 & 0 & \eta_1^2 & 0 & 0 \\ 0 & -\frac{q_2}{2} & 0 & 0 & \eta_2^2 & 0 \\ 0 & 0 & -\frac{q_2}{2} & 0 & 0 & \eta_3^2 \end{array}\right] \geq 0,$$

with M as in (6.56).

Figure 6.3 depicts the obtained results for three different Reynolds numbers. As the Reynolds number approaches the estimated Re_C for $Ro = 0.5$, the upper-bounds on the induced $\mathcal{L}^2$-norm from the body forces $\boldsymbol{d}$ to perturbation velocities $\boldsymbol{u}$ increase dramatically.

In order to check the ISS property, we check inequality (6.44) from Corollary 6.3.1 for the Taylor-Couette flow under study, *i.e.*,

$$P = \left[\begin{array}{ccc:ccc} & & & -\frac{q_1}{2} & 0 & 0 \\ & M - Q & & 0 & -\frac{q_2}{2} & 0 \\ & & & 0 & 0 & -\frac{q_2}{2} \\ \hdashline -\frac{q_1}{2} & 0 & 0 & \sigma_1 & 0 & 0 \\ 0 & -\frac{q_2}{2} & 0 & 0 & \sigma_2 & 0 \\ 0 & 0 & -\frac{q_2}{2} & 0 & 0 & \sigma_3 \end{array}\right] \geq 0$$

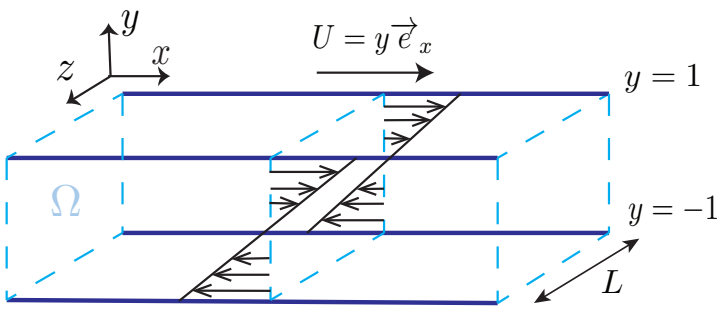

Figure 6.4: Schematic of the plane Couette flow geometry.

with M given in (6.56) and $Q = \begin{bmatrix} q_1\psi_1 & 0 & 0 \\ 0 & q_2\psi_2 & 0 \\ 0 & 0 & q_2\psi_3 \end{bmatrix}$. We fix $\psi_i = 10^{-4}$, $i = 1, 2, 3$ and $L = 2\pi$. Numerical experiments show that, for $Ro \in (0, 1)$, the maximum Reynolds number for which ISS certificates could be found Re_{ISS} and Re_C coincide. The limiting cases $Ro = 0, 1$ will be discussed in the next example.

6.4.2 Plane Couette Flow

We consider the flow of viscous fluid between two parallel plates, where the gap between the plates is much smaller than the length of the plates as illustrated in Figure 6.4.

We consider no-slip boundary conditions $\boldsymbol{u}|_{y=-1}^{1} = 0$ and $\boldsymbol{u}(t, y, z) = \boldsymbol{u}(t, y, z + L)$. The Poincaré constant is then given by $C = \frac{\pi^2}{\sqrt{L^2+2^2}}$.

We are interested in finding estimates of the critical Reynolds number Re_C using the following Lyapunov functional

$$V(u) = \int_0^L \int_{-1}^1 \begin{bmatrix} u_x \\ u_y \\ u_z \end{bmatrix}' \begin{bmatrix} q_x & 0 & 0 \\ 0 & q_y & 0 \\ 0 & 0 & q_z \end{bmatrix} \begin{bmatrix} u_x \\ u_y \\ u_z \end{bmatrix} \, dydz, \tag{6.57}$$

with $q_y = q_z$, which is the same as Lyapunov functional (6.18) considering invariance with respect to x.

For stability analysis, we need to check inequality (6.41) according to Item I in Corol-

lary 6.3.1. For this flow ($m = x, j = y, i = z$), we have

$$M = \begin{bmatrix} \frac{q_x C}{Re} & \frac{q_x}{2} & 0 \\ \frac{q_x}{2} & \frac{q_y C}{Re} & 0 \\ 0 & 0 & \frac{q_y C}{Re} \end{bmatrix} \geq 0 \tag{6.58}$$

This is a LMI feasibility problem with decision variables $q_x, q_y > 0$.

To find estimates of Re_C, applying Schur complement [19, p. 650] to (6.58), we have

$$\frac{q_x C}{Re} - \left(\frac{q_x}{2}\right)^2 \left(\frac{Re}{q_y C}\right) \geq 0, \ \frac{q_y C}{Re} \geq 0,$$

which yields the inequality

$$\frac{q_y}{q_x} \geq \left(\frac{Re}{2C}\right)^2. \tag{6.59}$$

This implies that the Couette flow subject to constant perturbations in the streamwise direction is stable for all Re. Hence, for Couette flow, $Re_C = \infty$ obtained using Lyapunov functional (6.18) coincides with linear stability limit $Re_L = \infty$ [101].

Let $L = \pi$. For energy growth analysis, we solve optimization problem (6.50) with M given by (6.58). The results are depicted in Figure 6.5. For small Reynolds numbers $\gamma^2 \propto O(Re)$, whereas for larger Reynolds numbers $\gamma^2 \propto O(Re^3)$. Therefore, it can be inferred that $\gamma^2 = c_0 Re + c_1 Re^3$ with $c_0, c_1 > 0$. This is consistent with the results by [15] where the maximum energy growth of steamwise constant (nonlinear) Couette flow was calculated analytically.

For induced $\mathcal{L}^2$-norm analysis, we apply inequality (6.43) which for this particular flow is given by the following LMI

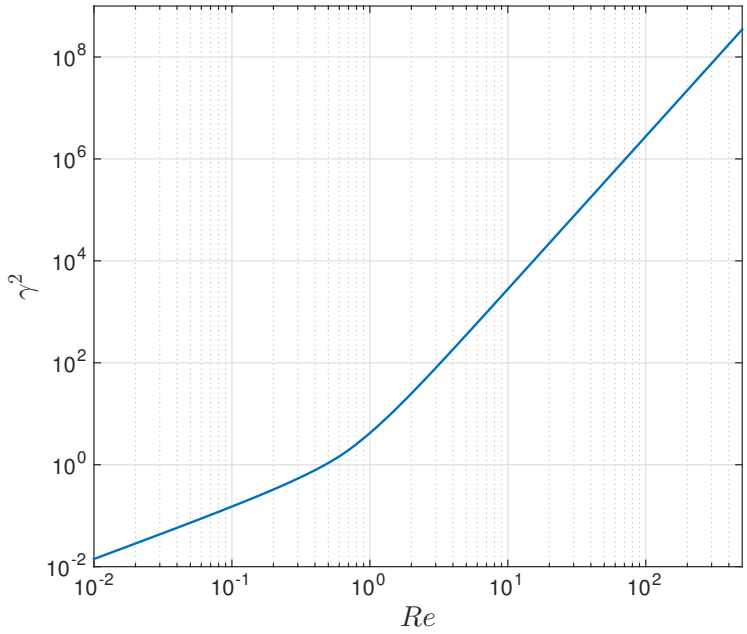

Figure 6.5: Upper bounds on the maximum energy growth for Couette flow in terms of Reynolds numbers.

$$N = \left[\begin{array}{ccc:ccc} & M - \mathrm{I}_{3\times 3} & & -\frac{q_x}{2} & 0 & 0 \\ & & & 0 & -\frac{q_y}{2} & 0 \\ & & & 0 & 0 & -\frac{q_y}{2} \\ \hdashline -\frac{q_x}{2} & 0 & 0 & \eta_x^2 & 0 & 0 \\ 0 & -\frac{q_y}{2} & 0 & 0 & \eta_y^2 & 0 \\ 0 & 0 & -\frac{q_y}{2} & 0 & 0 & \eta_z^2 \end{array}\right] \geq 0$$

with M as in (6.58).

The obtained upper-bounds on the induced $\mathcal{L}^2$-norm for Couette flow are given in Figure 6.6. Since the flow is stable for all Reynolds numbers, the induced $\mathcal{L}^2$-norms are monotone with Reynolds number. The obtained upper-bounds depicted in Figure 6.6 imply $\eta_x^2 = a_0 Re^2 + a_1 Re^3$, $\eta_y^2 = b_0 Re^2 + b_1 Re^4$ and $\eta_z^2 = c_0 Re^2 + c_1 Re^4$ with $a_0, a_1, b_0, b_1, c_0, c_1 > 0$. The obtained upper-bounds depicted in Figure 6.6 can be compared with Corollary D.0.2 (see Appendix D), wherein it was demonstrated that $\eta_x^2 = f_0 Re^2$, $\eta_y^2 = g_0 Re^2 + g_1 Re^4$ and

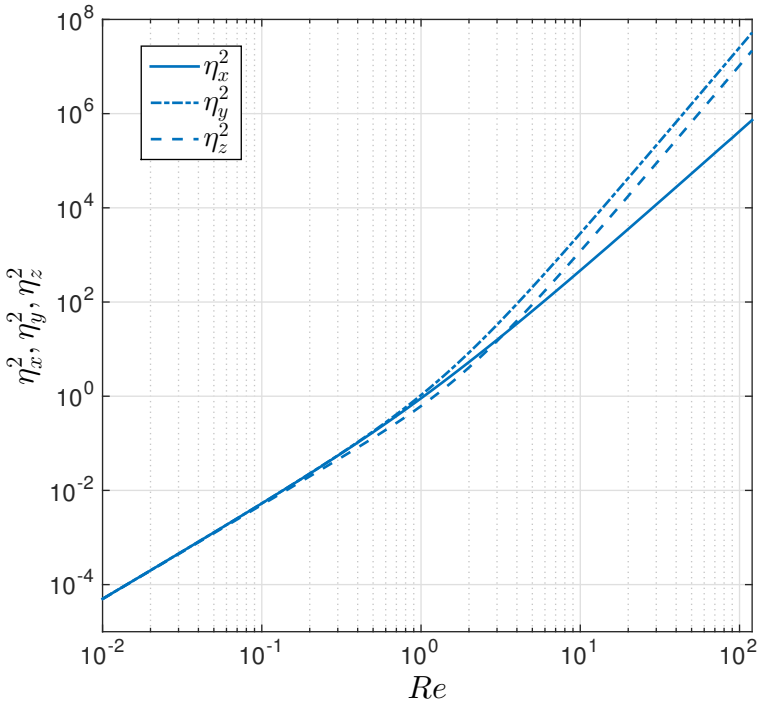

Figure 6.6: Upper bounds on induced $\mathcal{L}^2$-norms for perturbation velocities of Couette flow for different Reynolds numbers.

$\eta_z^2 = h_0 Re^2 + h_1 Re^4$ for the linearized Couette flow with $f_0, g_0, g_1, h_0, h_1 > 0$.

In order to check the ISS property, we check inequality (6.44) from Corollary 6.3.1 for the Couette flow under study, *i.e.,*

$$Z = \left[\begin{array}{ccc:ccc} & M - W & & -\frac{q_x}{2} & 0 & 0 \\ & & & 0 & -\frac{q_y}{2} & 0 \\ & & & 0 & 0 & -\frac{q_y}{2} \\ \hdashline -\frac{q_x}{2} & 0 & 0 & \sigma_x & 0 & 0 \\ 0 & -\frac{q_y}{2} & 0 & 0 & \sigma_y & 0 \\ 0 & 0 & -\frac{q_y}{2} & 0 & 0 & \sigma_z \end{array}\right] \geq 0$$

with M given in (6.58) and $W = \begin{bmatrix} q_x\psi_x & 0 & 0 \\ 0 & q_y\psi_y & 0 \\ 0 & 0 & q_y\psi_z \end{bmatrix}$. We fix $\psi_i = 10^{-4}$, $i = x, y, z$ and $L = 2\pi$. In this case, we obtain $Re_{ISS} = 316$ and $Re_C = \infty$. The quantity $Re_{ISS} = 316$ is the closest estimate to the empirical Reynolds number $Re \approx 350$ obtained by [120] above which transition to turbulence is observed. In this sense, it turns out that the Re_{ISS} gives

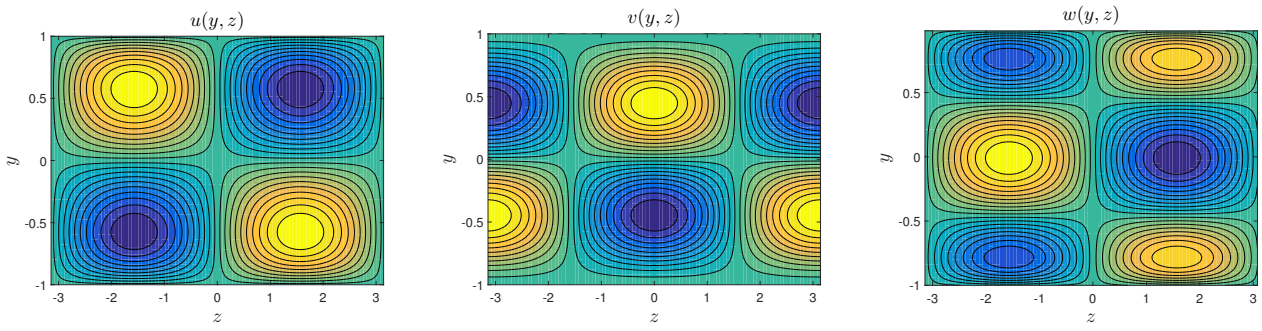

Figure 6.7: The perturbation flow structures with maximum ISS amplification at $Re = 316$.

lower bounds on the Reynolds number above which transition occurs.

In order to understand this ISS result, we carried out numerical experiments to obtain the flow structures that receive maximum amplification in the sense of ISS. The experiments were undertaken for the linearized Navier-Stokes equation through the Orr-Somerfield equations. Appendix C discusses the details of these numerical experiments. Notice that these results are based on solving LMIs that ensure ISS for the ODE space-discretizations of the Orr-Somerfield equations. This is carried out by making a 50×50 grid on the wave number space $k_x - k_z$ ($k_x, k_z \in [0, 150]$) and running the LMIs for each point in the grid. Then, the wave numbers corresponding to the maximum ISS amplification are selected (especially, we are interested to find k_x corresponding to maximum amplification, as this is the streamwise direction) and the corresponding flow structure is simulated. It turns out that the maximum ISS amplification corresponds to the streamwise constant case $k_x = 0$. Figure 6.7 illustrates the flow structures that receive maximum ISS amplification at $Re = 316$.

It is also worth mentioning that certificates for ISS of the linearized Navier-Stokes equation, as discussed in Appendix C, could be constructed for all Reynolds numbers, which is in contrast to the nonlinear case.

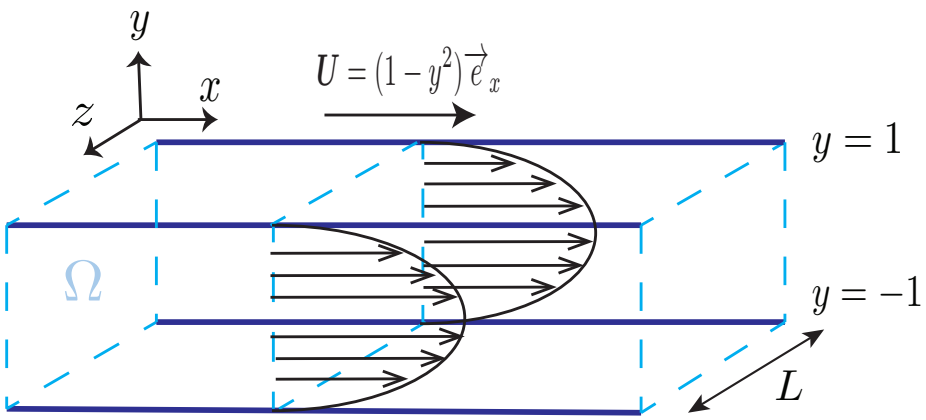

Figure 6.8: Schematic of the plane Poiseuille flow geometry.

6.4.3 Plane Poiseuille Flow

Similar to the plane Couette flow, we consider the flow of viscous fluid between two parallel plates, where the gap between the plates is much smaller than the length of the plates. Unlike the plane Couette flow, the plates are stationary and the flow is induced by a pressure gradient in the flow direction, flowing from the region of higher pressure to one of lower pressure. The flow geometry is depicted in Figure 6.8.

The domain Ω is defined as $\Omega = \{(y, z) \mid -1 < y < 1,\ 0 < z < L\}$. The flow perturbations are assumed constant in the streamwise direction x. The base flow is given by $\boldsymbol{U} = U_m(y)\vec{e}_x = (1 - y^2)\vec{e}_x$ and $P = 1 - \frac{4x}{Re}$. We consider no-slip boundary conditions $\boldsymbol{u}|_{y=-1}^{1} = 0$ and $\boldsymbol{u}(t, y, z) = \boldsymbol{u}(t, y, z + L)$. The Poincaré constant is then given by $C = \frac{\pi^2}{\sqrt{L^2+2^2}}$. We study the stability and the input-output properties of the flow using the storage functional (6.57).

In order to check stability, we need to verify inequality (6.41) according to Item I in

Corollary 6.3.1. For this flow ($m = x, j = y, i = z$), we have

$$M(y) = \begin{bmatrix} \frac{q_x C}{Re} & -yq_x & 0 \\ -yq_x & \frac{q_y C}{Re} & 0 \\ 0 & 0 & \frac{q_y C}{Re} \end{bmatrix} \geq 0, \quad y \in (-1, 1). \tag{6.60}$$

Using the Schur complement, we have

$$\frac{q_x C}{Re} - (yq_x)^2 \frac{Re}{q_y y} \geq 0, \ \frac{q_y C}{Re} \geq 0, \quad y \in (-1, 1).$$

That is, $\frac{q_y}{q_x} \geq \left(\frac{yRe}{C}\right)^2$ for all $y \in (-1, 1)$ which is satisfied whenever

$$\frac{q_y}{q_x} \geq \left(\frac{Re}{C}\right)^2. \tag{6.61}$$

Hence, the plane Poiseuille flow with streamwise constant perturbations is stable for all Reynolds numbers. Note that it is a known result that the Plane Poiseuille flow becomes unstable to perturbations that are streamwise dependent or three-dimensional perturbations [105]. Hence, the streamwise constant formulation does not provide a *good* estimate for stability Reynolds number in this case.

To find upper bounds on maximum energy growth for the plane Poiseuille flow, we solve the optimization problem (6.50) with M as given in (6.60). The results are illustrated in Figure 6.9. This implies that the maximum energy amplification is described by $\gamma^2 = b_0 Re + b_1 Re^2$, with $b_0, b_1 > 0$.

For induced $\mathcal{L}^2$-norm analysis, we use inequality (6.43) which for this flow is given by the following LMI

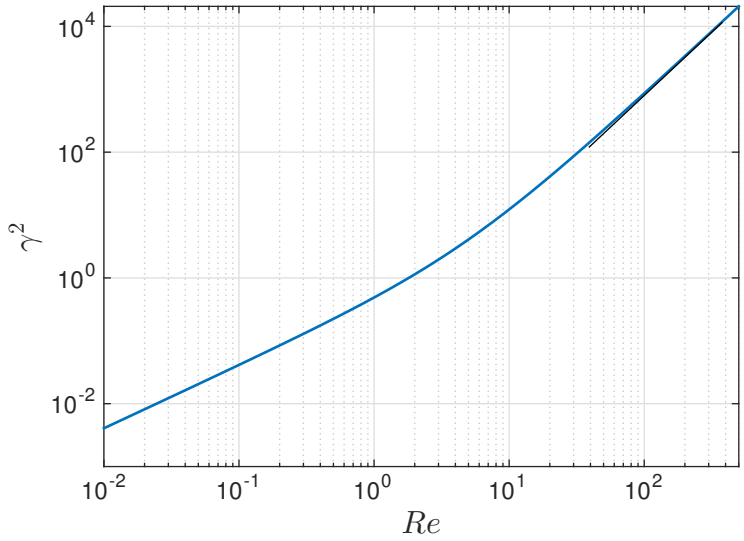

Figure 6.9: Upper bounds on the maximum energy growth for plane Poiseuille flow in terms of Reynolds numbers.

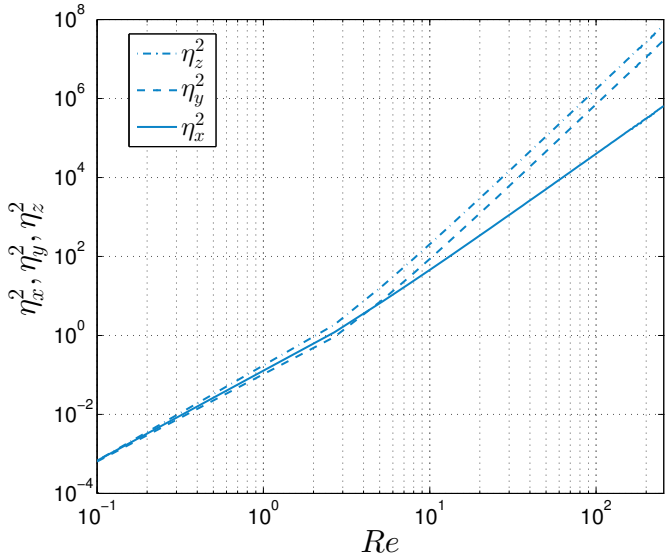

Figure 6.10: Upper bounds on induced $\mathcal{L}^2$-norms for perturbation velocities of plane Poiseuille flow for different Reynolds numbers.

$$N = \left[\begin{array}{ccc:ccc} & M(y) - \mathrm{I}_{3\times 3} & & -\frac{q_x}{2} & 0 & 0 \\ & & & 0 & -\frac{q_y}{2} & 0 \\ & & & 0 & 0 & -\frac{q_y}{2} \\ \hdashline -\frac{q_x}{2} & 0 & 0 & \eta_x^2 & 0 & 0 \\ 0 & -\frac{q_y}{2} & 0 & 0 & \eta_y^2 & 0 \\ 0 & 0 & -\frac{q_y}{2} & 0 & 0 & \eta_z^2 \end{array}\right] \geq 0, \quad y \in (-1, 1),$$

with M as in (6.60). The obtained upper-bounds on the induced $\mathcal{L}^2$-norm for the plane Poiseuille flow are also given in Figure 6.10. Since this flow is stable for all Reynolds numbers (as shown above), the induced $\mathcal{L}^2$-norms increases with Reynolds number. Form Figure 6.10 it can be inferred that $\eta_x^2 = a_0 Re^2 + a_1 Re^3$, $\eta_y^2 = b_0 Re^{2.2} + b_1 Re^4$ and $\eta_z^2 = c_0 Re^2 + c_1 Re^4$ with $a_0, a_1, b_0, b_1, c_0, c_1 > 0$.

For ISS analysis, we check inequality (6.44) from Corollary 6.3.1 for plane Poiseuille flow, *i.e.,*

$$Z = \left[\begin{array}{ccc:ccc} & M(y) - W & & -\frac{q_x}{2} & 0 & 0 \\ & & & 0 & -\frac{q_y}{2} & 0 \\ & & & 0 & 0 & -\frac{q_y}{2} \\ \hdashline -\frac{q_x}{2} & 0 & 0 & \sigma_x(y) & 0 & 0 \\ 0 & -\frac{q_y}{2} & 0 & 0 & \sigma_y(y) & 0 \\ 0 & 0 & -\frac{q_y}{2} & 0 & 0 & \sigma_z(y) \end{array}\right] \geq 0, \quad y \in (-1, 1)$$

with M given in (6.60) and $W = \left[\begin{smallmatrix} q_x\psi_x & 0 & 0 \\ 0 & q_y\psi_y & 0 \\ 0 & 0 & q_y\psi_z \end{smallmatrix}\right]$. We fix $\psi_i = 10^{-4},\ i = x, y, z$ and $L = 2\pi$. In this case, we obtain $Re_{ISS} = 1855$. The quantity $Re_{ISS} = 1855$ can be compared with the empirical Reynolds number at the onset of turbulence $Re \approx 2000$ as discussed in [43]. Once again, we infer that Re_{ISS} provides a lower bound for the Reynolds number for which transition to turbulence occurs.

Analogous to the plane Couette flow, we undertook numerical experiments to find the flow structures subject to maximum ISS amplification. Again, we found that the maximum amplification corresponds to the streamwise constant case $k_x = 0$. Figure 6.11 illustrates

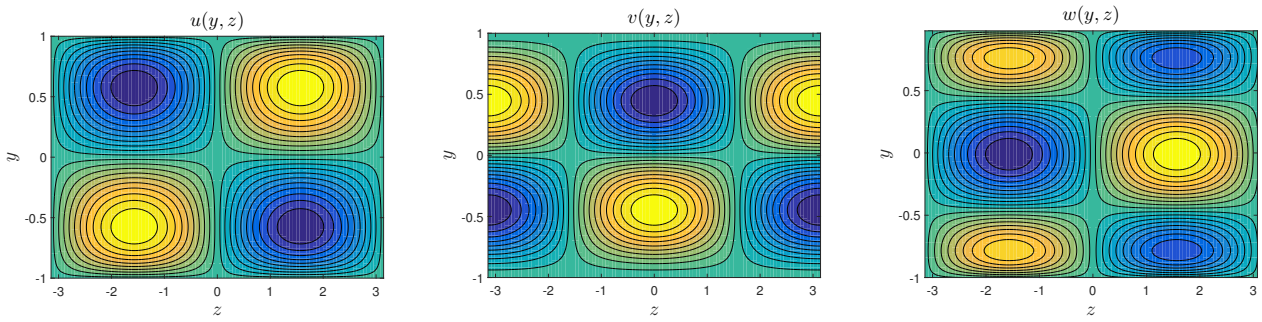

Figure 6.11: The perturbation flow structures with maximum ISS amplification at $Re = 1855$.

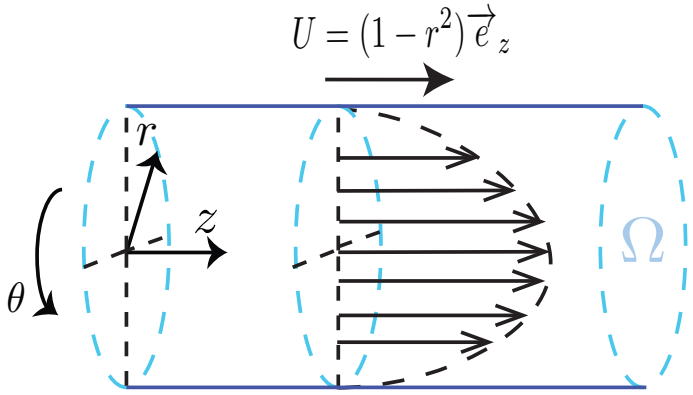

Figure 6.12: Schematic of the Hagen-Poiseuille flow geometry.

the flow structures that receive maximum ISS amplification at $Re = 1855$.

6.4.4 Hagen-Poiseuille Flow

We consider the flow of viscous fluid driven by the pressure gradient in a pipe as illustrated in Figure 6.12. The domain Ω is defined as $\Omega = \{(r,\theta) \mid 0 < r < 1,\ 0 < \theta < 2\pi\}$. The flow is invariant in the streamwise direction z. It was shown by [104] that streamwise constant perturbations are subject to maximum background energy amplification in pipe flow. The base flow is given by $\boldsymbol{U} = U_m(r)\vec{e}_z = (1-r^2)\vec{e}_z$ and $P = 1 - \frac{4z}{Re}$. Then, the perturbation dynamics is given by (6.33) with $F \equiv 0$ and $U_m(r) = 1 - r^2$. Moreover, we assume no-slip boundary conditions $\boldsymbol{u}|_{r=1} = 0$.

We consider the Lyapunov functional given in (6.34). Then, substituting U_m and F

in (6.52) yields

$$M_c(r) = \begin{bmatrix} \frac{q_z C}{Re} & -rq_z & 0 \\ -rq_z & \frac{q_r C}{Re} & 0 \\ 0 & 0 & \frac{q_\theta C}{Re} \end{bmatrix} \geq 0, \quad r \in (0,1). \tag{6.62}$$

Applying the Schur complement, we obtain the following conditions for exponential stability

$$\frac{q_z C}{Re} - (rq_z)^2 \frac{Re}{q_r r} \geq 0, \ \frac{q_\theta C}{Re} \geq 0, \quad r \in (0,1).$$

That is, $\frac{q_r}{q_z} \geq \left(\frac{rRe}{C}\right)^2$ for all $r \in (0,1)$ which is satisfied whenever

$$\frac{q_r}{q_z} \geq \left(\frac{Re}{C}\right)^2. \tag{6.63}$$

Hence, given q_r and q_z satisfying (6.63), the Hagen-Poiseuille flow with streamwise constant perturbations is exponentially stable for all Reynolds numbers, *i.e.,* the linear stability limit coincides with nonlinear stability limit.

In order to find upper bounds on maximum energy growth for Hagen-Poiseuille flow, we solve optimization problem (6.50) with $M = M_c(r)$ as (6.62). The results are illustrated in Figure 6.13. The results imply that the maximum energy amplification is described by $\gamma^2 = b_0 Re + b_1 Re^2$, with $b_0, b_1 > 0$.

This tallies with the numerical experiments of [104] on the transient growth based on the linearized Navier-Stokes equations for the pipe flow.

Considering $M_c(r)$ as in (6.62), inequality (6.54) becomes

$$N_c(r) = \left[\begin{array}{ccc:ccc} & & & -\frac{q_z}{2} & 0 & 0 \\ & M_c(r) - \mathrm{I}_{3\times 3} & & 0 & -\frac{q_r}{2} & 0 \\ & & & 0 & 0 & -\frac{q_\theta}{2} \\ \hdashline -\frac{q_z}{2} & 0 & 0 & \eta_z^2 & 0 & 0 \\ 0 & -\frac{q_r}{2} & 0 & 0 & \eta_r^2 & 0 \\ 0 & 0 & -\frac{q_\theta}{2} & 0 & 0 & \eta_\theta^2 \end{array}\right] \geq 0, \quad r \in (0,1). \tag{6.64}$$

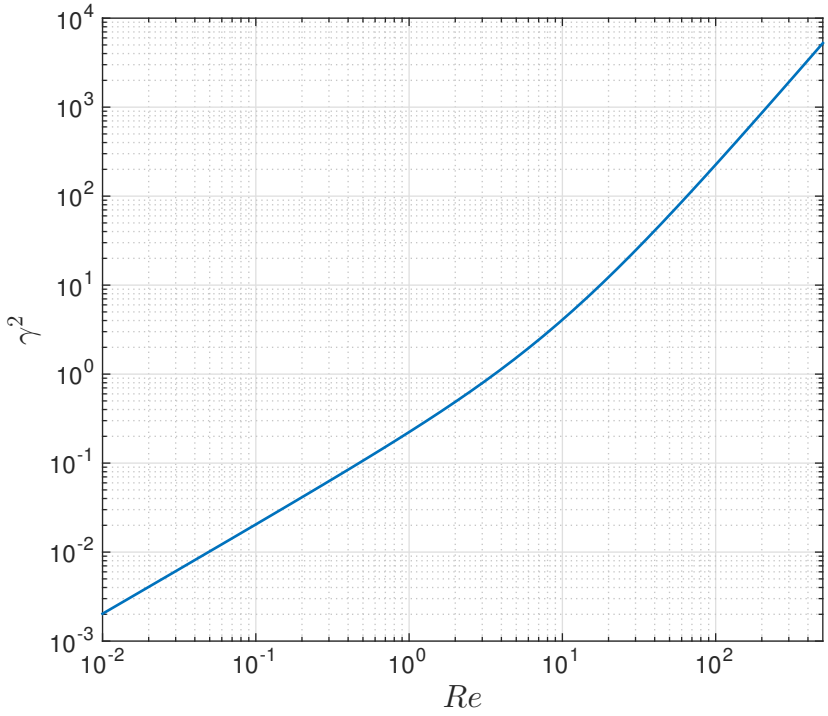

Figure 6.13: Upper bounds on the maximum energy growth for Hagen-Poiseuille Flow flow in terms of Reynolds numbers.

Minimizing η_z^2, η_r^2 and η_θ^2 subject to the above inequality provides upper-bounds on the induced $\mathcal{L}^2$-norms for pipe flow. The results are depicted in Figure 6.14. The interesting conclusion from the figure is that the perturbations are amplified as $\eta_z^2 = a_0 Re^2 + a_1 Re^3$, $\eta_\theta^2 = b_0 Re^2 + b_1 Re^4$, and $\eta_r^2 = c_0 Re^2 + c_1 Re^4$ with $a_0, a_1, b_0, b_1, c_0, c_1 > 0$.

Note that [59] just considered channel flows which does not include pipe flow.

For ISS analysis, the following polynomial matrix inequality

$$Z_c(r) = \left[\begin{array}{ccc:ccc} & & & -\frac{q_z}{2} & 0 & 0 \\ & M_c(r) - W_c & & 0 & -\frac{q_r}{2} & 0 \\ & & & 0 & 0 & -\frac{q_\theta}{2} \\ \hdashline -\frac{q_z}{2} & 0 & 0 & \sigma_z(r) & 0 & 0 \\ 0 & -\frac{q_r}{2} & 0 & 0 & \sigma_r(r) & 0 \\ 0 & 0 & -\frac{q_\theta}{2} & 0 & 0 & \sigma_\theta(r) \end{array}\right] \geq 0, \quad r \in (0,1), \tag{6.65}$$

where $W_c = \left[\begin{smallmatrix} \psi_z q_z & 0 & 0 \\ 0 & \psi_r q_r & 0 \\ 0 & 0 & \psi_\theta q_\theta \end{smallmatrix}\right]$ was checked. The maximum Reynolds number for which certificates of ISS could be found was $Re_{ISS} = 1614$ using degree 10 polynomials in $\sigma_z(r), \sigma_\theta(r)$ and $\sigma_r(r)$. Remarkably, this is a lower bound to the Reynolds number for which transition to turbulence was observed empirically by [87], *i.e.*, $Re \approx 1800$.

6.5 Conclusions

We studied stability and input-output properties of fluid flows with constant perturbations in one of the directions using dissipation inequalities. We proposed a class of appropriate Lyapunov/storage functionals for such flows that lead to a quadratic representation of the integrands of the dissipation inequalities. Conditions based on matrix inequalities were given for streamwise constant flow perturbations. When the base flow was given by a polynomial of spatial coordinates and the flow geometry was described by a semi-algebraic set, the matrix inequalities were checked using convex optimization. For illustration purposes, we applied the proposed method to study several flows.

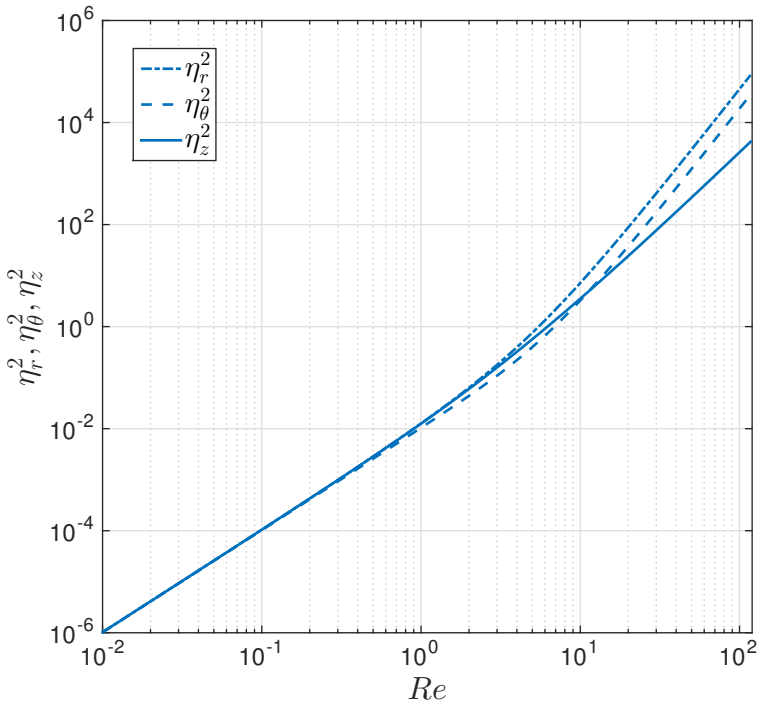

Figure 6.14: Upper bounds on induced $\mathcal{L}^2$-norms for perturbation velocities of pipe flow in terms of different Reynolds numbers.

Chapter 7

Conclusions and Future Work

In this dissertation, we proposed methods based on convex optimization for the analysis of systems described by PDEs. The analysis problems we considered included stability, input-state/output properties, safety verification and bounding output functionals of PDEs. We applied the stability and input-state/output analysis tools to problems from fluid mechanics. Before closing this dissertation, we provide a summary of the contents and present some directions for future research.

7.1 Summary

After a brief review of some mathematical preliminaries in Chapter 2, in Chapter 3, we proposed a method for solving integral inequalities with polynomial integrands using convex optimization. The method relied on a quadratic representation of the integrands and an application of Fundamental Theorem of Calculus to account for boundary conditions. We then used this method to check the integral inequalities encountered in the Lyapunov stability analysis of PDEs.

In Chapter 4, we studied the input-state/output properties of PDEs based on formulating a set of dissipation inequalities. In this respect, we considered passivity, reachability, induced norms, and ISS. The formulation based on dissipation inequalities allowed us to

investigate the properties of interconnections of PDE-PDE systems and PDE-ODE systems. In the case of polynomial data, we solved the dissipation inequalities using convex optimization.

In Chapter 5, we considered the safety verification problem of PDEs. The proposed analysis required the construction of barrier functionals satisfying two integral inequalities along the solutions of a PDE. We further demonstrated that the problem of bounding output functionals of PDEs can be addressed using barrier functionals. In the case of polynomial data, we solved the associated integral inequalities and we constructed the barrier functionals using SOS programming.

In Chapter 6, we applied the methods for stability analysis and input-output analysis proposed in Chapters 3 and 4, respectively, to the input-output analysis problems of fluid flows. Particularly, we studied flows with constant perturbations in one of the directions. A suitable structure of the Lyapunov/storage functional led to a set of matrix inequalities that can be checked via convex optimization in the case of polynomial base flow and semi-algebraic flow geometry. The method was applied to the input-output analysis problems of several channel and pipe flows.

7.2 Future Research Directions

In terms of the convex method to check integral inequalities, here, we treated integral inequalities defined over one dimensional domains. An extension has been made to integrals over domains of two spatial dimensions, of which [127] reports some preliminary results. In the two dimensional setting, we can apply Green's Theorem to obtain a set of quadratic representations of a given integral inequality. Then, the positivity of the surface integral can be analyzed by checking the positivity of the matrices in the quadratic representations. In [127], we detailed the method for unit square domains. Other domain topologies, e.g. the unit circle, are also worth studying. In addition, the extension to higher dimensions,

say three spatial dimensions, can be made by applying Stokes' Theorem.

In this dissertation, the function bases we selected were polynomials. This choice made it possible to derive SOS programs to verify integral inequalities. However, this choice may not be the best. In the time-delay systems literature, the Legendre basis functions were used in [107] to formulate LMI conditions for the stability tests of distributed time-delay systems using a complete Lyapunov-Krasovskii functional. In the context of PDEs, in [36], the authors propose an SDP-based method based on the Legendre basis functions to optimize a linear objective function subject to a quadratic integral inequality. The method has shown to be effective in handling PDE analysis problems [34, 35]. These contributions raise the question of whether exploiting other sequences of orthogonal functions such as trigonometric functions, Bernstein, Chebyshev or Laguerre polynomials would potentially lead to more efficient computational tools. In this regard, the case of Chebyshev polynomials is particularly interesting due to their convergence properties for function approximation [17], e.g. in spectral methods [122].

In terms of dissipation inequalities, more complicated interconnections can be considered. Furthermore, optimal controller synthesis algorithms for PDEs can be studied, where both in-domain and boundary actuation can be considered. In this regard, controller synthesis methods for PDEs based on convex optimization were recently proposed in [9, 38]. In particular, [38] considers the following Lyapunov functional structure

$$V(u) = \int_0^1 M(x)u^2\,dx + \int_0^1\int_0^1 u'(t,x)K(x,\zeta)u(t,\zeta)\,dxd\zeta,$$

where

$$K(x,\zeta) = \begin{cases} K_1(x,\zeta) & \zeta \leq x, \\ K_2(x,\zeta) & \zeta > x \end{cases}$$

with polynomials $M : (0,1) \to \mathbb{R}$, $K_1 : (0,1)^2 \to \mathbb{R}$ and $K_2 : (0,1)^2 \to \mathbb{R}$. Such K is referred to as a *semi-separable* kernel. The latter structure has been shown to be efficacious

in designing stabilizing controllers for linear PDEs. Yet, the extension to nonlinear PDEs is still an open problem.

In terms of barrier functionals, prospective research can consider bounding functionals of the states of nonlinear stochastic differential equations (SDEs). A preliminary result in this direction has been accepted for presentation at the 55th IEEE Conference on Decision and Control [1], where a method for safety verification of backward-in-time PDEs is developed and used to bound state functionals of SDEs thanks to the Feynman-Kac PDE. This method also has direct applications to optimal control of stochastic systems, wherein the Hamilton-Jacobi-Bellman equation can be used.

In the case of applications to fluid mechanics, an interesting problem for future research is identifying the regions of attraction for different flow configurations. For example, in the case of Taylor-Couette flow, after decomposing the Navier-Stokes equation about different flow regimes, one can search for estimates of the region of attraction inside which each flow regime is stable.

In addition, input-output amplification mechanisms of turbulent flows is also an intriguing prospective research direction. In this regard, [29, 98] consider a non-polynomial model for turbulent mean velocity profiles and turbulent eddy viscosities. Polynomial approximations (of high degrees) of such nonlinear models fit the formulation given in Chapter 6. Then, the method discussed in Chapter 6 can be used to study the input-output properties.

Lastly, more general Lyapunov/storage functional structures can be considered. More specifically, given the nonlinear dynamics of the Navier-Stokes equations, one can consider the following class of Lyapunov/storage functionals

$$V(\boldsymbol{u}) = \int_{\Omega} \begin{bmatrix} \boldsymbol{u} \\ \boldsymbol{u}^2 \end{bmatrix}' Q \begin{bmatrix} \boldsymbol{u} \\ \boldsymbol{u}^2 \end{bmatrix} \, d\Omega.$$

However, a convex formulation using the above structure is not clear at the moment.

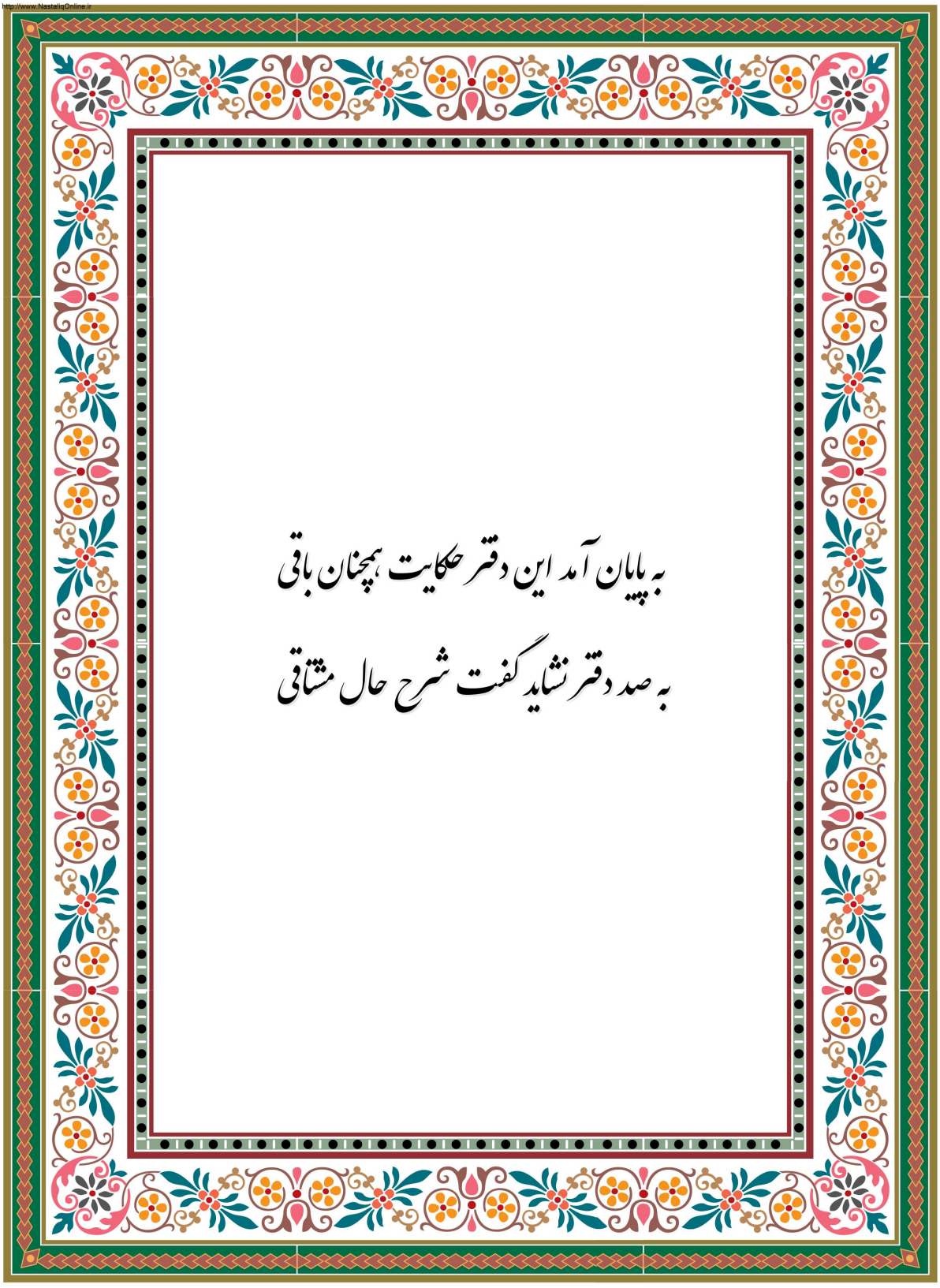

[1]

[1] This book has come to an end, but much still remains of what it aims to tell / For even in one hundred books, one cannot describe the state of he who is athirst [for knowledge] – Sa'di

Appendix A

Well-posedness of PDEs

In this dissertation, we consider the following (abstract) differential equations

$$\begin{cases} \partial_t u = \mathscr{F} u + \mathscr{G} d, \ t > 0, \\ u(0) = u_0 \in \mathcal{U}_0 \subset Dom(\mathscr{F}), \end{cases} \tag{A.1}$$

where $\mathscr{F}$ and $\mathscr{G}$ are operators. To see how this abstract representation can be used to analyze PDEs, let us go through the following example.

Example A.0.1 *Consider a heated metal bar of unit length, in which the two ends of the bar are insulated so that there is no heat flux. The heat distribution over the rod is described by the following PDE*

$$\begin{cases} \partial_t u(t,x) = \partial_x^2 u(t,x) + d(t,x) \quad t \geq 0, \ x \in \Omega = (0,1) \\ u(0,x) = u_0(x), \\ \partial_x u(t,0) = \partial_x u(t,1) = 0. \end{cases} \tag{A.2}$$

where $u(t,x)$ denotes the temperature at position x and time t, $u_0(x)$ the initial temperature distribution, and $d(t,x)$ the heat source. In order to use the abstract form (A.1)*, we take $\mathcal{U} = \mathcal{L}^2(\Omega)$ as the state space and the trajectory segment $u(t,\cdot) = \{u(t,x), \ x \in \Omega\}$ as the*

state. Now it suffices to define

$$\mathscr{F}h = \partial_x^2 h, \tag{A.3}$$

$$\mathscr{G}h = h, \tag{A.4}$$

$$Dom(\mathscr{F}) = \left\{h \in \mathcal{L}^2(\Omega) \mid h \in \mathcal{H}^2(\Omega) \text{ and } \partial_x h(0) = \partial_x h(1) = 0\right\} \tag{A.5}$$

and $u_0 \in \mathcal{L}^2(\Omega)$ *as the initial condition.*

A.1 Linear PDEs

In the case when $\mathscr{F}$ and $\mathscr{G}$ are linear operators, the well-posedness problem of (A.1) is tied to F being the generator of a *strongly continuous semigroup* denoted C^0-Semigroup [26, Chapter 2.1]. Let $\mathfrak{L}(\mathcal{U})$ be the space of bounded linear maps[1] on a Hilbert space $\mathcal{U}$.

Definition A.1.1 (C^0-Semigroup) *A C^0-semigroup is an operator valued function $T(t)$ from $\mathbb{R}_{\geq 0}$ to $\mathfrak{L}(U)$ that satisfies the following properties*

- $T(t+r) = T(t)T(r),\ \forall t, s \in \mathbb{R}_{\geq 0}$,
- $T(0) = I$,
- $\lim_{t\to 0^+} \|T(t)u_0 - u_0\| \to 0,\ \forall u_0 \in \mathcal{U}$.

Another important concept that we need in order to define the solutions to (A.1) is the *infinitesimal generator*.

[1] Let $\mathcal{X}$ and $\mathcal{Y}$ be two normed vector spaces. The operator $\mathscr{S} : \mathcal{X} \to \mathcal{Y}$ is a bounded linear operator, if there exists some $M > 0$ such that for all $v \in \mathcal{X}$

$$\|\mathscr{S}v\|_{\mathcal{Y}} \leq M\|v\|_{\mathcal{X}}.$$

The smallest such M is called the operator norm of $\mathscr{S}$.

Definition A.1.2 (Infinitesimal Generator) *The infinitesimal generator $\mathscr{F}$ of a C^0-semigroup on a Hilbert space $\mathcal{U}$ is defined by*

$$\mathscr{F}u = \lim_{t \to 0^+} \frac{T(t)u - u}{t}.$$

In principle, the above definition gives a way of calculating the infinitesimal generator of a C^0-semigroup, but this is rarely used as it is rather difficult to apply.

Example A.1.3 (Linear Systems) *Let $A \in \mathfrak{L}(\mathbb{R}^{n\times n})$, e.g. the matrix $A \in \mathbb{R}^{n\times n}$ and consider the following well-known C^0-semigroup for linear systems*

$$T(t) = e^{At}.$$

Then, the infinitesimal generator of $T(t)$ is described as

$$\mathscr{F}u = Au.$$

Although in the above example finding the infinitesimal generator seems trivial to obtain, such characterization is not straightforward in general. In this respect, the Hille-Yosida theorem [114, Theorem 3.4.1], [26, Theorem 2.1.12] provides necessary and sufficient conditions for such generators. To state the latter theorem, we need the *resolvent operator*, $R(\lambda, \mathcal{F}) = (\lambda\mathscr{I} - \mathscr{F})^{-1}$ with $\mathscr{I}$ denoting the identity operator, of the infinitesimal generator $\mathscr{F}$ of a C^0-semigroup. Lemma 2.1.11 in [26] demonstrates that $R(\lambda, \mathcal{F})$ is indeed the Laplace transform of the semigroup $T(t)$.

Theorem A.1.4 (Hille-Yosida Theorem) *A necessary and sufficient condition for a closed, densely defined, linear operator $\mathscr{F}$ on a Hilbert space $\mathcal{U}$ to be the infinitesimal generator of a C^0-semigroup is that there exist real numbers M and w, such that for all real $\alpha > w$,*

$\alpha \in \rho(\mathscr{F})$, *the resolvent set of* $\mathscr{F}$, *and*

$$\| \left(R(\alpha, \mathscr{F})\right)^r \| \leq \frac{M}{(\alpha - w)^r}, \ \forall r \geq 1,$$

In this case,

$$\|T(t)\| \leq Me^{wt}.$$

The Hille-Yosida Theorem concedes that every C^0-semigroup satisfies $\|T(t)\| \leq Me^{wt}$ for some M and w. The reader may have noted that in the case when $w < 0$, $\mathscr{F}$ is the infinitesimal generator of an exponentially stable semigroup $T(t)$. Another special and important case is when $M = 1$ (*quasicontraction semigroup*). Then, the semigroup $e^{-wt}T(t)$ satisfies $\|T(t)\| \leq 1$. Such semigroups are called contraction semigroups.

Definition A.1.5 (Contraction Semigroup) $T(t)$ *is a contraction semigroup if it is a* C^0*-semigroup that satisfies an estimate* $\|T(t)\| \leq 1$ *for all* $t \geq 0$.

In addition, the Lumer-Phillips theorem [114, Theorem 3.4.5],[69],[125, Theorem 3.8.6] presents conditions for the generator of a strongly continuous contraction semigroup that are easier to verify based on checking whether the operator is *dissipative*.

The next result gives sufficient conditions that resemble Lyapunov inequalities and can be used to show that the generator of a contraction semigroup exits or, in other words, that the operator is dissipative (when $w = 0$).

Corollary A.1.6 *Sufficient conditions for a closed, densely defined operator on a Hilbert space to be the infinitesimal generator of a* C^0*-semigroup satisfying* $\|T(t)\| \leq e^{wt}$ *are:*

$$Re \left\langle \mathscr{F}u, u \right\rangle \leq w\|u\|^2, \ u \in Dom(\mathscr{F}),$$

$$Re \left\langle \mathscr{F}^*u, u \right\rangle \leq w\|u\|^2, \ u \in Dom(\mathscr{F}*),$$

where $Re(\cdot)$ *denotes the real part.*

Let us illustrate this by an example.

Example A.1.7 *Let $\mathcal{U} = \mathcal{H}^2(\Omega;\mathbb{R})$ for an open and connected domain $\Omega \subseteq \mathbb{R}^n$ and let $\mathscr{F} = \Delta$, the Laplace operator, defined on the dense subspace of compactly supported smooth functions on Ω. Then, using integration by parts,*

$$\langle u, \Delta u\rangle = \int_\Omega u(x)\Delta u(x)\, dx = -\int_\Omega \left|\nabla u(x)\right|^2 dx = -\|\nabla u\|^2_{\mathcal{L}^2(\Omega;\mathbb{R})} \leq 0,$$

so the Laplacian is a dissipative operator.

Theorem 2.1.10 in [26] states that if an infinitesimal generator $\mathscr{F}$ exists for a C^0-semigroup $T(t)$, then the uncontrolled ($d = 0$) version of our system (A.1) has a solution with the properties of a dynamical system.

Theorem A.1.8 *Let $T(t)$ be a C^0-semigroup on a Hilbert space $\mathcal{U}$ with infinitesimal generator $\mathscr{F}$. Then, the following hold*

- *For $u_0 \in Dom(\mathscr{F})$, $T(t)u_0 \in Dom(\mathscr{F})$, $\forall t \geq 0$,*
- *$\partial_t\left(T(t)u_0\right) = \mathscr{F}T(t)u_0 = T(t)\mathscr{F}u_0$ for $u_0 \in Dom(\mathscr{F})$, $t > 0$,*
- *$u(t) = T(t)u_0 = u_0 + \int_0^t T(t)\mathscr{F}u_0\, dt$ for $Dom(\mathscr{F})$,*
- *$\mathscr{F}$ is a closed linear operator.*

Next, we present the first definition for a solution to (A.1). Subsequently, we will see that such solutions exist, if an infinitesimal generator exits. Let $z = \mathscr{G}d$.

Definition A.1.9 (Classical Solution, Definition 3.1.1 in [26]) *Consider equation* (A.1) *on the Hilbert space $\mathcal{U}$. Let $z \in \mathcal{C}^1([0,r];\mathcal{U})$. The function $u(t)$ is a classical solution of* (A.1) *on $[0,r]$ if $u(t) \in \mathcal{C}^1([0,r];\mathcal{U})$, $u(t) \in Dom(\mathscr{F})$ for all $t \in [0,r]$ and $u(t)$ satisfies* (A.1) *for all $t \in [0,r]$. The function $u(t)$ is a classical solution on $\mathbb{R}_{\geq 0}$, if $u(t)$ is a classical solution on $[0,r]$ for every $r \in \mathbb{R}_{\geq 0}$.*

Theorem A.1.10 (Theorem 3.1.3 in [26]) *If $\mathscr{F}$ is the infinitesimal generator of a C^0-semigroup $T(t)$ on a Hilbert space $\mathcal{U}$, $z \in \mathcal{C}^1([0,T];\mathcal{U})$ and $u_0 \in Dom(\mathscr{F})$, then*

$$u(t) = T(t)u_0 + \int_0^t T(t-s)z(s)\, ds \tag{A.6}$$

is continuously differentiable on $[0,T]$ and it is the unique classical solution of (A.1)*.*

For control applications, in general, we do not wish to assume that $u \in \mathcal{C}^1([0,r];\mathcal{U})$. So we introduce the following weaker concept of a solution of (A.1).

Definition A.1.11 (Mild Solution, Definition 3.1.4 in [26]) *If $u \in \mathcal{L}^p([0,r];\mathcal{U})$ for a $p \geq 1$ and $u_0 \in \mathcal{U}$, then we call* (A.6) *a mild solution of* (A.1) *on* $[0,r]$.

It can be shown that a weak solution is continuous on the domain $[0,r]$. In fact, this mild solution is the same as the concept of a weak solution [2] used in the study of PDEs.

Theorem A.1.12 (Theorem 3.1.7 in [26]) *For every $u_0 \in \mathcal{U}$ and every $z \in \mathcal{L}^p([0,r);\mathcal{U})$ there exists a unique weak solution of* (A.1) *that is the mild solution of* (A.1)*.*

A.2 Nonlinear PDEs

Set $\mathscr{G} = 0$. If $\mathscr{F}$ is a nonlinear dissipative operator, [72, Chapter 4] describes the conditions for which $\mathscr{F}$ generates a semigroup of contractions.

Definition A.2.1 *A nonlinear semi-group on a compact normed space $\mathcal{U}$ is a family of maps $\{T(t) \mid \mathcal{U} \to \mathcal{U},\ t \geq t_0\}$ such that*

[2] For $z \in \mathcal{L}^p([0,r);\mathcal{U})$ for a $p \geq 1$. We call u a weak solution of (A.1) on $[0,r)$, if the following holds:

- $u(t)$ is continuous on $[0,r]$,
- For all $g \in \mathcal{C}([0,r];\mathcal{U})$,

$$\int_0^r \langle u(t), g(t)\rangle\ dt + \int_0^r \langle z(t), s(t)\rangle\ dt + \langle u_0, s(0)\rangle = 0,$$

where $s(t) = -\int_t^r T^*(\tau - t)g(\tau)\, d\tau$, where T^* is the adjoint of the operator T.

We call u a weak solution of (A.1) on $\mathbb{R}_{\geq 0}$, if it is a weak solution on $[0,r)$ for every $r \geq 0$.

- *for each $t \geq t_0$, $T(t)$ is continuous from $\mathcal{U}$ to $\mathcal{U}$,*
- *for each $u \in \mathcal{U}$, the mapping $t \to T(t)u$ is continuous,*
- *$T(0)$ is the identity on $\mathcal{U}$,*
- *$T(t)(T(\tau)u) = T(t+\tau)u$ for all $u \in \mathcal{U}$ and all $t, \tau \geq 0$.*

Theorem A.2.2 (Theorem 4.2. in [72]) *Let $\mathscr{F}$ be a dissipative operator that satisfies the following condition*

$$Dom(\mathscr{F}) \subset Ran(\mathscr{I} - \lambda\mathscr{F}), \quad \forall \lambda > 0, \tag{A.7}$$

where $Ran(\mathscr{A}) = \bigcup_{u \in Dom(\mathscr{A})} \mathscr{A}u$ denotes the range of the operator $\mathscr{A}$, then there is a semigroup of contractions $\{T(t),\ t \geq 0\}$ on $\overline{Dom(\mathscr{F})}$ that satisfies

I) for every $u \in R \cap \overline{Dom(\mathscr{F})}$, where $R = \cap_{\lambda>0} R(\mathscr{I} - \lambda\mathscr{F})$,

$$T(t)u = \lim_{\lambda \to 0^+} (\mathscr{I} - \lambda\mathscr{F})^{-\frac{t}{\lambda}} u,\ t \geq 0,$$

where convergence is uniform on bounded some intervals of $\mathbb{R}_{\geq 0}$.

II) $\|T(t)u - T(s)u\| \leq \|\mathscr{F}u\||t-s|,\ u \in Dom(\mathscr{F}),\ t, s \geq 0$.

At this point, we are ready to state a wellposedness result for nonlinear semigroups.

Theorem A.2.3 (Theorem 4.10. in [72]) *Let $\mathscr{F}$ be a closed dissipative operator satisfying* (A.7) *and let $\{T(t),\ t \geq 0\}$ be a semigroup of contractions on $\overline{Dom(\mathscr{F})}$ as in Theorem A.2.2 and let $u \in Dom(\mathscr{F})$. If $T(t)u$ is differentiable a.e. $t \geq 0$, then $T(t)u : \mathbb{R}_{\geq 0} \to \mathcal{U}$ is a unique solution to* (A.1).

Appendix B

Converting Functionals to The Full Integral Form

In this appendix, we describe methods to convert functionals defined over subsets of the domain into the full integral form.

B.1 Boundaries

Consider functional (5.15) with $h_2 = 0$, $h_1 \in \mathcal{C}^1[x]$ and $x \in \{0, 1\}$, i.e.

$$y(t) = h\left(t, 0, D^{\alpha}u(t, 0)\right), \; x_0 \in \partial\Omega. \tag{B.1}$$

For some $p \in \mathcal{C}^1(\Omega)$ satisfying $p(1) = 0$, we obtain

$$p(0)h\left(t, 0, D^{\alpha}u(t, 0)\right) = -\int_0^1 \partial_x(ph) \; dx. \tag{B.2}$$

Therefore,

$$y(t) = h\left(t, 0, D^{\alpha}u(t, 0)\right) = \frac{-1}{p(0)} \int_0^1 \left((\partial_x p)h + p(\partial_x h)\right) \; dx. \tag{B.3}$$

In addition, if the functional is defined on the boundary $x = 1$, assuming $p(0) = 0$, we obtain

$$y(t) = h\left(t, 1, D^{\alpha}u(t,1)\right) = \frac{1}{p(1)}\int_0^1 \left((\partial_x p)h + p(\partial_x h)\right)\ dx. \tag{B.4}$$

Notice that, by fixing the values of $p(0)$ and $p(1)$ in (B.3) and (B.4), respectively, we can use equations (B.3) and (B.4) to study functionals evaluated at the boundaries using integral inequalities in the full integral form.

B.2 Single Points Inside the Domain

At this point, consider functional (5.15) with $h_2 = 0$, i.e.

$$y(t) = h\left(t, x_0, D^{\beta}u(t,x_0)\right),\ x_0 \in \Omega. \tag{B.5}$$

We split the domain into two subsets $\Omega_1 = (0, x_0]$ and $\Omega_2 = [x_0, 1)$. Then, PDE (5.10) can be represented by the following coupled PDEs

$$\partial_t u = \begin{cases} F(t,x,D^{\alpha}u), & x \in \Omega_1 \\ F(t,x,D^{\alpha}u), & x \in \Omega_2 \end{cases}$$

subject to $D^{\alpha-1}u(t,x_0) = D^{\alpha-1}u(t,x_0)$ and (5.12). Using appropriate change of variables, we obtain

$$\begin{cases} \partial_t u_1 = F_1(t,x,D^{\alpha}u_1), & x \in \Omega \\ \partial_t u_2 = F_2(t,x,D^{\alpha}u_2), & x \in \Omega \end{cases}$$

subject to $\frac{1}{x_0^{\alpha-1}} D^{\alpha-1} u_1(t,1) = \frac{1}{(1-x_0)^{\alpha-1}} D^{\alpha-1} u_2(t,0)$[1] and

$$B \begin{bmatrix} \frac{1}{x_0^{\alpha-1}} D^{\alpha-1} u_2(t,1) \\ \frac{1}{(1-x_0)^{\alpha-1}} D^{\alpha-1} u_1(t,0) \end{bmatrix} = 0,$$

where B is as in (5.12), $F_1 = F(t, x, \frac{1}{x_0^\beta} D^\beta u_1)$, and $F_2 = F(t, x, \frac{1}{(1-x_0)^\beta} D^\beta u_2)$. Then, functional (B.5) can be changed to either of the following

$$\begin{aligned} y(t) &= h\left(t, x_0, \frac{1}{x_0^\beta} D^\beta u_1(t,1)\right), \\ y(t) &= h\left(t, x_0, \frac{1}{(1-x_0)^\beta} D^\beta u_2(t,0)\right), \end{aligned}$$

and the method proposed for points at the boundaries described in previous subsection B.1.

B.3 Subsets Inside the Domain

Consider functional (5.15) with $g_1 = 0$, i.e.

$$y(t) = \int_{\tilde{\Omega}} g\left(t, x, D^\beta u(t,x)\right) \, dx, \tag{B.6}$$

where $\tilde{\Omega} = (x_1, x_2) \subset \Omega$. Similar to the previous section, we split the domain into three subsets $\Omega_1 = (0, x_1]$, $\Omega_2 = [x_1, x_2)$, and $\Omega_3 = [x_2, 1)$. Then, PDE (5.10) can be rewritten as

$$\partial_t u = \begin{cases} F(t, x, D^\alpha u), & x \in \Omega_1 \\ F(t, x, D^\alpha u), & x \in \Omega_2 \\ F(t, x, D^\alpha u), & x \in \Omega_3, \end{cases}$$

[1] To simplify the notation, we define

$$\frac{1}{x_0^{\alpha-1}} D^{\alpha-1} u = \left(u, \frac{1}{x_0} \partial_x u, \ldots, \frac{1}{x_0^{\alpha-1}} \partial_x^{\alpha-1} u\right)'.$$

subject to $D^{\alpha-1}u(t,x_1) = D^{\alpha-1}u(t,x_1)$, $D^{\alpha-1}u(t,x_2) = D^{\alpha-1}u(t,x_2)$, and (5.12). With appropriate change of variables, we have

$$\begin{cases} \partial_t u_1 = F_1(t,x,D^\alpha u_1), & x \in \Omega \\ \partial_t u_2 = F_2(t,x,D^\alpha u_2), & x \in \Omega \\ \partial_t u_3 = F_3(t,x,D^\alpha u_3), & x \in \Omega \end{cases}$$

subject to $\frac{1}{(x_1)^{\alpha-1}} D^{\alpha-1}u_1(t,1) = \frac{1}{(x_2-x_1)^{\alpha-1}} D^{\alpha-1}u_2(t,0)$ and $\frac{1}{(x_2-x_1)^{\alpha-1}} D^{\alpha-1}u_2(t,1) = \frac{1}{(1-x_2)^{\alpha-1}} D^{\alpha-1}u_3(t,0)$ in addition to

$$B \begin{bmatrix} \frac{1}{(1-x_2)^{\alpha-1}} D^{\alpha-1}u_3(t,1) \\ \frac{1}{(x_1)^{\alpha-1}} D^{\alpha-1}u_1(t,0) \end{bmatrix} = 0,$$

where B is the same matrix as the one in (5.12),

$$F_1 = F(t,x,\frac{1}{x_1^\beta} D^\beta u_1),\ F_2 = F(t,x,\frac{1}{(x_2-x_1)^\beta} D^\beta u_2),$$

and $F_3 = F(t,x,\frac{1}{(1-x_2)^\beta} D^\beta u_3)$. Finally, functional (B.6) can be converted to the following full integral form which is suitable for the integral inequalities

$$y(t) = (x_2 - x_1) \int_0^1 h\left(t,x,\frac{1}{(x_2-x_1)^\beta} D^\beta u_2(t,x)\right)\ dx.$$

Appendix C

Details of Numerical Experiments for Flow Structures

In the following, we describe the details of the numerical experiments carried out to obtain the flow structures for the plane Couette flow and the plane Poiseuille flow. We begin by describing the linearized Navier-Stokes equation and its corresponding discretization [37].

The non-dimensional linearized Navier-Stokes equations governing the evolution of disturbances in steady mean flow with streamwise velocity varying only in the cross-stream direction are

$$\begin{cases} (\partial_t + U\partial_x)\,\Delta v - \partial_y^2 U \partial_x v = \frac{1}{Re}\Delta\Delta v, \\ (\partial_t + U\partial_x)\,\eta + \partial_y U \partial_z v = \frac{1}{Re}\Delta\eta, \end{cases} \tag{C.1}$$

where $U(y)$ is the mean streamwise velocity component, v is the cross-section perturbation velocity, $\eta := \partial_z u - \partial_x w$, the cross-stream component of perturbation vorticity (z denotes the spanwise direction). Velocity has been non-dimensionalized by U_0, the maximum velocity in the channel; length has been non-dimensionalized by L, the width of the channel. The Reynolds number is defined as $Re := \frac{U_0 L}{\nu}$, where ν is the kinematic viscosity. Considering no-slip boundary conditions at $y = \pm 1$, we have $v = \partial_y v = \eta = 0$ at $y = \pm 1$. Recall that for the plane Couette flow $U = y$, and for the plane Poiseuille flow $U = 1 - y^2$.

Consider a single Fourier component

$$v = \hat{v}e^{ik_x x + ik_z z}, \tag{C.2}$$

$$\eta = \hat{\eta}e^{ik_x x + ik_z z}. \tag{C.3}$$

Physical variables being identified with the real part of these complex form. The field equations can be written in the compact form

$$\partial_t \begin{bmatrix} \hat{v} \\ \hat{\eta} \end{bmatrix} = \begin{bmatrix} \mathscr{L} & 0 \\ \mathscr{C} & \mathscr{S} \end{bmatrix} \begin{bmatrix} \hat{v} \\ \hat{\eta} \end{bmatrix}, \tag{C.4}$$

in which the Orr-Sommerfield operator $\mathscr{L}$, the Square operator $\mathscr{S}$, and the coupling operator $\mathscr{C}$ are defined as

$$\mathscr{L} = \Delta^{-1}\left(-ik_x U\Delta + ik_x\partial_y^2 U + \frac{\Delta\Delta}{Re}\right), \tag{C.5}$$

$$\mathscr{S} = -ik_x U + \frac{\Delta}{Re}, \tag{C.6}$$

$$\mathscr{C} = -ik_y\partial_y U, \tag{C.7}$$

with $K^2 = k_x^2 + k_y^2$ and $\Delta = \partial_y^2 - K^2$. Moreover, we have

$$\hat{u} = \frac{-i}{K^2}\left(k_y\hat{\eta} - k_x\partial_y\hat{v}\right), \tag{C.8}$$

$$\hat{w} = \frac{i}{K^2}\left(k_x\hat{\eta} + k_y\partial_y\hat{v}\right). \tag{C.9}$$

For numerical simulations of the Orr-Somerfield equation (C.1), we consider its discrete equivalent for an N-level discretization (over space)

$$\zeta = \begin{bmatrix} \hat{v}_1 & \cdots & \hat{v}_N & \hat{\eta}_1 & \cdots & \hat{\eta}_N \end{bmatrix}',$$

and the initial value problem (C.1) can be rewritten as

$$\dot{\zeta} = \mathscr{A}\zeta, \tag{C.10}$$

in which the linear dynamical operator, $\mathscr{A}$, is the discretized form of $\left[\begin{smallmatrix} \mathscr{L} & 0 \\ \mathscr{C} & \mathscr{J} \end{smallmatrix}\right]$. This means that the infinite dimensional dynamical system (C.1), is approximated as a finite dimensional dynamical systems.

The discretized operator $\mathscr{A}$ was calculated using the codes available in the Appendix A of [105] using Chebyshev discretization. For both flows, we considered $N = 50$. Then, the state-space form (C.10) is a linear system that has to be studied. In the following, we obtain LMI conditions to check ISS of a linear system.

Now, consider the following linear dynamical system

$$\dot{\zeta} = \mathscr{A}\zeta + Bd, \quad t > 0, \tag{C.11}$$

where $\zeta(0) = \zeta_0$, $\zeta \in \mathbb{R}^{2N}$, $d \in \mathbb{R}^{2N}$ and $B = \mathrm{I}_{2N\times 2N}$. This is the perturbed version of the discrete system (C.10). We are interested in studying the ISS of (C.10). That is, given $d \in \mathcal{L}^\infty$, we have the following inequality for all $\zeta_0 \in \mathbb{R}^{2N}$

$$\|\zeta(t)\|_2 \leq \beta\left(t, ||\zeta_0||_2\right) + \sigma\left(\|d\|_{\mathcal{L}^\infty_{[0,t)}}\right),\ t > 0 \tag{C.12}$$

where $\beta \in \mathcal{KL}$, $\sigma \in \mathcal{K}$ and $\|\zeta(t)\|_2$ is the Euclidean 2-norm, *i.e.,* $\|\zeta(t)\|_2 = \sqrt{\zeta'\zeta}$.

Theorem C.0.1 *Consider system* (C.11)*. If there exists an ISS-Lyapunov function $V(\zeta)$ and a positive semidefinite function S, $c_1, c_2 \in \mathcal{K}$, and a positive scalar ψ satisfying*

$$c_1(\|\zeta\|_2) \leq V(\zeta) \leq c_2(\|\zeta\|_2), \tag{C.13}$$

and

$$\partial_t V(\zeta) \leq -\psi V(\zeta) + S(d), \tag{C.14}$$

then solutions of (C.11) *satisfy estimate* (C.12) *with* $\beta(\cdot) = c_1^{-1}\left(2e^{-\psi t}c_2(\cdot)\right)$ *and* $\sigma(\cdot) = c_1^{-1}\left(\frac{2}{\psi}S(\cdot)\right)$.

Proof: Multiplying both sides of (C.14) by $e^{\psi t}$, gives

$$e^{\psi t}\partial_t V(\zeta) \leq -e^{\psi t}\psi V(\zeta) + e^{\psi t}S(d)$$

which implies $\frac{d}{dt}\left(e^{\psi t}V(\zeta)\right) \leq e^{\psi t}S(d)$. Integrating both sides of the latter inequality from 0 to t yields

$$e^{\psi t}V(\zeta(t)) - V(\zeta_0) \leq \int_0^t e^{\psi\tau}S(d(\tau))\ d\tau \leq \left(\int_0^t e^{\psi t}\ d\tau\right)\left(\sup_{\tau\in[0,t)} S\left(d(\tau)\right)\right).$$

where, in the last inequality, we applied the Hölder inequality. Then,

$$e^{\psi t}V(\zeta(t)) - V(\zeta_0) \leq \left(\frac{e^{\psi t}-1}{\psi}\right)\left(\sup_{\tau\in[0,t)} S\left(d(\tau)\right)\right) \leq \frac{e^{\psi t}}{\psi}\sup_{\tau\in[0,t)} S\left(d(\tau)\right).$$

Dividing both sides of the last inequality above by the non-zero term $e^{\psi t}$ and re-arranging the terms gives

$$V(\zeta(t)) \leq e^{-\psi t}V(\zeta_0) + \frac{1}{\psi}\sup_{\tau\in[0,t)} S\left(d(\tau)\right).$$

Applying the bounds in (C.13), we obtain

$$c_1(\|\zeta\|_2) \leq e^{-\psi t}c_2(\|\zeta_0\|_2) + \frac{1}{\psi}\sup_{\tau\in[0,t)} S\left(d(\tau)\right).$$

Since $c_1 \in \mathcal{K}$, its inverse exists and belongs to $\mathcal{K}$. Thus,

$$\|\zeta\|_2 \leq c_1^{-1}\left(e^{-\psi t}c_2(\|\zeta_0\|_2) + \frac{1}{\psi}\sup_{\tau\in[0,t)} S\left(d(\tau)\right)\right),$$

which can be further modified to

$$\|\zeta\|_2 \leq c_1^{-1}\left(2e^{-\psi t}c_2(\|\zeta_0\|_2)\right) + c_1^{-1}\left(\frac{2}{\psi}\sup_{\tau\in[0,t)} S\left(d(\tau)\right)\right).$$

Noting that S is positive semidefinite, we have

$$\|\zeta\|_2 \leq c_1^{-1}\left(2e^{-\psi t}c_2(\|\zeta_0\|_2)\right) + c_1^{-1}\left(\frac{2}{\psi}S\left(\|d\|_{\mathcal{L}^\infty_{[0,t)}}\right)\right).$$

□

The following corollary gives sufficient conditions based on linear matrix inequalities to check the conditions of Theorem C.0.1.

Corollary C.0.2 *Consider system* (C.11)*. If there exist symmetric matrices P and S, and a positive scalar ψ such that*

$$P > 0,\ S > 0 \tag{C.15}$$

and

$$\begin{bmatrix} \mathscr{A}'P + P\mathscr{A} + \psi P & B'P \\ PB & -S \end{bmatrix} \leq 0, \tag{C.16}$$

then the solutions to (C.11) *satisfy* (C.12) *with for $\beta(\cdot) = \left(\frac{2\lambda_M(P)}{\lambda_m(P)}e^{-\psi t}(\cdot)\right)^{\frac{1}{2}}$ and $\sigma(\cdot) = \left(\frac{2\lambda_M(S)}{\psi\lambda_m(P)}(\cdot)\right)^{\frac{1}{2}}$.*

Proof: This is a result of applying Theorem C.0.1 by considering $V(\zeta) = \zeta' P\zeta$ and $S(d) = d'Sd$. □

In order to the find the maximum ISS amplification, we solve the following optimization

problem

$$\text{minimize}_{P,S}\ (\lambda_1 - \lambda_2)$$

$$\text{subject to}$$

$$S \leq \lambda_1 I,\ P > \lambda_2 I,\ \text{(C.15)},\ \text{and (C.16)}. \tag{C.17}$$

Then, the system satisfies inequality (C.12) with $\beta(\cdot) = \left(\frac{2\lambda_M(P)}{\lambda_2} e^{-\psi t}(\cdot)\right)^{\frac{1}{2}}$ and $\sigma(\cdot) = \left(\frac{2\lambda_1}{\psi\lambda_2}(\cdot)\right)^{\frac{1}{2}}$. The upper-bound on the maximum ISS amplification is thus $\left(\frac{2\lambda_1}{\psi\lambda_2}(\cdot)\right)^{\frac{1}{2}}$. For the wave numbers that correspond to the maximum ISS amplification, we obtain the direction in which maximum amplification is attained. To this end, we carry out a singular-value decomposition of P (since P is symmetric the singular values and eigenvalues coincide) and we obtain the eigenvector in $\mathscr{A}$ that corresponds to the maximum singular value.

Appendix D

Induced $\mathcal{L}^2_{[0,\infty),\Omega}$-norms for the Linearized 2D/3C Model

In [58], the authors calculated componentwise $\mathcal{H}^\infty$-norms for the linearized 2D/3C model by finding the maximum singular values. This result is described as follows.

Theorem D.0.1 (Thoerem 11, p. 93 in [58]) *For any streamwise constant channel flows with nominal velocity $U(y)$, the $\mathcal{H}^\infty$ norms of operators $\mathcal{H}_{rs}(\omega, k_z, Re)$ that maps d_s into u_r, $\{r = x, y, z;\ s = x, y, z\}$, are given by*

$$\begin{bmatrix} \|\mathcal{H}_{xx}\|_\infty(k_z) & \|\mathcal{H}_{xy}\|_\infty(k_z) & \|\mathcal{H}_{xz}\|_\infty(k_z) \\ \|\mathcal{H}_{yx}\|_\infty(k_z) & \|\mathcal{H}_{yy}\|_\infty(k_z) & \|\mathcal{H}_{yz}\|_\infty(k_z) \\ \|\mathcal{H}_{zx}\|_\infty(k_z) & \|\mathcal{H}_{zy}\|_\infty(k_z) & \|\mathcal{H}_{zz}\|_\infty(k_z) \end{bmatrix} = \begin{bmatrix} h_{xx}(k_z)Re & h_{xy}(k_z)Re^2 & h_{xz}(k_z)Re^2 \\ 0 & h_{yy}(k_z)Re & h_{yz}(k_z)Re \\ 0 & h_{zy}(k_z)Re & h_{zz}(k_z)Re \end{bmatrix}, \tag{D.1}$$

where k_z represent the wavenumber in x_z (spanwise direction).

We are interested in studying the induced $\mathcal{L}^2$-norms from inputs d_x, d_y, d_z to $\boldsymbol{u} = (u_x, u_y, u_z)'$. The following corollary provides the induced norms of interest.

Corollary D.0.2 *For any streamwise constant channel flows with nominal velocity $U(y)$,*

we have

$$\frac{\|\boldsymbol{u}\|^2_{\mathcal{L}^2_{[0,\infty),\Omega}}}{\|d_x\|^2_{\mathcal{L}^2_{[0,\infty),\Omega}}} = f_1(k_z)Re^2, \tag{D.2}$$

$$\frac{\|\boldsymbol{u}\|^2_{\mathcal{L}^2_{[0,\infty),\Omega}}}{\|d_y\|^2_{\mathcal{L}^2_{[0,\infty),\Omega}}} = f_2(k_z)Re^2 + g_2(k_z)Re^4, \tag{D.3}$$

$$\frac{\|\boldsymbol{u}\|^2_{\mathcal{L}^2_{[0,\infty),\Omega}}}{\|d_z\|^2_{\mathcal{L}^2_{[0,\infty),\Omega}}} = f_3(k_z)Re^2 + g_3(k_z)Re^4. \tag{D.4}$$

Proof: From (D.1), we infer that

$$\begin{bmatrix} \|u_x\|_{\mathcal{L}^2_{[0,\infty),\Omega}} \\ \|u_y\|_{\mathcal{L}^2_{[0,\infty),\Omega}} \\ \|u_z\|_{\mathcal{L}^2_{[0,\infty),\Omega}} \end{bmatrix} = \begin{bmatrix} h_{xx}(k_z)Re & h_{xy}(k_z)Re^2 & h_{xz}(k_z)Re^2 \\ 0 & h_{yy}(k_z)Re & h_{yz}(k_z)Re \\ 0 & h_{zy}(k_z)Re & h_{zz}(k_z)Re \end{bmatrix} \begin{bmatrix} \|d_x\|_{\mathcal{L}^2_{[0,\infty),\Omega}} \\ \|d_y\|_{\mathcal{L}^2_{[0,\infty),\Omega}} \\ \|d_z\|_{\mathcal{L}^2_{[0,\infty),\Omega}} \end{bmatrix}. \tag{D.5}$$

Thus, we have

$$\begin{bmatrix} \|u_x\|_{\mathcal{L}^2_{[0,\infty),\Omega}} \\ \|u_y\|_{\mathcal{L}^2_{[0,\infty),\Omega}} \\ \|u_z\|_{\mathcal{L}^2_{[0,\infty),\Omega}} \end{bmatrix} = \begin{bmatrix} h_{xx}(k_z)Re\|d_x\|_{\mathcal{L}^2_{[0,\infty),\Omega}} + h_{xy}(k_z)Re^2\|d_y\|_{\mathcal{L}^2_{[0,\infty),\Omega}} + h_{xz}(k_z)Re^2\|d_z\|_{\mathcal{L}^2_{[0,\infty),\Omega}} \\ h_{yy}(k_z)Re\|d_y\|_{\mathcal{L}^2_{[0,\infty),\Omega}} + h_{yz}(k_z)Re\|d_z\|_{\mathcal{L}^2_{[0,\infty),\Omega}} \\ h_{zy}(k_z)Re\|d_y\|_{\mathcal{L}^2_{[0,\infty),\Omega}} + h_{zz}(k_z)Re\|d_z\|_{\mathcal{L}^2_{[0,\infty),\Omega}} \end{bmatrix}. \tag{D.6}$$

Then, multiplying both sides of the above equality by the transpose of vector $\begin{bmatrix} \|u_x\|_{\mathcal{L}^2_{[0,\infty),\Omega}} \\ \|u_y\|_{\mathcal{L}^2_{[0,\infty),\Omega}} \\ \|u_z\|_{\mathcal{L}^2_{[0,\infty),\Omega}} \end{bmatrix}$ gives

$$\begin{bmatrix} \|u_x\|_{\mathcal{L}^2_{[0,\infty),\Omega}} \\ \|u_y\|_{\mathcal{L}^2_{[0,\infty),\Omega}} \\ \|u_z\|_{\mathcal{L}^2_{[0,\infty),\Omega}} \end{bmatrix}' \begin{bmatrix} \|u_x\|_{\mathcal{L}^2_{[0,\infty),\Omega}} \\ \|u_y\|_{\mathcal{L}^2_{[0,\infty),\Omega}} \\ \|u_z\|_{\mathcal{L}^2_{[0,\infty),\Omega}} \end{bmatrix}$$

$$= \begin{bmatrix} h_{xx}(k_z)Re\|d_x\|_{\mathcal{L}^2_{[0,\infty),\Omega}} + h_{xy}(k_z)Re^2\|d_y\|_{\mathcal{L}^2_{[0,\infty),\Omega}} + h_{xz}(k_z)Re^2\|d_z\|_{\mathcal{L}^2_{[0,\infty),\Omega}} \\ h_{yy}(k_z)Re\|d_y\|_{\mathcal{L}^2_{[0,\infty),\Omega}} + h_{yz}(k_z)Re\|d_z\|_{\mathcal{L}^2_{[0,\infty),\Omega}} \\ h_{zy}(k_z)Re\|d_y\|_{\mathcal{L}^2_{[0,\infty),\Omega}} + h_{zz}(k_z)Re\|d_z\|_{\mathcal{L}^2_{[0,\infty),\Omega}} \end{bmatrix}'$$

$$\begin{bmatrix} h_{xx}(k_z)Re\|d_x\|_{\mathcal{L}^2_{[0,\infty),\Omega}} + h_{xy}(k_z)Re^2\|d_y\|_{\mathcal{L}^2_{[0,\infty),\Omega}} + h_{xz}(k_z)Re^2\|d_z\|_{\mathcal{L}^2_{[0,\infty),\Omega}} \\ h_{yy}(k_z)Re\|d_y\|_{\mathcal{L}^2_{[0,\infty),\Omega}} + h_{yz}(k_z)Re\|d_z\|_{\mathcal{L}^2_{[0,\infty),\Omega}} \\ h_{zy}(k_z)Re\|d_y\|_{\mathcal{L}^2_{[0,\infty),\Omega}} + h_{zz}(k_z)Re\|d_z\|_{\mathcal{L}^2_{[0,\infty),\Omega}} \end{bmatrix}. \quad \text{(D.7)}$$

That is,

$$\overbrace{\|u_x\|^2_{\mathcal{L}^2_{[0,\infty),\Omega}} + \|u_y\|^2_{\mathcal{L}^2_{[0,\infty),\Omega}} + \|u_z\|^2_{\mathcal{L}^2_{[0,\infty),\Omega}}}^{\|\boldsymbol{u}\|^2_{\mathcal{L}^2_{[0,\infty),\Omega}}}$$

$$= \left(h_{xx}(k_z)Re\|d_x\|_{\mathcal{L}^2_{[0,\infty),\Omega}} + h_{xy}(k_z)Re^2\|d_y\|_{\mathcal{L}^2_{[0,\infty),\Omega}} + h_{xz}(k_z)Re^2\|d_z\|_{\mathcal{L}^2_{[0,\infty),\Omega}}\right)^2$$

$$+ \left(h_{yy}(k_z)Re\|d_y\|_{\mathcal{L}^2_{[0,\infty),\Omega}} + h_{yz}(k_z)Re\|d_z\|_{\mathcal{L}^2_{[0,\infty),\Omega}}\right)^2$$

$$+ \left(h_{zy}(k_z)Re\|d_y\|_{\mathcal{L}^2_{[0,\infty),\Omega}} + h_{zz}(k_z)Re\|d_z\|_{\mathcal{L}^2_{[0,\infty),\Omega}}\right)^2. \quad \text{(D.8)}$$

In order to see the influence of each d_x on $\|\boldsymbol{u}\|^2_{\mathcal{L}^2_{[0,\infty),\Omega}}$, we set $d_y = d_z = 0$ obtaining

$$\|\boldsymbol{u}\|^2_{\mathcal{L}^2_{[0,\infty),\Omega}} = h^2_{xx}(k_z)Re^2\|d_x\|^2_{\mathcal{L}^2_{[0,\infty),\Omega}}.$$

It suffices to set $f_1(k_z) = h_{xx}^2(k_z)$. Similarly, we have

$$\|\boldsymbol{u}\|_{\mathcal{L}^2_{[0,\infty),\Omega}}^2 = h_{xy}^2(k_z) Re^4 \|d_y\|_{\mathcal{L}^2_{[0,\infty),\Omega}}^2 + \left(h_{yy}^2(k_z) + h_{zy}^2(k_z)\right) Re^2 \|d_y\|_{\mathcal{L}^2_{[0,\infty),\Omega}}^2,$$

$$\|\boldsymbol{u}\|_{\mathcal{L}^2_{[0,\infty),\Omega}}^2 = h_{xz}^2(k_z) Re^4 \|d_z\|_{\mathcal{L}^2_{[0,\infty),\Omega}}^2 + \left(h_{yz}^2(k_z) + h_{zz}^2(k_z)\right) Re^2 \|d_z\|_{\mathcal{L}^2_{[0,\infty),\Omega}}^2,$$

wherein $f_2(k_z) = h_{yy}^2(k_z) + h_{zy}^2(k_z)$, $g_2(k_z) = h_{xy}^2(k_z)$, $f_3(k_z) = h_{yz}^2(k_z) + h_{zz}^2(k_z)$ and $g_3(k_z) = h_{xz}^2(k_z)$. □

Bibliography

[1] M. Ahmadi, A. K. Harris, and A. Papachristodoulou. An optimization-based method for bounding state functionals of nonlinear stochastic systems. In *Decision and Control (CDC), 2016 IEEE 55th Annual Conference on*, Las Vegas, NV, 2016.

[2] M. Ahmadi, G. Valmorbida, and A. Papachristodoulou. Input-output analysis of distributed parameter systems using convex optimization. In *53rd IEEE Conference on Decision and Control*, pages 4310–4315. IEEE, 2014.

[3] M. Ahmadi, G. Valmorbida, and A. Papachristodoulou. Barrier functionals for output functional estimation of PDEs. In *2015 American Control Conference (ACC)*, pages 2594–2599. IEEE, 2015.

[4] M. Ahmadi, G. Valmorbida, and A. Papachristodoulou. A convex approach to hydrodynamic analysis. In *2015 54th IEEE Conference on Decision and Control (CDC)*, pages 7262–7267. IEEE, 2015.

[5] M. Ahmadi, G. Valmorbida, and A. Papachristodoulou. Barrier functionals for the analysis of complex systems: An optimization-based approach. *arXiv preprint arXiv:1603.08716*, 2016.

[6] M. Ahmadi, G. Valmorbida, and A. Papachristodoulou. Dissipation inequalities for the analysis of a class of PDEs. *Automatica*, 66:163–171, 2016.

[7] J. Anderson and A. Papachristodoulou. On validation and invalidation of biological models. *BMC Bioinformatics*, 132(10), 2009.

[8] Z. Artstein. Stabilization with relaxed controls. *Nonlinear Analysis: Theory, Methods & Applications*, 7(11):1163–1173, jan 1983.

[9] P. Ascencio, A. Astolfi, and T. Parisini. Backstepping PDE design, Volterra and Fredholm operators: A convex optimization approach. In *2015 54th IEEE Conference on Decision and Control (CDC)*, pages 7048–7053. IEEE, 2015.

[10] I. Babuska and M. Suri. The p and h-p versions of the finite element method, basic principles and properties. *SIAM Review*, 36(4):pp. 578–632, 1994.

[11] S. Bagheri, L. Brandt, and D. S. Hennigson. Input-output analysis, model reduction and control of the flat-plate boundary layer. *Journal of Fluid Mechanics*, 620:263–298, 2 2009.

[12] S. Bagheri, D. S. Henningson, J. Hoepffner, and P. J. Schmid. Input-output analysis and control design applied to a linear model of spatially developing flows. *Applied Mechanics Reviews*, 62, 2009.

[13] B. Bamieh and M. Dahleh. Energy amplification in channel flows with stochastic excitation. *Physics of Fluids*, 13(11):3258–3269, 2001.

[14] D. Bertsimas and C. Caramanis. Bounds on linear PDEs via semidefinite optimization. *Math. Program.*, 108(1):135–158, August 2006.

[15] K.M. Bobba, B. Bamieh, and J.C. Doyle. Highly optimized transitions to turbulence. In *Decision and Control, 2002, Proceedings of the 41st IEEE Conference on*, volume 4, pages 4559–4562, Dec 2002.

[16] D. P. Bovet, P. Crescenzi, and D. Bovet. *Introduction to the Theory of Complexity*. Prentice Hall Englewood Cliffs, NJ, 1994.

[17] J.P. Boyd. *Chebyshev and Fourier Spectral Methods: Second Revised Edition*. Dover Books on Mathematics. Dover Publications, 2001.

[18] S. Boyd, L. El Ghaoui, E. Feron, and V. Balakrishnan. *Linear Matrix Inequalities in System and Control Theory*. SIAM Studies in Applied Mathematics, 1994.

[19] S. Boyd and L. Vandenberghe. *Convex Optimization*. Cambridge University Press, 2004.

[20] F. Bribiesca Argomedo, C. Prieur, E. Witrant, and S. Bremond. A strict control Lyapunov function for a diffusion equation with time-varying distributed coefficients. *Automatic Control, IEEE Transactions on*, 58(2):290–303, 2013.

[21] F. Castillo, E. Witrant, C. Prieur, and L. Dugard. Boundary observers for linear and quasi-linear hyperbolic systems with application to flow control. *Automatica*, 49(11):3180 – 3188, 2013.

[22] S. Chernyshenko, P. Goulart, D. Huang, and A. Papachristodoulou. Polynomial sum of squares in fluid dynamics: a review with a look ahead. *Royal Society of London. Philosophical Transactions A. Mathematical, Physical and Engineering Sciences*, 372(2020), 2014.

[23] G. Chesi, A. Tesi, A. Vicino, and R. Genesio. On convexification of some minimum distance problems. In *5th European Control Conference*, Karlsruhe, Germany, 1999.

[24] M.D. Choi, T.Y. Lam, and B. Reznick. Sums of squares of real polynomials. In *Symposia in Pure Mathematics*, volume 58, pages 103–126, 1995.

[25] J.-M. Coron and B. D'Andrea-Novel. Stabilization of a rotating body beam without damping. *Automatic Control, IEEE Transactions on*, 43(5):608–618, May 1998.

[26] R. F. Curtain and H. J. Zwart. *An Introduction to Infinite-Dimensional Linear Systems Theory*, volume 21 of *Texts in Applied Mathematics*. Springer-Verlag, Berlin, 1995.

[27] S. Dashkovskiy and F. Mironchenko. Input-to-state stability of infinite-dimensional control systems. *Mathematics of Signals, Controls and Systems*, 25:1–35, 2013.

[28] R. Datko. Extending a theorem of A. M. Liapunov to Hilbert space. *Journal of Mathematical Analysis and Applications*, 32(3):610 – 616, 1970.

[29] J. C. del Alamo and J. Jiménez. Linear energy amplification in turbulent channels. *Journal of Fluid Mechanics*, 559:205–213, 7 2006.

[30] P. G. Drazin and W. H. Reid. *Hydrodynamic Stability*. Cambridge University Press, New York, 1981.

[31] C. Ebenbauer and F. Allgöwer. Analysis and design of polynomial control systems using dissipation inequalities and sum of squares. *Computers & Chemical Engineering*, 30(10-12):1590 – 1602, 2006.

[32] N. H. El-Farra, A. Armaou, and P. D. Christofides. Analysis and control of parabolic PDE systems with input constraints. *Automatica*, 39(4):715 – 725, 2003.

[33] L. C. Evans. *Partial Differential Equations*. Graduate studies in mathematics. American Mathematical Society, 2010.

[34] G. Fantuzzi and A. Wynn. Construction of an optimal background profile for the Kuramoto–Sivashinsky equation using semidefinite programming. *Physics Letters A*, 379(1):23–32, 2015.

[35] G. Fantuzzi and A. Wynn. Optimal energy dissipation bounds for 2D and 3D stress-driven shear flows. *Bulletin of the American Physical Society*, 60, 2015.

[36] G. Fantuzzi, A. Wynn, P. Goulart, and A. Papachristodoulou. Optimization with affine homogeneous quadratic integral inequality constraints. *arXiv preprint arXiv:1607.04210*, 2016.

[37] Brian F. Farrell and Petros J. Ioannou. Stochastic forcing of the linearized Navier-Stokes equations. *Physics of Fluids A*, 5(11):2600–2609, 1993.

[38] A. Gahlawat and M. M. Peet. Output feedback control of inhomogeneous parabolic PDEs with point actuation and point measurement using SOS and semi-separable kernels. In *2015 54th IEEE Conference on Decision and Control (CDC)*, pages 1217–1223. IEEE, 2015.

[39] A. Garulli, A. Masi, G. Valmorbida, and L. Zaccarian. Global stability and finite $\mathcal{L}_{2m}$-gain of saturated uncertain systems via piecewise polynomial Lyapunov functions. *Automatic Control, IEEE Transactions on*, 58(1):242–246, Jan 2013.

[40] D. F. Gayme, B. J. McKeon, B. Bamieh, A. Papachristodoulou, and J. C. Doyle. Amplification and nonlinear mechanisms in plane Couette flow. *Physics of Fluids*, 23(6), 2011.

[41] S. Glavaski, D. Subramanian, K. Ariyur, R. Ghosh, N. Lamba, and A. Papachristodoulou. A nonlinear hybrid life support system: Dynamic modeling, control design, and safety verification. *Control Systems Technology, IEEE Transactions on*, 15(6):1003–1017, Nov 2007.

[42] P. J. Goulart and S. Chernyshenko. Global stability analysis of fluid flows using sum-of-squares. *Physica D: Nonlinear Phenomena*, 241(6):692 – 704, 2012.

[43] S. Grossmann. The onset of shear flow turbulence. *Rev. Mod. Phys.*, 72:603–618, Apr 2000.

[44] H. Guéguen, M. Lefebvre, J. Zaytoon, and O. Nasri. Safety verification and reachability analysis for hybrid systems. *Annual Reviews in Control*, 33(1):25 – 36, 2009.

[45] L. H. Gustavsson. Energy growth of three-dimensional disturbances in plane Poiseuille flow. *Journal of Fluid Mechanics*, 224:241–260, 3 1991.

[46] W. M. Haddad and V. S. Chellaboina. *Nonlinear Dynamical Systems and Control: A Lyapunov-based Approach*. Princeton University Press, Princeton, New Jersey,, 2008.

[47] G. H. Hardy, J. E. Littlewood, and G. Polya. *Inequalities*. Cambridge University Press, 2nd edition, 1988.

[48] D. Henrion and M. Korda. Convex computation of the region of attraction of polynomial control systems. *Automatic Control, IEEE Transactions on*, 59(2):297–312, Feb 2014.

[49] D. Henry. *Geometric Theory of Semilinear Parabolic Equations*. Lecture Notes in Mathematics. Springer-Verlag, Berlin, 1981.

[50] T. I. Hesla, F. R. Pranckh, and L. Preziosi. Squire's theorem for two stratified fluids. *Physics of Fluids*, 29(9):2808–2811, 1986.

[51] D. Hill and P. Moylan. The stability of nonlinear dissipative systems. *Automatic Control, IEEE Transactions on*, 21(5):708–711, Oct 1976.

[52] D. Huang, S. Chernyshenko, P. Goulart, D. Lasagna, O. Tutty, and F. Fuentes. Sum-of-squares of polynomials approach to nonlinear stability of fluid flows: an example of application. *Proceedings of the Royal Society of London A: Mathematical, Physical and Engineering Sciences*, 471(2183), 2015.

[53] Y. Hwang and C. Cossu. Linear non-normal energy amplification of harmonic and stochastic forcing in the turbulent channel flow. *Journal of Fluid Mechanics*, 664:51–73, 12 2010.

[54] R. Al Jamal. *Bounded Control of the Kuramoto–Sivashinsky equation*. PhD thesis, University of Waterloo, Waterloo, Ontario, Canada, 2013.

[55] D. D. Joseph. *Stability of fluid motions*. Springer Tracts in Natural Philosophy. Springer-Verlag, Berlin, 1976.

[56] D. D. Joseph and W. Hung. Contributions to the nonlinear theory of stability of viscous flow in pipes and between rotating cylinders. *Archive for Rational Mechanics and Analysis*, 44(1):1–22, 1971.

[57] M. Jovanović and B. Bamieh. The spatio-temporal impulse response of the linearized Navier-Stokes equations. In *Proceedings of 2001 American Control Conference*, volume 3, pages 1948–1953, June 2001.

[58] M. R. Jovanović. *Modeling, analysis, and control of spatially distributed systems*. PhD thesis, University of California, Santa Barbara, 2004.

[59] M. R. Jovanović and B. Bamieh. Componentwise energy amplification in channel flows. *Journal of Fluid Mechanics*, 534:145–183, 2005.

[60] R. E. Kalman. Lyapunov functions for the problem of Luré in automatic control. *Proceedings of the National Academy of Sciences*, 49(2):201–205, 1963.

[61] H. K. Khalil and J. W. Grizzle. *Nonlinear systems*. Prentice hall New Jersey, 1996.

[62] M. Krstić, L. Magnis, and R. Vazquez. Nonlinear stabilization of shock-like unstable equilibria in the viscous Burgers PDE. *Automatic Control, IEEE Transactions on*, 53(7):1678–1683, Aug 2008.

[63] A. Kurzhanski and P. Varaiya. Ellipsoidal techniques for reachability analysis: internal approximation. *Systems & Control Letters*, 41(3):201 – 211, 2000.

[64] I. Lasiecka and R. Triggiani. *Control theory for partial differential equations: Volumes 1 & 2*. Number 74,75 in Encyclopedia of Mathematics and Its Applications. Cambridge University Press, Cambridge, UK, 2000.

[65] J. B. Lasserre. *Moments, Positive Polynomials and Their Applications*. Imperial College Press, London, 2009.

[66] J. B. Lasserre, D. Henrion, C. Prieur, and E. Trelat. Nonlinear optimal control via occupation measures and LMI relaxations. *SIAM J. Control and Optimization*, 47(4):1643—1666, 2008.

[67] W. Liu and M. Krstić. Stability enhancement by boundary control in the Kuramoto–Sivashinsky equation. *Nonlinear Analysis: Theory, Methods & Applications*, 43(4):485–507, 2001.

[68] J. Löfberg. YALMIP : a toolbox for modeling and optimization in MATLAB. In *Computer Aided Control Systems Design, 2004 IEEE International Symposium on*, pages 284–289, Sept 2004.

[69] G. Lumer and R. S. Phillips. Dissipative operators in a banach space. *Pacific J. Math.*, 11(2):679–698, 1961.

[70] Z. Luo, B. Guo, and O. Murgol. *Stability and Stabilization of Infinite Dimensional Systems with Applications*. Communications and Control Engineering. Springer-Verlag, London, UK, 1999.

[71] F. Mazenc and C. Prieur. Strict Lyapunov functions for semilinear parabolic partial differential equations. *Mathematical Control and Related Fields*, 1(2):231–250, 2011.

[72] I. Miyadera. *Nonlinear Semigroups*. Translations of Mathematical Monographs. American Mathematical Society, Providence, Rhode Island, 2005.

[73] P. Monk and E. Süli. The adaptive computation of far-field patterns by a posteriori error estimation of linear functionals. *SIAM J. Numer. Anal.*, 36(1):251–274, 1998.

[74] T. S. Motzkin. The arithmetic-geometric inequality. In *1967 Inequalities Symposium*, pages 205–224, Wright-Patterson Air Force Base, Ohio, 1965.

[75] A.A Movchan. The direct method of Liapunov in stability problems of elastic systems. *Journal of Applied Mathematics and Mechanics*, 23(3):686–700, 1959.

[76] M. R. Opmeer, T. Reis, and W. Wollner. Finite-rank ADI iteration for operator Lyapunov equations. *SIAM Journal on Control and Optimization*, 51(5):4084–4117, 2013.

[77] W. Orr. The stability or instability of the steady motions of a perfect liquid and of a viscous liquid. part II: A viscous liquid. *Proceedings of the Royal Irish Academy. Section A: Mathematical and Physical Sciences*, 27:pp. 69–138, 1907.

[78] F. Otto. Optimal bounds on the Kuramoto-Sivashinsky equation. *Journal of Functional Analysis*, 257(7):2188 – 2245, 2009.

[79] A. Papachristodoulou, J. Anderson, G. Valmorbida, S. Prajna, P. Seiler, and P.A. Parrilo. SOSTOOLS: Sum of squares optimization toolbox for MATLAB V3.00, 2013.

[80] A. Papachristodoulou and M.M. Peet. On the analysis of systems described by classes of partial differential equations. In *Decision and Control, 2006 45th IEEE Conference on*, pages 747–752, 2006.

[81] A. Papachristodoulou and S. Prajna. A tutorial on sum of squares techniques for systems analysis. In *American Control Conference, 2005. Proceedings of the 2005*, pages 2686–2700 vol. 4, 2005.

[82] N. Parés, J. Bonet, A. Huerta, and J. Peraire. The computation of bounds for linear-functional outputs of weak solutions to the two-dimensional elasticity equations. *Computer Methods in Applied Mechanics and Engineering*, 195(4):406 – 429, 2006.

[83] P. C. Parks and A. J. Pritchard. On the construction and use of Lyapunov functionals. In *4th IFAC World Congress*, pages 59–76, 1969.

[84] P. Parrilo. *Structured semidefinite programs and semialgebraic geometry methods in robustness and optimization*. PhD thesis, California Institute of Technology, 2000.

[85] L.E. Payne and H.F. Weinberger. An optimal Poincare inequality for convex domains. *Archive for Rational Mechanics and Analysis*, 5(1):286–292, 1960.

[86] M. M. Peet, A. Papachristodoulou, and S. Lall. Positive forms and stability of linear time-delay systems. *SIAM J. Control and Optimization*, 47(6):3237—3258, 2007.

[87] J. Peixinho and T. Mullin. Decay of turbulence in pipe flow. *Phys. Rev. Lett.*, 96:094501, Mar 2006.

[88] J. Peraire and A. T. Patera. Bounds for linear-functional outputs of coercive partial differential equations: linear indicators and adaptive refinement. In P. Ladevéze and J. T. Oden, editors, *Advances in adaptive computational methods in mechanics*, volume 47 of *Studies in Applied Mechanics*, pages 199–217. Elsevier Science Ltd., Oxford, UK, 1998.

[89] N. A. Pierce and M. B. Giles. Adjoint and defect error bounding and correction for functional estimates. *Journal of Computational Physics*, 200(2):769 – 794, 2004.

[90] I. Pólik and T. Terlaky. A survey of the S-Lemma. *SIAM Review*, 49(3):371–418, 2007.

[91] S. Prajna. Barrier certificates for nonlinear model validation. *Automatica*, 42(1):117 – 126, 2006.

[92] S. Prajna and A. Jadbabaie. Methods for safety verification of time-delay systems. In *Decision and Control, 2005 and 2005 European Control Conference. CDC-ECC '05. 44th IEEE Conference on*, pages 4348–4353, Dec 2005.

[93] S. Prajna, A Jadbabaie, and G.J. Pappas. A framework for worst-case and stochastic safety verification using barrier certificates. *Automatic Control, IEEE Transactions on*, 52(8):1415–1428, Aug 2007.

[94] S. Prajna, A. Papachristodoulou, and F. Wu. Nonlinear control synthesis by sum of squares optimization: a Lyapunov-based approach. In *5th Asian Control Conference*, volume 1, pages 157–165, 2004.

[95] S. Prajna and A. Rantzer. On the necessity of barrier certificates. In *Proceedings of the 16th IFAC World Congress, 2005*, pages 742–742, 2005.

[96] Stephen Prajna, Antonis Papachristodoulou, and Fen Wu. Nonlinear control synthesis by sum of squares optimization: A Lyapunov-based approach. In *Control Conference, 2004. 5th Asian*, volume 1, pages 157–165. IEEE, 2004.

[97] C. Prieur and F. Mazenc. ISS-Lyapunov functions for time-varying hyperbolic systems of balance laws. *Mathematics of Signals, Controls and Systems*, 24:111–134, 2012.

[98] G. Pujals, M. Garćia-Villalba, C. Cossu, and S. Depardon. A note on optimal transient growth in turbulent channel flows. *Physics of Fluids*, 21(1), 2009.

[99] O. Reynolds. An experimental investigation of the circumstances which determine whether the motion of water shall be direct or sinuous and the law of resistance in parallel channels. *Philos. Trans.*, 935(51), 1883.

[100] B. Reznick. Some concrete aspects of Hilbert's 17th problem. *Contemporary Mathematics*, 253:251–272, 2000.

[101] V.A. Romanov. Stability of plane-parallel Couette flow. *Functional Analysis and Its Applications*, 7(2):137–146, 1973.

[102] A. J. Schaft. *L_2-Gain and Passivity Techniques in Nonlinear Control*. Springer-Verlag New York, Inc., Secaucus, NJ, USA, 1st edition, 1996.

[103] P. J. Schmid. Nonmodal stability theory. *Annual Review of Fluid Mechanics*, 39(1):129–162, 2007.

[104] P. J. Schmid and D. S. Henningson. Optimal energy density growth in Hagen—Poiseuille flow. *Journal of Fluid Mechanics*, 277:197–225, 10 1994.

[105] P. J. Schmid and D. S. Henningson. *Stability and transition in shear flows*. Applied Mathematical Sciences. Springer-Verlag, New York, 2001.

[106] J. Serrin. On the stability of viscous fluid motions. *Arch. Ration. Mech. Anal.*, 3:1–13, 1959.

[107] A. Seuret, F. Gouaisbaut, and Y. Ariba. Complete quadratic Lyapunov functionals for distributed delay systems. *Automatica*, 62:168–176, 2015.

[108] A. Seuret, F. Gouaisbaut, and E. Fridman. Stability of systems with fast-varying delay using improved Wirtinger's inequality. In *Decision and Control (CDC), 2013 IEEE 52nd Annual Conference on*, pages 946–951, Dec 2013.

[109] A. S. Sharma, J. F. Morrison, B. J. McKeon, D. J. N. Limebeer, W. H. Koberg, and S. J. Sherwin. Relaminarisation of $Re_\tau = 100$ channel flow with globally stabilising linear feedback control. *Physics of Fluids*, 23(125105), 2011.

[110] C. Sloth, R. Wisniewski, and G.J. Pappas. On the existence of compositional barrier certificates. In *Decision and Control (CDC), 2012 IEEE 51st Annual Conference on*, pages 4580–4585, Dec 2012.

[111] E. D. Sontag. A universal construction of Artstein's theorem on nonlinear stabilization. *Systems & Control Letters*, 13(2):117–123, aug 1989.

[112] E. D. Sontag. Smooth stabilization implies coprime factorization. *Automatic Control, IEEE Transactions on*, 34(4):435–443, Apr 1989.

[113] E. D. Sontag and Y. Wang. On characterizations of the input-to-state stability property. *Systems & Control Letters*, 24(5):351 – 359, 1995.

[114] O. Staffans. *Well-Posed Linear Systems*. Cambridge University Press, 2005.

[115] J. Steinhardt and R. Tedrake. Finite-time regional verification of stochastic nonlinear systems. *The International Journal of Robotics Research*, 31(7):901–923, 2012.

[116] B. Straughan. *The Energy Method, Stability, and Nonlinear Convection*, volume 91 of *Applied Mathematical Sciences*. Springer-Verlag, Berlin, 2nd edition, 2004.

[117] Jos F. Sturm. Using SeDuMi 1.02, a MATLAB toolbox for optimization over symmetric cones, 1998.

[118] E. Summers, A. Chakraborty, W. Tan, U. Topcu, P. Seiler, G. Balas, and A. Packard. Quantitative local L2-gain and reachability analysis for nonlinear systems. *International Journal of Robust and Nonlinear Control*, 23(10):1115–1135, 2013.

[119] R. Temam. *Infinite-dimensional dynamical systems in mechanics and physics*, volume 68. Springer, 2nd edition, 1988.

[120] N. Tillmark and P. H. Alfredsson. Experiments on transition in plane Couette flow. *Journal of Fluid Mechanics*, 235:89–102, 1992.

[121] C.J. Tomlin, I. Mitchell, A.M. Bayen, and M. Oishi. Computational techniques for the verification of hybrid systems. *Proceedings of the IEEE*, 91(7):986–1001, July 2003.

[122] L. N. Trefethen. *Spectral methods in MATLAB*. SIAM, 2000.

[123] L. N. Trefethen, A. E. Trefethen, S. C. Reddy, and T. A. Driscoll. Hydrodynamic stability without eigenvalues. *Science*, 261(5121):578–584, 1993.

[124] H. L. Trentelman and J. C. Willems. Every storage function is a state function. *Systems & Control Letters*, 32(5):249 – 259, 1997.

[125] M. Tucsnak and G. Weiss. *Observation and Control for Operator Semigroups*. Birkhäuser Advanced Texts. Birkhäuser, 2009.

[126] G. Valmorbida, M. Ahmadi, and A. Papachristodoulou. Semi-definite programming and functional inequalities for distributed parameter systems. In *53rd IEEE Conference on Decision and Control*, pages 4304–4309. IEEE, 2014.

[127] G. Valmorbida, M. Ahmadi, and A. Papachristodoulou. Convex solutions to integral inequalities in two-dimensional domains. In *Decision and Control, 2015 54th IEEE Conference on*, pages –, Dec 2015.

[128] G. Valmorbida, M. Ahmadi, and A. Papachristodoulou. Stability analysis for a class of partial differential equations via semidefinite programming. *IEEE Transactions on Automatic Control*, 61(6):1649–1654, 2016.

[129] G. Valmorbida, S. Tarbouriech, and G. Garcia. Design of polynomial control laws for polynomial systems subject to actuator saturation. *Automatic Control, IEEE Transactions on*, 58(7):1758–1770, July 2013.

[130] R. Vazquez, Schuster E., and M. Krstic. Magnetohydrodynamic state estimation with boundary sensors. *Automatica*, 44(10):2517 – 2527, 2008.

[131] A. J. Walker. *Dynamical Systems and Evolution Equations: Theory and applications*. Plenum Press, New York, 1980.

[132] G. Weiss, O. Staffans, and M. Tucsnak. Well-posed linear systems - a survey with emphasis on conservative systems. *International Journal of Applied Mathematics and Computer Science*, 11(1):7–33, 2001.

[133] G. Weiss and M. Tucsnak. How to get a conservative well-posed linear system out of thin air. Part I. Well-posedness and energy balance. *ESAIM: COCV*, 9:247–273, 2003.

[134] P. Wieland and F. Allgöwer. Constructive safety using control barrier functions. In *7th IFAC Symposium on Nonlinear Control Systems*, pages 473–478, 2007.

[135] J. C. Willems. Dissipative dynamical systems part I: General theory. *Archive for Rational Mechanics and Analysis*, 45(5):321–351, 1972.

[136] R. Wisniewski, M. Svenstrup, A.S. Pedersen, and C.S. Steiniche. Certificate for safe emergency shutdown of wind turbines. In *American Control Conference (ACC), 2013*, pages 3667–3672, June 2013.

[137] E. Witrant, E. Joffrin, S. Brémond, G. Giruzzi, D. Mazon, O. Barana, and P. Moreau. A control-oriented model of the current profile in Tokamak plasma. *Plasma Physics and Controlled Fusion*, 49(7):1075, 2007.

[138] Z.C. Xuan, K.H. Lee, and J. Peraire. A posteriori output bound for partial differential equations based on elemental error bound computing. In Vipin Kumar, Marina L. Gavrilova, Chih Jeng Kenneth Tan, and Pierre Ecuyer, editors, *Computational Science and Its Applications ICCSA 2003*, volume 2667 of *Lecture Notes in Computer Science*, pages 1035–1044. Springer Berlin Heidelberg, 2003.

[139] Z.C. Xuan, N. Parés, and J. Peraire. Computing upper and lower bounds for the J-integral in two-dimensional linear elasticity. *Computer Methods in Applied Mechanics and Engineering*, 195(406):430 – 443, 2006.